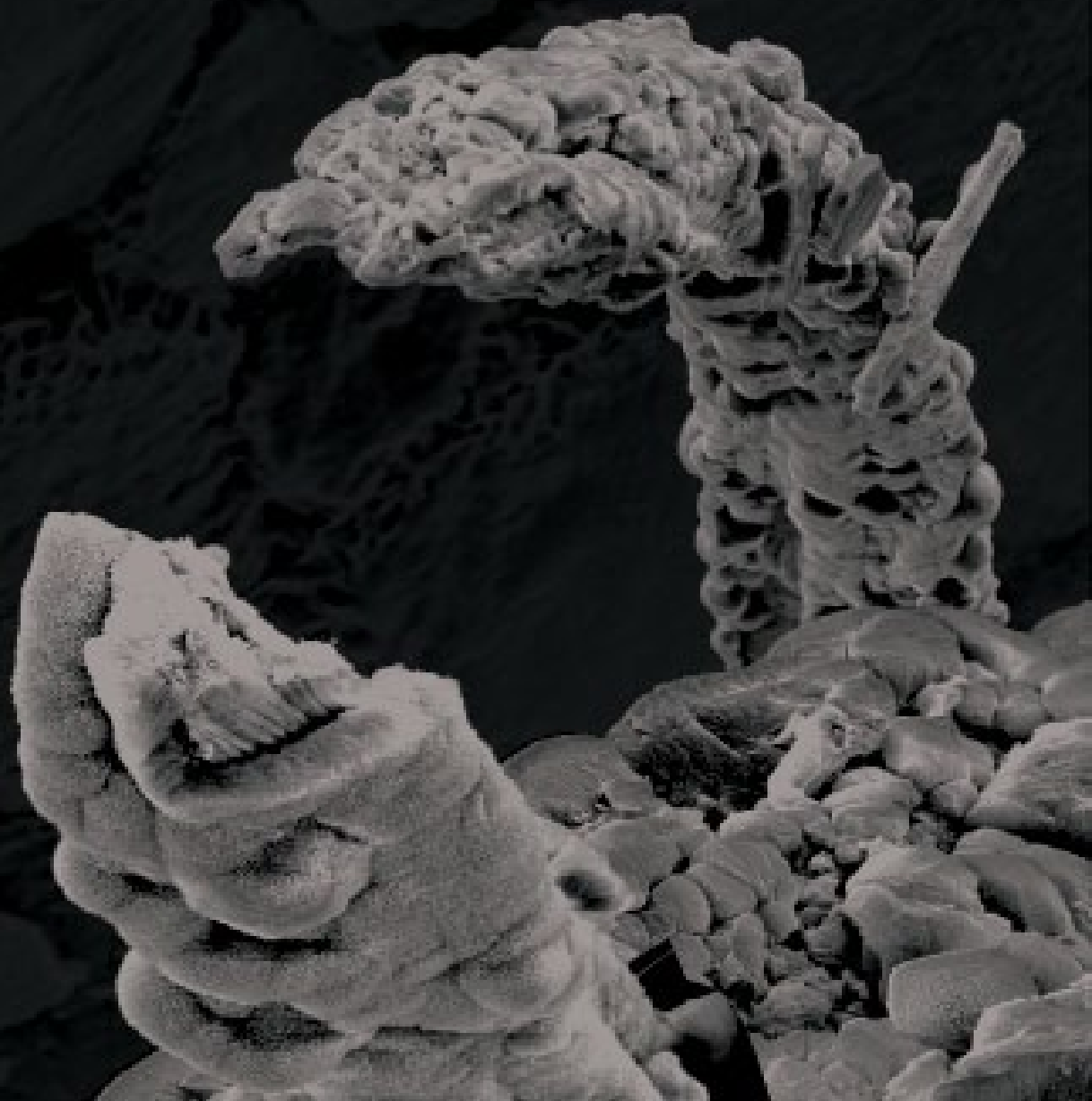# Calcium Phosphate Coatings for Bone Regeneration

Liang Yang

Calcium Phosphate Coatings for Bone Regeneration

Liang Yang

2010

Members of the Committee:

Prof. dr. J. Engbersen	Chairman	(University of Twente)
Prof. dr. C.A. van Blitterswijk	Promoter	(University of Twente)
Dr. P. Habibovic	Co-Promoter	(University of Twente)

Prof. Dr. J.de Bruijn	(Queen Mary University, London)
Dr. F. de Groot-Barrere	(Progentix BV)
Dr. Y. Liu	(Acta)
Prof. Dr. D. Grijpma	(University of Twente)
Prof. Dr. N. Verdonschot	(University of Twente)

Liang Yang
Calcium Phosphate Coatings for Bone Regeneration

CALCIUM PHOSPHATE COATINGS FOR BONE REGENERATION

DISSERTATION

to obtain
the degree of doctor at the University of Twente,
on the authority of the rector magnificus,
prof. dr. H. Brinksma
on account of the decision of the graduation committee,
to be publicly defended
on Friday 11th June 2010 at 15:00

by

Liang Yang
born on June 12th 1982
in Linchuan, Jiangxi Province, China

To my beloved parents and Yunjie

Table of Content

Chapter 1

General Introduction

I - Biomaterials for bone repair and regeneration

Bone has self-healing function, which is called fracture healing. The whole process consists of five phases: fracture and inflammatory phase - construction of blood vessels and formation of blood clot; granulation tissue formation phase - formation of a loose aggregate of cells, interspersed with small blood vessels; callus formation phase - formation of hyaline cartilage bridging the fracture gap; lamellar bone deposition phase - replacement of the hyaline cartilage and woven bone with lamellar bone by a process called endochondral ossification; phase of remodeling to original bone contour - resorption of trabecular bone and deposition of new compact bone by osteoblasts. While immobilization and surgery may facilitate healing, a fracture ultimately heals through physiological processes. The healing process is mainly determined by the periosteum (the connective tissue membrane covering the bone). The periosteum is the primary source of precursor cells which develop into chondroblasts and osteoblasts that are essential to the healing of bone. The bone marrow (when present), endosteum, small blood vessels, and fibroblasts are secondary sources of precursor cells.

When the bone self-healing mechanism fails as a result of magnitude, infection or other causes, bone grafting has been shown to be a successful therapy. Disadvantages of using patient's own bone or bone from a donor to treat bone defects lay in limited availability, need for a second surgery sometimes associated with donor site morbidity, and possible immunogenic response and disease transmission. Therefore, alternatives to autograft and allograft are sought for. Tissue engineering is a novel approach to repair and regenerate damaged and degraded bone tissue. This is an emerging interdisciplinary field applying the principles of biology and engineering to the development of viable substitutes that restore and maintain the function of human bone tissues [1-4]. Tissue engineering constructs usually consist of cells and/or growth factors in combination with a natural or synthetic scaffold. Ideally, the engineered bone, as bone graft substitute, becomes integrated within the patient, affording a potentially permanent and specific cure of the tissue. Fully synthetic alternatives to autologous bone and tissue engineered constructs, i.e. synthetic bone graft substitutes are attractive because of their off-the-shelf availability in large quantities and relatively low production and storage costs. Bone-graft substitute should ideally be: biocompatible, i.e. accepted by the body without adverse tissue responses, osteoconductive, i.e. able to facilitate and guide new bone formation from the host bone, osteoinductive, i.e. able to induce new bone formation, bio-resorbable, and structurally similar to bone. A large number of bone-graft substi-

tutes are currently commercially available for orthopedic and cranio-maxillo-facial use. They vary in composition, mechanism of action, and special characteristics.

I.1 - Metals

Metals and their alloys have a long history as orthopedic implants and bone graft substitutes for their well-known strength (elastic modulus larger than 100 GPa), especially in load-bearing areas [5]. Conventional implants have typically been produced from stainless steel, cobalt–chromium (CoCr), or titanium alloys. A lot of processes of surface modification have been developed to enhance biological fixation of these implants to bone for use in orthopedic procedures [6]. The advantages of metallic alloys include a light-weight nature, high strength and biocompatibility. Their use is however also associated with several limitations, which include permanence, cracking, low volumetric porosity, relatively high modulus of elasticity and the potential of releasing metallic ions and introducing corrosion products into the body from these materials [7-12]. Most metals cannot be used to produce a complete tissue replacement for bone defects because they are not biodegradable. In addition, the released metal particles have been found to affect the release of inflammatory factors, inhibit expression of osteogenic cell markers, and stimulate bone loss or resumption. For example, studies have shown that titanium and its alloy particles inhibit bone-cell proliferation and osteogenic differentiation [13]. Moreover, metal implants could not integrate well with the surrounding tissues due to the lack of bioactivity and a significant difference in stiffness between implants and the surrounding bone tissue. These metal implants are always stiffer than the natural bone tissue, which may lead to the stress shielding effect and poor osteointegration.

To address some of the limitations of these traditional solid metals, several modifications have been suggested.

Porous tantalum has an open-cell tantalum structure of repeating dodecahedrons, which resembles structure of cancellous bones. Tantalum-based implants have been reported to have an exceptional biocompatibility and safety record in orthopedic, cranio-facial, and dentistry literature [14]. The kind of structure has a high volumetric porosity, a low modulus of elasticity, and relatively high frictional characteristics. Bermudez et al. have reported that tantalum, secondary to stable surface oxidation layer, showed excellent corrosion–erosion resistance in a highly acidic environment, with no significant weight or roughness change comparing to titanium and stainless steel implants [15].

Magnesium is another potentially useful metal in bone substitution, because of its light-weight and biodegradability. The fracture toughness of magnesium is greater than that of ceramic biomaterials such as hydroxyapatite, while its elastic modulus and compressive yield strength are closer to those of the natural bone as compared to other commonly used metallic implants [16]. Moreover, magnesium can be found in bone tissue as a trace element, where it plays an essential role [17-22]. Magnesium is a co-factor for many enzymes, and helps to stabilize the structures of DNA and RNA [22]. Reports suggested that magnesium may actually stimulate the growth of new bone tissue [23-26]. Thus, magnesium and its alloys could be used as lightweight, biodegradable, load bearing orthopedic implants, which

would remain present in the body and maintain mechanical integrity over 12–18 weeks. Eventually the implants are replaced by natural tissue [27, 28].

In general, metals are bioinert and do not bond to bone. Recently, Kokubo and colleagues showed that titanium, tantalum and their alloys could spontaneously bond to living bone after a pre-treatment with NaOH solution and a subsequent heat treatment [29]. Coating metal surfaces with a bioactive layer of e.g. calcium-phosphate is another way to improve their bioactivity [30].

I.2 - Polymers

Polymer cements, such as polymethylmethacrylate (PMMA), have been utilized for decades as bone substitute in filling defects and reconstruction of complex fractures. However, PMMA is not biodegradable and may initiate an osteolytic foreign body giant cell reaction when fragmented [31]. That is why nowadays many researches focus on biodegradable polymers. In an ideal situation, as the growth of bone into the scaffold promulgates and the bone cells naturally build an infrastructure, the initial supporting scaffold is degraded and a handoff of mechanical stress and strain is passed onto the neo-tissue structure [32]. There are two types of biodegradable polymers: one is the natural-based material, including polysaccharides (starch, alginate, chitin/chitosan, hyaluronic acid derivatives), proteins (soy, collagen, fibrin gels, silk) and a variety of biofibers such as lignocellulosic natural fibers [33-36]; the other is synthetic biodegradable polymers.

Synthetic biodegradable polymers, based primarily on a hydroxyl-acids, have been used clinically in the form of sutures for the past 40 years and as internal fixation devices such as pins, screws, and plates for over 20 years [37-39]. These polymers can be produced under controlled conditions and therefore exhibit in general predictable and reproducible mechanical and physical properties such as tensile strength, elastic modulus and degradation rate. Furthermore, material impurities and biocompatibility can be well controlled. Possible risks such as toxicity, immunogenicity and inflammations are also very low for pure synthetic polymers with a well-known simple structure [40-42]. With all these advantages, synthetic polymers are playing a very important role as bone graft substitutes and as scaffolds for tissue engineering constructs [43]. The in vivo degradation process of polymers includes chain scission by hydrolysis or oxidation, followed by conversion into metabolites and exertion [39]. Abundant evidences show that these materials can degrade during the healing process and be replaced by new tissue [44-50]. Kieswetter et al [51] reported that large segmental defects in rabbits treated with a porous granular polymeric scaffold had been healed to the extent which was comparable to those treated with autograft at 12 weeks, as indicated by radiographic evaluations and mechanical tests. However, in general, the performance of synthetic materials in regeneration of bone defects is still inferior to that of natural graft. The most often utilized biodegradable synthetic polymers in bone tissue engineering and for bone graft substitutes are saturated poly-a-hydroxy esters, including poly(lactic acid) (PLA) and poly(glycolic acid) (PGA), as well as poly(lactic-coglycolide) (PLGA) copolymers [52-54]. Biodegradable polyester degradation occurs by uptake of water followed by the hydrolysis of ester bonds. Once degraded, the monomeric components of each polymer, such as lactic and glycolic acids, are removed by natural

pathways which are harmless to human body.

PGA is converted to metabolites or eliminated by other mechanisms, and PLA can be cleared through the tricarboxylic acid cycle. Both degradation rates and physical and mechanical properties are adjustable over a wide range by changing molecular weight and components of copolymer. However, scaffolds made of PLA or PGA could fail prematurely by a bulk erosion process. In addition, abrupt release of the acidic degradation products can cause a strong inflammatory response [55, 56].

Different factors affect the degradation kinetics of polymers, such as: chemical composition and configurational structure, processing, molar mass (Mw), poly-dispersity (Mw/Mn), environmental conditions, stress and strain, crystallinity, device size, morphology (e.g. porosity), chain orientation, distribution of chemically reactive compounds within the matrix, additives [57, 58], presence of original monomers and overall hydrophilicity. PLGA, for instance, has a wide range of degradation rates, which can be controlled by both hydrophobic/hydrophilic balance and crystallinity. The composition of chains (i.e. contents in L-LA and D-LA and/or GA units) also influences the degradation rate of PLGA polymers. Blends containing the larger amount of PGA have been shown to degrade relatively fast [58]. Poly (e-caprolactone) (PCL) on the other hand, can take several years to degrade in vivo [59, 60].

Crystallinity is another important factor in degradation. In general, the initial degree of crystallinity of polyesters affects the rate of hydrolytic degradation, as the crystal segments are chemically more stable than amorphous segments and reduce water permeation into the matrix. Hydrolysis of amorphous polymers, e.g. PDLLA, is faster due to the lack of crystalline regions. Degradation takes longer with the stereoisomers of the polymer, e.g. PLA composed of L-lactic repeating units takes more than 5 years for total absorption, whereas only about 1 year is needed for amorphous PLA (or PDLLA) [59].

However, biodegradation can also be harmful to bone healing process due to debris and crystalline by-products, as well as particularly acidic degradation products of PLA, PGA, PCL and their copolymers [60, 61]. To remove these side facts and control degradation rate, several groups have incorporated basic compounds to stabilize the pH of the environment surrounding the polymer using bioactive glasses and calcium phosphates [57-59, 62].

I.3 - Calcium phosphate- based materials

Around 60 wt% of human bone is made of a calcium phosphate (CaP) mineral with a chemical composition similar to that of hydroxyapatite (HA - $Ca_{10}(PO_4)_6(OH)_2$). Therefore HA and related CaPs such as octacalcium phosphate, tricalcium phosphate etc. have been extensively used for the purpose of bone graft substitute and bone tissue engineering [63, 64]. Because of their similarity to bone mineral, CaP based materials are biocompatible, osteoconductive and bone-bonding. Various studies illustrated that CaP-based biomaterials can be used as a reasonable alternative to bone grafts [65-69], depending on the relevant properties, such as porosity [70-72], particle size [73, 74], and chemical composition [75-77]. Most CaP based biomaterials are not osteoinductive, unless growth factors such as BMPs, or other osteoinductive substances are added to create a composite graft. Other disadvantages of most CaP based biomaterials include poor mechanical properties such as brittleness and low tensile strength [78, 79].

CaP based biomaterials in bone repair and regeneration are usually ceramics, i.e. materials with ionic bonding between their atoms, with a variety of properties depending on their composition, degree of crystallinity and structure. They exist in the form of bulk or porous (sintered) ceramics, bioglasses, cements and coatings.

I.3.1 - Bulk (sintered) ceramics

Sintered CaP ceramics were the first synthetic materials used in bone repair. Degradation properties of the ceramics are considered an important parameter for their success in bone repair and regeneration. Many different factors are important for the degradation properties of the ceramics, such as thermodynamic solubility (HA<TCP<OCP<DCPD), crystallinity features (crystalline<amorphous), presence of impurities and additives and structural properties (dense<porous). The degradation is also dependent on the external factors, such as pH, temperature, degree of the saturation and concentration of the buffered or unbuffered solutions, and solid/solution ratio [80]. Another factor to consider in the use of CaP ceramics is their porosity. Porosity is needed to allow cell- and blood vessel infiltration, transportation of oxygen and nutrients and ingrowth of bone. The ceramics should therefore possess and open and interconnected porous structure, with a pore size in the range of 150 to 500 μm [81]. However, when the porosity is too high, the mechanical properties, and in particular the compressive strength of the ceramic are negatively influenced. It is therefore imperative to reach a compromise between porosity and mechanical properties, depending on the intended application. The most widely used sintered ceramics are HA, TCP, or the combinations of the two, the so called Biphasic Calcium Phosphate (BCP) ceramics.

Synthetic HA is manufactured as a ceramic through a sintering process. These ceramics can be obtained in block, granular, powder, or putty form. Porous HA is brittle and has poor tensile properties, but its mechanical properties will improve if bone apposition and ingrowth occur. Animal studies have suggested that HA may be osteoinductive, in addition to its osteoconductive capability [75, 82]. Although HA is not soluble at neutral pH, it can be dissolved in the acidic environment created by osteoclasts. This process is often, but not always, coupled with new bone formation. One of the earliest materials for clinical use was ProOsteon (Interpore Cross International, Irvine, CA) [83]. This material is derived from the conversion of the calcium carbonate of sea coral into a highly crystalline HA. ProOsteon was first approved by the US Food and Drug Administration in 1992 for use in filling bony voids, and it has been used to help healing of selected fractures, to augment bone in maxillofacial surgery, and as a graft extender for spinal fusion [84]. Besides ProOsteon, there exist a large number of other HA products, most of which are synthesized by powder precipitation, followed by slurry production and final sintering. TCP ceramics are generally more soluble than HA.. Animal studies have demonstrated that 95% of TCP was degraded in twenty-six to eighty-six weeks of implantation [85, 86]. Degradation rate of BCP can be tailored by HA to TCP ratio.

I.3.2 - Bioglasses

In 1969, Hench et al. discovered that certain glass compositions had excellent biocompatibility as well as bone bonding ability [87]. In general, these bioglasses contain less than 60 mole% SiO_2, have high Na_2O

and CaO content, and a CaO/P ratio similar to that of native bone [88]. After implantation, they develop a carbonated hydroxyapatite (CHA) surface layer that allows chemical bonding to host bone, through interfacial and cell mediated reactions [87, 89-92]. The formation of this bioactive CHA layer can be significantly affected by the bioglass composition [31]. Various reports have shown that bioglasses could support enzyme activity [93], vascularization [94, 95], foster osteoblast adhesion, growth, and differentiation, as well as induction of differentiation of mesenchymal cells into osteoblasts [96-98]. Release of soluble Si, Ca, P and Na ions, due to reactions of body fluids with bioactive ceramics surfaces, has been shown to induce intracellular and extracellular responses [99, 100].

Another significant advantage of bioglasses is the possibility of controlling a range of chemical properties and thus the bioresorption rate. The structure and chemistry of ceramics, especially sol-gel derived glasses [91], can be tailored at a molecular level by varying either composition, or thermal and environmental processing parameters.

However, it was reported that crystallization of bioglasses decreased the level of bioactivity [101] rendering them inert [102]. Another drawback of bioglasses is their low fracture toughness and mechanical strength, especially in a porous form, limiting their use to non load-bearing applications.

I.3.3 - Cements

The concept of developing CaP cement was introduced by LeGeros et.al. and Chow et.al. [103, 104]. The cements consist of solid and liquid components and are produced by mixing one or more calcium orthophosphates with an aqueous solution. The great advantages of the cements above CaP materials in the shape of blocks and granules, are their injectability, ability to custom-fill defects and relatively high compressive strength [66].

Cements are able to set and harden within the body after implantation. The product obtained after the setting of the cement is dependent on the reaction between solid and liquid components. Reports showed that the cements are highly biocompatible and osteoconductive [105, 106]. In addition, CaP cements were shown to be useful as drug carrier whereby the porosity and other microstructural parameters play an important role in the kinetics of drug release [107-109]. An important drawback of cement is that they can be extruded beyond the boundaries of the fracture, potentially damaging the surrounding tissue.

The category of CaP coatings will be discussed in detail in the following section.

II - Coatings and coating methods

In the late 1960s, the concept of biological fixation of load-bearing implants using CaP coatings and bioactive HA was proposed as an alternative to cemented fixation. In 1985, for the first time, HA-coated implants were used for clinical trials by Furlong and Osborn. Since then, it has been reported that HA coating can successfully improve clinical success of total hip arthroplasty to a failure rate of less than 2% after 10 years. For the last forty years, many studies have been carried out on optimization of coating properties for maximum tissue response by adjusting coating process. There are now various

methods available for making calcium phosphate coatings on implants.

II.1 - Plasma spraying methods

Plasma spraying of HA is a common practice used to modify the surfaces of orthopedic and dental implants. Complex thermal changes between the plasma zone, powder particles, and the substrate occur during the process. After injection into the 10,000°C plasma jet, HA particles undergo an extremely strong heating within a few seconds. However, some large particles may remain unmolten because of their short stay in the plasma zone. Various studies have shown that both amorphous calcium phosphates and crystalline HA are present in the plasma-sprayed coatings. The Ca/P ratio of the coating is lower than that of the starting HA powder, possibly due to the high sintering temperature [110]. Because of the relatively short duration of high temperatures, crystallization of the particles can be incomplete, explaining the presence of the amorphous calcium phosphates [111].

Due to the spraying process, plasma-sprayed coatings exhibit some poor characteristics, including failure within the coating, discontinued dissolution of the coating after implantation, variation in bond strength between the coatings and metallic substrate, non-uniformity in coating density, poor adhesion between the coatings and substrates, micro cracks on the coating surface [112], and poor resistance to delamination [113].

II.2 - Sol-gel coating methods

A number of studies reported the coating of titanium surfaces with HA by the so called sol-gel coating process [114-116]. In this method, Ca-P coatings are prepared by soaking the substrate into calcium (nitrate salt usually) and phosphorus gels. The sol-gel coatings are porous, allowing the circulation of physiological fluids to provide nutrients upon implantation [115]. However, poor adhesion is a serious drawback. Therefore, sintering process at high temperatures was used to improve their density and adhesion. Depending on the sintering temperatures, different calcium phosphates were obtained [116]. Although HA phase is favorable, presence of TCP can be advantageous to increase the biodegradability of the coating [116]. Despite extensive research, sol-gel coatings are not widely used due to the long process time and post-sintering requirements.

II.3 - Laser methods

HA, amorphous calcium phosphate, and β-TCP can be applied onto the surface of titanium and its alloys by pulsed laser deposition (PLD) methods [117-121]. Inside a vacuum chamber, a pulsed laser beam is focused onto a rotating HA target. Upon ejection from each laser pulse releases the species form the coating as soon as they reach the heated substrate. HA coatings with different compositions and crystallinity can be produced, depending on the starting material and process parameters. Laser-deposited coatings are generally thin and exhibit therefore high fatigue resistance. Both the amorphous and crystalline HA coatings adhere well to the substrates, without delamination.

As amorphous and low crystalline HA dissolve fast under physiological conditions, increase of the crys-
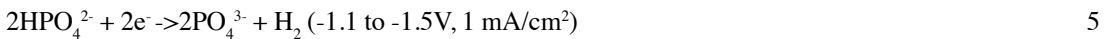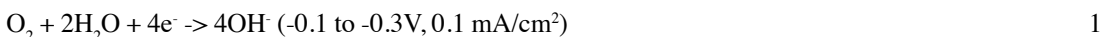
tallinity of laser-deposited coatings is sometimes needed. Because of the high cost of the equipment, the PLD method is not widely used for coating orthopaedic implants.

II.4 - RF sputtering methods

Calcium phosphate coating can be prepared by rf-magnetron sputtering from calcium phosphate glass targets followed by post-annealing. These sputtering methods can be used to produce thin coatings with strong adhesion and compact microstructure [110]. For example, thin apatite films can be formed on the surface of the substrate by rf-magnetron sputtering using calcium phosphate glass with a Ca/P ratio of 0.6 to 0.75; however; when the ratio is changed to 0.25 - 0.65, tri-calcium and pyro-calcium phosphate films will be formed. RF-sputtered Ca-P coatings have shown a pronounced dissolution rate as compared to heat-treated Ca-P coatings due to a more amorphous structure [122]. Studies reported a good bonding strength to substrate and satisfying initial osteointegration rate and it was suggested that their bioactivity is related to their degradation behavior [122]. In addition, it was suggested that once early osteointegration is achieved, biodegradation of the thin Ca-P coatings is not detrimental to bone-coating-implant fixation and does not compromise bone responses to the coated implant surfaces [123]. Sputtering methods are not currently used as a commercial deposition process, but they may potentially become a valuable way of coating orthopaedic and maxillo-facial implants.

II.5 - Electrochemical cathodic deposition methods

Under the ambient temperature, cathodic deposition of CaP coating results in good conformability to the shape of the substrate [124]. The process is comprised of two steps: in the first step, a CaP precursor is formed on the surface, and in the second, this CaP precursor is converted to HA [125]. Cathodic reactions under these conditions (potential range of -0.1 to 3 V vs. Ag/AgCl; bath pH 4.76) are as follows [126]:

$$O_2 + 2H_2O + 4e^- \to 4OH^- \text{ (-0.1 to -0.3V, 0.1 mA/cm}^2) \tag{1}$$

$$H_2PO_4^- + H_2O + 2e^- \to H_2PO_3^- + 2OH^- \tag{2}$$

$$2H^+ + 2e^- \to H_2 \text{ (-0.3 to -1.1V, 0.3 mA/cm}^2) \tag{3}$$

$$2H_2PO_4^- + 2e^- \to 2HPO_4^{2-} + H_2 \tag{4}$$

$$2HPO_4^{2-} + 2e^- \to 2PO_4^{3-} + H_2 \text{ (-1.1 to -1.5V, 1 mA/cm}^2) \tag{5}$$

$$2H_2O + 2e^- \to H_2 + 2OH^- \text{ (-1.5 to -3V, 3 mA/cm}^2) \tag{6}$$

With the assistance of an electric field, positive calcium ions migrate to the cathode and further react with PO_4^{3-} and OH^- to form a calcium phosphate layer. If alkalization at the cathode is insufficient, Dicalcium Phosphate Dihydrate (DCPD) is formed, which can be converted to HA by further cathodic deposition or by hydrothermal treatment. If sufficient alkalization is produced by reactions 1, 2 and 6, then HA coating is formed directly.

II.6 - Electrophoretic deposition methods

In this method, coating process occurs upon migration of charged particles under the electric field. Deposition relies on the coagulation of particles to a dense mass. In order for coating to be formed, the
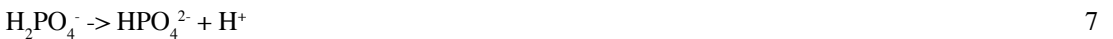
particles have to be small enough to remain in suspension in the liquid medium, which should be dielectric constant [127]. Coatings with various thicknesses can be formed by altering the voltage applied during the process. A constant voltage applied during the process results in coatings with high bonding strength and porous structure. When low voltages (20 V) are applied, deposition of small HA particles has been reported [128]. In contrast, the application of higher voltages (200 V) for periods longer than 10s, has been shown to result in larger HA particles with a more porous microstructure [129]. Electrophoretic deposition is simple, cost efficient and applicable to substrates with geometrically complex and porous shapes. A disadvantage is the need for post-coating sintering at about 800°C to increase coating crystallinity and bonding strength.

II.7 - Biomimetic coating methods

Biomimetic coating method is based on immersion of substrates in aqueous solutions that resemble mineral composition of human blood plasma, the so called Simulated Body Fluid (SBF). A brief summary of classical SBF preparation was given by Cho et al. [130]. The ion concentrations of SBF and related solutions are given in Table 1. The pH of SBF is typically adjusted to 7.25 at 36.5°C. Sometimes, the pH of the SBF is adjusted to 7.40, if the apatite-forming ability of the substrate is not very high. The method has undergone improvement and refinement by several groups of investigators [131-136]. In the present thesis, for example, supersaturated SBF was used to increase the rate of the coating process. The process with supersaturated SBF consists of two steps. In the first step, the substrate is immersed in supersaturated SBF that is five times more concentrated than the classical solution [Table 1]. The supersaturation of the solution is obtained by bubbling mildly acidic carbon-dioxide gas into the solution, to decrease its pH. Upon immersion, the coating process is initiated by the slow increase of pH achieved by the release of the CO2 gas from the solution. The first step of the process results in the formation of a thin (<3 μm), dense and amorphous CaP layer. This amorphous layer serves as a seeding substratum for the subsequent growth of a crystalline layer that is formed in the second step of the process, in a similar supersaturated SBF, but with decreased amounts of magnesium and carbonate ions, the known inhibitors of crystal formation [Table 1] [137-139].

The chemical reactions involved in the process are as follows:

$$H_2PO_4^- \rightarrow HPO_4^{2-} + H^+ \tag{7}$$

$$HPO_4^{2-} \rightarrow PO_4^{3-} + H^+ \tag{8}$$

$$H^+ + HCO_3^- \rightarrow H_2O + CO_2 \tag{9}$$

$$10Ca^{2+} + 6PO_4^{3-} + 2OH^- \rightarrow Ca_{10}(PO_4)_6(OH)_2 \tag{10}$$

$$Ca^{2+} + HPO_4^{2-} + 2H_2O \rightarrow CaHPO_4 \cdot 2H_2O \tag{11}$$

The first and second reactions release hydrogen ions into the solution. The third reaction increases the pH of the solution by consuming the H^+ ions released from the first two reactions. The consumption of hydroxide ions, shown in Eq. 10, is responsible for the drop of pH value in the solutions. $NaHCO_3$ elevates the pH of the solution gradually and thus leads to high Ca^{2+} supersaturation level in the solution.

Table 1 Inorganic ion composition (mmol/L) of coating solutions						
Solutions	**Na$^+$**	**Ca^{2+}**	**Cl$^-$**	**HPO$_4^{2-}$**	**Mg^{2+}**	**HCO$_3^-$**
SBF^a	142.0	2.5	147.8	1.0	1.5	4.2
SBFx5^b	733.0	12.5	720.0	5.0	7.5	21.0
SBFx5^c	702.0	12.5	714.5	5.0	2.5	10.0

[a] Simulated Body Fluid
[b] SBFx5 biomimetic coating solution which is used in step 1
[c] SBFx5m biomimetic coating solution which is used in step 2

The biomimetic method, that takes place at near-physiological pH and low temperatures, is simple to perform, cost-effective and may be applied to heat-sensitive, nonconductive and porous materials of large dimensions and with complex surface geometries [134, 140-143]. The biomimetic method is particularly attractive because it offers possibilities for incorporation of a variety of molecules into the coating, such as proteins [134, 144], which can change the coating properties and improve their in vivo behavior

III - New developments in bone regeneration strategies

Synthetic implants and bone graft substitutes are steadily improving; however, in most applications, their performance is still inferior to that of autograft and biological growth factors. In order to form a more comprehensive alternative to autograft, synthetic biomaterials are often combined with cells and/ or growth factors to form tissue engineered constructs.

III.1 - Cell-based approaches

In the process of natural bone growth, cells play a crucial and irreplaceable role and a cell-based approach to bone regeneration strategies is a logical one. To be used in tissue engineering constructs, cells require a reliable source as well as the ability to expand, and create new tissue. Regarding the cell source, osteoblasts, i.e. bone-forming cells would be a logical choice. However, the source of patient's own osteoblasts is limited and, as mature cell, osteoblasts have a low proliferation potential. Osteoblasts derived from a human- or animal donor present important drawbacks related to the risk of immune response, disease transmission, etc [145, 146]. As an alternative to mature, differentiated cells, the use of stem cells has gained much attention in bone tissue engineering approaches.

Stem cells are defined as undifferentiated cells capable of self-renewal that can differentiate into more than one specialized cell type [147]. In other words, stem cells possess two important properties: 1) Self-renewal: the ability to go through numerous cycles of cell division while maintaining the undifferentiated state; 2) Potency: the capacity to differentiate into specialized cell types. In the strictest sense, this requires stem cells to be either totipotent (e.g. early mammalian embryo) or pluripotent (e.g. embryonic stem cells) to be able to give rise to any mature cell type, although multipotent (e.g. mesenchymal stem cells) or unipotent (e.g. epidermal stem cells) progenitor cells are commonly also referred to as stem cells [148].

It is because of the superb proliferation ability as well as the ability of differentiation down the osteogenic differentiation pathway and bone formation that stem cells are perceived as the most potential cell type to improve the performance of tissue engineering strategy. Two types of stem cells are under investigation, embryonic stem cells (ESCs) and adult stem cells.

ESCs are pluripotent, which means they are able to differentiate into all derivatives of the three primary germ layers: ectoderm, endoderm, and mesoderm. ESCs are derived from the inner cell mass of an early stage embryo known as a blastocyst. When cultured with the leukaemia inhibitory factor (LIF) or with a feeder layer of murine embryonic fibroblasts, ESCs remain undifferentiated [149]. When cultured with other specific media and growth factors, ESCs can be differentiated into all derivatives of the primary germ layers. Many studies reported that ESCs can be differentiated into cardiomyocytes, endothelial cells, neurons, chondrocytes etc [150-156]. Buttery and colleagues reported differentiation of ESCs into the osteogenic lineage when cultured in presence of dexamethasone [157]. Although ESCs have many advantages as compared to other cell types, practical and ethical concerns currently restrict the depth of the researches and potential applications of ESCs.

Adult stem cells from a number of different sources have also found their application in bone tissue engineering, bone marrow being the most explored one. Over 100 years ago, Cohnheim found that there was a nonhematopoietic cell type located in the adult bone marrow [158]. The evidence followed that these cells possess the potential to form osseous tissue upon implantation under the renal capsule as well as the ability to differentiate into different cell types, including osteoblasts [159]. These cells were finally named Mesenchymal Stem Cells in 1991 [160].

Besides their differentiation potential, MSCs present other important properties. As described by Bruder [161], they can be extensively expanded in vitro. Pittinger [162] also showed that, with an increased number of passages, they do not spontaneously differentiate. Furthermore, it was demonstrated that these cells may possess immunosuppressive effects which may render them either ''immune privileged'' or perhaps immunosuppressive in vivo, making them suitable for allogeneic or xenogeneic transplantation [163].

In vivo, bone formation and maturation were shown after ectopic implantation of ceramic scaffolds with rat bone marrow derived stem cells [164, 165]. In addition, the constructs of bioactive materials and the in vitro expanded MSC were tested in critical-sized bone defects in a number of animal models [166-168]. Ohgushi and colleagues showed that 8 mm defects of rat long bones can be restored using porous ceramics seeded with expanded MSCs [168]. The number of studies in which tissue engineered constructs based on MSCs were tested in clinically-relevant defects, such as segmental femur defects in large animal models is more limited [169-171]. Successful bone formation has been reported in skull and mandibular defects in sheep, and in iliac wing defects in goats [172-174].

Clinically, MSCs have been used to optimize bone structure and function in children with osteogenesis imperfecta [175, 176] which resulted in improved growth velocities, homing of mesenchymal stem cells in bone as well as the production of normal collagen by transplanted MSCs. For the repair of large bone defects, autologous MSCs were mixed with hydroxyapatite scaffolds [177].

Other sources of adult stem cells under current investigation for use in bone tissue engineering include muscle-, adipose tissue and peripheral blood-derived stem cells [178-180].

III.2 - Growth factor-based approaches

A number of proteins, also known as growth factors, have been shown to stimulate proliferation and/or differentiation of osteogenic cells in vitro and in vivo, such as bone morphogenetic proteins (BMPs) and other members of the transforming growth factor β (TGFs-β) family, fibroblast growth factors (FGFs), plateled-derived growth factors (PDGFs) and insuline derived growth factors (IGFs). Some of them have been produced by gene techniques and are commercially available as recombinant proteins. In vitro studies have shown that these proteins can regulate the proliferation and differentiation of stem cells into the osteoblastic lineage and in vivo studies have demonstrated that some of them can improve bone healing process and lead to new bone formation. BMPs for example are highly potent osteoinductive factors. A large number of studies has shown that application of BMPs can indeed lead to successful bone formation in various applications, such as spinal fusion, long bone defects, mandibular and cranial bone defects, fracture healing, as well as in periodontal regeneration, alveolar ridge augmentation and osteointegration of dental implants [181]. In addition, various preclinical and clinical studies have been performed, showing a beneficial effect of BMPs in nonunions and segmental defects, like traumatic tibial defect [182, 183] and femoral defects [184].

IV - Objectives of the present thesis

Although cell- and growth factor based approaches are steadily becoming a comprehensive alternative to patients' own bone graft in repair and regeneration of osseous defects, their use is logistically rather complex and often associated with high costs. This explains the attractiveness of fully synthetic alternatives to autograft, that are readily available in large quantities, easy to produce and store and relatively inexpensive. The aim of the present thesis was to explore the possibilities to improve the biological performance of the existing biomaterials in bone repair and regeneration, without the use of cells and growth factors. Calcium-phosphate coatings were thereby used as the model biomaterial. As an alternative to cells and growth factors, plasmid DNA and trace elements were investigated. Furthermore, CaP coatings were combined with natural and synthetic polymers in an attempt to develop a mechanically suitable yet bioactive bone graft substitute.

The first part of the thesis is dedicated to finding a proper system to introduce different molecules into CaP coatings and evaluating their biological effect. In Chapter 2, a literature review is given on the role of selected trace elements in general, and in bone metabolism in particular. Different methods to incorporate some of these elements into CaP ceramics and their effect on ceramic properties and processes related to bone formation and remodeling are also reviewed. Chapter 3 investigates the possibility of co-depositing lithium into CaP coatings by biomimetic and electrodeposition process. Chapters 4 and 5 explore the possibility of co-precipitating a number of trace elements into biomimetic CaP coatings using a medium-throughput protocol. Chapter 6 describes an attempt to co-precipitate plasmid DNA

into the CaP coatings using a biomimetic method. The second part of the thesis describes the studies in which CaP coatings were combined with other biomaterials in order to obtain a more suitable bone graft substitute for clinical applications. Chapter 7 explores the mechanism of biomineralization of a novel recombinant spider silk in biomimetic coating solutions and evaluates the characteristics of the silk/CaP coating construct. In Chapter 8, the possibilities of coating electrospun polymers with CaPs were explored. Finally, in the last chapter, the results of the thesis are discussed.

References:

1.   Dawson, J.I. and R.O. Oreffo, Bridging the regeneration gap: stem cells, biomaterials and clinical translation in bone tissue engineering. Arch Biochem Biophys, 2008. 473(2): p. 124-31.

2.   Betz, V.M., et al., Bone tissue engineering and repair by gene therapy. Front Biosci, 2008. 13: p. 833-41.

3.   Hardouin, P., et al., Tissue engineering and skeletal diseases. Joint Bone Spine, 2000. 67(5): p. 419-24.

4.   Braddock, M., et al., Born again bone: tissue engineering for bone repair. News Physiol Sci, 2001. 16: p. 208-13.

5.   Wang, M., Developing bioactive composite materials for tissue replacement. Biomaterials, 2003. 24(13): p. 2133-51.

6.   Bobyn, J.D., et al., Characteristics of bone ingrowth and interface mechanics of a new porous tantalum biomaterial. J Bone Joint Surg Br, 1999. 81(5): p. 907-14.

7.   Jacobs, J.J., et al., Metal degradation products: a cause for concern in metal-metal bearings? Clin Orthop Relat Res, 2003(417): p. 139-47.

8.   Jacobs, J.J., J.L. Gilbert, and R.M. Urban, Corrosion of metal orthopaedic implants. J Bone Joint Surg Am, 1998. 80(2): p. 268-82.

9.   Vermes, C., et al., The potential role of the osteoblast in the development of periprosthetic osteolysis: review of in vitro osteoblast responses to wear debris, corrosion products, and cytokines and growth factors. J Arthroplasty, 2001. 16(8 Suppl 1): p. 95-100.

10.   Puleo, D.A. and W.W. Huh, Acute toxicity of metal ions in cultures of osteogenic cells derived from bone marrow stromal cells. J Appl Biomater, 1995. 6(2): p. 109-16.

11.   Lhotka, C., et al., Four-year study of cobalt and chromium blood levels in patients managed with two different metal-on-metal total hip replacements. J Orthop Res, 2003. 21(2): p. 189-95.

12.   Jacobs, J.J., et al., Metal release in patients who have had a primary total hip arthroplasty. A prospective, controlled, longitudinal study. J Bone Joint Surg Am, 1998. 80(10): p. 1447-58.

13.   Goodman, S.B., et al., Effects of orthopaedic wear particles on osteoprogenitor cells. Biomaterials, 2006. 27(36): p. 6096-101.

14.   Kato, H., et al., Bonding of alkali- and heat-treated tantalum implants to bone. J Biomed Mater Res, 2000. 53(1): p. 28-35.

15.   Bermude, M.D., et al., Erosion-corrosion of stainless steels, titanium, tantalum and zirconium.

Wear, 2005(258): p. 693-700.

16.   DeGarmo, P.E., Materials and processes in manufacturing. 5th ed ed. 1979, New York: Collin Macmillan.

17.   Slinde, F., et al., Individual dietary intervention in patients with COPD during multidisciplinary rehabilitation. Respir Med, 2002. 96(5): p. 330-6.

18.   Saris, N.E., et al., Magnesium. An update on physiological, clinical and analytical aspects. Clin Chim Acta, 2000. 294(1-2): p. 1-26.

19.   Okuma, T., Magnesium and bone strength. Nutrition, 2001. 17(7-8): p. 679-80.

20.   Vormann, J., Magnesium: nutrition and metabolism. Mol Aspects Med, 2003. 24(1-3): p. 27-37.

21.   Wolf, F.I. and A. Cittadini, Chemistry and biochemistry of magnesium. Mol Aspects Med, 2003. 24(1-3): p. 3-9.

22.   Hartwig, A., Role of magnesium in genomic stability. Mutat Res, 2001. 475(1-2): p. 113-21.

23.   Revell, P.A., et al., The effect of mangesium ions on bone bonding to hydroxyapatite. Key Eng Mater, 2004: p. 447-450.

24.   Zreiqat, H., et al., Mechanisms of magnesium-stimulated adhesion of osteoblastic cells to commonly used orthopaedic implants. J Biomed Mater Res, 2002. 62(2): p. 175-84.

25.   Yamasaki, Y., et al., Synthesis of functionally graded MgCO3 apatite accelerating osteoblast adhesion. J Biomed Mater Res, 2002. 62(1): p. 99-105.

26.   Yamasaki, Y., et al., Action of FGMgCO3Ap-collagen composite in promoting bone formation. Biomaterials, 2003. 24(27): p. 4913-20.

27.   Witte, F., et al., In vivo corrosion of four magnesium alloys and the associated bone response. Biomaterials, 2005. 26(17): p. 3557-63.

28.   Wen, C.E., et al., Processing of biocompatible prous Ti and Mg. Scripta Mater, 2001. 45: p. 1147-1153.

29.   Kokubo, T., et al., Bioactive metals: preparation and properties. J Mater Sci Mater Med, 2004. 15(2): p. 99-107.

30.   Granchi, D., et al., Cytokine release in mononuclear cells of patients with Co-Cr hip prosthesis. Biomaterials, 1999. 20(12): p. 1079-86.

31.   Glowacki, J., M. Jasty, and S. Goldring, Comparison of multinucleated cells elicited in rats by particulate bone, polyethylene, or polymethylmethacrylate. J Bone Miner Res, 1986. 1(4): p. 327-31.

32.   Athanasiou, K.A., et al., Orthopaedic applications for PLA-PGA biodegradable polymers. Arthroscopy, 1998. 14(7): p. 726-37.

33.   Reis, R.L., et al., Mechanical behavior of injection-molded starch-based polymers. Polym Adv Technol, 1996(7): p. 784-790.

34.   Di Martino, A., M. Sittinger, and M.V. Risbud, Chitosan: a versatile biopolymer for orthopaedic tissue-engineering. Biomaterials, 2005. 26(30): p. 5983-90.

35.   Lee, S.B., et al., Study of gelatin-containing artificial skin V: fabrication of gelatin scaffolds using a salt-leaching method. Biomaterials, 2005. 26(14): p. 1961-8.

36.   Mohanty, A.K., M. Misra, and G. Hinrichsen, Biofibres, biodegradable polymers and biocomposites: an overview. Macromol Mater Eng, 2000: p. 1-24.

37.   Horton, C.E., et al., Vicryl synthetic absorbable sutures. Am Surg, 1974. 40(12): p. 729-31.

38.   Salthouse, T.N., Biologic response to sutures. Otolaryngol Head Neck Surg, 1980. 88(6): p. 658-64.

39.   Viljanen, V.V. and T.S. Lindholm, Background of the early development of absorbable fixation devices. Tech Ortho, 1998. 13: p. 117-122.

40.   Chen, G.Q. and Q. Wu, The application of polyhydroxyalkanoates as tissue engineering materials. Biomaterials, 2005. 26(33): p. 6565-78.

41.   Middleton, J.C. and A.J. Tipton, Synthetic biodegradable polymers as orthopedic devices. Biomaterials, 2000. 21(23): p. 2335-46.

42.   Gunatillake, P.A. and R. Adhikari, Biodegradable synthetic polymers for tissue engineering. Eur Cell Mater, 2003. 5: p. 1-16; discussion 16.

43.   Ishaug, S.L., et al., Osteoblast function on synthetic biodegradable polymers. J Biomed Mater Res, 1994. 28(12): p. 1445-53.

44.   Eppley, B.L. and C.D. Prevel, Nonmetallic fixation in traumatic midfacial fractures. J Craniofac Surg, 1997. 8(2): p. 103-9.

45.   Kumar, A.V., et al., Bioabsorbable plates and screws in pediatric craniofacial surgery: a review of 22 cases. J Craniofac Surg, 1997. 8(2): p. 97-9.

46.   Weisberger, E.C. and B.L. Eppley, Resorbable fixation plates in head and neck surgery. Laryngoscope, 1997. 107(6): p. 716-9.

47.   Bostman, O., et al., Absorbable polyglycolide pins in internal fixation of fractures in children. J Pediatr Orthop, 1993. 13(2): p. 242-5.

48.   Bucholz, R.W., S. Henry, and M.B. Henley, Fixation with bioabsorbable screws for the treatment of fractures of the ankle. J Bone Joint Surg Am, 1994. 76(3): p. 319-24.

49.   Burns, A.E., Biofix fixation techniques and results in foot surgery. J Foot Ankle Surg, 1995. 34(3): p. 276-82.

50.   Hope, P.G., et al., Biodegradable pin fixation of elbow fractures in children. A randomised trial. J Bone Joint Surg Br, 1991. 73(6): p. 965-8.

51.   Kieswetter, K., Z. Schwartz, and G.G. Niederauer, Segmental defect repair with biodegradable tissue scaffolds. Trans Orthoped Res Soc, 1998.

52.   Mano, J.F., et al., Bioinert, biodegradable and injectable polymeric matrix composites for hard tissue replacement: state of the art and recent developments. Compos Sci Technol, 2004. 64: p. 789-817.

53.   Kohn, J.R.L., Bioresorbable and bioerodible materials, in Biomaterials science: an introduction to materials in medicine, B.D. Ratner, A.S. Hoffman, and F.J. Schoen, Editors. 1996, Academic Press: New York. p. 64-72.

54.   Jagur-Grodzinski, J., Biomedical application of functional polymers. Reactive Funct Polym, 1999. 39: p. 99-138.

55.   Martin, C., H. Winet, and J.Y. Bao, Acidity near eroding polylactide-polyglycolide in vitro and in vivo in rabbit tibial bone chambers. Biomaterials, 1996. 17(24): p. 2373-80.

56.   Bergsma, E.J., et al., Foreign body reaction to resorbable poly(L-lactic) bone plates and screws used for the fixation of unstable zygomatic fractures. J Oral Maxillofac Surg, 1993. 51: p. 666-670.

57.   Heidemann, W., et al., Degradation of poly(D,L)lactide implants with or without addition of calciumphosphates in vivo. Biomaterials, 2001. 22(17): p. 2371-81.

58.   Dunn, A.S., P.G. Campbell, and K.G. Marra, The influence of polymer blend composition on the degradation of polymer/hydroxyapatite biomaterials. J Mater Sci Mater Med, 2001. 12(8): p. 673-7.

59.   Rich, J., et al., In vitro evaluation of poly(epsilon-caprolactone-co-DL-lactide)/ bioactive glass composites. Biomaterials, 2002. 23(10): p. 2143-50.

60.   Yang, S., et al., The design of scaffolds for use in tissue engineering. Part I. Traditional factors. Tissue Eng, 2001. 7(6): p. 679-89.

61.   Niiranen, H., et al., In vitro and in vivo behavior of self-reinforced bioabsorbable polymer and self-reinforced bioabsorbable polymer/bioactive glass composites. J Biomed Mater Res A, 2004. 69(4): p. 699-708.

62.   Boccaccini, A.R. and V. Maquet, Bioresorbable and bioactive polymer/Bioglass(R) composites with tailored pore structure for tissue engineering applications. Compos Sci Technol, 2003. 63: p. 2417-2429.

63.   Hench, L.L. and J. Wilson, An introduction to bioceramics. 2nd ed. ed. 1999, London: Word Scientific.

64.   Yamamuro, T., L.L. Hench, and J. Wilson, Handbook of bioactive ceramics. 1990., Boca Raton, FL: CRC Press.

65.   Friedman, C.D., et al., BoneSource hydroxyapatite cement: a novel biomaterial for craniofacial skeletal tissue engineering and reconstruction. J Biomed Mater Res, 1998. 43(4): p. 428-32.

66.   Larsson, S. and T.W. Bauer, Use of injectable calcium phosphate cement for fracture fixation: a review. Clin Orthop Relat Res, 2002(395): p. 23-32.

67.   Lee, Y.M., et al., Tissue-engineered growth of bone by marrow cell transplantation using porous calcium metaphosphate matrices. J Biomed Mater Res, 2001. 54(2): p. 216-23.

68.   Manjubala, I., T.P. Sastry, and R.V. Kumar, Bone in-growth induced by biphasic calcium phosphate ceramic in femoral defect of dogs. J Biomater Appl, 2005. 19(4): p. 341-60.

69.   Suzuki, O., et al., Bone formation enhanced by implanted octacalcium phosphate involving conversion into Ca-deficient hydroxyapatite. Biomaterials, 2006. 27(13): p. 2671-81.

70.   del Real, R.P., et al., In vivo bone response to porous calcium phosphate cement. J Biomed Mater Res A, 2003. 65(1): p. 30-6.

71.   Galois, L. and D. Mainard, Bone ingrowth into two porous ceramics with different pore sizes: an experimental study. Acta Orthop Belg, 2004. 70(6): p. 598-603.

72.   Gauthier, O., et al., Macroporous biphasic calcium phosphate ceramics: influence of macropore diameter and macroporosity percentage on bone ingrowth. Biomaterials, 1998. 19(1-3): p. 133-9.

73.   Balasundaram, G., M. Sato, and T.J. Webster, Using hydroxyapatite nanoparticles and decreased crystallinity to promote osteoblast adhesion similar to functionalizing with RGD. Biomaterials, 2006. 27(14): p. 2798-805.

74.   Moon, H.J., et al., Effect of calcium phosphate glass on bone formation in calvarial defects of Sprague-Dawley rats. J Mater Sci Mater Med, 2006. 17(9): p. 807-13.

75.   Gosain, A.K., et al., A 1-year study of osteoinduction in hydroxyapatite-derived biomaterials in an adult sheep model: part I. Plast Reconstr Surg, 2002. 109(2): p. 619-30.

76.   Manjubala, I., et al., Bioactivity and osseointegration study of calcium phosphate ceramic of different chemical composition. J Biomed Mater Res, 2002. 63(2): p. 200-8.

77.   Pekkarinen, T., et al., The effect of different mineral frames on ectopic bone formation in mouse hind leg muscles induced by native reindeer bone morphogenetic protein. Arch Orthop Trauma Surg, 2005. 125(1): p. 10-5.

78.   Xu, H.H., et al., Injectable and macroporous calcium phosphate cement scaffold. Biomaterials, 2006. 27(24): p. 4279-87.

79.   Zhang, Y., et al., In-situ hardening hydroxyapatite-based scaffold for bone repair. J Mater Sci Mater Med, 2006. 17(5): p. 437-45.

80.   Barrere, F., et al., degradation of bioceramics, in Tissue engineering. 2008, Elsevier. p. 223-254.

81.   Flatley, T.J., K.L. Lynch, and M. Benson, Tissue response to implants of calcium phosphate ceramic in the rabbit spine. Clin Orthop Relat Res, 1983(179): p. 246-52.

82.   Ripamonti, U., Osteoinduction in porous hydroxyapatite implanted in heterotopic sites of different animal models. Biomaterials, 1996. 17(1): p. 31-5.

83.   Holmes, R.E., R.W. Bucholz, and V. Mooney, Porous hydroxyapatite as a bone-graft substitute in metaphyseal defects. A histometric study. J Bone Joint Surg Am, 1986. 68(6): p. 904-11.

84.   Bucholz, R.W., A. Carlton, and R. Holmes, Interporous hydroxyapatite as a bone graft substitute in tibial plateau fractures. Clin Orthop Relat Res, 1989(240): p. 53-62.

85.   Knaack, D., et al., Resorbable calcium phosphate bone substitute. J Biomed Mater Res, 1998. 43(4): p. 399-409.

86.   Wiltfang, J., et al., Degradation characteristics of alpha and beta tri-calcium-phosphate (TCP) in minipigs. J Biomed Mater Res, 2002. 63(2): p. 115-21.

87.   Hench, L.L., R.J. Splinter, and W.C. Allen, Bonding mechanisms at the interface of ceramic prosthetic materials. J Biomed Mater Res Symp, 1971. 2: p. 117-141.

88.   Hench, L.L., Bioactive Bone Substitutes, in Bone Grafts and Bone Graft Substitutes. , M.B. Habal and A.H. Reddi, Editors. 1992 WB Saunders. : Philadelphia:. p. 263-275.

89.   Hench, L.L., Bioactive glasses and glasses-ceramics, in Bioceramics -applications of ceramic and glass materials in medicine, J.F. Shackelford, Editor. 1999, Trans Tech Publication: Switzerland. p. 37-64.

90.   Hench, L.L. and J. Wilson, eds. An introduction to bioceramics. 2nd ed. ed. 1999, Word Scientific: London.

91.   Pereira, M.M., A.E. Clark, and L.L. Hench, Calcium phosphate formation on sol-gel-derived bioactive glasses in vitro. J Biomed Mater Res, 1994. 28(6): p. 693-8.

92.   Wilson, J., et al., Toxicology and biocompatibility of bioglasses. J Biomed Mater Res, 1981. 15(6): p. 805-17.

93.   Ohgushi, H., et al., Osteogenic differentiation of cultured marrow stromal stem cells on the surface of bioactive glass ceramics. J Biomed Mater Res, 1996. 32(3): p. 341-8.

94.   Day, R.M., et al., Assessment of polyglycolic acid mesh and bioactive glass for soft-tissue engineering scaffolds. Biomaterials, 2004. 25(27): p. 5857-66.

95.   Keshaw, H., A. Forbes, and R.M. Day, Release of angiogenic growth factors from cells encapsulated in alginate beads with bioactive glass. Biomaterials, 2005. 26(19): p. 4171-9.

96.   Gatti, A.M., G. Valdre, and O.H. Andersson, Analysis of the in vivo reactions of a bioactive glass in soft and hard tissue. Biomaterials, 1994. 15(3): p. 208-12.

97.   Lu, H.H., et al., Compositional effects on the formation of a calcium phosphate layer and the response of osteoblast-like cells on polymer-bioactive glass composites. Biomaterials, 2005. 26(32): p. 6323-34.

98.   Roether, J.A., et al., Novel bioresorbable and bioactive composites based on bioactive glass and polylactide foams for bone tissue engineering. J Mater Sci Mater Med, 2002. 13(12): p. 1207-14.

99.   Xynos, I.D., et al., Ionic products of bioactive glass dissolution increase proliferation of human osteoblasts and induce insulin-like growth factor II mRNA expression and protein synthesis. Biochem Biophys Res Commun, 2000. 276(2): p. 461-5.

100.   Xynos, I.D., et al., Gene-expression profiling of human osteoblasts following treatment with the ionic products of Bioglass 45S5 dissolution. J Biomed Mater Res, 2001. 55(2): p. 151-7.

101.   Peitl Filho, O., G.P. LaTorre, and L.L. Hench, Effect of crystallization on apatite-layer formation of bioactive glass 45S5. J Biomed Mater Res, 1996. 30(4): p. 509-14.

102.   Li, P., F. Zhang, and T. Kokubo, The effect of residual glassy phase in a bioactive glass-ceramic on the formation of its surface apatite layer in vitro. J Mater Sci: Mater Med 1992: p. 452–456.

103.   Chohayeb, A.A., L.C. Chow, and P.J. Tsaknis, Evaluation of calcium phosphate as a root canal sealer-filler material. J Endod, 1987 13(8): p. 384-7.

104.   LeGeros, R.Z., Calcium phosphate materials in restorative dentistry: a review. Adv Dent Res. , 1988 2(1): p. 164-80.

105.   Jansen, J., et al., Injectable calcium phosphate cement for bone repair and implant fixation. Orthop Clin North Am, 2005. 36(1): p. 89-95, vii.

106.   Le Nihouannen, D., et al., The use of RANKL-coated brushite cement to stimulate bone remodelling. Biomaterials, 2008. 29(22): p. 3253-9.

107.   Hofmann, M.P., et al., High-strength resorbable brushite bone cement with controlled drug-releasing capabilities. Acta Biomater, 2009. 5(1): p. 43-9.

108.   Xu, H.H., M.D. Weir, and C.G. Simon, Injectable and strong nano-apatite scaffolds for cell/growth factor delivery and bone regeneration. Dent Mater, 2008. 24(9): p. 1212-22.

109.   Blom, E.J., et al., Transforming growth factor-beta1 incorporation in a calcium phosphate bone cement: material properties and release characteristics. J Biomed Mater Res, 2002. 59(2): p. 265-72.

110.   Massaro, C., et al., Surface and biological evaluation of hydroxyapatite-based coatings on titanium deposited by different techniques. J Biomed Mater Res, 2001. 58(6): p. 651-7.

111.   Khor, K.A., et al., Microstructure investigation of plasma sprayed HA/Ti6Al4V composites by TEM. Mater Sci Eng A 2000. 281: p. 221-228.

112.   Zhu, X., et al., Characterization of hydrothermally treated anodic oxides containing Ca and P on titanium. J Mater Sci Mater Med, 2003. 14(7): p. 629-34.

113.   Willmann, G., Coating of implants with hydroxyapatite materials connections between bone and metals. Adv Eng Mater, 1999. 1: p. 95-105.

114.   Kim, H.W., et al., Hydroxyapatite coating on titanium substrate with titania buffer layer processed by sol-gel method. Biomaterials, 2004. 25(13): p. 2533-8.

115.   Liu, D.M., T. Troczynski, and W.J. Tseng, Water-based sol-gel synthesis of hydroxyapatite: process development. Biomaterials, 2001. 22(13): p. 1721-30.

116.   Thian, E.S., et al., Processing of HA-coated Ti-6Al-4V by a ceramic slurry approach: an in vitro study. Biomaterials, 2001. 22(11): p. 1225-32.

117.   Cleries, L., J.M. Fernandez-Pradas, and J.L. Morenza, Bone growth on and resorption of calcium phosphate coatings obtained by pulsed laser deposition. J Biomed Mater Res, 2000. 49(1): p. 43-52.

118.   Cleries, L., J.M. Fernandez-Pradas, and J.L. Morenza, Behavior in simulated body fluid of calcium phosphate coatings obtained by laser ablation. Biomaterials, 2000. 21(18): p. 1861-5.

119.   Cleries, L., et al., Application of dissolution experiments to characterise the structure of pulsed laser-deposited calcium phosphate coatings. Biomaterials, 1999. 20(15): p. 1401-5.

120.   Cleries, L., et al., Mechanical properties of calcium phosphate coatings deposited by laser ablation. Biomaterials, 2000. 21(9): p. 967-71.

121.   Fernandez-Pradas, J.M., et al., Influence of thickness on the properties of hydroxyapatite coatings deposited by KrF laser ablation. Biomaterials, 2001. 22(15): p. 2171-5.

122.   Yang, Y., K.H. Kim, and J.L. Ong, A review on calcium phosphate coatings produced using a sputtering process--an alternative to plasma spraying. Biomaterials, 2005. 26(3): p. 327-37.

123.   Wolke JGC, et al., Studies on the thermal spraying of apatite bioceramics. . J Therm Spray Technol 1992: p. 75-82.

124.   Royer P and R. C., Calcium phosphate coatings for orthopedic prosthesis. Surf Coat Technol 1991. 45: p. 171-177.

125.   Kumar, M., H. Dasarathy, and C. Riley, Electrodeposition of brushite coatings and their transformation to hydroxyapatite in aqueous solutions. J Biomed Mater Res, 1999. 45(4): p. 302-10.

126.   Yen SK and L. CM., Cathodic reactions of electrolytic hydoxyapatite coating on pure titanium. Mater ChemPhys 2002. 77: p. 70-76.

127.   Stoch A, et al., Electrophoretic coating of hydroxyapatite on titanium implants. J Mol Struct 2001. 596: p. 191-200.

128. Zhitomirsky, I. and L. Gal-Or, Electrophoretic deposition of hydroxyapatite. J Mater Sci Mater Med, 1997. 8(4): p. 213-9.

129. Cortez PM and G.r. GV., Electrophoretic deposition of hydroxyapatite submicron particles at high voltages. Mater Lett 2005. 58: p. 1336-1339.

130. Cho SB, Nakanishi K, and Kokubo T, Dependence of apatite formation on silica gel on its structure: effect of heat treatment. J Am Ceram Soc 1995 78: p. 1769-1774.

131. Barrere, F., et al., In vitro and in vivo degradation of biomimetic octacalcium phosphate and carbonate apatite coatings on titanium implants. J Biomed Mater Res A, 2003. 64(2): p. 378-87.

132. Du, C., et al., Biomimetic calcium phosphate coatings on Polyactive 1000/70/30. J Biomed Mater Res, 2002. 59(3): p. 535-46.

133. Kim, H.M., et al., Biomimetic apatite formation on polyethylene photografted with vinyltri-methoxysilane and hydrolyzed. Biomaterials, 2001. 22(18): p. 2489-94.

134. Liu, Y., et al., Biomimetic coprecipitation of calcium phosphate and bovine serum albumin on titanium alloy. J Biomed Mater Res, 2001. 57(3): p. 327-35.

135. Stigter, M., K. de Groot, and P. Layrolle, Incorporation of tobramycin into biomimetic hy-droxyapatite coating on titanium. Biomaterials, 2002. 23(20): p. 4143-53.

136. Wen, H.B., et al., Preparation of bioactive Ti6Al4V surfaces by a simple method. Biomaterials, 1998. 19(1-3): p. 215-21.

137. Barrere, F., et al., Biomimetic calcium phosphate coatings on Ti6AI4V: a crystal growth study of octacalcium phosphate and inhibition by Mg2+ and HCO3. Bone, 1999. 25(2 Suppl): p. 107S-111S.

138. Barrere, F., et al., Nucleation of biomimetic Ca-P coatings on ti6A14V from a SBF x 5 solution: influence of magnesium. Biomaterials, 2002. 23(10): p. 2211-20.

139. Barrere, F., et al., Influence of ionic strength and carbonate on the Ca-P coating formation from SBFx5 solution. Biomaterials, 2002. 23(9): p. 1921-30.

140. de Groot, K., Hydroxylapatite coated implants. J Biomed Mater Res, 1989. 23(11): p. 1367-71.

141. Kokubo, T., Bioactive glass ceramics: properties and applications. Biomaterials, 1991. 12(2): p. 155-63.

142. Kokubo, T., et al., Solutions able to reproduce in vivo surface-structure changes in bioactive glass-ceramic A-W. J Biomed Mater Res, 1990. 24(6): p. 721-34.

143. Wen, H.B., et al., Incorporation of bovine serum albumin in calcium phosphate coating on tita-nium. J Biomed Mater Res, 1999. 46(2): p. 245-52.

144. Liu, Y.M., K. de Groot, and E.B. Hunziker, Cell-mediated protein release from calcium-phos-phate-coated titanium implants. J Control Release, 2005. 101(1-3): p. 346-7.

145. Heath, C.A., Cells for tissue engineering. Trends Biotechnol, 2000. 18(1): p. 17-9.

146. Platt, J.L., The immunological barriers to xenotransplantation. Crit Rev Immunol, 1996. 16(4): p. 331-58.

147. Weissman, I.L., Translating stem and progenitor cell biology to the clinic: barriers and oppor-tunities. Science, 2000. 287(5457): p. 1442-6.

148.   Tumbar, T., et al., Defining the epithelial stem cell niche in skin. Science, 2004. 303(5656): p. 359-63.

149.   Martin, G.R., Isolation of a pluripotent cell line from early mouse embryos cultured in medium conditioned by teratocarcinoma stem cells. Proc Natl Acad Sci U S A, 1981. 78(12): p. 7634-8.

150.   Guan, K., et al., Embryonic stem cell-derived neurogenesis. Retinoic acid induction and lineage selection of neuronal cells. Cell Tissue Res, 2001. 305(2): p. 171-6.

151.   Kramer, J., et al., Embryonic stem cell-derived chondrogenic differentiation in vitro: activation by BMP-2 and BMP-4. Mech Dev, 2000. 92(2): p. 193-205.

152.   Nakayama, N., et al., Macroscopic cartilage formation with embryonic stem-cell-derived mesodermal progenitor cells. J Cell Sci, 2003. 116(Pt 10): p. 2015-28.

153.   Schuldiner, M., et al., Induced neuronal differentiation of human embryonic stem cells. Brain Res, 2001. 913(2): p. 201-5.

154.   Wang, R., R. Clark, and V.L. Bautch, Embryonic stem cell-derived cystic embryoid bodies form vascular channels: an in vitro model of blood vessel development. Development, 1992. 114(2): p. 303-16.

155.   Wiles, M.V. and G. Keller, Multiple hematopoietic lineages develop from embryonic stem (ES) cells in culture. Development, 1991. 111(2): p. 259-67.

156.   Yamashita, J., et al., Flk1-positive cells derived from embryonic stem cells serve as vascular progenitors. Nature, 2000. 408(6808): p. 92-6.

157.   Buttery, L.D., et al., Differentiation of osteoblasts and in vitro bone formation from murine embryonic stem cells. Tissue Eng, 2001. 7(1): p. 89-99.

158.   J., C., Über Entzündung und Eiterung. Virchows Arch Pathol Anat Physiol Klin Med, 1867. 40: p. 1-79.

159.   Friedenstein, A.J., R.K. Chailakhyan, and U.V. Gerasimov, Bone marrow osteogenic stem cells: in vitro cultivation and transplantation in diffusion chambers. Cell Tissue Kinet, 1987. 20(3): p. 263-72.

160.   Caplan, A.I., Mesenchymal stem cells. J Orthop Res, 1991. 9(5): p. 641-50.

161.   Bruder, S.P., N. Jaiswal, and S.E. Haynesworth, Growth kinetics, self-renewal, and the osteogenic potential of purified human mesenchymal stem cells during extensive subcultivation and following cryopreservation. J Cell Biochem, 1997. 64(2): p. 278-94.

162.   Pittenger, M.F., et al., Multilineage potential of adult human mesenchymal stem cells. Science, 1999. 284(5411): p. 143-7.

163.   Devine, S.M., Mesenchymal stem cells: will they have a role in the clinic? J Cell Biochem Suppl, 2002. 38: p. 73-9.

164.   Ohgushi, H. and A.I. Caplan, Stem cell technology and bioceramics: from cell to gene engineering. J Biomed Mater Res, 1999. 48(6): p. 913-27.

165.   Yoshikawa, T., H. Ohgushi, and S. Tamai, Immediate bone forming capability of prefabricated osteogenic hydroxyapatite. J Biomed Mater Res, 1996. 32(3): p. 481-92.

166.   Boyan, B.D., et al., Osteochondral progenitor cells in acute and chronic canine nonunions. J

Orthop Res, 1999. 17(2): p. 246-55.

167.   Niedzwiedzki, T., et al., Bone healing after bone marrow stromal cell transplantation to the bone defect. Biomaterials, 1993. 14(2): p. 115-21.

168.   Ohgushi, H., V.M. Goldberg, and A.I. Caplan, Repair of bone defects with marrow cells and porous ceramic. Experiments in rats. Acta Orthop Scand, 1989. 60(3): p. 334-9.

169.   Bruder, S.P., et al., Bone regeneration by implantation of purified, culture-expanded human mesenchymal stem cells. J Orthop Res, 1998. 16(2): p. 155-62.

170.   Kon, E., et al., Autologous bone marrow stromal cells loaded onto porous hydroxyapatite ceramic accelerate bone repair in critical-size defects of sheep long bones. J Biomed Mater Res, 2000. 49(3): p. 328-37.

171.   Petite, H., et al., Tissue-engineered bone regeneration. Nat Biotechnol, 2000. 18(9): p. 959-63.

172.   Kruyt, M.C., et al., Bone tissue engineering in a critical size defect compared to ectopic implantations in the goat. J Orthop Res, 2004. 22(3): p. 544-51.

173.   Schliephake, H., et al., Use of cultivated osteoprogenitor cells to increase bone formation in segmental mandibular defects: an experimental pilot study in sheep. Int J Oral Maxillofac Surg, 2001. 30(6): p. 531-7.

174.   Shang, Q., et al., Tissue-engineered bone repair of sheep cranial defects with autologous bone marrow stromal cells. J Craniofac Surg, 2001. 12(6): p. 586-93; discussion 594-5.

175.   Horwitz, E.M., et al., Transplantability and therapeutic effects of bone marrow-derived mesenchymal cells in children with osteogenesis imperfecta. Nat Med, 1999. 5(3): p. 309-13.

176.   Horwitz, E.M., et al., Clinical responses to bone marrow transplantation in children with severe osteogenesis imperfecta. Blood, 2001. 97(5): p. 1227-31.

177.   Quarto, R., et al., Repair of large bone defects with the use of autologous bone marrow stromal cells. N Engl J Med, 2001. 344(5): p. 385-6.

178.   Lee, J.Y., et al., Clonal isolation of muscle-derived cells capable of enhancing muscle regeneration and bone healing. J Cell Biol, 2000. 150(5): p. 1085-100.

179.   Peterson, B., et al., Healing of critically sized femoral defects, using genetically modified mesenchymal stem cells from human adipose tissue. Tissue Eng, 2005. 11(1-2): p. 120-9.

180.   Kuznetsov, S.A., et al., Circulating skeletal stem cells. J Cell Biol, 2001. 153(5): p. 1133-40.

181.   Kirker-Head, C.A., Potential applications and delivery strategies for bone morphogenetic proteins. Adv Drug Deliv Rev, 2000. 43(1): p. 65-92.

182.   Johnson, E.E., M.R. Urist, and G.A. Finerman, Repair of segmental defects of the tibia with cancellous bone grafts augmented with human bone morphogenetic protein. A preliminary report. Clin Orthop Relat Res, 1988(236): p. 249-57.

183.   Geesink, R.G., N.H. Hoefnagels, and S.K. Bulstra, Osteogenic activity of OP-1 bone morphogenetic protein (BMP-7) in a human fibular defect. J Bone Joint Surg Br, 1999. 81(4): p. 710-8.

184.   Johnson, E.E. and M.R. Urist, Human bone morphogenetic protein allografting for reconstruction of femoral nonunion. Clin Orthop Relat Res, 2000(371): p. 61-74.

Chapter 2

Calcium-phosphate ceramics with inorganic additives

An increasing number of orthopaedic and cranio-maxillo-facial surgeries is one of the consequences of the current progressive population aging. Availability of patient's own bone, the golden standard in bone regeneration, is limited, and therefore novel approaches are needed. Tissue engineering, both growth factor- and cell-based, is a promising alternative, however, its complexity makes the transfer from laboratory to the clinic, long and difficult one. Synthetic biomaterials form an interesting alternative to autograft, because they are off-the-shelf available in large quantities, and relatively easy to adapt to various applications. Particularly calcium phosphate based synthetic bone graft substitutes such as calcium phosphate ceramics are of great interest, as they resemble chemical composition of bone mineral and are therefore not only biocompatible, but also bioactive. Biological performance of currently available calcium phosphate ceramics in bone regeneration is nevertheless still inferior to that of autograft, as their osteoconductive, osteoinductive and ostegenic potential is generally less pronounced. Improving the biological performance of bone graft substitutes, while retaining their synthetic character is a challenge. Use of inorganic compounds, which are present in bone as trace elements, and known to be involved in processes related to bone formation and remodeling, as additives to synthetic bone graft substitutes is a potentially interesting approach to improvement of their biological performance. In this chapter, five inorganic additives have been selected: zinc, copper, strontium, fluoride and carbonate. First, their role in bone metabolism and processes related to bone formation and resorption is discussed. Then, a number of methods are described by which these elements can be incorporated into calcium-phosphate ceramics. Their effect on ceramic properties, as well as their, direct or indirect effect on bone formation and resorption processes in vitro and in vivo, are also discussed. Finally, some conclusions and future perspectives are given for further research into synthetic bone graft substitutes. Keywords: synthetic bone graft substitutes, calcium-phosphate ceramics, trace elements, inorganic additives

1 INTRODUCTION

Regenerative medicine, a field that is aimed at restoring, rather than replacing the function of damaged and degraded organs and tissue, is becoming increasingly important in our society with aging population. In the areas of orthopaedic- and cranio-maxillofacial surgery, for example, there exist great demand for bone regeneration strategies. Restoration of bone defects caused by tumor removal, infections, traumas, as well as spinal fusion are some of the frequently performed surgeries in the clinic. Currently, treatments of bone defects include the use of natural bone grafts, synthetic bone graft substitutes and tissue engineered constructs (Figure 1).

The rationale behind these different strategies is a simple one: providing an environment that is similar to natural bone and facilitating bone regeneration in the defect area as optimally as possible. Approaches to bone regeneration are therefore developed based on the properties of bone tissue, which will in short be summarize in the next section.
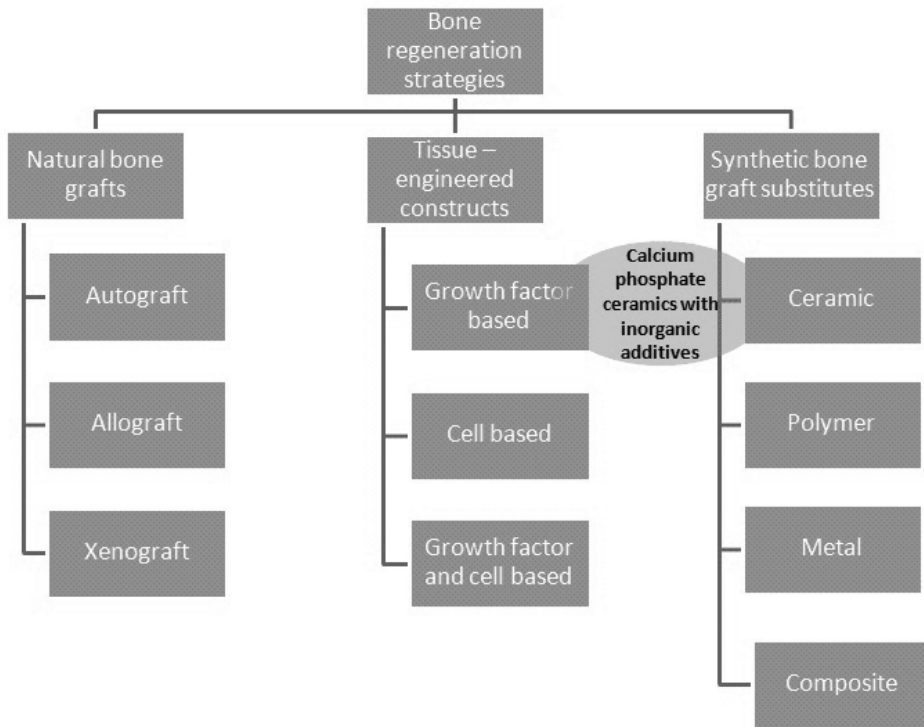
Figure 1: An overview of current strategies in bone repair and regeneration.

2 BONE

Bone is a highly specialized form of connective tissue that is nature's provision for an internal support system in most higher vertebrates. Bone provides for the attachment of the muscles and tendons essential for movement, protects the vital organs of the cranial and thoracic cavities, and it encloses the bloodforming elements of the bone marrow. In addition to these mechanical functions, bone plays an

important metabolic role as a mobilizable store of calcium and phosphate, which can be drawn upon when needed in the homeostatic regulation of the calcium and phosphate in blood and other fluids of the body [1].

Morphologically there are two forms of bone: cortical (compact) bone and cancellous (trabecular) bone. Compact bone, which is rigid and dense, is found mainly in the middle shaft of long bones or shells of other bones. Found predominantly in epiphysis, ribs and spine, cancellous bone has a highly porous structure (>75%), with numerous small bone trusses or trabeculae interconnected with each other, and tends to orient along the principal directions in adaptation to the external loading environment.

Bone is composed of four different cell types. Osteoblasts, osteoclasts and bone lining cells are present on bone surface, whereas osteocytes permeate the mineralized interior. Osteoblasts, osteoclasts and bone lining cells originate from local osteoprogenitor cells, whereas osteoclasts arise from the fusion of mononuclear precursors, which originate in the various hemapoietic tissues. Osteoblasts are the fully differentiated cells responsible for the production of the bone matrix and regulation of its mineralization. The osteocyte is a mature osteoblast within the bone matrix and is responsible for the matrix maintenance. Bone lining cells are flat, elongated cells that cover bone surfaces that are undergoing neither bone formation nor resorption. Little is known regarding the function of these cells, however, it has been speculated that bone lining cells can be precursors for osteoblasts. Osteoclasts are large, multinucleated cells, which are able of resorbing bone mineral.

By weight, bone contains approximately 60% mineral, 10% water and about 30% organic matrix. Type I collagen constitutes approximately 90% of the organic matrix; the remaining 10% is composed of proteoglycans and numerous noncallogeneous proteins, such as osteocalcin, osteopontin, osteonectin, bone sialoprotein, decorin and biglycan [2, 3].

The inorganic component of bone mineral consists of non-stoichiometric hydroxyapatite, the exact composition of which varies depending on the location and function in the body, species and age. Carbonate is the most abundant substitute in biological apatite crystal lattice, accounting for 2-8 wt% of total bone mineral in most mammals [4]. Apart from calcium, phosphate and carbonate, bone mineral contains a great number of other inorganic compounds in varying quantities.

3 CURRENT METHODS IN BONE REGENERATION

3.1 Natural Bone Grafts

Patient's own bone meets all the requirements for successful bone regeneration, and it is therefore little surprising that autologous bone is still considered the golden standard in most applications. Autologous bone grafts do not cause immunogenic reaction upon surgery [5-8]. Furthermore, they possess a great biological performance in terms of osteogenicity (supply of bone forming cells by the bone marrow) [9], osteoinductivity (initiation of the differentiation of mesenchymal stem cells towards the osteogenic lineage by e.g. bone morphogenetic proteins (BMPs) present in the graft) [5, 6, 9, 10] and osteoconductivity (facilitation of cell- en nutrient infiltration through the 3D porous structure) [6, 9, 11]. Several drawbacks are however associated with harvesting of autologous bone grafts, for which

an additional surgery is required, which is occasionally the cause of donor site morbidity [5, 6, 9, 12], chronic post-operative pain [6, 13-15], hypersensitivity [6] and infections [10, 13, 16]. In addition to these drawbacks, limited availability of autologous bone is probably the most important reason why alternative bone regeneration strategies are needed. Other natural bone grafts, allografts and xenografts, are less limited in available quantity, but their performance is often inferior to that of autografts [9, 15, 17-19], because they need to undergo a number of treatments in order not to cause immunogenic reaction [20, 21].

3.2 Synthetic Bone Graft Substitutes

Synthetic bone graft substitutes present an attractive alternative to natural bone grafts, in the first place because of their unlimited and off-the-shelf availability. But also the fact that they do not cause an immunogenic response and that they can easily be tailored to meet requirements of a specific application explains a great number of substitutes developed in the past decades. Although all three material types, metals, polymers and ceramics and combinations thereof, have been used to develop bone graft substitutes, the use of calcium-phosphate based biomaterials, mostly ceramics, has gained the largest interest. Considering the fact that the inorganic component of bone is basically a calcium phosphate mineral is the main reason for this interest and emphasizes again the fact that the rationale behind a tissue regeneration strategy is often an attempt to create an optimal environment for regeneration.
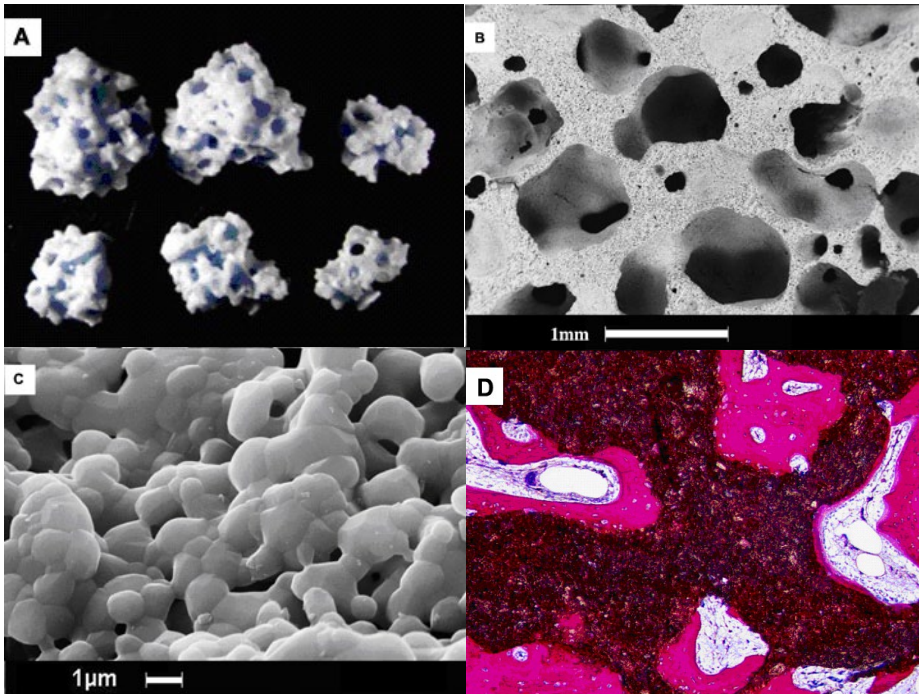
3.2.1 Calcium Phosphate Ceramics

Calcium phosphate (CaP) ceramics possess chemical composition similar to that of bone and tooth mineral. In addition to an excellent biocompatibility, their bioactivity is remarkable.

As reviewed by Damien and Parsons [6], various CaP biomaterials have shown some distinct clinical successes. Hydroxyapatites (HA) for example, both of natural (coral- and bovine bone derived) and synthetic origin, have widely been tested and successfully used for clinical applications. Due to its low resorption rate, hydroxyapatite has proven to be a good material for alveolar ridge augmentation, pulp capping, and filling of periodontal defects, where the use of autologous bone, that is resorbable, has been found to be less than optimal. In orthopaedics, porous hydroxyapatite blocks have been used for filling defects remaining after tumor excision, as well as in spinal fusion of vertebral bodies. Tricalcium phosphate (TCP) is another widely used ceramic, in particular in applications where degradation of the material is required. Dental applications of TCP ceramics include the filling of defects due to periodontal loss, as well as repairing cleft palates. In orthopaedics, tricalcium phosphate has been used in spinal fusion. A ceramic receiving much attention is biphasic calcium phosphate, consisting of HA and TCP. By altering the ratio of HA to TCP, variable rates of degradation can be achieved, an example of adaptability of synthetic bone graft substitutes to an intended application. Clinically, biphasic calcium phosphate has been tested for treatment of patient with scoliosis and for filling defects after tumor removal. Currently, calcium phosphate ceramics can be made in the form of particles, dense and porous scaffolds, [22, 23], and even in more defined shapes using free form fabrication techniques [24]. Their

microstructure can be modified by controlling production process, in order to control their bioactivity in vivo [25]. Figure 2 shows an example of calcium-phosphate ceramic particles (a), macro- (b) and microstructure (c) of porous calcium phosphate ceramic and its bonding to bone (d) which is a sign of bioactivity.

It should be noted that ceramics, especially sintered ones, are intrinsically brittle. This is an important limitation, because restoring the function of bone tissue includes restoration of mechanical properties of bone. However, brittle materials cannot be used in load-bearing applications, where mechanical load needs to be (temporarily) taken over by the implant. In order to overcome this limitation, ceramics are

Figure 2: Calcium phosphate ceramic: (a) digital micrograph showing ceramic particles, (b) low magnification Scanning Electron Microscopy micrograph of an open porous macrostructure; (c) high magnification Scanning Electron Microscopy micrograph showing microstructure with ceramic grains among which micropores are found and (d) Light Microscopy micrograph of a histological slide showing bone that has formed inside the ceramic pores and is in close contact with ceramic surface.

often combined with other materials, such as metals and polymers in the form of coatings [26-30] or composite materials [31-33].

3.3 Tissue Engineering

Despite intensive research and continuous improvements of synthetic biomaterials, so far these materials have not shown a biological performance that is equal to that of autologous bone grafts. Bone conduction over the material surface and the replacement by bone as well as their mechanical properties are usually inferior to autologous bone grafts [6, 17, 34-36]. Tissue engineering is relatively recent devel-

opment that has in 1993 been defined as an "interdisciplinary field that applies principles of engineering and life sciences toward the development of biological substitutes that restore, maintain, or improve tissue function" by Langer and Vacanti [37]. In practice, in tissue engineering, attempts are made to create constructs with properties and function similar to that of natural tissue. In other words, rather than using a bioactive calcium-phosphate ceramic that resembles bone mineral, an additional step is made to add cells and/or growth factors to the ceramic, creating thereby a construct that resembles both mineral and organic component of bone. Bone tissue engineering construct most often consist of a (synthetic) carrier loaded with either bone inducing substances (chemical stimulation of bone formation-growth factor based tissue engineering), osteogenic cells/tissue (cell-based tissue engineering) or both [37].

To date numerous growth factors have been identified and subsequently produced by recombinant gene technology, such as bone morphogenetic proteins (BMPs) and other members of the transforming growth factor β (TGFs-β) family, fibroblast growth factors (FGFs), plateled-derived growth factors (PDGFs) and insuline derived growth factors (IGFs). Various studies have shown that bone growth factors have several regulating effects on cells from the osteoblastic lineage and in vivo studies have demonstrated that some factors can induce bone formation and/or stimulate bone healing. Kirker-Head has reviewed the application of BMPs in a number of animal models at various orthotopic sites, such as spinal fusion, long bone defects, mandibular and cranial bone defects, fracture healing, as well as in periodontal regeneration, alveolar ridge augmentation and osteointegration of dental implants [38]. In addition, various preclinical and clinical studies have shown positive effects of BMP in nonunions and segmental defects, like traumatic tibial defect [39, 40] and femoral defects [41].

The combination of autologous cells with carriers is another way to produce tissue-engineered hybrids. Various cell types such as calvarial [42, 43] and periostal [44, 45] cells, osteoblasts of trabecular bone [46, 47], chondrocytes [48] and vascular pericytes [49] have been tested as potential sources of bone forming cells. Nevertheless, the most widely used source of osteogenic cells is bone marrow. Bone marrow has been recognized as a source of osteoprogenitor cells that can differentiate towards bone forming cells when cultured under adequate conditions [50-53]. In addition, bone marrow has been shown to be the most abundant source of osteoprogenitors, which possess high proliferative ability and great capacity for differentiation [54, 55]. Studies in rodents have shown the feasibility of the tissue-engineered hybrids, consisting of a carrier and bone marrow stromal cells, after ectopic [56, 57] and orthotopic implantation [56-60]. In larger animals, there are a few studies showing the biological performance of the TE hybrids, in ectopic [61-63] and orthotopic sites [64-66]. In a small number of studies in which cell-based tissue engineered construct have been tested in humans, the results obtained showed varying degrees of success [67].

Although both growth factors-based and cell-based tissue-engineered constructs have shown the capability to enhance bone formation when implanted orthotopically, their biological performance is for a big part dependent on the construct carrier. For example, when BMPs are implanted without a carrier, they are reported to diffuse too rapidly to be able to induce or to enhance new bone formation. Furthermore, the amount of BMP necessary to achieve a certain dose in vivo is also carrier dependent [68-70].

Similarly, a suitable carrier is a prerequisite for the success of a cell-based tissue-engineered construct. For instance, recent studies have shown that bone formation in tissue-engineered constructs is restricted to confined areas of the scaffold. Furthermore, bone bridging between individual tissue-engineered material granules is exceptional. In addition, the findings of the clinically relevant studies suggest that the effect of tissue engineering is moderate and may be irrelevant at long-term implantation intervals [71]. The tissue engineering technique is also associated with some drawbacks. The production of recombinant growth factors, collection and transport of the biopsies, culture of autologous cells are some of the factors that make tissue engineering time-, money- and labor-consuming.

4 IMPROVEMENT OF SYNTHETIC BONE GRAFT SUBSTITUTES

From the above given overview of the current status of bone regeneration strategies, the following summary can be made: (1) autologous bone is the gold standard with regard to biological performance, but its limited availability creates a need for comprehensive alternatives; (2) synthetic bone graft substitutes have a great advantage of being off-the-shelf available in large quantities and relatively inexpensive, but their biological performance needs improvement for them to become a comprehensive alternative to autograft and (3) tissue engineering is a strategy with great possibilities, but due to its complexity, extensive research is needed before tissue engineering is widely applied in the clinic.

For material scientists, real challenge lies in the improvement of the biological performance of the existing bone graft substitutes, while retaining their synthetic character. In this chapter, the potential use of inorganic additives to bone graft substitutes will be discussed as "synthetic growth factors" (Figure 1). These inorganic additives are compounds found in bone mineral as trace elements. As mentioned in the section on bone composition, the inorganic component of bone is non-stoichiometric hydroxyapatite, mainly consisting of calcium (36.6 wt%), phosphorus (17.1 wt%) and carbonate (4.8 wt%). In addition, a number of other components are also found in bone minerals, such as sodium (1 wt%), potassium (0.07 wt%), fluorine (0.1 wt%), chlorine (0.1 wt%), magnesium (0.6 wt%), and strontium (0.05 wt%) [72]. In an early work by Becker and co-workers, presence of alumunium, copper, iron, manganese, lead, silicon, tin, vanadium and zinc has also been determined in human bone [73]. In 1997, El-Amri and El-Kabroun used neutron activation analysis and showed that also barium and bromine are present in human bone [74]. Most of these elements have an effect on properties of bone mineral, such as mechanical and degradation properties. In addition, a number of them can influence processes of angiogenesis, bone formation and remodeling, all of which are of importance in the field of bone regeneration. Probably the best example of use of trace elements in bone regeneration and bone-related diseases is clinical use of strontium ranelate in patients with osteoporosis. But there is also evidence that other elements can influence processes related to bone formation and remodeling. We have chosen three metallic-, zinc, copper and strontium, and two non-metallic components of bone, fluoride and carbonate, to discuss their potential use in bone regeneration. Occurrence of these five elements in bone is summarized in Table 1.

First, their importance will be discussed in bone metabolism and a literature review will be given on

their effect on processes related to bone formation and remodeling. Then, a number of methods will be discussed to incorporate these elements in calcium phosphate based ceramics and an overview of studies in which ic expression of a range of proteins [79]. The amount of zinc in bone is relatively high as compared to other tissues. As reviewed by Colhoun and coworkers, human bone ash contains between 150 and 250 μg/g zinc, depending on the location in body. Zinc deficiency is associated with a number of skeletal anomalies in fetal and postnatal development, such as depressed bone age, which can be treated with zinc supplementation. It was demonstrated that nutritional zinc deficiency results in a decrease of zinc concentrations in bone. Early studies indicated an increase in uptake of zinc in the areas of bone healing, in particular in the areas in close proximity to the sites of calcification, as well as during ectopic bone formation, suggesting the influence of zinc in osteogenesis [75]. The role of zinc in the bone has been shown to be twofold: (1) zinc plays a structural role in the bone matrix that consist of hydroxyapatite crystals, which contain zinc complexed with fluoride and (2) zinc is involved in the stimulation of bone formation by osteoblasts and inhibition of bone resorption by osteoclasts [80].

Table 1: occurrence of zinc, copper, strontium, fluoride and carbonate in bone

Element	Content
Zinc	60-85 ppm (in ash of human cortical bone)[1]
	153-266 ppm (in ash of various human bones)[2]
	54-315 ppm (in lyophilized human bone)[3]
Copper	5 ppm (in ash of human cortical bone)1
Strontium	62-130 ppm (in ash of human cortical bone)[1]
	11-418 ppm (in lyophilized human bone)[3]
Fluoride	0.1 wt% (in mineral of bovine cortical bone)[4]
	0.08-0.69 wt% (in ash of human iliac crest bone)[5]
Carbonate	4.8 wt% (in mineral of bovine cortical bone)[4]
	5.1-5.8 wt% (ash of human iliac crest bone)[5]

1[73]   2[75]   3[74]   4[72]   5[169]

Yamaguchi and coworkers, for example, showed an increase of Runx-2, osteoprotegerin and regucalcin mRNA expression by MC3T3-E1 osteoblasts in presence of zinc sulfate in concentrations $10^{-6} - 10^{-4}$ M) [81]. More recently, Kwun and colleagues showed that zinc deficiency reduced osteogenic activity of MC3T3-E1 cells in vitro by decreasing bone marker gene transcription through reduced and delayed Runx-2 expression and by reduction of extracellular matrix mineralization through a decrease in ALP activity [82]. The effect of zinc on human osteoblast-like cell line SaOS-2 was also investigated and it was observed that both ALP expression and the formation of mineral nodules were stimulated in presence of zinc at concentrations of 1 and 10 μM but inhibited at concentrations higher than 25 μM [83]. When primary murine bone marrow stromal cells and osteoblast were treated with zinc at concentrations of 10^{-9} M and lower, no effect was observed on proliferation, and inhibitory effect was proven on both osteogenic and adipogenic differentiation [84].

As recently reviewed by Yamaguchi, zinc has been shown to have an inhibitory effect on bone resorption in tissue culture systems in vitro and to suppress osteoclastogenesis of osteoclastic cells derived from bone marrow [85].

5.2 Copper

Copper deficiency is generally associated with syndromes of anemia and pancytopenia, as well as with neuro-degeneration in humans and other mammals. In the metabolism of the skeleton, copper performs a key catalytic function in the first step of the maturation of collagen to form stable fibrils [86, 87]. This effect can be contributed primarily to the copper-dependent enzyme lysys oxidase, for which copper acts as cofactor. Lysyl oxidase is required for the formation of lysine-derived cross-links in collagen and elastin [88]. Several reports suggested that mild copper deficiency may contribute to bone defects such as osteoporotic-like lesions and bone fragility in humans and animals [89, 90], as well as in a variety of bone developmental defects in preterm infants [91, 92]. Oral supplementation with copper, however, resulted in complete healing of fractures and improvement in other bone defects [91, 92].

Copper was shown to affect both the proliferation and differentiation behavior of mesencymal stem cells (MSCs) in vitro. It decreased the proliferation rate of MSCs and induced an increase in their differentiation towards the osteogenic and adipogenic lineage [93]. Copper was also reported to affect the timing of expression of ALP activity, which reached its maximum earlier than in the controls in absence of copper.

Copper also plays a role in the inhibition of bone resorption, through its action as a cofactor for superoxidase dismutase, an antioxidant enzyme containing two atoms of zinc and copper which act as a free radical scavenger, neutralizing the superoxide radicals produced by osteoclasts during bone resorption [80]. While an inhibition in osteoclast function was observed in copper-deficient animals [94], Wilson suggested that higher concentrations of copper in cell culture medium (10^{-5} M copper sulfate) reduced bone resorption and inhibited hydroxyproline, protein, and DNA synthesis in vitro [95].

In a number of studies, copper was also shown to have an effect on angiogenesis, a process which is of great importance in bone regeneration. Angiogenesis is essential for the survival of osteoblasts, as well as for the regulation of fracture healing and bone remodeling [96, 97]. Previous reports showed that copper can enhance growth of endothelial cells in vivo [98-100], and copper found in wound tissues is known to be involved in generation of free radicals during tissue regeneration [101].

5.3 Strontium

Strontium is, like calcium, a group IIa element and, from a chemical point of view, they behave similarly. Although strontium is not an essential trace element, a substantial amount of research has been performed on its properties and effects due to its chemical analogy to calcium. Strontium is a bone-seeking element, of which 98% in human body can be found in the skeleton [102]. It is therefore not surprising that among the trace metals present in human bone, strontium was the only one that was correlated with bone compressive strength [103]. Strontium was shown to have dose-dependent ef-

fects on bone formation, which was further affected by presence or absence of renal failure. While low doses (0.19% - 0.34% in drinking water during 9 weeks) were reported to improve the vertebral bone density and stimulate bone formation in rats with normal renal function [104-106]; high doses (> 0.4% in drinking water) were shown to have deleterious effects on bone minerlization [104, 105]. However, in animals with chronic renal failure, 0.34% of strontium (as chloride compound) in drinking water induced a bone lesion histologically characterized as osteomalacia [107]. This and further studies on a similar model showed the effect of strontium to be complex and dose dependent.

Similar, dose-dependent effect of strontium was also observed in cell culture experiments. Studies with primary osteoblasts isolated from fetal rat calvaria showed that at low doses (1 μg/ml strontium in the culture medium) a reduced nodule formation occurred in the presence of an intact mineralization; at intermediate concentration (5 μg/ml), no effect was observed, while at high concentrations (20-100 μg/ml), an intact nodule formation was accompanied by a reduced mineralization [108].

Strontium was also shown to reduce excessive bone resorption in rats with osteopenia, which was associated with a decrease in the number of osteoclasts [109]. Baron and Tsouderos further showed that a distrontium salt, S12911 dissolved into the culture medium inhibited osteolcast differentiation and osteoclast activity in a dose-dependent manner, without affecting the attachment of the osteoclast [110]. As mentioned before, current clinical use of strontium ranelate for treatment of osteoporosis is an excellent example of application of inorganic trace elements in bone related conditions. The dual anabolic and antiresorptive role of strontium ranelate has been described in vitro [111]. As recently reviewed by O'Donnell and coworkers, there is evidence that supports the efficacy of strontium ranelate in reducing vertebral, and to a lesser extent, non-vertebral fractures in postmenopausal osteoporotic women and in increasing bone matrix density in postmenopausal women with and without osteoporosis [112, 113].

5.4 Fluoride

Fluoride has been recognized as an important element in mineralized tissues, such as teeth and bone, for over a century. Initial attention was paid on environmental overexposure to this element as a cause of crippling bone disease. However, research that followed led to some major clinical successes, in particular with regard to dental use with eradication of endemic dental fluorosis worldwide and a successful water and topical fluoridation program that has reduced prevalence of dental caries [114]. The role of fluoride in the prevention and control of dental caries in both humans and animals has been shown to be predominant in the maturation stage of enamel formation [115-119]. Fluoride was also found to be the single most effective agent for increasing bone volume in the osteoporotic skeleton [120] and an effective anabolic agent to increase spinal bone density by increasing bone formation and mineralization [121, 122]. Like strontium, fluoride was shown to have a dose related effect on bone formation are: low doses of fluoride (50 mg sodium fluoride daily) increased the trabecular bone density of osteoporotic patient [123-125], whereas a dose of 75 mg/day had no beneficial effects on bone mineral density in postmenopausal women [126]. 0.8 mg/kg fluoride intake also stimulated bone formation in rats [106]. Complex, and dose-dependent effects of fluoride together with reports showing an increase in occur-

rence of osteoporotic hip fractures related to regular fluoride intake, were important reasons for the lack of major achievements in of fluoride treatment in orthopaedics.

Also in vitro, dose dependent effects of fluoride were observed. Bellows et.al. demonstrated an increase in proliferation of fetal rat calvarial osteoblasts with increasing dose of sodium fluoride in cell culture medium in concentrations between 10 and 500 μM, with higher concentrations being cytotoxic [127]. A positive effect on proliferation of 10 μM sodium fluoride in culture medium was also observed on embryonic chick calvarial cells, while no effect was found human osteoblast cultures [114]. Recently, dose dependent effect of sodium fluoride was found on proliferation and differentiation of caprine osteoblasts: at concentrations below 10^{-5} M of sodium fluoride in cell culture medium, cell proliferation and ALP expression were enhanced, whereas above this dose, apoptosis occurred and a decrease in ALP expression was observed [128]. Burgener and coworkers suggested that fluoride enhances protein tyrosine phosphorylation in osteoblast-like cells UMR-106, by enhancing tyrosine kinase activity, postulating that this signal transduction pathway is involved in the osteogenic effect of fluoride [129].

The effect of fluoride on the behavior of osteoclasts has been reported in a study where rabbit primary osteoclasts were cultured on thin slices of bovine bone. Sodium fluoride in concentrations of 0.5-1.0 mM in medium decreased the number of resorption lacunae made by individual osteoclasts as well as the resorbed area per osteoclast [130]. It was further shown that the suppression of the resorption was enhanced by increasing the sodium fluoride concentration of the cell culture medium [131].

5.5 Carbonate

Carbonate is, together with calcium and phosphate, major constituent of bone mineral, which makes it potentially an interesting compound for treatment of damaged and degraded bone tissue. Bone mineral of most mammals contains between about 2 and 8 wt% carbonate [4, 72, 132], depending on the age of the individual [133]. Type B carbonated apatite (CO_3^{2-} for PO_4^{3-} substitution, coupled with Na^+ for Ca^{2+} substitution) prevails in biological apatites [132]. A small amount CO_3^{2-} is believed to be a substituent for OH^- groups, known as type A substitution [134]. Type A to type B ratio in biological apatites is between 0.7 and 0.9 [135]. Introducing carbonate groups in the structure of hydroxyapatite mineral in general results in a decrease of crystallinity and increase of solubility in vitro and in vivo [136]. Possible effects of carbonate are generally investigated and discussed in relation to a bone graft substitute to which it has been added as a direct addition to, for example, cell culture medium, mainly has an effect on the pH. Carbonate will therefore be discussed in more detail in the section on calcium phosphate ceramics with inorganic additives.

6 INORGANIC ADDITIVES IN CALCIUM PHOSPHATE CERAMICS
6.1 Methods of Preparation

A great advantage of inorganic additives in comparison with organic compounds such as growth factors, is their thermal stability, i.e. inorganic additives do not require physiological conditions to retain their stability and functionality. However, although standard methods of preparation can often be used,

processes sometimes need adaptations for various additives to be efficiently incorporated into a calcium phosphate ceramic. Method of incorporation determines the way an element is a part of the ceramic and therewith also the release profile and the efficiency of the element upon release.

Powder preparation is often a first step in the process of ceramic production. Depending on the ceramic type to be produced, the produced powder then undergoes a number of subsequent processes. For sintered, porous or dense ceramics, for example, calcination, slurry preparation, drying and sintering are frequently the steps following powder preparation. In the case of non-sintered ceramics, or cements, powder is often mixed with a liquid phase to initiate setting of cement. A great number of different coating techniques also exist, which are used to provide surfaces of, for example metallic, implants with a calcium phosphate ceramic layer. The most widely used coating method is plasma-spraying [137, 138], but alternative methods such as double decomposition- [139], biomimetic- [140-142], electrolytic deposition- [143, 144], sol-gel- [145-147], laser- [148-152], magnetic sputtering- [137] and hydrothermal coating methods [153-156] have gained interest in the past decades. For a number of these methods, powder is a starting point, for others, precipitation of the coating directly from a solution is a part of the process.

Inorganic additives are frequently incorporated into a ceramic (coating) during the process of powder production, either by addition of an element salt into the solution from which calcium-phosphate phase is precipitated, or by adding a precursor containing the additive of choice into a sol-gel process. Another way of additive incorporation is in the later stage of ceramic processing, by a solid state reaction. In this case a ceramic powder, such as hydroxyapatite or β-tricalcium phosphate is mixed with a salt of choice, followed by heating at high temperatures, which allows incorporation of the inorganic additive into the ceramic powder.

Metallic ion additives can be doped into the crystal lattice, which is one of the most widely used methods of incorporation. A maximum exist in the amount of dopant that can be added, above which impurities are formed.

Zinc, for example, is often incorporated into β-TCP ceramics [157]. Incorporation of zinc into β-TCP stabilizes the crystal lattice, preventing conversion to α-tricalcium phosphate [158], thus increasing the thermal stability of the β- TCP. To manufacture a zinc TCP (ZnTCP) powder, an adapted co-precipitation process as used for the preparation of β-TCP and HA production can be applied. First, to a solution of calcium oxide, zinc nitrate is added with a final molar ratio of 10 % in Zn:(Ca+Zn). Up to 12 mol % zinc can be taken up, as at higher concentrations an impurity appears in the form of $Zn_2Ca(PO_4)_2$. Then, phosphoric acid is added as a source of phosphate, resulting in precipitation of zinc containing powder, which is then used for further ceramic preparation [157, 159]. Also sol-gel reaction, with, for example zinc nitrite as a precursor [160] and solid-state reactions, wherein β-TCP powder is mixed with zinc phosphate powder and heated [158] were used to produce zinc containing ceramic.

Incorporation of zinc into HA results in instability of the crystal lattice, because of the lack of adequate atomic sites. Zinc exhibits an inhibitory effect on crystallization of HA, and heat treatment of HA in presence of zinc resulted in conversion into β-TCP, with a reduced lattice constant in comparison to

pure β-TCP [161].

A way to obtain strontium-doped β-TCP is by mixing tri-strontium phosphate (α-TSrP/$Sr_3(PO_4)_2$), obtained by solid state reaction of strontium carbonate and ammonium phosphate at a ratio of 3:2, with β-TCP powders, followed by heat treated [158]. Strontium has also been added to HA powders, either by a co-precipitation process or sol-gel method. In the co-precipitation process, strontium substitution occurred by the replacement of a part of calcium nitrate with strontium nitrate in the reaction with ammonium phosphate. The overall molar ratio was kept at 10:6 with $(NH_4)_2HPO_4$:($Ca(NO_3)_2$+ $Sr(NO_3)_2$), which is the desired Ca/P ratio for HA [162].

To create a single phase strontium hydroxyapatite a sol-gel route was followed. A solution of sodium diphosphate was added to a strontium nitrate solution, with a molar ratio for Sr:P of 2:1. Then, sodium alginate (Na-Alg) was added to the aqueous solution containing $Sr(NO_3)_2$ and $Na_4P_2O_7$ according to the molar ratios of Sr:P:Na-Alg = 2/1/2.5, followed by drying and calcinations of the sol. The phase composition appeared highly dependent amount Na-Alg added. When other ratios were used, phases like $Sr_2P_2O_7$ and/or $Sr_3(PO_4)_2$ also formed [163].

In contrast to zinc- and strontium doping, a relatively limited amount of work has been done on copper doping of calcium phosphate ceramics. In a paper by Belik and coworkers, it was reported that $Ca_{10.5-x}Cu_x(PO_4)_7$ with x =0, 1/6, 1/3, 1/2, 2/3, 5/6, 1, 7/6, 4/3 and 1.5 can be synthesized after the substitution of calcium by copper within the structure of β-TCP through a solid-state reaction [164].

.Fluoridated apatite powders can be readily made by adding a fluoride donor during calcium-phosphate precipitation process, whereby F^- substitutes the OH^- [165-167], leading to a reduction in crystal size and an increase in structure stability [168, 169].

Synthetic carbonated apatite type A (CO_3^{2-} for OH^- substitution) has been successfully produced by using a time-consuming process of sintering HA powder under CO_2 supply or by soaking HA powder in an aqueous solution saturated with CO_2 [72, 170]. Preparation of type B (CO_3^{2-} for PO_4^{3-} substitution, coupled with Na^+ for Ca^{2+} substitution) or type AB is more complex, and occurs predominantly via closely controlled aqueous precipitation reactions [171-175]. However, when carbonated apatite powders are sintered to produce highly crystalline, porous ceramics, excessive loss of carbonate may occur [174, 176, 177] due to thermal instability of carbonated apatites [178, 179].

6.2 Effect of Inorganic Additives on Ceramic Properties

Incorporation of zinc into the calcium-phosphate crystal lattice occurs by substitution of calcium ion. As earlier mentioned, zinc generally destabilizes the crystal structure, except for that of β-TCP, which has an atomic site, known as a Mg site, that can incorporate divalent cations with an ionic radius ranging from 0.060 to 0.080 nm, where the ionic radius of zinc belongs to [180]. By heating of the zinc doped β-TCP at temperatures above 800°C, the zinc doped β-TCP started to transform into zinc doped α-TCP which had higher solubility than β-TCP [181]. The highest content of zinc in the zinc doped β-TCP was 6 wt%, which was higher than maximum zinc content of 1.26 wt% in zinc doped α-TCP at 1450°C [182]. While the zinc content increases, the solubility of TCP decreases. The negative loga-

rithm of the Ksp is expressed as pKsp = 28.686 +1.7414C − 0.42239C^2 + 0.063911C^3 − 0.0051037C^4 + 0.0001595C^5, where C is the zinc content in TCP in mol% [183]. XRD results showed that TCP structure did not undergo great changes after substitution [157, 184, 185]. Rietveld refinement of the XRD data confirmed that the lattice parameters a and c decreased with an increase of the zinc content in β-TCP from 2 mol% to 9 mol%, leading to contraction in the unit cell volume [186]. This effect on the unit cell volume was consistent with the reports on the effect of magnesium and copper and is probably caused by the lower ionic radius of zinc comparing with that of calcium [187, 188]. Reports also revealed that the replacement of M(5) site of calcium ions in the β-TCP structure was favored, consistent with reports on copper [164, 186], which can be explained by the fact that the Ca-O bond at M(5) site was the shortest mean distances in the β-TCP structure [189].

Although substitution of zinc into HA is more difficult than substitution into β-TCP, Chung et. al. successfully synthesized the ZnHA powders by a sol-gel method through addition of zinc ranging from 200 to 20000 ppm by atomic ratio versus calcium atoms [190]. The TGA analyses, however implied that the amount incorporated was relatively small. XRD results, supported by the FTIR analysis showed that the only phase present was that of HA [185, 190, 191].

HA was also doped with zinc using a hydrothermal method [191, 192]. In this study, it was shown that the crystallinity of HA decreased an increasing zinc content from 10 mol% to 20 mol%. Dissolution behavior of HA ceramic was affected in presence of zinc: while Mayer and Featherstone observed a decrease in dissolution, in another study, an increase in solubility was observed, possibly due to differences in production methods [191, 193, 194].

In a study, in which copper substituted β-TCP was prepared through a solid-state reaction, it was shown that the maximum copper content was 8.5 wt%. XRD data showed that the calcium cations on the M(4) and M(5) sites in the β-TCP structure can be replaced by copper cations and also confirmed the dependence of unit cell parameters on the copper concentration [164]. Replacement of Ca^{2+} with Cu^{2+} reduces the bond lengths between calcium and oxygen atoms in the crystalline lattice mainly due to the lower ionic radius of Cu^{2+} and compared with that of the Ca^{2+} [187, 195]. From the energy point of view, the total molecular energy decreases with the replacement of Ca^{2+} with Cu^{2+} [187], meaning that copper ions are theoretically are preferred to calcium ions.

In a study wherein single-phase strontium doped β-TCP was produced by preparing a calcium-deficient apatite through aqueous precipitation and consequent heat-treatment at a temperature above 700°C, substitution of calcium by strontium was shown to have an effect on the lattice constant of the resulting β-TCP [196]. Substitution of calcium by strontium led to a significant expansion in both the a- and c- axis, which was increased with an increasing strontium content due to the larger ionic radius of strontium of 1.13 Å compared with that of calcium (0.96 Å). β-TCP showed the ability to host up to 80 at.% of strontium without provoking a remarkable rearrangement of the unit cell [196-198]. These findings were consistent with studies on strontium-substituted α-TCP [199].

The substitution of calcium by strontium in the HA was proven possible to an extent of Sr/Ca atomic ratio of 30%. Also here, substitution resulted in larger crystal lattice and increased solubility of the

ceramic, due to the relatively large ionic radius of strontium compared with that of calcium [200, 201]. These findings were consistent with other reports where the XRD and FTIR analyses in strontium-containing HA indicated the substantial expansion of the crystal lattice dimensions as compared to pure HA [202, 203].

Replacement of OH^- with F^- in an apatite lattice can bring about a reduction in the volume of the unit cell and a concomitant increase in structure stability [72, 204]. FHA nano-powders with composition of $Ca_{10}(PO_4)_6OH_{2-x}F_x$ (x in the range of 0 to 2) were successfully synthesized by mechanical alloying method whereby XRD and FTIR analyses only revealed presence of apatite [205]. XRD patterns showed that some peaks gradually shifted to the right with the increasing of fluoride content in FHA, due to the decrease in a-axis of the unit cell, caused by lower ionic radius of F^- compared with that of OH^- [206-208]. Dissolution tests showed that solubility decreased with the increase in fluoride content. The minimum solubility was observed at x values of 0.8-1.1, because the substitution of OH^- by F^- resulted in a stronger hydrogen bond between F^- and nearby OH^-, resulting in a more stable structure with lower solubility [206, 209-211].

An increase of carbonate content in a carbonated apatite by both A and B substitution, resulted in contraction of a-axis and expansion of c-axis of the unit cell, and therefore in a decrease in crystal size and an increase in crystal strain, which in turn resulted in a higher solubility [212, 213]. Figure 3 shows microstructure of an HA and a carbonated apatite ceramic, produced using a similar method, from which it is obvious that even a carbonate content of about 5 wt.% leads to a great decrease of grain size of the ceramic.
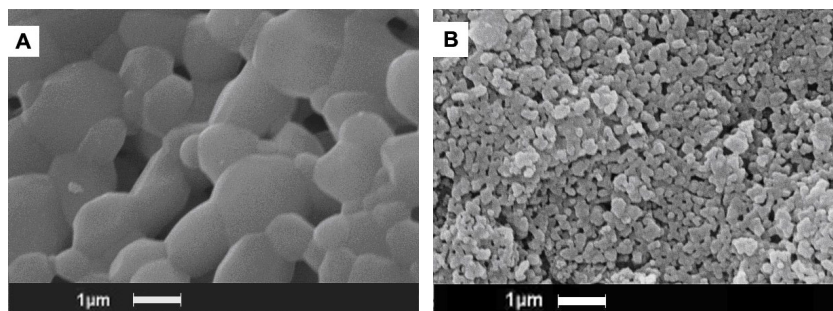

Figure 3: High magnification Scanning Electron Microscopy micrographs showing microstructure of (a) hydroxyapatite and (b) type B carbonated apatite ceramic containing ca. 4 wt.% carbonate, produced using a similar process. Note a significant decrease in crystal size in presence of carbonate.

6.3 Biological Performance of Ceramics Containing Inorganic Additives

In this section, release profiles of the inorganic additives from the ceramics are discussed in physiological conditions as well as their effect in in vitro and in vivo systems related to bone formation and remodeling.

Studies on the in vitro release profiles of zinc for the ZnTCP in Simulated Body Fluid (SBF), showed an initial burst release of zinc, followed by a sustained release over a longer period of time. The amount of

zinc released increased with the increasing zinc content of the ceramic ranging from 0.6 wt% to 6 wt% [184]. The rate of zinc release was shown to increase when the calcium content of the release medium was decreased [184].

In a study by Tas et.al. it was demonstrated that presence of zinc β-TCP in concentrations 2900 and 4100 ppm increased viability of murine osteoblast-like cells, whereas further increase in zinc content has an opposite effect. ALP activity of these cells was found to reach its maximum on ceramics containing 4100 ppm zinc [214]. Dose dependent effects on osteoblastic cell attachment and growth were observed in both zinc containing HA and β-TCP, with a positive effect up 1.5 wt% and a negative effect above this level, possibly due to toxic effects on cells [185, 215]. Ito and colleagues also reported a more pronounced MC3T3-E1 osteoblasts proliferation in vitro for ZnTCP/HAp ceramics with zinc content ranging from 0.6 and 1.2 wt% as compared to the control [157], which was consistent with other in vitro reports [216, 217].

Resorption by mature osteoclasts attached to ZnTCP in the presence of zinc in concentrations of 0.316 wt% and especially 0.633 wt%, compared to pure TCP, which was possibly die to an increase in apoptosis of osteoclasts [183, 218]. At zinc level of 0.633 wt%, the number of apoptotic osteoclasts was 2.8 times higher than on pure TCP after 24h of culture. These findings were consistent with the laser microscopic measurement experiments on osteoclastic resorption pits, which showed that ZnTCP slightly reduced the resorption area by 15.5%, remarkably reduced the depth of resorption pits by 25.4% and therewith the volume of resorption pits by 53.9% compared to pure TCP [219].

In vivo studies in rabbit femora showed that 0.316 wt% of zinc was the optimum concentration at which the largest area of new bone was formed, in both ZnTCP and ZnTCP/HAp, whereas zinc content of 0.633 wt% was too high, enlarging the medullary cavity area by stimulated bone resorption [220]. Interestingly, the optimum zinc content in vivo was much lower than the zinc amount needed to exert a positive effect of osteoblast proliferation in vitro [157].

Copper-containing calcium phosphate ceramics have not been extensively investigated with regard to their bioactivity in bone regeneration, however, simple adsorption of copper ions on a calcium phosphate ceramic prepared at room temperature, showed a positive effect on angiogenesis in vitro and in vivo [221, 222]. This is an interesting finding, because poor vascularization is considered an important reason failure in timely and complete regeneration of large critically-sized bone defects.

In vitro bioactivity studies in SBF showed that Sr-HA, with a strontium content below 10 mol% showed a more pronounced apatite layer formation on the surface than pure HA, which can be contributed to a higher dissolution rate of strontium-containing ceramic [201, 223]. A similar observation was made in strontium-containing TCP [199]. Experiments with osteoprecursor cells (OPC1) showed that both the attachment and proliferation were increased in HA containing 20 mol% strontium as compared to the control without strontium. An increase in ALP and osteopontin were also increased, suggesting that strontium stimulated osteogenic differentiation of OPC1 cells [223]. Similar findings were also obtained in a study where osteoblast-like cells were cultured on strontium substituted biphasic calcium phosphate ceramic [224]. Pulsed-laser deposition was successfully used to apply a coating of

strontium-doped HA, prepared by an aqueous precipitation method, on metallic substrates. Osteogenic differentiation of human osteoblasts MG-63 was stimulated by strontium (3-7 at.% in the coating), whereas proliferation of osteoclasts was negatively affected [225].

Injection of strontium containing calcium-phosphate cement into rabbit iliac crest cancellous bone revealed that Sr-HA stimulated the formation of osteoblast, osteoid layers and hence new bone formation [226].

Fluoridated HA showed a positive effect on proliferation and osteogenic differentiation of cells. In a study by Wang and coworkers, MG-63 human osteosarcoma cells were cultured on fluoridated HA coatings produced by a sol-gel dipping method. Positive effect on fluoride on cell attachment, as well as ALP and osteocalcin production were observed in a certain concentration range [209], at which the ceramic coating had the lowest solubility. A positive effect fluoride on cell proliferation and osteogenic differentiation was also observed when SaOS-3 rat osteosarcoma cells were cultured on fluoridated HA discs in comparison to fluoride-free controls [227]. In a study by Inoue and co-workers, fluoridated apatite ceramics were tested in a short-term implantation model in rat tibia. A more pronounced bone formation was observed in fluoride containing ceramic as compared to the an unsintered calcium-deficient apatite ceramic [228].

Redey and coworkers showed a poor attachment and low collagen production of human primary osteoblasts on carbonated apatite ceramic as compared to HA ceramic, possibly caused by the difference in wettability between the two ceramics [229], which is in agreement with other reports showing a positive correlation between surface energy and attachment of cells [230-232]. After initial cell attachment, however, no significant difference was found in further proliferation of the cells between carbonated and pure HA ceramic. Similar to osteoblast attachment, osteoclast attachment was more pronounced on carbonate-free ceramics as compared to the carbonated one, while no difference was observed on the spreading of cells after initial attachment [233]. Doi et. al. showed that CA was resorbed by osteoclasts in 2-day cultures, while HA remained unresorbed, suggesting that the presence of carbonate may play an crucial role in osteoclastic resorption [234], which was in accordance with the results obtained in an in vivo experiment in rats [235]. A possible reason could be the released carbonate that stimulates carbonic anhydrase activity and hence promotes acid secretion by osteoclasts [236]. Also Spence and co-workers recently observed an increase in osteoclastic resorption with an increase of carbonate content in an HA ceramic [237]. In an in vivo study in rabbits by Landi and coworkers, higher amount of new bone formation was found in sintered carbonated apatite ceramic, as compared to the pure HA ceramic [238]. An increase in the amount of newly formed bone with increasing carbonate content in an apatite ceramic was also observed in a rat femur model [239]. In a recent study in a critical-size iliac wing model in goats, it was shown that an increase in carbonate content of a ceramic does not necessarily lead to more bone formation if other ceramic properties are not controlled [179].

Simultaneous incorporation of fluoride and carbonate into apatites led to inhibition of osteoclast proliferation and pit formation in vitro as compared to pure HA and carbonated apatites, whereas in vivo, faster bone remodeling was observed [240].

7 FUTURE PERSPECTIVES

Incorporation of inorganic additives in order to improve the biological performance of the existing bone graft substitutes is a complex matter, as we tried to demonstrate in the previous sections, in which we summarized some of the work performed on preparation, characterization and biological activity assessment of ceramics containing zinc, copper, strontium, fluoride and carbonate. Incorporation of these additives into calcium-phosphate bone graft substitutes not only adds an additional element into the structure, that can exert a certain function, but it also changes intrinsic properties of the recipient material. The way and the efficiency of incorporation are dependent on the method used. That in turn affects the release profile of the incorporated additive, but it also affects the solubility of the recipient itself. And all this affects the behavior of osteoblasts and osteoclasts in vitro, as well as the in vivo bone formation and remodeling. And although it is almost impossible to make general statements on the effect of additives to the existing bone graft substitutes, some careful conclusions can be drawn from the work performed so far. Zinc incorporation into β-TCP is responsible for a reduction in cell unit and a decrease in solubility of the ceramic. Zinc has shown positive effects on proliferation and osteogenic differentiation of bone forming cells and decreased osteoclastic resorption in vitro, but this effect was dose dependent. Some promising results were observed with regard to bone forming capacity in in vivo preclinical models with zinc doped β-TCP. Copper was shown to have similar effect on crystal properties as zinc, and although copper doped ceramics have not been tested in detail, there is some evidence that copper can stimulate angiogenesis, which is of great importance in bone regeneration. Strontium, that is substituent to calcium, increases the size of the cell unit as well as the solubility of the ceramic. Proliferation and osteogenic differentiation of osteoblastic cells were shown to be increased in strontium-substituted ceramics, whereas the effect on osteoclast growth was negative. Replacement of OH^- with F^- in an apatite lattice can bring about a reduction in the volume of the unit cell and a concomitant increase in structure stability. Fluoridated apatites can stimulate osteoblast proliferation and osteogenic differentiation, but in a dose dependent manner. Finally, carbonate is responsible for a decrease in crystal size of an apatitic crystal and an increase in ceramic solubility. Attachment of osteoblastic cells on carbonated ceramics was poorer than on the hydroxyapatite ones, but proliferation was not affected. Osteoclast proliferation and resorption potential were higher on the carbonate-containing calcium-phosphate ceramics as compared to the control ceramics without carbonate.

As already mentioned, these are some general remarks about the effects of various additives on properties and efficiency of the existing bone graft substitutes. But due to variations in the preparation and characterization methods and assessment of biological performance of these materials, a comparison among the studies and the results obtained is hard to make, and hence general conclusions cannot be drawn. This problem is not only associated with the materials discussed here, but it holds for the whole field of biomaterials research. We therefore believe that standardized, high-throughput methods of investigating the behavior of materials in vitro to predict their performance in vivo, are required in order to obtain true directions for how to improve the existing bone graft substitutes. We have recently published a study, in which thin apatitic coatings, containing a number of inorganic additives in vary-

ing concentrations were deposited into the wells of the standard tissue culture well plates, to assess the effect of additives on the behavior of osteoblasts and osteoclasts. This medium-throughput approach was a first step to investigate a large number of parameters in a systematic way in a single study [241]. Further work focuses on developing true high-throughput systems using microfluidics, in which gradients of additives and their combinations can be established to investigate the effect of large number of concentrations as well as combinations of additives at varying concentration in a controlled and systematic manner.

REFERENCES

1.   Fawcett, D.W., Bone, in A textbook of histology, W. Bloom and D.W. Fawcett, Editors. 1986, W.B. Saunders Company: Philadelphia, USA. p. 199-238.

2.   Derkx, P., et al., Immunolocalization and quantification of noncollagenous bone matrix proteins in methylmethacrylate-embedded adult human bone in combination with histomorphometry. Bone, 1998. 22(4): p. 367-73.

3.   Marks, S.C. and D.C. Hermey, Jr., The structure and development of bone, in Principles of bone biology, J.P. Bilezikian, L.G. Raisz, and G.A. Rodan, Editors. 1996, Academic Press: San Diego, USA. p. 3-14.

4.   Bigi, A., et al., Chemical and structural characterization of the mineral phase from cortical and trabecular bone. J Inorg Biochem, 1997. 68(1): p. 45-51.

5.   Brown, K.L. and R.L. Cruess, Bone and cartilage transplantation in orthopaedic surgery. A review. J Bone Joint Surg Am, 1982. 64(2): p. 270-9.

6.   Damien, C.J. and J.R. Parsons, Bone graft and bone graft substitutes: a review of current technology and applications. J Appl Biomater, 1991. 2(3): p. 187-208.

7.   de Boer, H.H., The history of bone grafts. Clin Orthop, 1988. 226(226): p. 292-8.

8.   Yaszemski, M.J., et al., Evolution of bone transplantation: molecular, cellular and tissue strategies to engineer human bone. Biomaterials, 1996. 17(2): p. 175-85.

9.   Lane, J.M., E. Tomin, and M.P. Bostrom, Biosynthetic bone grafting. Clin Orthop, 1999. 367 Suppl: p. S107-17.

10.   Urist, M.R., Bone: formation by autoinduction. Science, 1965. 150(698): p. 893-9.

11.   Cornell, C.N. and J.M. Lane, Current understanding of osteoconduction in bone regeneration. Clin Orthop, 1998. 355 Suppl: p. S267-73.

12.   Coombes, A.G. and M.C. Meikle, Resorbable synthetic polymers as replacements for bone graft. Clin Mater, 1994. 17(1): p. 35-67.

13.   Arrington, E.D., et al., Complications of iliac crest bone graft harvesting. Clin Orthop, 1996. 329: p. 300-309.

14.   Cowley, S.P. and L.D. Anderson, Hernias through donor sites for iliac-bone grafts. J Bone Joint Surg Am, 1983. 65(7): p. 1023-5.

15.   Prolo, D.J. and J.J. Rodrigo, Contemporary bone graft physiology and surgery. Clin Orthop,

1985. 200: p. 322-42.

16.   Younger, E.M. and M.W. Chapman, Morbidity at bone graft donor sites. J Orthop Trauma, 1989. 3(3): p. 192-5.

17.   Anderson, M., et al., Critical size defect in the goat's os ilium. A model to evaluate bone grafts and substitutes. Clin Orthop, 1999. 364: p. 231-9.

18.   Oikarinen, J. and L.K. Korhonen, The bone inductive capacity of various bone transplanting materials used for treatment of experimental bone defects. Clin Orthop, 1979. 140: p. 208-15.

19.   Oklund, S.A., et al., Quantitative comparisons of healing in cranial fresh autografts, frozen autografts and processed autografts, and allografts in canine skull defects. Clin Orthop, 1986. 205: p. 269-91.

20.   Brantigan, J.W., et al., Compression strength of donor bone for posterior lumbar interbody fusion. Spine, 1993. 18(9): p. 1213-21.

21.   Urist, M.R., et al., The bone induction principle. Clin Orthop, 1967. 53: p. 243-83.

22.   Habibovic, P., et al., Comparative in vivo study of six hydroxyapatite-based bone graft substitutes. J Orthop Res, 2008. 26(10): p. 1363-70.

23.   Le Nihouannen, D., et al., Ectopic bone formation by microporous calcium phosphate ceramic particles in sheep muscles. Bone, 2005. 36(6): p. 1086-93.

24.   Habibovic, P., et al., Osteoconduction and osteoinduction of low-temperature 3D printed bioceramic implants. Biomaterials, 2008. 29(7): p. 944-53.

25.   Habibovic, P., et al., 3D microenvironment as essential element for osteoinduction by biomaterials. Biomaterials, 2005. 26(17): p. 3565-75.

26.   Ben-Nissan, B., C.S. Chai, and K.A. Gross, Effect of solution aging on sol-gel hydroxyapatite coatings. Bioceramics, 1997. 10: p. 175-178.

27.   Ducheyne, P., et al., Structural analysis of hydroxyapatite coatings on titanium. Biomaterials, 1986. 7(2): p. 97-103.

28.   Havelin, L.I., et al., The Norwegian Arthroplasty Register: 11 years and 73,000 arthroplasties. Acta Orthop Scand, 2000. 71(4): p. 337-53.

29.   Ong, J.L., et al., Structure, solubility and bond strength of thin calcium phosphate coatings produced by ion beam sputter deposition. Biomaterials, 1992. 13(4): p. 249-54.

30.   Liu, Y., Hunziker, E. B., Layrolle, P., de Bruijn, J. D. and de Groot, K., Bone morphogenetic protein 2 incorporated into biomimetic coatings retains its biological activity. Tissue Eng, 2004. 10(1-2): p. 101-8.

31.   Guan, L. and J.E. Davies, Preparation and characterization of a highly macroporous biodegradable composite tissue engineering scaffold. J Biomed Mater Res A, 2004. 71(3): p. 480-7.

32.   Zardiackas, L.D., et al., Torsional properties of healed canine diaphyseal defects grafted with a fibrillar collagen and hydroxyapatite/tricalcium phosphate composite. J Appl Biomater, 1994. 5(4): p. 277-83.

33.   Zhang, R. and P.X. Ma, Poly(alpha-hydroxyl acids)/hydroxyapatite porous composites for

bone-tissue engineering. I. Preparation and morphology. J Biomed Mater Res, 1999. 44(4): p. 446-55.

34.	Blokhuis, T.J., et al., Resorbable calcium phosphate particles as a carrier material for bone marrow in an ovine segmental defect. J Biomed Mater Res, 2000. 51(3): p. 369-75.

35.	Boden, S.D., et al., The use of coralline hydroxyapatite with bone marrow, autogenous bone graft, or osteoinductive bone protein extract for posterolateral lumbar spine fusion. Spine, 1999. 24(4): p. 320-7.

36.	Zdeblick, T.A., et al., Anterior cervical discectomy and fusion using a porous hydroxyapatite bone graft substitute. Spine, 1994. 19(20): p. 2348-57.

37.	Langer, R. and J.P. Vacanti, Tissue engineering. Science, 1993. 260(5110): p. 920-6.

38.	Kirker-Head, C.A., Potential applications and delivery strategies for bone morphogenetic proteins. Adv Drug Deliv Rev, 2000. 43(1): p. 65-92.

39.	Geesink, R.G., N.H. Hoefnagels, and S.K. Bulstra, Osteogenic activity of OP-1 bone morphogenetic protein (BMP-7) in a human fibular defect. J Bone Joint Surg Br, 1999. 81(4): p. 710-8.

40.	Johnson, E.E., M.R. Urist, and G.A. Finerman, Repair of segmental defects of the tibia with cancellous bone grafts augmented with human bone morphogenetic protein. A preliminary report. Clin Orthop, 1988(236): p. 249-57.

41.	Johnson, E.E. and M.R. Urist, Human bone morphogenetic protein allografting for reconstruction of femoral nonunion. Clin Orthop, 2000. 371: p. 61-74.

42.	Nefussi, J.R., et al., Sequential expression of bone matrix proteins during rat calvaria osteoblast differentiation and bone nodule formation in vitro. J Histochem Cytochem, 1997. 45(4): p. 493-503.

43.	Wada, Y., et al., Changes in osteoblast phenotype during differentiation of enzymatically isolated rat calvaria cells. Bone, 1998. 22(5): p. 479-85.

44.	Miura, Y. and S.W. O'Driscoll, Culturing periosteum in vitro: the influence of different sizes of explants. Cell Transplant, 1998. 7(5): p. 453-7.

45.	Takushima, A., Y. Kitano, and K. Harii, Osteogenic potential of cultured periosteal cells in a distracted bone gap in rabbits. J Surg Res, 1998. 78(1): p. 68-77.

46.	Gundle, R., C.J. Joyner, and J.T. Triffitt, Interactions of human osteoprogenitors with porous ceramic following diffusion chamber implantation in a xenogeneic host. J Mater Sci Mater Med, 1997. 8(8): p. 519-23.

47.	Robey, P.G. and J.D. Termine, Human bone cells in vitro. Calcif Tissue Int, 1985. 37(5): p. 453-60.

48.	Bruder, S.P. and B.S. Fox, Tissue engineering of bone. Cell based strategies. Clin Orthop, 1999. 367 Suppl: p. S68-83.

49.	Doherty, M.J., et al., Vascular pericytes express osteogenic potential in vitro and in vivo. J Bone Miner Res, 1998. 13(5): p. 828-38.

50.	Friedenstein, A.J., R.K. Chailakhyan, and U.V. Gerasimov, Bone marrow osteogenic stem cells: in vitro cultivation and transplantation in diffusion chambers. Cell Tissue Kinet, 1987. 20(3): p. 263-72.

51. Maniatopoulos, C., J. Sodek, and A.H. Melcher, Bone formation in vitro by stromal cells obtained from bone marrow of young adult rats. Cell Tissue Res, 1988. 254(2): p. 317-30.

52. Ohgushi, H. and M. Okumura, Osteogenic capacity of rat and human marrow cells in porous ceramics. Experiments in athymic (nude) mice. Acta Orthop Scand, 1990. 61(5): p. 431-4.

53. Owen, M., Marrow stromal stem cells. J Cell Sci Suppl, 1988. 10: p. 63-76.

54. Beresford, J.N., Osteogenic stem cells and the stromal system of bone and marrow. Clin Orthop, 1989(240): p. 270-80.

55. Muschler, G.F., C. Boehm, and K. Easley, Aspiration to obtain osteoblast progenitor cells from human bone marrow: the influence of aspiration volume. J Bone Joint Surg Am, 1997. 79(11): p. 1699-709.

56. Allay, J., et al., LacZ and interleukin-3 expression in vivo after retroviral transduction of marrow-derived human osteogenic mesenchymal progenitors. Hum Gene Ther, 1997. 8(12): p. 1417-27.

57. Friedenstein, A.J., et al., Marrow microenvironment transfer by heterotopic transplantation of freshly isolated and cultured cells in porous sponges. Exp Hematol, 1982. 10(2): p. 217-27.

58. Bruder, S.P., et al., Bone regeneration by implantation of purified, culture-expanded human mesenchymal stem cells. J Orthop Res, 1998. 16(2): p. 155-62.

59. Cui, Q., et al., Comparison of lumbar spine fusion using mixed and cloned marrow cells. Spine, 2001. 26(21): p. 2305-10.

60. Krebsbach, P.H., et al., Repair of craniotomy defects using bone marrow stromal cells. Transplantation, 1998. 66(10): p. 1272-8.

61. Anselme, K., et al., Association of porous hydroxyapatite and bone marrow cells for bone regeneration. Bone, 1999. 25(2 Suppl): p. 51S-54S.

62. Kruyt, M.C., et al., Viable osteogenic cells are obligatory for tissue-engineered ectopic bone formation in goats. Tissue Eng, 2003. 9(2): p. 327-36.

63. Kruyt, M.C., et al., Optimization of bone-tissue engineering in goats. J Biomed Mater Res, 2004. 69B(2): p. 113-20.

64. Bruder, S.P., et al., The effect of implants loaded with autologous mesenchymal stem cells on the healing of canine segmental bone defects. J Bone Joint Surg Am, 1998. 80(7): p. 985-96.

65. Kruyt, M.C., et al., Bone tissue engineering in a critical size defect compared to ectopic implantations in the goat. J Orthop Res, 2004. 22(3): p. 544-51.

66. Petite, H., et al., Tissue-engineered bone regeneration. Nat Biotechnol, 2000. 18(9): p. 959-63.

67. Meijer, G.J., et al., Cell-based bone tissue engineering. PLoS Med, 2007. 4(2): p. e9.

68. Boden, S.D., Bioactive factors for bone tissue engineering. Clin Orthop, 1999. 367 Suppl: p. S84-94.

69. Hollinger, J.O., H. Uludag, and S.R. Winn, Sustained release emphasizing recombinant human bone morphogenetic protein-2. Adv Drug Deliv Rev, 1998. 31(3): p. 303-318.

70. Winn, S.R., H. Uludag, and J.O. Hollinger, Carrier systems for bone morphogenetic proteins. Clin Orthop, 1999. 367 Suppl: p. S95-106.

71.   Kruyt, M.C., Tissue engineering of bone: the applicability of cell-based strategies. 2003, Thesis, Department of Orthopaedics, University Medical Center Utrecht: Utrecht, The Netherlands. p. 186.

72.   Elliot, J.C., Structure and chemistry of the apatites and other calcium orthophosphates. 1994, Amsterdam: Elsevier.

73.   Becker, R.O., J.A. Spadaro, and E.W. Berg, The trace elements of human bone. J Bone Joint Surg Am, 1968. 50(2): p. 326-34.

74.   El-Amri, F.A. and M.A.R. El-Kabroun, Trace element concentration in human bone using instrumental neutron activation analysis. Journal of Radioanalytical and Nuclear Chemistry, 1997. 217(2): p. 205-207.

75.   Calhoun, N.R., J.C. Smith, Jr., and K.L. Becker, The role of zinc in bone metabolism. Clin Orthop Relat Res, 1974(103): p. 212-34.

76.   Oteiza, P.I. and G.G. Mackenzie, Zinc, oxidant-triggered cell signaling, and human health. Mol Aspects Med, 2005. 26(4-5): p. 245-55.

77.   Vallee, B.L. and D.S. Auld, Zinc coordination, function, and structure of zinc enzymes and other proteins. Biochemistry, 1990. 29(24): p. 5647-59.

78.   Vallee, B.L. and K.H. Falchuk, The biochemical basis of zinc physiology. Physiol Rev, 1993. 73(1): p. 79-118.

79.   Prasad, A.S., et al., Antioxidant effect of zinc in humans. Free Radic Biol Med, 2004. 37(8): p. 1182-90.

80.   Lowe, N.M., W.D. Fraser, and M.J. Jackson, Is there a potential therapeutic value of copper and zinc for osteoporosis? Proc Nutr Soc, 2002. 61(2): p. 181-5.

81.   Yamaguchi, M., et al., Effect of zinc on gene expression in osteoblastic MC3T3-E1 cells: enhancement of Runx2, OPG, and regucalcin mRNA expressions. Mol Cell Biochem, 2008. 312(1-2): p. 157-66.

82.   Kwun, I.S., et al., Zinc deficiency suppresses matrix mineralization and retards osteogenesis transiently with catch-up possibly through Runx 2 modulation. Bone, 2009.

83.   Cerovic, A., et al., Effects of zinc on the mineralization of bone nodules from human osteoblast-like cells. Biol Trace Elem Res, 2007. 116(1): p. 61-71.

84.   Wang, T., et al., Effect of zinc ion on the osteogenic and adipogenic differentiation of mouse primary bone marrow stromal cells and the adipocytic trans-differentiation of mouse primary osteoblasts. J Trace Elem Med Biol, 2007. 21(2): p. 84-91.

85.   Yamaguchi, M., Role of nutritional zinc in the prevention of osteoporosis. Mol Cell Biochem, 2009.

86.   O'Dell, B.L., Roles for iron and copper in connective tissue biosynthesis. Philos Trans R Soc Lond B Biol Sci, 1981. 294(1071): p. 91-104.

87.   Tinker, D., N. Romero, and R. Rucker, The role of copper and crosslinking in elastin accumulation., in Trace element in man and animals L. Hurley, et al., Editors. 1988, Plenum Press: New York. p. 277-278.

88.   Rucker, R.B., et al., Copper, lysyl oxidase, and extracellular matrix protein cross-linking. Am J Clin Nutr, 1998. 67(5 Suppl): p. 996S-1002S.

89.   Howell, J.M. and A.N. Davison, The copper content and cytochrome oxidase activity of tissues from normal and swayback lambs. Biochem J, 1959. 72(2): p. 365-8.

90.   Strain, J.J., A reassessment of diet and osteoporosis--possible role for copper. Med Hypotheses, 1988. 27(4): p. 333-8.

91.   Paterson, C.R., Osteogenesis imperfecta and other bone disorders in the differential diagnosis of unexplained fractures. J R Soc Med, 1990. 83(2): p. 72-4.

92.   Allen, T.M., A. Manoli, 2nd, and R.L. LaMont, Skeletal changes associated with copper deficiency. Clin Orthop Relat Res, 1982(168): p. 206-10.

93.   Fromigue, O., P.J. Marie, and A. Lomri, Bone morphogenetic protein-2 and transforming growth factor-beta2 interact to modulate human bone marrow stromal cell proliferation and differentiation. J Cell Biochem, 1998. 68(4): p. 411-26.

94.   Rico, H., Minerals and osteoporosis. Osteoporos Int, 1991. 2(1): p. 20-5.

95.   Wilson, T., J.M. Katz, and D.H. Gray, Inhibition of active bone resorption by copper. Calcif Tissue Int, 1981. 33(1): p. 35-9.

96.   Eriksen, E.F., G.Z. Eghbali-Fatourechi, and S. Khosla, Remodeling and vascular spaces in bone. J Bone Miner Res, 2007. 22(1): p. 1-6.

97.   Ito, H., et al., Remodeling of cortical bone allografts mediated by adherent rAAV-RANKL and VEGF gene therapy. Nat Med, 2005. 11(3): p. 291-7.

98.   Hu, G.F., Copper stimulates proliferation of human endothelial cells under culture. J Cell Biochem, 1998. 69(3): p. 326-35.

99.   Parke, A., et al., Characterization and quantification of copper sulfate-induced vascularization of the rabbit cornea. Am J Pathol, 1988. 130(1): p. 173-8.

100.   Sen, C.K., et al., Copper-induced vascular endothelial growth factor expression and wound healing. Am J Physiol Heart Circ Physiol, 2002. 282(5): p. H1821-7.

101.   Halliwell, B. and J.M. Gutteridge, Role of free radicals and catalytic metal ions in human disease: an overview. Methods Enzymol, 1990. 186: p. 1-85.

102.   Skoryna, S., Metabolic aspects of the pharmacologic uses of the trace elements in human subjects with specific reference to stable strontium. Trace Subst Environ Health, 1984(18): p. 3-23.

103.   Jensen, J.-E., H. Stang, and B. Kringsholm, Relationship between trace element content and mechanical bone strength. Bone, 1997(20).

104.   Grynpas, M.D. and P.J. Marie, Effects of low doses of strontium on bone quality and quantity in rats. Bone, 1990. 11(5): p. 313-9.

105.   Marie, P.J., et al., Effect of low doses of stable strontium on bone metabolism in rats. Miner Electrolyte Metab, 1985. 11(1): p. 5-13.

106.   Marie, P.J. and M. Hott, Short-term effects of fluoride and strontium on bone formation and resorption in the mouse. Metabolism, 1986. 35(6): p. 547-51.

107.   Schrooten, I., et al., Strontium causes osteomalacia in chronic renal failure rats. Kidney Int, 1998. 54(2): p. 448-56.

108.   Verberckmoes, S.C., M.E. De Broe, and P.C. D'Haese, Dose-dependent effects of strontium on osteoblast function and mineralization. Kidney Int, 2003. 64(2): p. 534-43.

109.   Marie, P.J., et al., S12911, a new agent containing strontium, inhibits bone loss due to immobilization in rats. J bone Miner Res, 1995. 10(Suppl. 1).

110.   Baron, R. and Y. Tsouderos, In vitro effects of S12911-2 on osteoclast function and bone marrow macrophage differentiation. Eur J Pharmacol, 2002. 450(1): p. 11-7.

111.   Canalis, E., A. Giustina, and J.P. Bilezikian, Mechanisms of anabolic therapies for osteoporosis. N Engl J Med, 2007. 357(9): p. 905-16.

112.   O'Donnell, S., et al., Strontium ranelate for preventing and treating postmenopausal osteoporosis. Cochrane Database Syst Rev, 2006(4): p. CD005326.

113.   Meunier, P.J., et al., The effects of strontium ranelate on the risk of vertebral fracture in women with postmenopausal osteoporosis. N Engl J Med, 2004. 350(5): p. 459-68.

114.   Kleerekoper, M., Fluoride and the skeleton, in Principles of bone biology, J.P. Bilezikian, L.G. Raisz, and G.A. Rodan, Editors. 1996, Academic Press: San Diego. p. 1053-1062.

115.   Richards, A., Nature and mechanisms of dental fluorosis in animals. J Dent Res, 1990. 69 Spec No: p. 701-5; discussion 721.

116.   Richards, A., et al., Dental fluorosis developed in post-secretory enamel. J Dent Res, 1986. 65(12): p. 1406-9.

117.   Kierdorf, U., et al., Structural changes in fluorosed dental enamel of red deer (Cervus elaphus L.) from a region with severe environmental pollution by fluorides. J Anat, 1996. 188 (Pt 1): p. 183-95.

118.   Larsen, M.J., et al., Enamel fluoride, dental fluorosis and dental caries among immigrants to and permanent residents of five Danish fluoride areas. Caries Res, 1986. 20(4): p. 349-55.

119.   Suckling, G., D.C. Thurley, and D.G. Nelson, The macroscopic and scanning electron-microscopic appearance and microhardness of the enamel, and the related histological changes in the enamel organ of erupting sheep incisors resulting from a prolonged low daily dose of fluoride. Arch Oral Biol, 1988. 33(5): p. 361-73.

120.   Farley, S.M., et al., Fluoride therapy for osteoporosis: characterization of the skeletal response by serial measurements of serum alkaline phosphatase activity. Metabolism, 1987. 36(3): p. 211-8.

121.   Gabuda, S., et al., Structural forms of fl uorides in bone tissue of animals under chronic fluoride intoxication. J Struct Chem (Engl Transl), 2006(47): p. 258-266.

122.   Mackie, E.J., Osteoblasts: novel roles in orchestration of skeletal architecture. Int J Biochem Cell Biol, 2003. 35(9): p. 1301-5.

123.   Briancon, D. and P.J. Meunier, Treatment of osteoporosis with fluoride, calcium, and vitamin D. Orthop Clin North Am, 1981. 12(3): p. 629-48.

124.   Mamelle, N., et al., Risk-benefit ratio of sodium fluoride treatment in primary vertebral osteoporosis. Lancet, 1988. 2(8607): p. 361-5.

125.   Riggs, B.L., et al., Effect of the fluoride/calcium regimen on vertebral fracture occurrence in postmenopausal osteoporosis. Comparison with conventional therapy. N Engl J Med, 1982. 306(8): p. 446-50.

126.   Riggs, B.L., et al., Effect of fluoride treatment on the fracture rate in postmenopausal women with osteoporosis. N Engl J Med, 1990. 322(12): p. 802-9.

127.   Bellows, C.G., J.N. Heersche, and J.E. Aubin, The effects of fluoride on osteoblast progenitors in vitro. J Bone Miner Res, 1990. 5 Suppl 1: p. S101-5.

128.   Qu, W.J., et al., Sodium fluoride modulates caprine osteoblast proliferation and differentiation. J Bone Miner Metab, 2008. 26(4): p. 328-34.

129.   Burgener, D., J.P. Bonjour, and J. Caverzasio, Fluoride increases tyrosine kinase activity in osteoblast-like cells: regulatory role for the stimulation of cell proliferation and Pi transport across the plasma membrane. J Bone Miner Res, 1995. 10(1): p. 164-71.

130.   Okuda, A., J. Kanehisa, and J.N. Heersche, The effects of sodium fluoride on the resorptive activity of isolated osteoclasts. J Bone Miner Res, 1990. 5 Suppl 1: p. S115-20.

131.   Taylor, M.L., et al., The effect of fluoride on the resorption of dentine by osteoclasts in vitro. J Bone Miner Res, 1990. 5 Suppl 1: p. S121-30.

132.   LeGeros, R.Z., Calcium phosphates in oral biology and medicine. Vol. 15. 1991, Basel, Switserland: Karger. 200.

133.   Rey, C., et al., Fourier transform infrared spectroscopic study of the carbonate ions in bone mineral during aging. Calcif Tissue Int, 1991. 49(4): p. 251-8.

134.   Elliott, J.C., D.W. Holcomb, and R.A. Young, Infrared determination of the degree of substitution of hydroxyl by carbonate ions in human dental enamel. Calcif Tissue Int, 1985. 37(4): p. 372-5.

135.   Rey, C., et al., The carbonate environment in bone mineral: a resolution-enhanced fourier transform infrared spectroscopy study. Calcif Tissue Int, 1989. 45: p. 157-64.

136.   Legeros, R.Z., et al., Apatite Crystallites: Effects of Carbonate on Morphology. Science, 1967. 155(3768): p. 1409-1411.

137.   Massaro, C., et al., Surface and biological evaluation of hydroxyapatite-based coatings on titanium deposited by different techniques. J Biomed Mater Res, 2001. 58(6): p. 651-7.

138.   Willmann, G., Coating of implants with hydroxyapatite materials connections between bone and metals. Adv Eng Mater, 1999. 1: p. 95-105.

139.   Bonel, G., et al., Apatitic calcium orthophosphates and related compounds for biomaterials preparation. Ann N Y Acad Sci, 1988. 523: p. 115-30.

140.   Barrere, F., et al., Biomimetic calcium phosphate coatings on Ti6AI4V: a crystal growth study of octacalcium phosphate and inhibition by Mg2+ and HCO3. Bone, 1999. 25(2 Suppl): p. 107S-111S.

141.   Barrere, F., et al., Nucleation of biomimetic Ca-P coatings on ti6A14V from a SBF x 5 solution: influence of magnesium. Biomaterials, 2002. 23(10): p. 2211-20.

142.   Patntirapong, S., P. Habibovic, and P.V. Hauschka, Effects of soluble cobalt and cobalt incorporated into calcium phosphate layers on osteoclast differentiation and activation. Biomaterials, 2009.

30(4): p. 548-55.

143.   T, K., et al., Apatite coating on various substrates in simulated body fluid. Bioceramics, 1989. 2: p. 235-242.

144.   Zhitomirsky, I., New developments in electrolytic deposition of ceramic films. Am Ceram Soc Bull, 2000(79): p. 57-63.

145.   Kim, H.W., et al., Hydroxyapatite coating on titanium substrate with titania buffer layer processed by sol-gel method. Biomaterials, 2004. 25(13): p. 2533-8.

146.   Liu, D.M., T. Troczynski, and W.J. Tseng, Water-based sol-gel synthesis of hydroxyapatite: process development. Biomaterials, 2001. 22(13): p. 1721-30.

147.   Thian, E.S., et al., Processing of HA-coated Ti-6Al-4V by a ceramic slurry approach: an in vitro study. Biomaterials, 2001. 22(11): p. 1225-32.

148.   Cleries, L., J.M. Fernandez-Pradas, and J.L. Morenza, Bone growth on and resorption of calcium phosphate coatings obtained by pulsed laser deposition. J Biomed Mater Res, 2000. 49(1): p. 43-52.

149.   Cleries, L., J.M. Fernandez-Pradas, and J.L. Morenza, Behavior in simulated body fluid of calcium phosphate coatings obtained by laser ablation. Biomaterials, 2000. 21(18): p. 1861-5.

150.   Cleries, L., et al., Application of dissolution experiments to characterise the structure of pulsed laser-deposited calcium phosphate coatings. Biomaterials, 1999. 20(15): p. 1401-5.

151.   Cleries, L., et al., Mechanical properties of calcium phosphate coatings deposited by laser ablation. Biomaterials, 2000. 21(9): p. 967-71.

152.   Fernandez-Pradas, J.M., et al., Influence of thickness on the properties of hydroxyapatite coatings deposited by KrF laser ablation. Biomaterials, 2001. 22(15): p. 2171-5.

153.   Ishizawa, H., M. Fujino, and M. Ogino, Histomorphometric evaluation of the thin hydroxyapatite layer formed through anodization followed by hydrothermal treatment. J Biomed Mater Res, 1997. 35(2): p. 199-206.

154.   Ishizawa, H. and M. Ogino, Formation and characterization of anodic titanium oxide films containing Ca and P. J Biomed Mater Res, 1995. 29(1): p. 65-72.

155.   Ishizawa, H. and M. Ogino, Characterization of thin hydroxyapatite layers formed on anodic titanium oxide films containing Ca and P by hydrothermal treatment. J Biomed Mater Res, 1995. 29(9): p. 1071-9.

156.   Jolly, W.L., ed. The Synthesis and Characterization of Inorganic Compounds. 1970, Prentice Hall, Englewood Cliffs, : NJ. 231.

157.   Ito, A., et al., Preparation, solubility, and cytocompatibility of zinc-releasing calcium phosphate ceramics. J Biomed Mater Res, 2000. 50(2): p. 178-83.

158.   Bigi, A., et al., Isomorphous substitutions in [beta]-tricalcium phosphate: The different effects of zinc and strontium. J Inorg Biochem, 1997. 66: p. 259-265.

159.   Ito, A., et al., Zinc-releasing calcium phosphate for stimulating bone formation. Materials Science and Engineering: C, 2002. 22(1): p. 21-25.

160.   Jallot, E., et al., STEM and EDXS characterisation of physico-chemical reactions at the periphery of sol-gel derived Zn-substituted hydroxyapatites during interactions with biological fluids. Colloids Surf B Biointerfaces, 2005. 42(3-4): p. 205-10.

161.   Bigi, A., et al., Inhibiting effect of zinc on hydroxylapatite crystallization. J Inorg Biochem, 1995. 58: p. 49-58.

162.   Li, Z.Y., et al., Chemical composition, crystal size and lattice structural changes after incorporation of strontium into biomimetic apatite. Biomaterials, 2007. 28(7): p. 1452-60.

163.   Balamurugan, A., et al., Sol-gel synthesis and spectrometric structural evaluation of strontium substituted hydroxyapatite. Materials Science and Engineering: C, 2009. 29: p. 1006-1009.

164.   Belik, A.A., B.I. Yanov, and Lazoryak, Synthesis and crystal structure of Ca9Cu1.5(PO4)7 and reinvestigation of Ca9.5Cu(PO4)7. Materials Reasearch Bulletin 2001. 36: p. 1863-1871.

165.   Okazaki, M., et al., Functionally graded fluoridated apatites. Biomaterials, 1999. 20(15): p. 1421-6.

166.   Okazaki, M., et al., Fluoridated apatite synthesized using a multi-step fluoride supply system. Biomaterials, 1999. 20(14): p. 1303-7.

167.   Bouslama, N., F. Ben Ayed, and J. Bouaziz, Effect of fluorapatite additive on densification and mechanical properties of tricalcium phosphate. J Mech Behav Biomed Mater, 2010. 3(1): p. 2-13.

168.   Elliot, J.C., Studies in inorganic chemistry: structure and chemistry of the apatites and other calcium orthophosphates. 1994, Amsterdam, The Netherlands: Elsevier Science. 389.

169.   Grynpas, M.D., Fluoride effects on bone crystals. J Bone Miner Res, 1990. 5 Suppl 1: p. S169-75.

170.   Elliott, J.C., The problems of the composition and structure of the mineral components of the hard tissues. Clin Orthop Relat Res, 1973(93): p. 313-45.

171.   Nelson, D.G. and J.D. Featherstone, Preparation, analysis, and characterization of carbonated apatites. Calcif Tissue Int, 1982. 34 Suppl 2: p. S69-81.

172.   Vignoles, M., G. Bonel, and R.A. Young, Occurrence of nitrogenous species in precipitated B-type carbonated hydroxyapatites. Calcif Tissue Int, 1987. 40(2): p. 64-70.

173.   Doi, Y., et al., Carbonate apatites from aqueous and non-aqueous media studied by ESR, IR, and X-ray diffraction: effect of NH4+ ions on crystallographic parameters. J Dent Res, 1982. 61(2): p. 429-34.

174.   Gibson, I.R. and W. Bonfield, Novel synthesis and characterization of an AB-type carbonate-substituted hydroxyapatite. J Biomed Mater Res, 2002. 59(4): p. 697-708.

175.   Landi, E., et al., Influence of synthesis and sintering parameters on the characteristics of carbonate apatite. Biomaterials, 2004. 25(10): p. 1763-70.

176.   Barralet, J.E., S.M. Best, and W. Bonfield, Effect of sintering parameters on the density and microstructure of carbonate hydroxyapatite. J Mater Sci Mater Med, 2000. 11(11): p. 719-24.

177.   Ellies, L.G., D.G. Nelson, and J.D. Featherstone, Crystallographic structure and surface morphology of sintered carbonated apatites. J Biomed Mater Res, 1988. 22(6): p. 541-53.

178.   Barinov, S.M., et al., Carbonate release from carbonated hydroxyapatite in the wide tempera-ture rage. J Mater Sci Mater Med, 2006. 17(7): p. 597-604.

179.   Habibovic, P., et al., Comparison of two carbonated apatite ceramics in vivo. Acta Biomater, 2009.

180.   Schroeder, L.W., B. Dickens, and W.E. Brown, Crystallographic studies of the role of Mg as a stabilizing impurity in h-Ca3(PO4)2: II. Refinement of Mg-containing B-Ca3(PO4)2. J. Solid State Chem., 1977. 22: p. 253-262.

181.   Sogo, Y., et al., Hydrolysis and cytocompatibility of zinc-containing a-tricalcium phosphate powder. Materials Science and Engineering C, 2004. 24: p. 709-715.

182.   Ito, A., et al., Zinc-concontaining tricalcium phosphate and related materials for promoting bone formation. Current Applied Physics, 2005. 5: p. 402-406.

183.   Ito, A., et al., Resorbability and solubility of zinc-containing tricalcium phosphate. J Biomed Mater Res, 2002. 60(2): p. 224-31.

184.   Otsuka, M., et al., Calcium level-responsive in-vitro zinc release from zinc containing trical-cium phosphate (ZnTCP). J Biomed Mater Res, 2000. 52(4): p. 819-24.

185.   Bandyopadhyay, A., et al., Influence of Zno doping in calcium phosphate ceramics. Materials Science and Engineering C, 2007. 27: p. 14-17.

186.   Kannan, S., et al., Synthesis and structure refinement of zinc-doped B-Tricalcium Phosphate powders. J. Am. Ceram. Soc., 2009. 92(7): p. 1592-1595.

187.   Gutowska, I., Z. Machoy, and B. Machalinski, The role of bivalent metals in hydroxyapatite structures as revealed by molecular modeling with the HyperChem software. J Biomed Mater Res A, 2005. 75(4): p. 788-93.

188.   Enderle, R., et al., Influence of magnesium doping on the phase transformation temperature of beta-TCP ceramics examined by Rietveld refinement. Biomaterials, 2005. 26(17): p. 3379-84.

189.   B.Dickens, L.W. Schroeder, and W.E. Brown, Crystallographic studies of the role of Mg as a stabilizing impurity in B-Ca3(PO4)2. I. The crystal structure of pure B-Ca3(PO4)2. J. Solid State Chem., C1974. 10: p. 232-248.

190.   Chung, R.-J., et al., Anti-Microbial Hydroxyapatite Particles Synthesized by a Sol - Gel Route. Journal of Sol-Gel Science and Technology, 2005. 33: p. 229-239.

191.   Webster, T.J., et al., Osteoblast response to hydroxyapatite doped with divalent and trivalent cations. Biomaterials, 2004. 25(11): p. 2111-21.

192.   Li, M., et al., Structural characterization of zinc-substituted hydroxyapatite prepared by hydro-thermal method. J Mater Sci Mater Med, 2008. 19(2): p. 797-803.

193.   Ito, A., et al., Dissolution studies of Zn-containing carbonated hydroxyapatites. Key Eng Mater, 2001: p. 192-195.

194.   I, M. and F. JDB, Dissolution studies of Zn-containing carbonated hydroxyapatites. J Crystal Growth, 2000. 219: p. 98-101.

195.   Shannon, R. and C. Prewitt, Effective ionic radii in oxides and fluorides. Acta Cryst, 1969(B25).

196.   Kannan, S., S. Pina, and J.M.F. Ferreira, Formation of strontium-stabilized B-tricalcium phosphate from calcium-deficient apatite. J. Am. Ceram. Soc., 2006. 89(10): p. 3277-3280.

197.   Bigi, A., et al., Isomorphous Substitutions in b-Tricalcium Phosphate: The Different Effects of Zinc and Strontium. J. Inorg. Biochem., 1997. 66(4): p. 259-265.

198.   Bigi, A., et al., Rietveld Structure Refinement of SyntheticMagnesium Substituted b-Tricalcium Phosphate. Z. Kristallogr, 1996. 211(2): p. 13-16.

199.   Saint-Jean, S.J., et al., Study of the reactivity and in vitro bioactivity of Sr-substituted alpha-TCP cements. J Mater Sci Mater Med, 2005. 16(11): p. 993-1001.

200.   Legeros, R.Z., et al. effect of the strontium on some properties of apatites. in the 5th Interantional Symposium. 1989.

201.   Christoffersen, J., et al., Effects of strontium ions on growth and dissolution of hydroxyapatite and on bone mineral detection. Bone, 1997. 20(1): p. 47-54.

202.   Verberckmoes, S.C., et al., Effects of strontium on the physicochemical characteristics of hydroxyapatite. Calcif Tissue Int, 2004. 75(5): p. 405-15.

203.   Wang, X. and J. Ye, Variation of crystal structure of hydroxyapatite in calcium phosphate cement by the substitution of strontium ions. J Mater Sci Mater Med, 2008. 19(3): p. 1183-6.

204.   Aoba, T., The effect of fluoride on apatite structure and growth. Crit Rev Oral Biol Med, 1997. 8(2): p. 136-53.

205.   Fathi, M.H. and E.M. Zahrani, Fabrication and characterization of fluoridated hydroxyapatite nanopowders via mechanical alloying. Journal of alloys and compounds, 2009. 475: p. 408-414.

206.   Chen, Y. and X. Miao, Thermal and chemical stability of fluorohydroxyapatite ceramics with different fluorine contents. Biomaterials, 2005. 26(11): p. 1205-10.

207.   Rodriguez-Lorenzo, L.M., J.N. Hart, and K.A. Gross, Influence of fluorine in the synthesis of apatites. Synthesis of solid solutions of hydroxy-fluorapatite. Biomaterials, 2003. 24(21): p. 3777-85.

208.   Cheng, K., et al., In vitro behavior of osteoblast-like cells on fluoridated hydroxyapatite coatings. Biomaterials, 2005. 26(32): p. 6288-95.

209.   Wang, Y., et al., Osteoblastic cell response on fluoridated hydroxyapatite coatings. Acta Biomater, 2007. 3(2): p. 191-7.

210.   Kay, M.I., R.A. Young, and A.S. Posner, Crystal Structure of Hydroxyapatite. Nature, 1964. 204: p. 1050-2.

211.   Harrison, J., et al., Sintered hydroxyfluorapatites--IV: The effect of fluoride substitutions upon colonisation of hydroxyapatites by mouse embryonic stem cells. Biomaterials, 2004. 25(20): p. 4977-86.

212.   LeGeros, R., Apatites in biological systems. Prog Cryst Growth Charact, 1981. 4: p. 1-45.

213.   Baig, A.A., et al., Relationships among carbonated apatite solubility, cyrstallite size, and microstrain parameters. Calcif Tissue Int, 1998. 64: p. 437-449.

214.   Tas, A.C., S.B. Bhaduri, and S. Jalota, Preparation of Zn-doped B-tricalcium phsophate (B-Ca3(PO4)2) bioceramics. Materials Science and Engineering C, 2007. 27.

215.   Webster, T.J., et al., Hydroxylapatite with substituted magnesium, zinc, cadmium, and yttrium. II. Mechanisms of osteoblast adhesion. J Biomed Mater Res, 2002. 59(2): p. 312-7.

216.   Sogo, Y., et al., The most appropriate (Ca+Zn)/P molar ratio to minimize the zinc content of ZnTCP/HAP ceramic used in the promotion of bone formation. J Biomed Mater Res, 2002. 62(3): p. 457-63.

217.   Ikeuchi, M., et al., Osteogenic differentiation of cultured rat and human bone marrow cells on the surface of zinc-releasing calcium phosphate ceramics. J Biomed Mater Res A, 2003. 67(4): p. 1115-22.

218.   Yamada, Y., et al., Inhibitory effect of Zn2+ in zinc-containing -tricalcium phosphate on resorbing activity of mature osteoclasts Journal of Biomedical Materials Research Part A, 2007. 84A(2): p. 344-352.

219.   Yamada, Y., et al., Laser microscopic measurement of osteoclastic resorption pits on biomaterials. Materials Science and Engineering C, 2007. 27: p. 762-766.

220.   Kawamura, H., et al., Stimulatory effect of zinc-releasing calcium phosphate implant on bone formation in rabbit femora. J Biomed Mater Res, 2000. 50(2): p. 184-90.

221.   Barralet, J., et al., Angiogenesis in calcium phosphate scaffolds by inorganic copper ion release. Tissue Eng, 2008. accepted for publication.

222.   Gerard, C., et al., The stimulation of angiogenesis and collagen deposition by copper. Biomaterials, 2010. 31(5): p. 824-31.

223.   Xue, W., et al., Osteoprecursor cell response to strontium-containing hydroxyapatite ceramics. J Biomed Mater Res A, 2006. 79(4): p. 804-14.

224.   Kim, H.W., et al., Strontium substituted calcium phosphate biphasic ceramics obtained by a powder precipitation method. J Mater Sci Mater Med, 2004. 15(10): p. 1129-34.

225.   Capuccini, C., et al., Strontium-substituted hydroxyapatite coatings synthesized by pulsed-laser deposition: in vitro osteoblast and osteoclast response. Acta Biomater, 2008. 4(6): p. 1885-93.

226.   Wong, C.T., et al., In vivo cancellous bone remodeling on a strontium-containing hydroxyapatite (sr-HA) bioactive cement. J Biomed Mater Res A, 2004. 68(3): p. 513-21.

227.   Qu, H. and M. Wei, The effect of fluoride contents in fluoridated hydroxyapatite on osteoblast behavior. Acta Biomater, 2006. 2(1): p. 113-9.

228.   Inoue, M., et al., In vivo effect of fluoride-substituted apatite on rat bone. Dent Mater J, 2005. 24(3): p. 398-402.

229.   Redey, S.A., et al., Behavior of human osteoblastic cells on stoichiometric hydroxyapatite and type A carbonate apatite: role of surface energy. J Biomed Mater Res, 2000. 50(3): p. 353-64.

230.   Dekker, A., et al., Adhesion of endothelial cells and adsorption of serum proteins on gas plasma-treated polytetrafluoroethylene. Biomaterials, 1991. 12(2): p. 130-8.

231.   Schakenraad, J.M., et al., Thermodynamic aspects of cell spreading on solid substrata. Cell Biophys, 1988. 13(1): p. 75-91.

232.   van Kooten, T.G., et al., Influence of substratum wettability on the strength of adhesion of hu-

man fibroblasts. Biomaterials, 1992. 13(13): p. 897-904.

233.   Redey, S.A., et al., Osteoclast adhesion and activity on synthetic hydroxyapatite, carbonated hydroxyapatite, and natural calcium carbonate: relationship to surface energies. J Biomed Mater Res, 1999. 45(2): p. 140-7.

234.   Doi, Y., et al., Osteoclastic responses to various calcium phosphates in cell cultures. J Biomed Mater Res, 1999. 47(3): p. 424-33.

235.   Hasegawa, M., Y. Doi, and A. Uchida, Cell-mediated bioresorption of sintered carbonate apatite in rabbits. J Bone Joint Surg Br, 2003. 85(1): p. 142-7.

236.   Anderson, R.E., W.S. Jee, and D.M. Woodbury, Stimulation of carbonic anhydrase in osteoclasts by parathyroid hormone. Calcif Tissue Int, 1985. 37(6): p. 646-50.

237.   Spence, G., et al., Osteoclastogenesis on hydroxyapatite ceramics: The effect of carbonate substitution. J Biomed Mater Res A, 2009.

238.   Landi, E., et al., Carbonated hydroxyapatite as bone substitute. J Eur Ceram Soc, 2003(23): p. 2931-2937.

239.   Ellies, L.G., et al., Quantitative analysis of early in vivo tissue response to synthetic apatite implants. J Biomed Mater Res, 1988. 22(2): p. 137-48.

240.   Yao, F., J.P. LeGeros, and R.Z. LeGeros, Simultaneous incorporation of carbonate and fluoride in synthetic apatites: Effect on crystallographic and physico-chemical properties. Acta Biomater, 2009. 5(6): p. 2169-77.

241.   Yang, L., et al., The effects of inorganic additives to calcium phosphate on in vitro behavior of osteoblasts and osteoclasts Biomaterials, 2010. in press.

Chapter 3

Deposition of lithium ions into calcium-phosphate coatings by biomimetic and electrolytic method

Lithium ions are involved in the Wnt signaling pathway and we previously reported that proliferation of in vitro cultured human mesenchymal stem cells can be enhanced by incubation with lithium. In the present study, we prepared calcium phosphate coatings containing lithium, by applying biomimetic and electrolytic deposition techniques. For both techniques, coatings were prepared from solutions containing 0, 0.5 and 5 g/L lithium chloride. ICP-MS analysis showed that lithium was incorporated into both biomimetic and electrolytic coatings; however the efficiency of incorporation was higher in electrolytic coatings than in the biomimetic ones. Scanning electron microscopy demonstrated that increasing concentrations of lithium decreased crystal size, independent on the coating method. FTIR and XRD analyses showed that electrolytic coating method resulted in the formation of a crystalline coating that was a mixture of carbonated apatite and octacalcium phosphate. The biomimetic coating approach led to the formation of AB type carbonated apatite structure. A burst release profile was observed upon immersion into PBS, reaching 80% of maximum within half an hour for both biomimetic and electrolytic coatings.

INTRODUCTION

Bone is characterized by its large regenerative potential as witnessed by continuous remodeling and fracture healing. However, bone defects beyond a critical size do not heal spontaneously and require orthopedic intervention. Calcium phosphate ceramics are widely applied in orthopedic and cranio-facial surgery as bone filler and as coating on metallic implants [1-4]. Calcium phosphate-based bone graft substitutes are osteoconductive, i.e. able of guiding osteoblasts from the surrounding bone tissue in- or onto the implant improving therewith bone healing to some extend. Most calcium phosphate ceramics, in particular those with porous structure, cannot be used as unique material for load-bearing applications due to their poor mechanical properties [5]. Nevertheless, they can be applied as coating by different techniques so that the strong mechanical properties of metals and the bioactivity of calcium phosphates are combined. The classical method of providing metallic surfaces with a calcium-phosphate ceramic layer is plasma-spraying. Plasma-spraying occurs at very high temperatures, limiting this technique to the production of thermally stable calcium-phosphate phases [6-8]. Besides, this line-of-sight process is not applicable to geometrically complex and porous shapes. Clinical successes of hydroxyapatite coated hip prostheses using plasma-spraying have been satisfying, while occasional failures were associated with implant loosening due to an uncontrolled dissolution of the amorphous part of the coating. Alternative coating methods have been developed that allow for coating porous structures with a range of calcium phosphate phases. Some of these coating processes require energy such as sol-gel- [9-11], sputter- [7, 12] and electrolytic deposition [13, 14]. Another approach of depositing calcium-phosphate layer on metallic implants is by biomimetic route from a simulated body fluid that mimics the mineral composition of human blood plasma [15-17]. With small modifications, both approaches allow for formation of varying calcium phosphate phases, such as dicalcium phosphate, octacalcium phosphate (OCP), carbonate apatite (CA), and hydroxyapatite. Furthermore, unlike plasma-spraying, these processes take place at (near) physiological pH and temperature, allowing for coprecipitation of e.g. growth factors such as Bone Morphogenetic Protein (BMP) [18].

Although calcium phosphate bone graft substitutes are osteoconductive, their performance with regard to healing of large, critically-sized bone defects remains inferior to that of autograft, the golden standard in orthopedic surgery. One way to further improve the bone healing process is by combining calcium phosphate bone graft substitutes with osteoinductive growth factors, such as BMPs, or with osteogenic cells. A more elegant approach is to modify physioco-chemical and structural properties of these bone graft substitutes in such a way that they become intrinsically osteoinductive. Other than osteogenic differentiation, calcium phosphate bone graft substitutes could be further improved if other critical steps of osteogenesis could be controlled as well, such as osteoprogenitor proliferation or mineral production. For instance, we and others reported that a family of chemical inhibitors of so-called histone-deacetylases (HDAC) stimulates mineralisation of osteoblasts and inhibits osteoclast mediated bone resorption. Controlled release of HDAC inhibitors could therefore be used to enhance mineralisation and inhibit resorption. Another signal transduction pathway that has been associated with bone and cartilage formation is Wnt signaling. Wnts are a family of secreted glycoproteins that initiate a signal transduction

cascade upon binding to the frizzled family of receptors and their low density lipoprotein-related protein (LRP) co-receptors [19, 20]. The Wnt signaling pathway acts via the bipartite transcription factor β-catenin/T cell factor (TCF), which binds to the promoter of Wnt responsive genes and thus initiates their transcription. In unstimulated cells, cytoplasmic β-catenin is phosphorylated by a complex of proteins containing axin, the adenomatous polyposis coli protein (APC) and glycogen synthase kinase 3 (GSK3), which earmarks β-catenin for degradation by the proteasome. Upon binding of Wnt to frizzled receptors, the axin/APC/GSK3 complex is inactivated, resulting in the accumulation of cytoplasmic β-catenin, which will translocate to the nucleus and activate Wnt responsive genes. Lithium ions can block the GSK3-mediated phosphorylation of β-catenin, which leads to the accumulation of β-catenin and thus stimulates Wnt signaling. In our previous experiments, we demonstrated that lithium enhances proliferation of tissue cultured human mesenchymal stem cells at 4 mM but inhibits proliferation at higher concentrations [21]. Furthermore, cells that were extensively expanded in the presence of 4 mM lithium chloride could still differentiate into both the osteogenic and adipogenic lineage. This opens the possibility to use lithium as a mitogenic compound in calcium phosphate coatings and ceramics.

In the present study, we have investigated the possibility of incorporating lithium ions into calcium phosphate coatings produced by electrolytic deposition and biomimetic method. The coatings were fully characterized in terms of composition, morphology and crystallinity and the release profile from different coating types was determined as a function of lithium ions content.

MATERIALS AND METHODS

Coating preparation

20 x 20 x 1 mm Ti6Al4V plates (Smitfort Staal BV, Zwijndrecht, The Netherlands) were sandblasted by alumina particles at a pressure of 4 bar to obtain an average roughness (Ra) of 4.0 μm. Prior to coating, the samples were ultrasonically cleaned with acetone, 70% ethanol and demineralised water for 15 minutes. Next, they were etched in a mixture of 2 ml 40% HF and 4 ml 66% HNO_3 in 994 ml water for 10 minutes to form a fresh titanium oxide surface.

1. Electrolytic deposition coating

Table 1 Inorganic ion composition (mM) of coating solutions and SPS						
Solutions	Na$^+$	Ca^{2+}	Cl$^-$	HPO$_4{}^{2-}$	Mg^{2+}	HCO$_3{}^-$
ELD[a]	141.0	4.0	>185.0	2.0	-	-
SBFx5[b]	733.0	12.5	720.0	5.0	7.5	21.0
SBFx5m[c]	702.0	12.5	714.5	5.0	2.5	10.0
SPS[d]	>137.0	-	137.0	-	-	-
[a] ELD calcium phosphate solution [b] SBFx5 biomimetic coating solution [c] SBFx5m biomimetic coating solution [d] simulated physiologic solution						

The electrolyte ("CaP solution") was prepared by first dissolving reagent-grade chemicals of HCl, NaCl, $CaCl_2 \cdot 2H_2O$ and $Na_2HPO_4 \cdot 2H_2O$ into demineralised water as listed in Table 1. CaP solution, with or without LiCl (EMD Biosciences, San Diego, USA) was finally buffered to pH 7.0 at room temperature with 50 mM Tris (see Table 1). The titanium alloy plates were placed as cathode and a platinum electrode (10mm x 10mm x 0.1mm) was placed as anode. The electrolytic deposition was conducted at 52°C and maintained at 2.0 mA/cm² through a galvanostat power supply (BioRad PowerPac 1000, USA) under continuous stirring. Four different calcium phosphate coatings were prepared: Standard electrolytic deposition in CaP solution for 8 hours (ELD coating), electrolytic deposition in CaP solution with 0.5 g/L LiCl for 8 hours (ELD0.5Li coating) and electrolytic deposition in CaP solution with 5 g/L LiCl for 8 hours (ELD5Li coating).

2. Biomimetic coating

For the preparation of biomimetic coating, a two-step method as described earlier was used [16]. In short, in the first step a solution was prepared that was 5 times more concentrated than classical simulated body fluid [22] (SBFx5) by addition of carbon dioxide gas (CO_2). The composition of the SBFx5 solution is shown in Table 1. After dissolution of all salts, the CO_2 gas source was removed and under continuous stirring at 37°C the gas was allowed to slowly escape. Consequent increase of the pH of the solution resulted in the formation of an amorphous pre-calcification layer on Titanium plates during 24 hours. In the second step, a solution similar to SBFx5 solution, but with decreased Mg^{2+} and CO_3^{2-} concentration (Table 1) (SBFx5m) was prepared using the same method. LiCl salt, in concentrations 0 g/l, 0.5 g/l and 5 g/l was added to the SBFx5m solution, and crystalline coatings without Lithium (BM) and with varying amounts of lithium (BM0.5Li and BM5Li coating, respectively) were allowed to form during 24h at 50°C..

Physicochemical characterization

The coatings were observed with an environmental scanning electron microscope (ESEM, Philips XL-30, The Netherlands) in the secondary electron mode. The composition of the coatings was determined by Fourier transform infrared spectroscopy (FTIR, PerkinElmer spectrum 1000, UK) and the crystal structure was studied using X-ray diffraction (XRD, Rigaku Miniflex goniometer, Japan). The crystallinity index was inferred from the XRD pattern and based on the integration of the amorphous wide hump and the crystalline peaks in the range of $2\theta = 25-360$. The crystallinity index was calculated according to the formula [8]:

crystallinity (%)= (area of crystalline peaks / area of amorphous hump and crystalline peaks) x 100%

The coating thickness was measured in situ (n=3) with a magnetic induction probe (ElectroPhysik Minitest 2100, Germany). The lithium content was determined by atomic absorption spectrometry (SpectrAA-100, Varian) after dissolving calcium phosphate coating into given amount of hydrochloric acid (n=3).

Lithium release profile

Simulated physiological solution (SPS) buffered at pH 7.3 with NaOH and HEPES (Table 1) was used to determine the lithium release behavior. Ten coated plates were soaked into 50 ml SPS maintained at 37°C in a double-jacketed reactor and stirred with a magnetic bar at 200 rpm. At each interval point, i.e. 0.5 hour, 1 hour, 2 hours, 8 hours, 1 day, 2 days, 4 days and 7 days, 200 μl of solution was removed to determine the lithium concentration ([Li]) by Atomic Absorption Spectrometer (SpectrAA-100, Varian) or Ion Coupled Plasma – Mass Spectroscopy (ICP-MS) (Elan 6000, Perkin Elmer). The experiment was performed in triplicate.

RESULTS

Coating characteristics

We prepared ELD coatings (ELD, ELD0.5Li and ELD5Li) and biomimetic coatings (BM, BM0.5Li and BM5Li) and analyzed the coating morphology using ESEM (Figure 1). Consistent with our previous results [23], ELD coatings without lithium exhibited a rough surface composed of CaP globules, with a diameter of about 50-100 μm and crystals of approximately 5-6 μm (Fig. 1A, 1C). Biomimetic coating, on the other hand showed a rougher surface with CaP globules with a diameter of about 10-20 μm and more irregular boundaries between the globules (Fig. 1B, 1D). Also the crystal size of the biomimetic coatings (3-4 μm) was systematically smaller than that of ELD coatings. Addition of LiCl into coating solutions resulted in a visual decrease of roughness for both coating types (1E, 1F). Low concentration of LiCL (0.5 g/l) did not affect the crystal size of either coating (Fig. 1G, 1H). LiCl concentration of 5 g/l LiCl clearly affected the visual roughness of both coatings, resulting in almost complete disappearance of the globules (Fig. 1I, 1J). Crystal size for both coating types also decreased in presence of 5 g/l LiCl in the solution (Fig. 1K, 1L).

To further investigate the effect of lithium on crystallinity, we established XRD patterns of the coatings (Fig. 2). The ELD coating demonstrated a pattern typical of carbonate apatite and had a crystallinity of about 80% (Fig 2.1A). The XRD patterns of ELD0.5Li and ELD5Li coating presented the same diffraction lines but relatively broader peaks (Fig. 2.1B and 2.1C), which was in accordance with a lower crystallinity of about 60%. Similar observations were obtained for the XRD patterns of biomimetic coating (Fig. 2.2): crystallinity of the coating decreased with increasing LiCl concentration of the solution from about 55% of BM coating (Fig. 2.2A) to about 50% of BM0.5Li (Fig. 2.2B) and BM5Li coatings (Fig. 2.2C).
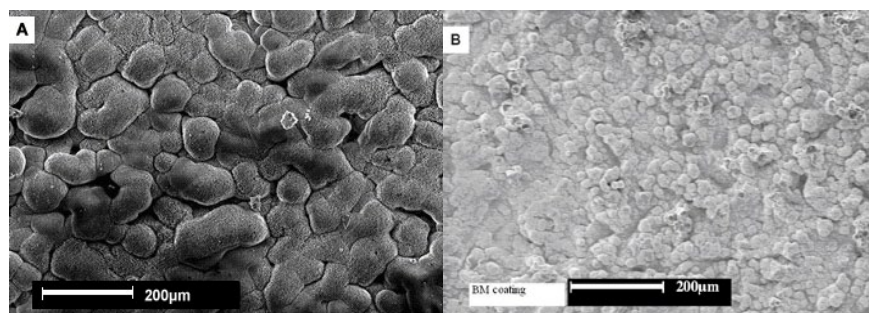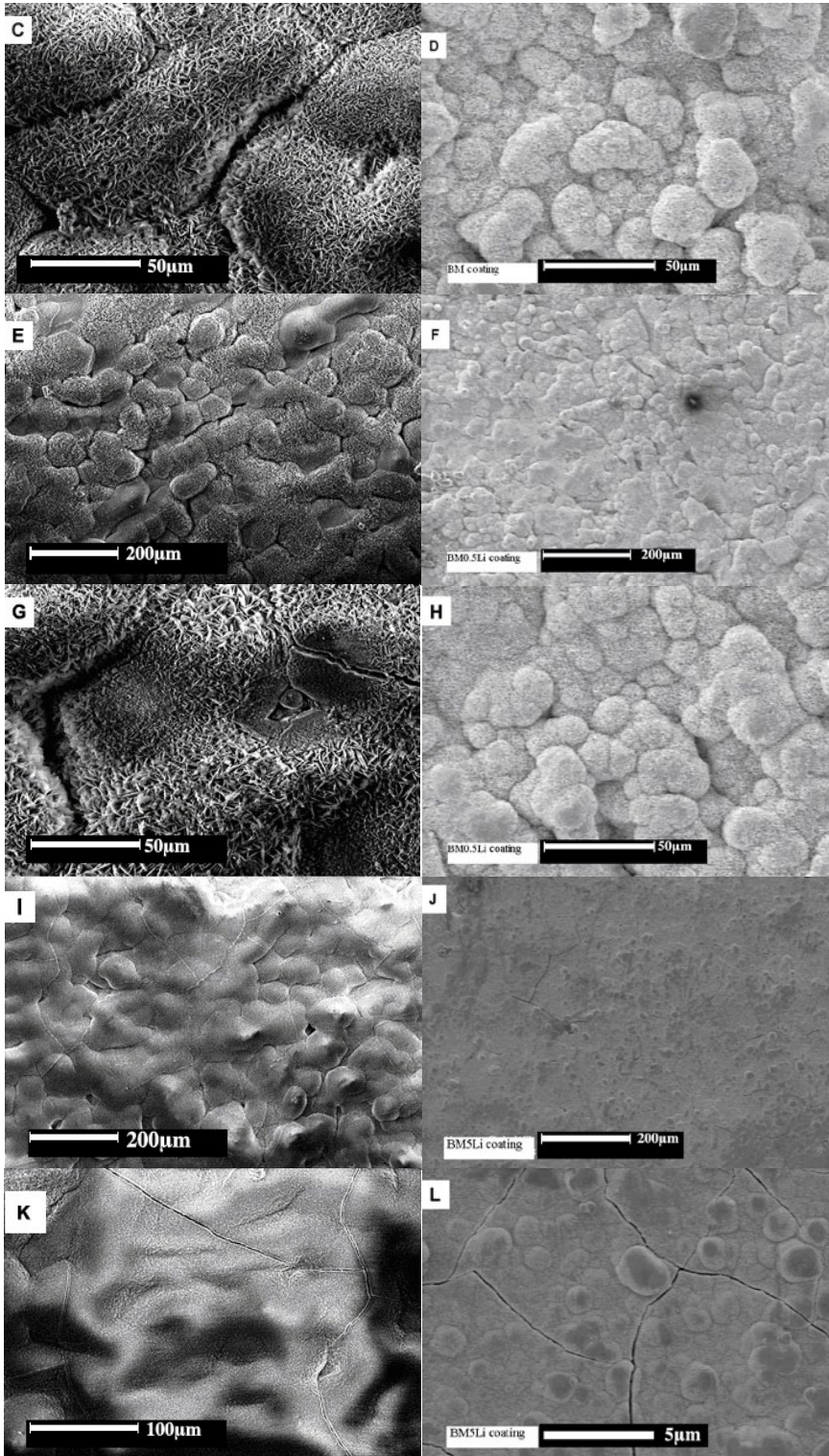
Figure1: The ESEM micrographs of ELD coatings (left column) and biomimetic coatings (right column): A)&C) LD coating without LiCl; B)&D) biomimetic coating without LiCl; E)&G) ELD0.5Li coating; F)&H) BM0.5Li coating; I)&K) ELD5Li coating; J)&L) BM5Li coating.
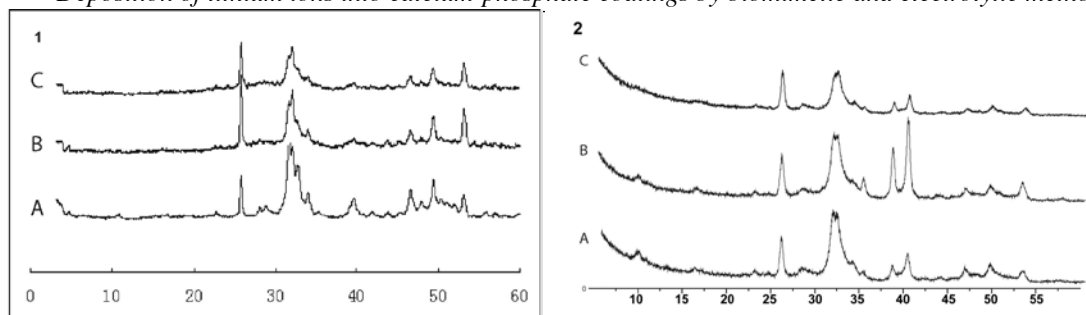
Figure 2: The XRD patterns of ELD coatings (2.1) and biomimetic coatings (2.2): A) the coating made in absence of LiCl; B) the coating made in presence of 0.5g/l LiCl; C) the coating made in presence of 5g/l LiCl.
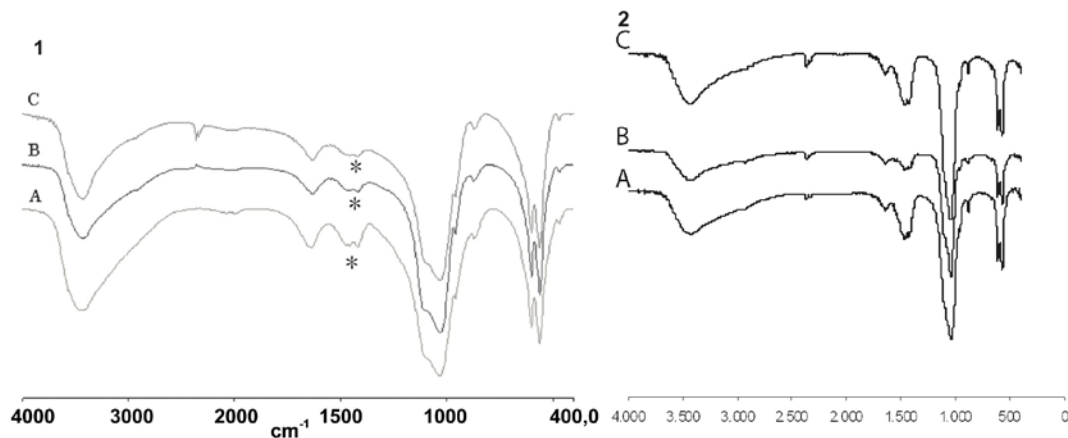

Figure 3: The FTIR spectra of ELD coatings (3.1) and biomimetic coatings (3.2): A) the coating made in absence of LiCl; B) the coating made in presence of 0.5g/l LiCl; C) the coating made in presence of 5g/l LiCl.

To analyze the chemical composition of the coatings, FTIR spectra were obtained. (Fig. 3). ELD coatings exhibited broad band at 1021 cm^{-1} with two shoulders at 1104 and 960 cm^{-1}, as well as carbonate peaks at 880 cm^{-1} (CO_3^{2-} replacing OH$^-$, type A substitution), as well as at 1465, 1413, and 873 cm^{-1} (CO_3^{2-} replacing PO_4^{3-}, type B substitution), (Fig. 3.1A), suggesting a mix between carbonated apatite and octacalcium phosphate phases. The biomimetic coatings exhibited a broad band at around 960 cm^{-1}, without pronounced shoulders (Fig. 3.2A). Carbonate peaks were found at the same locations as for ELD coatings, indicating AB type carbonated apatite phase (Fig. 3.2A). The spectra of coatings with lithium were similar to those of the control coatings for both coating types, with only small difference in intensities of carbonate bands at 1459 and 1408 cm^{-1} (Fig. 3.1B&C, 3.2B&C).

Table 2 The lithium concentration and coating thickness		
Coatings	Lithium concentration (µg/mg)	Coating thickness (µm)
ELD	0	40.3 ± 4.2
ELD0.5Li	2.22 ± 0.24	29.4 ± 4.5
ELD5Li	5.46 ± 0.36	25.8 ± 4.2
BM	0	38.1 ± 3.9
BM0.5Li	0.12 ± 0.06	31 ± 4.1
BM5Li	1.18 ± 0.25	22 ± 4.2

The lithium concentration and coating thickness are summarized in Table 2. The thickness of the control biomimetic coating was around 38 μm, and no lithium was detected. Biomimetic coatings prepared in solutions with 0.5 g/l LiCl contained 0.12 μg/mg lithium. Lithium content of the coating further increased to 1.18 μg/mg, in the BM5Li coatings. In presence of lithium, coating thickness decreased to 31 μm and 22 μm in BM0.5Li and BM5Li coating, respectively. ELD coating without lithium had a thickness of about 40 μm decreasing to 29 μm in ELD0.5Li and to 26 μm in ELD5Li coatings. The lithium content of the coating was 2.2 μg/mg and 5.5 μg/mg in ELD0.5Li and ELD5Li coating, respectively.

Lithium release profile

The biological activity of lithium in the coatings is determined by the amount of lithium incorporated and/or its release profile upon implantation. To investigate the in vitro release profile, BM5Li and ELD5Li coatings were immersed in Simulated Physiological Solution and lithium concentration was measured in time. Both ELD5Li and BM5Li coating exhibited a typical burst release profile; however, the total amount of lithium released from the ELD5Li coating was 4-5 times higher than what was released from BM5Li coating, corresponding to the total amount of incorporated lithium in the coating. For both coating types, 70-80% of the final lithium concentration was reached within half an hour and the release curve reached a plateau after 24 hours (Fig. 4). We detected around 0.2 μg/mg lithium in the BM5Li coating and 0.6 μg/mg lithium in the ELD5Li coating after 180 hours of release, indicating that 80~90% of the total lithium was released from in the coating.
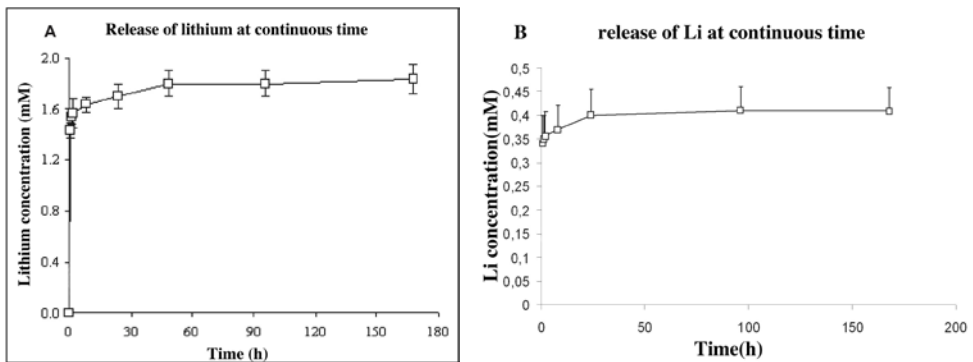
Figure 4: The lithium release profile of ELD5Li (A) and BM5Li (B) coating.

To explore whether this phenomenon was caused by the saturation of the release solution with lithium, or calcium and phosphate ions, inhibiting further dissolution of the coating, additional test was carried out on the ELD5Li coatings. Smaller volume of SPS solution (5ml for one plate) was used and refreshed every day. Lithium concentration of the solution on day 1 was 2.13 mM, decreasing to 0.2 mM on days 2 and 7. This confirmed that the release of lithium from the coatings indeed had a burst profile.

Discussion

This study showed that lithium can be co-precipitated into calcium phosphate coatings by both biomi-

metic and electrolytic route, by a simple addition of LiCl salt into the coating solution. The lithium content of the coating can be controlled by the LiCl concentration of the coating solution. In the biomimetic process used here, a mildly acidic gas carbon dioxide was used to temporary decrease the pH of the coating solution in order to prepare a supersaturated simulated body fluid. After removing the its source from the solution, the CO_2 gas slowly releases from the solution, leading to a gradual increase in pH of the solution and consequent precipitation of a calcium phosphate layer on the surface of the titanium alloy substrate. Addition of LiCl into the coating solution slightly disturbed the balance among the contents of simulated body fluid as well as the pH of the coating, which may explain the effect on the coating morphology, crystallinity and thickness observed. Electrolytic deposition involves a series of reactions induced by electric currents occurring at the surface of the cathode. First, the increase of local pH around the cathode occurs followed by a reaction of calcium and phosphate ions with the hydroxyl group and finally the electrostatic adsorption of homogeneous nucleated calcium phosphate clusters on the substrate [24]. In this situation, the addition of LiCl to the supersaturated CaP solution in the presence of electric field results not only in normal electrolytic calcium phosphate deposition [25], but also in deposition of the positively charged lithium on the cathode. For both biomimetic and ELD method, lithium may be incorporated by two alternative mechanisms: chemical incorporation in the crystal lattice by partial substitution of calcium ions by lithium ions and physical incorporation whereby lithium ions are adsorbed on the coating surface or adjoined to apatite crystals filling the space between them. Our results suggest that the latter mechanism was more pronounced in the coatings described here for a number of reasons. Firstly, the amount of lithium in the coating was relatively small. Respectively, only 1.18 µg and 5.5 µg lithium per mg of coating were present in BM5Li and ELD5Li coatings, which were produced from a coating solution with LiCl concentration of 5 g/L. In other words, the atomic ratio of Ca/Li in BM5Li coating was about 43, strongly contrasting the Ca/Li of the coating solution of 0.017. Similarly, the atomic Ca/Li ratio of ELD5Li coating was about 11, whereas the ratio of electrolyte was about 0.03. Also, the presence of lithium did not strongly affect the composition of the coating, judging from the FTIR spectra as opposed to crystallinity and crystal size which were obviously affected, Finally, lithium released from the coatings showed a typical "burst release" profile, independent on the coating type, which can be expected when lithium is not part of the crystal lattice. However, we can not completely rule out the possibility that lithium was partly chemically incorporated into the crystal lattice, since small amounts of lithium were found in the coating after 7 days of in vitro release.. Further studies are required to elucidate the exact mechanism of lithium incorporation into these coatings

Despite the relatively small amounts in the coatings, lithium had an obvious dose-dependent effect on their properties. Lithium interfered with calcium phosphate crystal formation, as was suggested by lower crystallinity, smaller globules, smaller crystals and thinner coatings. This inhibitory effect was similar to that of magnesium [16, 26, 27]. Eanes et al. concluded that magnesium ions could markedly influence calcium phosphate crystallization without being significantly incorporated into the precipitate [28].

The efficiency of lithium incorporation into biomimetic coatings was lower than in electrolytic ones,

although the biomimetic solution was much more supersaturated than the electrolytic one. This could be explained by the fact that electric current increases the rate of coating formation and helps depositing the positively charged lithium ions onto the substrate.

CONCLUSIONS

Lithium can be co-precipitated with calcium phosphates as coating on titanium alloy surface by both biomimetic and electrolytic method. However, the incorporation of lithium interferes with the formation of calcium phosphate layer, resulting in a change of coating morphology, and decrease of coating crystallinity and thickness. The in vitro release of lithium from the coatings has a "burst" profile. Further studies should aim at determining biological effect of incorporated lithium.

ACKNOWLEDGEMENTS

REFERENCES

1.	Vallet-Regi, M., Revisiting ceramics for medical applications. Dalton Trans, 2006(44): p. 5211-20.

2.	El-Ghannam, A., Bone reconstruction: from bioceramics to tissue engineering. Expert Rev Med Devices, 2005. 2(1): p. 87-101.

3.	Hench, L.L. and J. Wilson, An introduction to bioceramics. 2nd ed. ed. 1999, London: Word Scientific.

4.	Kokubo, T., Bioactive glass ceramics: properties and applications. Biomaterials, 1991. 12(2): p. 155-63.

5.	Gauthier, O., et al., Macroporous biphasic calcium phosphate ceramics: influence of macropore diameter and macroporosity percentage on bone ingrowth. Biomaterials, 1998. 19(1-3): p. 133-9.

6.	Khor, K.A., et al., Microstructure investigation of plasma sprayed HA/Ti6Al4V composites by TEM. Mater Sci Eng A 2000. 281: p. 221-228.

7.	Yang, Y., K.H. Kim, and J.L. Ong, A review on calcium phosphate coatings produced using a sputtering process--an alternative to plasma spraying. Biomaterials, 2005. 26(3): p. 327-37.

8.	Tsui, Y.C., C. Doyle, and T.W. Clyne, Plasma sprayed hydroxyapatite coatings on titanium substrates. Part 1: Mechanical properties and residual stress levels. Biomaterials, 1998. 19(22): p. 2015-29.

9.	Choi, A.H. and B. Ben-Nissan, Sol-gel production of bioactive nanocoatings for medical applications. Part II: current research and development. Nanomed, 2007. 2(1): p. 51-61.

10.	Kim, H.W., et al., Hydroxyapatite coating on titanium substrate with titania buffer layer processed by sol-gel method. Biomaterials, 2004. 25(13): p. 2533-8.

11.	Liu, D.M., T. Troczynski, and W.J. Tseng, Water-based sol-gel synthesis of hydroxyapatite:

process development. Biomaterials, 2001. 22(13): p. 1721-30.

12.   Ong, J.L., et al., Structure, solubility and bond strength of thin calcium phosphate coatings produced by ion beam sputter deposition. Biomaterials, 1992. 13(4): p. 249-54.

13.   Kumar, M., H. Dasarathy, and C. Riley, Electrodeposition of brushite coatings and their transformation to hydroxyapatite in aqueous solutions. J Biomed Mater Res, 1999. 45(4): p. 302-10.

14.   Redepenning, J., et al., Characterization of electrolytically prepared brushite and hydroxyapatite coatings on orthopedic alloys. J Biomed Mater Res, 1996. 30(3): p. 287-94.

15.   Du, C., et al., Biomimetic calcium phosphate coatings on Polyactive 1000/70/30. J Biomed Mater Res, 2002. 59(3): p. 535-46.

16.   Barrere, F., et al., Nucleation of biomimetic Ca-P coatings on ti6A14V from a SBF x 5 solution: influence of magnesium. Biomaterials, 2002. 23(10): p. 2211-20.

17.   Cho SB, Nakanishi K, and Kokubo T, Dependence of apatite formation on silica gel on its structure: effect of heat treatment. J Am Ceram Soc 1995 78: p. 1769-1774.

18.   Liu, Y., K. de Groot, and E.B. Hunziker, BMP-2 liberated from biomimetic implant coatings induces and sustains direct ossification in an ectopic rat model. Bone, 2005. 36(5): p. 745-57.

19.   Cadigan, K.M. and R. Nusse, Wnt signaling: a common theme in animal development. Genes Dev, 1997. 11(24): p. 3286-305.

20.   Moon, R.T., et al., The promise and perils of Wnt signaling through beta-catenin. Science, 2002. 296(5573): p. 1644-6.

21.   De Boer, J., H.J. Wang, and C. Van Blitterswijk, Effects of Wnt signaling on proliferation and differentiation of human mesenchymal stem cells. Tissue Eng, 2004. 10(3-4): p. 393-401.

22.   Kokubo, T., et al., Solutions able to reproduce in vivo surface-structure changes in bioactive glass-ceramic A-W. J Biomed Mater Res, 1990. 24(6): p. 721-34.

23.   Wang, J., et al., Biomimetic and electrolytic calcium phosphate coatings on titanium alloy: physicochemical characteristics and cell attachment. Biomaterials, 2004. 25(4): p. 583-92.

24.   Rossler, S., et al., Electrochemically assisted deposition of thin calcium phosphate coatings at near-physiological pH and temperature. J Biomed Mater Res A, 2003. 64(4): p. 655-63.

25.   Ban, S. and S. Maruno, Morphology and microstructure of electrochemically deposited calcium phosphates in a modified simulated body fluid. Biomaterials, 1998. 19(14): p. 1245-53.

26.   Barrere, F., et al., Biomimetic calcium phosphate coatings on Ti6AI4V: a crystal growth study of octacalcium phosphate and inhibition by Mg2+ and HCO3. Bone, 1999. 25(2 Suppl): p. 107S-111S.

27.   Barrere, F., et al., Influence of ionic strength and carbonate on the Ca-P coating formation from SBFx5 solution. Biomaterials, 2002. 23(9): p. 1921-30.

28.   Eanes, E.D. and S.L. Rattner, The effect of magnesium on apatite formation in seeded supersaturated solutions at pH 7.4. J Dent Res, 1981. 60(9): p. 1719-23.

Chapter 4

A medium-throughput method for studying the effect of trace elements on bone formation: incorporation into calcium-phosphate coatings

Biomimetic coating method possesses a number of advantages in comparison with the classical methods for providing orthopaedic and dental implants with a calcium phosphate layer. For example, we have previously reported that biologically active molecules, such as growth factors and antibiotics can be incorporated into and gradually released from biomimetically produced coating, adding therewith to their functionality. In the present study, we have set up a medium-throughput protocol which can be used to investigate the effect of trace elements on bone formation by coating cell culture well plates with calcium-phosphate coatings containing varying concentrations of copper-, zinc-, strontium-, fluoride- and carbonate ions. Energy Dispersive X-ray analyses showed that all trace elements were homogenously incorporated into the coatings. Environmental Scanning Electron Microscopy analysis showed that in particular fluoride and carbonate ions affected the morphology of calcium phosphate coating. These findings were confirmed by the Raman microscopy analysis. Ion Coupled Plasma – Mass Spectroscopy indicated that the amount of incorporated ions can be controlled by controlling their concentration in the coating solution. Furthermore, ICP-MS analysis suggested the mechanisms of ion incorporation into the crystalline lattice of calcium phosphate. Further studies will be performed to investigate the effect of trace elements on cells related to bone growth and resorption by using this system.

INTRODUCTION

The concept of biological fixation of load-bearing implants using calcium phosphate coatings and bio-active hydroxyapatite (HA) was proposed as an alternative to cemented fixation in the early '80s [1]. In 1985, for the first time, HA-coated implants were used for clinical trials by Furlong and Osborn [2]. Since then, it has been reported that HA coating can successfully enhance clinical successes of total hip arthroplasty to a failure rate lower than 2% [3].

Plasma spraying of hydroxyapatite is a common practice used to modify the surfaces of orthopedic and dental implants. Plasma spraying employs a gas stream to carry hydroxyapatite powders, which are then passed through electrical plasma to ensure bonding on the coating to the substrate material. This allows for rapid coating of implants at low costs [4]. However, there are some inherent problems associated with this method: mechanical failure within the coating, discontinued dissolution of the coating after implantation, variations in bond strength between the coatings and metallic substrate and non-uniformity in coating density as a result of the process. Furthermore, plasma-spraying can only be used for depositing thermally stable calcium phosphate phases on dense and geometrically simple surfaces. For the last forty years, many researchers have investigated alternative coating methods to overcome problems associated with plasma spraying, resulting in development of electrophoretic- [5], sputter- [6], sol-gel- [7] and biomimetic methods.

The biomimetic coating method, which is based on immersion of a biomaterial into a solution that mimics the inorganic composition of human blood plasma (the so-called Simulated Body Fluid (SBF)) at physiological conditions, was originally developed by Kokubo in 1990 [8], and has since been improved by several groups of investigators. In our group for example, supersaturating SBF resulted in successful formation of bone-like apatite coating on metallic surfaces in a considerably shorter period of time than when classical SBF was used [9, 10]. Biomimetic coating process has many advantages over the traditional ones. The process is relatively simple and takes place at low temperature and physiological pH. It is furthermore applicable to a large range of materials with varying chemical composition and geometrically complex and porous shapes [11, 12]. The most valuable aspect about this process is that biologically active molecules, such as growth factors [13] and antibiotics [14] can be co-precipitated with the coating, offering controlled release of these agents.

Biomimetic coating method can also be used for depositing calcium phosphate coatings, containing growth factors or other additives on tissue culture plastic. This allows for in vitro investigation of effect of coatings on relevant cells under standardized conditions. For example, recently a study was performed in which Co^{2+} ions at varying concentrations were coprecipitated with calcium phosphate coatings inside cell culture well plates, in order to study the effect of cobalt ions on resorptive activity of osteoclasts. This method elegantly mimicked bone mineral surrounding a Co-Cr implant. In the present study, we have employed this method to explore the possibility of co-precipitating trace elements into biomimetic coating in order to setup a standard medium-throughput protocol to investigate the effect of trace elements on bone formation. Calcium phosphate solutions with varying concentrations of Cu^{2+}, Zn^{2+}, Sr^{2+}, F^- and CO_3^{2-} were used to deposit trace elements containing coatings inside 48-well plates.

The coatings were then characterized using Environmental Scanning Electron Microscopy (ESEM), coupled with Energy Dispersive X-Ray Analyzer (EDX) and Raman Spectroscopy. Ion-Coupled Plasma-Mass Spectroscopy (ICP-MS) was used to investigate the efficiency of the system by measuring the total amounts of trace elements co-precipitated into the coatings and the effect of the presence of elements on calcium to phosphorus ratio of the coatings.

MATERIALS AND METHODS

Preparation of biomimetic coatings on 48-well plates

For preparation of coating, 48 tissue-culture treated plates (Nunclon^R MultiDishes, NUNC^{TM}) were used. All the salts and reagents were purchased at either Merck or Sigma-Aldrich.

The coating process consisted of two steps:

Step 1. Pre-calcification

48-well plates were pre-calcified by pouring a 2.5 times supersaturated Simulated Body Fluid (SBF x2.5) solution into the wells (500 μl/well). In order to prepare SBF x2.5 solution, three solutions were made: 1) Buffer solution by dissolving 24.2 g Tris base and 164ml 1M HCl in the pure MilliQ water to a total volume of 4L (final pH=7.4); 2) Calcium solution by dissolving 1.37 M NaCl, 15mM $MgCl_2 \cdot 6H_2O$ and 25mM $CaCl_2 \cdot 2H_2O$ in the buffer solution; 3) Phosphate solution by dissolving 42mM $NaHCO_3$ and 11.1mM $Na_2HPO_4 \cdot H_2O$ in the buffer solution. SBF x2.5 solution was prepared by mixing the three solutions at 2:1:1 ratio. SBF x2.5 was refreshed 3 days consecutively. At the end of day 3, the well plates were thoroughly washed with MilliQ water.

Step 2. Crystal growth

Pre-calcified 48-well plates were treated with a calcium phosphate supersaturated solution (CPS) at physiological pH of 7.40 (500 μl/well) to deposit a crystallized layer onto amorphous calcium phosphate layer formed in Step 1. CPS were prepared by dissolving 0.14M NaCl, 4mM $CaCl_2 \cdot 2H_2O$, 2.25mM $Na_2HPO_4 \cdot H_2O$ and 50 mM Tris in MilliQ water, adjusting the pH of the solution to 7.4 using 1M HCl.

Incorporation of trace elements in biomimetic Ca-P coatings

In order to prepare stock solutions, mineral salts (CuAc, ZnAc, SrAc, NaF, $NaHCO_3$) were dissolved in TRIS solution and buffered with HCl 1M at pH=7.4 to reach the molar concentration of 0.1 M (for Sr^{2+}, F^-, and CO_3^{2-}) or 0.01 M (for Cu^{2+} and Zn^{2+}).

After pre-calcification step, mineral stock solutions were added into the CPS solution, so as to obtain molar concentrations of elements in the range 0.1 μM-1000 μM. We prepared coating solutions with Cu^{2+} and Zn^{2+} in concentrations of 10, 1 and 0.1 μM, Sr^{2+} and F^- in concentrations 1000, 100, 10 and 1 μM and CO_3^{2-} in concentrations 10000, 1000, 100, 10 and 1 μM. These solutions were refreshed 3 days consecutively. In the rest of the article, the coatings will be labeled Cu0.1, Cu1, Cu10; Zn0.1, Zn1, Zn10; Sr1, Sr10, Sr100, Sr1000; F1, F10, F100, F1000; $CO_3$1, $CO_3$10, $CO_3$100, $CO_3$1000, $CO_3$10000 respectively. The reason that different concentrations of Cu^{2+} and Zn^{2+} were used was that at concentrations higher than 10uM, the coating solutions become unstable with inhomogeneous coatings as a result.

Coating characterisation

The morphology and the presence of trace elements were investigated on gold-sputtered coatings using Environmental Scanning Electron Microscopy (ESEM, XL-30 ESEM-FEG, Philips) in the secondary electron mode, coupled with Energy Dispersive X-ray analyser.

The coated well plates were gently washed with MilliQ water and dried at 50ºC overnight, and the walls of the well plates were cut off. For assessing the compositions of the coatings, measurements were performed with a custom made confocal Raman microscope using a diode laser ($\lambda = 685$ nm) with 15-20 mW effective power at the sample surface and a spatial resolution of 700nm. The position and the Full Width Half Height (FWHH) values of the PO_4^{3-} peak (around 960 cm^{-1}) were determined for the control coating and coatings containing highest concentration of trace elements on three well per samples and ten points per well. The values of the coatings with trace elements were compared with the control using one-way ANOVA with Dunnett's 2-sided t-test as post-hoc test. The significance level was set at $p < 0.05$.

Efficiency of trace elements incorporation

500μl ultrapure 25% HNO_3 was used for dissolving coating in each well. After 20 minutes, HNO_3 solution was taken out and diluted to 10ml by MilliQ water. Ion Coupled Plasma – Mass Spectroscopy (ICP-MS) (Elan 6000, Perkin Elmer) was used for determining the total amount of Cu^{2+}, Zn^{2+} and Sr^{2+} incorporated into the coatings. This method was not suitable for determining total amounts of F$^-$ and CO_3^{2-}. In addition, the amounts of calcium and phosphorus were investigated for all coatings.

RESULTS

ESEM and EDX analysis

After immersion into SBFx2.5 for 3 days, ESEM indicated that a dense and uniform amorphous Ca-P film was deposited on the plastic well plates (micrograph not shown). This layer was composed of spherical Ca-P globules with a diameter of about 0.1 μm. The 3-day coating process in CPS solution resulted in formation of crystalline layer consisting of globules with a diameter of around 4μm. These globules were composed of sharp platelet-like crystals with the size of around 0.5μm (figure 1a). Presence of Cu^{2+} and Zn^{2+} did not affect the morphology at low concentrations (micrographs not shown), whereas at the highest concentration of 10 μM, the size of the crystals was slightly larger as compared to the control (Figs. 1b and 1c, respectively)). Also Sr^{2+} did not affect the morphology of the coating over the range of tested concentrations (Fig. 1d). Presence of F$^-$ appeared to have an effect on the coating morphology over the total concentration range tested, with the strongest effect at the highest con-
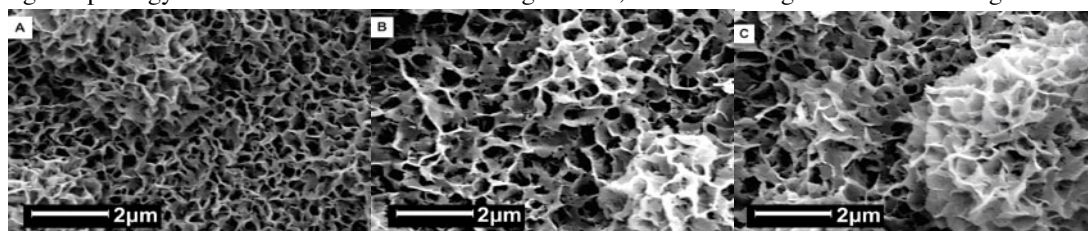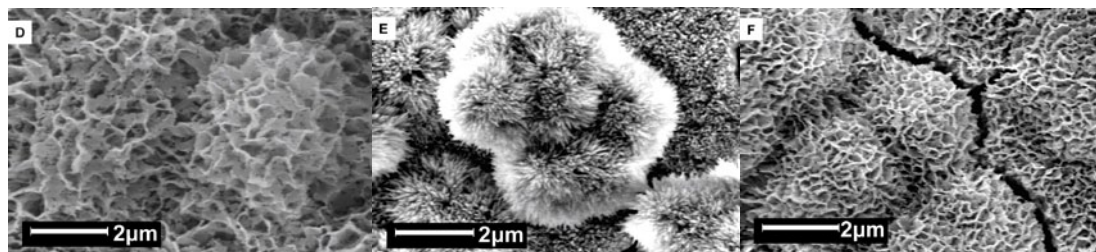
Figure1: ESEM micrographs showing morphology of: a) control coating without trace elements, b) Cu10, c) Zn10, d) Sr1000, e) F1000, and f) CO310000. (scale bar = 2 µm) .

centration. F1000 coatings also consisted of globules with a diameter of about 4 µm, however, instead of sharp, platelet-like crystals of the control coating, they were built out of rod-like apatite crystals with the size below 0.2 µm (Fig. 1e). Presence of CO_3^{2-} in the coating solution also resulted in a decrease of crystal size, with the strongest effect at the highest concentration (Fig. 1f).

EDX analysis revealed a homogenous distribution on the surface of the coatings of all trace elements at all concentrations. Figure 2 shows elemental mapping of F1000 coating and Zn0.1 coatings, which are representative for all other coatings.
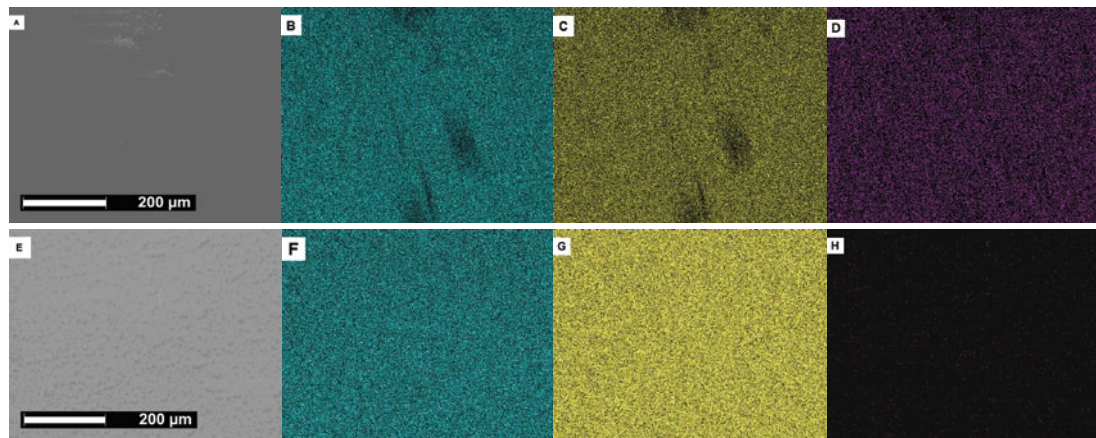
Figure 2: Xmap micrographs showing: a) morphology of the F1000 coating; b) distribution of P, c) Ca and d) F on the surface of the F1000 coating; e) morphology of the Zn0.1 coating; f) distribution of P, g) Ca and h) Zn on the surface of the Zn0.1 coating. Trace elements were homogenously distributed throughout the surface of the coating. This micrograph is respresentative for coatings with other trace elements at all concentrations.

Raman analysis

Fig. 3A shows some representative Raman spectra of coatings with different trace elements. All coatings showed a spectrum that is typical of hydroxyapatite-like phase, with the position of main PO_4^{3-} peak in v1 mode at around 960 cm^{-1}. In fig. 3B, the position and FWHH values of this peak are given for the control coating and coatings with highest content of trace elements as measured by Gaussian fit. The coating process in presence of the highest concentrations of Cu^{2+} and Zn^{2+} did not result in significant shift of PO_4^{3-} peak as compared to the control. The presence of Sr^{2+} and CO_3^{2-} however led to a significant shift of the phosphate peak to the left, whereas the presence of F$^-$ led to a significant shift

to the right. The FWHH values of the v1 mode of PO_4^{3-} of all coatings with trace elements differed significantly from the control. A decrease in the FWHH value was observed in presence of Cu^{2+}, Zn^{2+} and F^-, with the strongest effect of F^-, whereas the presence of Sr^{2+} and CO_3^{2-} led to a slight increase of the FWHH value as compared to the control (Fig. 3B).
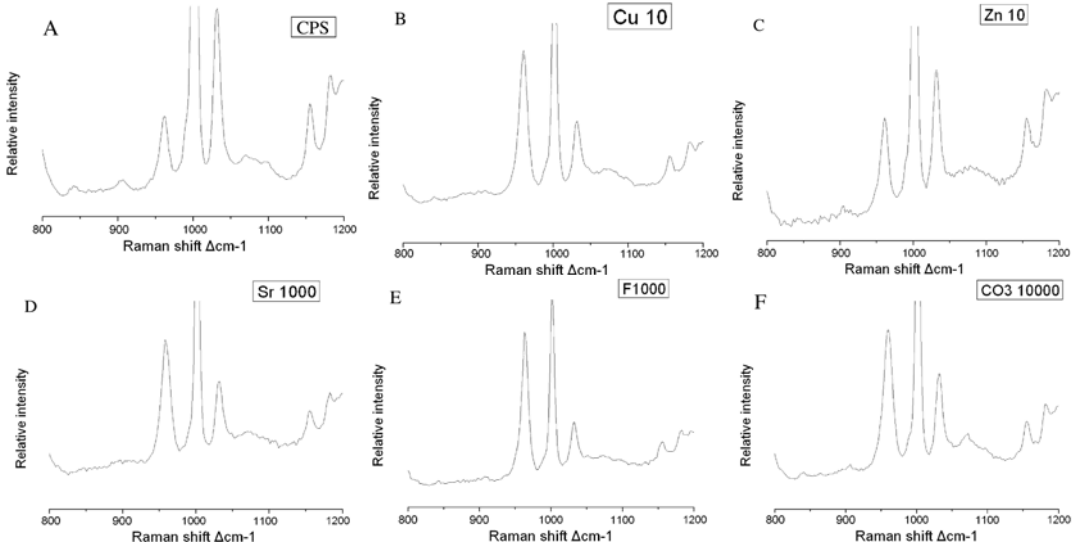

Figure 3A: Raman spectra of a) CPS coating; b) Cu10 coating; c) Zn10 coating; d) Sr1000 coating; e) F1000 coating and f) $CO_3$10000 coating.
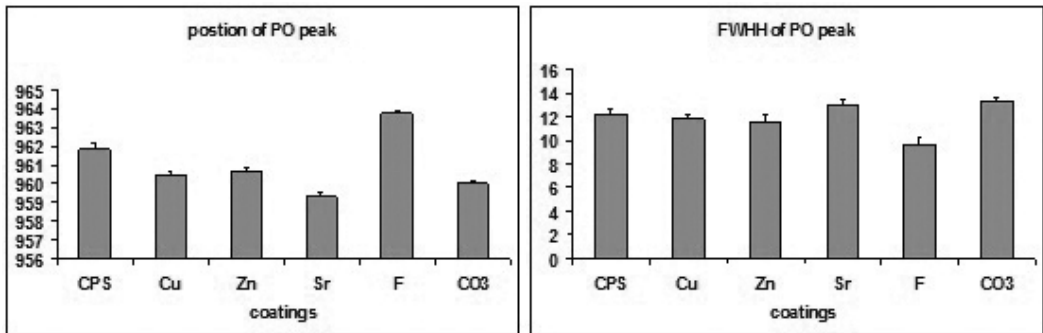
Figure 3B: Positions (left) and FWHH values (right) of PO_4 peaks for the control coating and coatings with highest concentrations of trace elements. In presence of CO_3^{2-} and Sr^{2+}, a significant shift to the left was observed, whereas the presence of F^- led to a shift to the right. The FWHH values of coatings containing Cu^{2+}, Zn^{2+} and F^- were significantly lower than that of the control, whereas the coatings with CO_3^{2-} and Sr^{2+} showed higher values than the control.

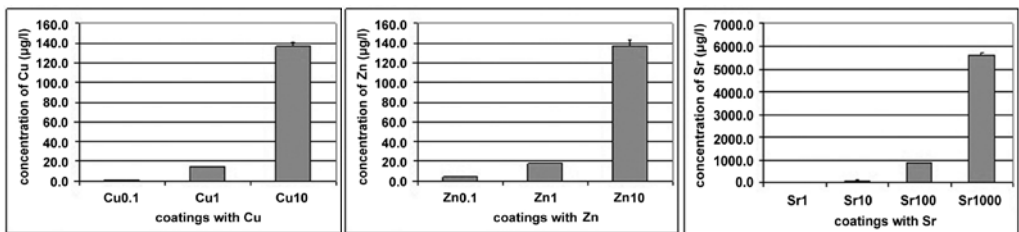Figure 4A: total amount of a) Cu^{2+} b) Zn^{2+} and c) Sr^{2+} incorporated in calcium phosphate coatings at different concentrations of ions in the solution, as measured by ICP-MP. An increase in concentration of trace elements in the solution resulted in an increase of the total incorporated amount of ions in the coating.
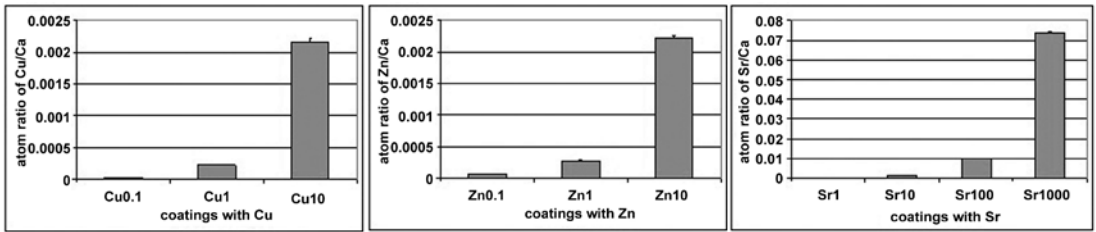
Figure 4B: atom ratio of trace elements to Ca in coatings with different concentrations of: a) Cu, b) Zn and c) Sr as measured by ICP-MP. Increase in concentration of the trace elements in coating solution led to an increase in total amounts of trace elements incorporated into the coating.

ICP-MS analysis

ICP-MS results showed that for Cu^{2+}, Zn^{2+} and Sr^{2+}, the total amount of incorporated ions increased with an increase on concentration of ions in the solution (Fig. 4A). Trace element to Ca ratio as determined by ICP-MS for the three cations showed a similar efficiency of incorporation into the coatings (Fig. 4B).

Table 1: Ca/P ratio			
coating	Ca/P atom ratio	coating	Ca/P atom ratio
CPS	1.49 ± 0.01	F1	1.50 ± 0.01
Cu0.1	1.45 ± 0.00	F10	1.52 ± 0.00
Cu1	1.46 ± 0.01	F100	1.52 ± 0.01
Cu10	1.45 ± 0.01	F1000	1.62 ± 0.01
Zn0.1	1.46 ± 0.02	CO_3 1	1.44 ± 0.01
Zn1	1.45 ± 0.00	CO_3 10	1.46 ± 0.01
Zn10	1.46 ± 0.01	CO_3 100	1.46 ± 0.01
Sr1	1.44 ± 0.01	CO_3 1000	1.48 ± 0.01
Sr10	1.45 ± 0.01	CO_3 10000	1.55 ± 0.00
Sr100	1.44 ± 0.01		
Sr1000	1.34 ± 0.00		

The effect of the presence of ions on Ca to P atomic ratio is summarized in Table 1. Ca to P ratio of the control coating was 1.49. Cu^{2+} and Zn^{2+} showed a slight decrease of the ratio, which was not dependent on the concentration of the elements in the coating solution. Sr^{2+} showed a slightly stronger decrease of the ratio, in particular at the highest concentration. F^- increased the Ca to P ratio and the effect was increased with an increase in ion concentration in the solution. Finally, CO_3^{2-} showed a slight decrease in the ration at all concentrations but the highest one, where an increase was observed.

Discussion

Biomimetic coating method has been developed as an alternative to plasma-spraying and other techniques such as electrodeposition and sol-gel for providing surfaces of (metallic) orthopaedic and dental implants with a calcium phosphate layer in order to improve their bioactivity in bone repair [15]. Important advantages of biomimetic approach as compared to other methods lies in the fact that the biomimetic coating process takes place in solutions at physiological pH and low temperatures, allowing

for coating of a variety of materials, independent on their shape and structure with a range of calcium phosphate phases. Furthermore, coprecipitation of biological agents, such as antibiotics and growth factors into calcium phosphate coatings is possible, adding new functions to their activity in vivo [13, 14]. In the present study, we have employed biomimetic aproach to develop a standardized medium-throughput in vitro method for studying the effect of additives to the coating on the behavior of cells relevant for bone formation and resorption. This simple approach consisted of providing tissue culture well plates with a thin calcium phosphate layer containing additives in different concentrations. This resulted in a system that mimics a coated implant and yet allows for the standardized cell culture, with known cell numbers, culture medium volume and direct comparison with the controls. Furthermore, by using 48-well plates, and the possibility to work in 96-well plates, the assays are medium-throughput, without being labour-intensive.

Instead of using growth factors or other biological agents, we have used a number of trace elements as additives to the coatings. Trace elements, although present at very low concentrations, play a pivotal role in the functioning of human body. Also in biological process related to bone, such as angiogenesis, osteogenesis and osteoclastogenesis, the role of a number of trace elements has been shown to be of great importance [16-19]. It is therefore highly conceivable that trace elements, when combined with bone graft substitutes under appropriate conditions, could become a valuable inexpensive alternative to growth factor- and cell-based tissue engineering. Another scientifically interesting reason behind the choice of trace elements as additives was the expectation that their presence would, to a certain extent, interfere with the formation of calcium phosphate coating from the coating solution.

For this study, we have chosen copper, zinc, strontium, fluoride and carbonate as relevant ions, all of which have been shown to interfere with bone formation in vitro and in vivo [20-25]. The choice of their salts was such that, when dissolved in the biomimetic solution, their effect on the local pH would be minimal.

The results of the present study showed that the biomimetic coating method was successfully employed to provide wells of tissue culture well-plates with a uniform thin layer of calcium phosphate containing varying concentrations of the five investigated trace elements. The calcium phosphate phase formed in absence of trace elements was a mix between octacalcium phosphate and hydroxyapatite, as was shown by the calcium to phosphorus ratio [26]. Elemental mapping using EDX demonstrated a homogenous distribution of the trace elements in the coating. Measurements of the total amount of incorporated elements as well as the element to calcium ratio showed that with increasing concentration of the element in coating solution the final element content of the coating also increased. Although these measurements were only performed for Cu^{2+}, Zn^{2+} and Sr^{2+}, it is expected that they were also representative for CO_3^{2-} and F^-. This assumption was confirmed by performing trace element to calcium measurement on the surface of the F- coatings using EDX elemental mapping (results not shown). Absolute amounts of incorporated element into the coating as well as its effect on the coating morphology largely differed based on the element type.

For Cu^{2+} and Zn^{2+}, the increase of total amount found inside the coating and the increase of Cu/Ca and

Zn/Ca ratio were consistent with the increase of concentration of the Cu^{2+} and Zn^{2+} in the coating solution. For example, the total amount of Cu^{2+} and Cu/Ca ratio in the coating made from Cu10 solution was more than 9 times higher than that made from Cu1 solution. Similarly, difference in the total amount of Zn^{2+} incorporated and Zn/Ca ratio between coatings made in solutions Zn1 and Zn10, respectively was about 8 times. Changes in the trace element to calcium ratios indicated that both Cu^{2+} and Zn^{2+} were incorporated into the CaP lattice. Indeed, observed decrease of calcium to phosphorus ratio in presence of these ions indicated that Cu^{2+} and Zn^{2+} ions occupied the Ca^{2+} sites in the crystalline lattice, which is consistent with other studies on incorporation of these ions into calcium phosphate crystals [27]. Zn^{2+} and Cu^{2+} show much chemical similarity with the alkaline earth metals and this may explain their ability to enter the apatite lattice. Replacement of Ca^{2+} with Cu^{2+} and Zn^{2+} reduces the bond lengths between calcium and oxygen atoms in the crystalline lattice mainly due to the lower ionic radius of Cu^{2+} and Zn^{2+} compared with that of the Ca^{2+} [28, 29]. The total molecular energy decreases with the replacement of Ca^{2+} with Cu^{2+} or Zn^{2+} according to Gutowska [28], meaning that copper and zinc are preferred to calcium from the energy point of view. With regard to crystal morphology, we observed a very slight increase of crystal size between the control coating and coatings containing Cu^{2+} or Zn^{2+}. Raman spectroscopy revealed a non-significant shift of the position of v1 mode of PO_4 bond and a relatively small change of the FWHH of this bond of Cu^{2+} or Zn^{2+} coatings as compared to the control. This relatively small effect of the presence of copper and zinc ions on the basic crystal structure may be contributed to a small absolute amount of these elements present in the coatings.

Similar to Cu^{2+} and Zn^{2+}, the total amount of incorporated Sr^{2+} increased with the increase in concentration of the coating solution, as confirmed by the measurements of coating efficiency and Sr/Ca ratio. A decrease in calcium to phosphorus ratio in presence of Sr^{2+} indicated the replacement of Ca^{2+} by Sr^{2+}, which is plausible, considering that both elements belong to the group of alkaline earth metals. Unlike Cu^{2+} and Zn^{2+}, Sr^{2+} allowed formation of a homogenous coating at concentrations higher than 10 μM. Although no obvious differences in crystal morphology were observed based on from the ESEM analysis, a significant increase of FWHH of v1 mode of PO_4 bond, together with shifting of this peak to lower frequency (shift related to a increase in the unit cell volume), indicated a reduced crystallinity in comparison with the control coating. This observation is related to the replacement of Ca^{2+} with Sr^{2+} which has a larger ionic radius than Ca^{2+} and is in accordance with earlier studies on the effect of strontium on calcium phosphate crystallinity [30-32].

Regarding incorporation of F^- into the coating, it is known that the replacement of OH^- with F^- can decrease solubility of calcium phosphate crystal, and bring about a reduction in the volume of the unit cell [26, 33-35]. This was confirmed by the ESEM observations which showed replacement of large, platelet-like crystals of the control coating by smaller, rod-like crystals in F^- coatings. The significant decrease of FWHH of v1 mode of PO_4 bond, together with shift of this peak to higher frequency in F1000, indicated an increase in crystallinity as compared to the control coating. Similar observations were previously discussed in relation to the presence of fluoride ions in hydroxyapatite and octacalcium phosphate structures [36, 37].

CO_3^{2-} ions can occupy phosphate positions (A type substitution) and/or hydroxyl positions (B type) in the lattice of calcium phosphate [36, 38]. ICP-MS result showed an increase in calcium to phosphorus ratio with the increasing concentrations of carbonate in coating solution, suggesting an increase in A type substitution. The B type substitution is favored energetically, and prevails at low concentration of carbonate. At higher carbonate concentrations, however, the probability of the two substitution types is mainly determined by the number of sites available for substitution, explaining the prevalence of type A substitution in this study [39, 40]. The presence of carbonate in the lattice reduced the crystallinity which was confirmed by the significant increase of FWHH of v1 mode of PO_4 bond and its significant shift to the left. The ESEM micrographs also showed a decrease in crystal size as compared to the control, which is consistent with the A type substitution [41, 42].

The present study showed that the biomimetic coating approach can successfully be used to develop a medium-throughput in vitro system for studying the effect of trace elements incorporated into calcium phosphates. All trace elements were incorporated into the crystalline lattice by substitution of Ca^{2+}, OH^- or PO_4^{3-} sites and were homogenously distributed throughout the coating. The amount of elements incorporated was controlled by changing trace element concentration of the coating solution. A drawback of the system is that there is a limit up to which certain elements can be coprecipitated so as that the coating formation and homogeneity are not affected. Besides trace elements, this system can also be used to investigate the effect of other compounds, such as growth factors at varying concentrations. A next step in our investigation will be experiments with cells related to bone formation and resorption in order to investigate the effect of trace elements using this system.

CONCLUSION

This study presents a standard medium-throughput protocol which can be used to investigate the effect of trace elements on bone formation based on biomimetic coating process. The incorporation of copper, zinc, strontium, fluoride and carbonate into calcium phosphate coating is possible and the amount of incorporated elements can be controlled by varying the concentration of elements in the coating solution. Different elements affected the calcium phosphate crystallization by altering the coating morphology, the coating crystallinity and the coating solubility. Further studies will be performed to test the effect of trace elements on cells related to bone formation and resorption by using this protocol.

ACKNOWLEDGEMENTS

REFERENCES

1.   Epinette, J.-A. and M. Manley, eds. Fifteen years of ckinical experience with hydroxyapatie coatings in joint arthroplasty. 2003, Springer-Verlag. 250.

2.   Furlong, R.J. and J.F. Osborn, Fixation of hip prostheses by hydroxyapatite ceramic coatings. J Bone Joint Surg Br, 1991. 73(5): p. 741-5.

3.   Havelin, L.I., et al., The Norwegian Arthroplasty Register: 11 years and 73,000 arthroplasties. Acta Orthop Scand, 2000. 71(4): p. 337-53.

4.   Yang, Y., K.H. Kim, and J.L. Ong, A review on calcium phosphate coatings produced using a sputtering process--an alternative to plasma spraying. Biomaterials, 2005. 26(3): p. 327-37.

5.   Ducheyne, P., et al., Structural analysis of hydroxyapatite coatings on titanium. Biomaterials, 1986. 7(2): p. 97-103.

6.   Ong, J.L., et al., Structure, solubility and bond strength of thin calcium phosphate coatings produced by ion beam sputter deposition. Biomaterials, 1992. 13(4): p. 249-54.

7.   Choi, A.H. and B. Ben-Nissan, Sol-gel production of bioactive nanocoatings for medical applications. Part II: current research and development. Nanomed, 2007. 2(1): p. 51-61.

8.   Kokubo, T., et al., Solutions able to reproduce in vivo surface-structure changes in bioactive glass-ceramic A-W. J Biomed Mater Res, 1990. 24(6): p. 721-34.

9.   Barrere, F., et al., Influence of ionic strength and carbonate on the Ca-P coating formation from SBFx5 solution. Biomaterials, 2002. 23(9): p. 1921-30.

10.   Barrere, F., et al., Nucleation of biomimetic Ca-P coatings on ti6A14V from a SBF x 5 solution: influence of magnesium. Biomaterials, 2002. 23(10): p. 2211-20.

11.   Du, C., et al., Biomimetic calcium phosphate coatings on Polyactive 1000/70/30. J Biomed Mater Res, 2002. 59(3): p. 535-46.

12.   Varma, H.K., et al., Porous calcium phosphate coating over phosphorylated chitosan film by a biomimetic method. Biomaterials, 1999. 20(9): p. 879-84.

13.   Liu, Y., K. de Groot, and E.B. Hunziker, BMP-2 liberated from biomimetic implant coatings induces and sustains direct ossification in an ectopic rat model. Bone, 2005. 36(5): p. 745-57.

14.   Stigter, M., et al., Incorporation of different antibiotics into carbonated hydroxyapatite coatings on titanium implants, release and antibiotic efficacy. J Control Release, 2004. 99(1): p. 127-37.

15.   Narayanan, R., et al., Calcium phosphate-based coatings on titanium and its alloys. J Biomed Mater Res B Appl Biomater, 2008. 85(1): p. 279-99.

16.   Suttle, N.F., et al., Osteoporosis in copper-depleted lambs. J Comp Pathol, 1972. 82(1): p. 93-7.

17.   ten Cate, J.M., Review on fluoride, with special emphasis on calcium fluoride mechanisms in caries prevention. Eur J Oral Sci, 1997. 105(5 Pt 2): p. 461-5.

18.   Dahl, S.G., et al., Incorporation and distribution of strontium in bone. Bone, 2001. 28(4): p. 446-53.

19.   Burch, R.E., H.K. Hahn, and J.F. Sullivan, Newer aspects of the roles of zinc, manganese, and copper in human nutrition. Clin Chem, 1975. 21(4): p. 501-20.

20.   Otsuka, M., et al., Efficacy of the injectable calcium phosphate ceramics suspensions containing magnesium, zinc and fluoride on the bone mineral deficiency in ovariectomized rats. J Pharm Sci, 2008. 97(1): p. 421-32.

21.   Zhang, Y.H., et al., [Effects of zinc deficiency on bone mineralization and its mechanism in rats]. Zhonghua Yu Fang Yi Xue Za Zhi, 2003. 37(2): p. 121-4.

22.   Takahashi, N., et al., S 12911-2 inhibits osteoclastic bone resorption in vitro. J Bone Miner Res, 2003. 18(6): p. 1082-7.

23.   Khandare, A.L., et al., Beneficial effect of copper supplementation on deposition of fluoride in bone in fluoride- and molybdenum-fed rabbits. Calcif Tissue Int, 2005. 77(4): p. 233-8.

24.   Hott, M., et al., Proliferation and differentiation of human trabecular osteoblastic cells on hydroxyapatite. J Biomed Mater Res, 1997. 37(4): p. 508-16.

25.   Fatokun, A.A., T.W. Stone, and R.A. Smith, Responses of differentiated MC3T3-E1 osteoblast-like cells to reactive oxygen species. Eur J Pharmacol, 2008. 587(1-3): p. 35-41.

26.   Elliott, J., Structure and Chemistry of the Apatites and Other Calcium Orthophosphates. ed. . Vol. . 1994, Amsterdam-London-New York-Tokyo: Elsevier. 389.

27.   LeGeros, R., Apatites in biological systems. Prog Cryst Growth Charact, 1981. 4: p. 1-45.

28.   Gutowska, I., Z. Machoy, and B. Machalinski, The role of bivalent metals in hydroxyapatite structures as revealed by molecular modeling with the HyperChem software. J Biomed Mater Res A, 2005. 75(4): p. 788-93.

29.   Shannon, R. and C. Prewitt, Effective ionic radii in oxides and fluorides. Acta Cryst, 1969(B25).

30.   Legeros, R.Z., et al. effect of the strontium on some properties of apatites. in the 5th Interantional Symposium. 1989.

31.   Wang, X. and J. Ye, Variation of crystal structure of hydroxyapatite in calcium phosphate cement by the substitution of strontium ions. J Mater Sci Mater Med, 2008. 19(3): p. 1183-6.

32.   Verberckmoes, S.C., et al., Effects of strontium on the physicochemical characteristics of hydroxyapatite. Calcif Tissue Int, 2004. 75(5): p. 405-15.

33.   Young, R. large effects from the small structural differences in apatites. in Pro Int Cong Phosphorous Compounds. 1980.

34.   legeros, R.Z. and J.P. Legeros, in An introduction to bioceramics, L. Hench and J. WIlson, Editors. 1993, World Scientific: Singpore.

35.   Aoba, T., The effects of the fluoride on apatite structure and growth. Crit Rev Oral Dent Med, 1997(8): p. 136-153.

36.   Elliott, J.C., D.W. Holcomb, and R.A. Young, Infrared determination of the degree of substitution of hydroxyl by carbonate ions in human dental enamel. Calcif Tissue Int, 1985. 37(4): p. 372-5.

37.   Shimoda, S., et al., Effect of solution composition on morphological and structural features of carbonated calcium apatites. J Dent Res, 1990. 69(11): p. 1731-40.

38.   Aoba, T. and E.C. Moreno, Changes in the nature and composition of enamel mineral during porcine amelogenesis. Calcif Tissue Int, 1990. 47(6): p. 356-64.

39.   Vignoles, M., et al., Influence of preparation conditions on the composition of type B carbonated hydroxyapatite and on the localization of the carbonate ions. Calcif Tissue Int, 1988. 43(1): p. 33-40.

78

40.   Gibson, I.R. and W. Bonfield, Novel synthesis and characterization of an AB-type carbonate-substituted hydroxyapatite. J Biomed Mater Res, 2002. 59(4): p. 697-708.

41.   McClellan, G. and J. Lehr, Crystal-chemical investigations of natural apatites. Am Min, 1969. 54: p. 1374-1391.

42.   LeGeros, R.Z., et al., Two types of carbonate substitution in the apatite structure. Experientia, 1969. 25(1): p. 5-7.

Chapter 5

Effect of trace elements on in vitro behavior of osteoblasts and osteoclasts: a medium-throughput study

Despite small amounts in which they are present, trace elements play crucial roles in the development and turnover of human bone and teeth. In a previous study, we have successfully setup a medium-throughput in vitro system to study the effect of trace elements on cells related to bone formation and resorption. This system is based on coating multiwell cell culture plates with a thin calcium-phosphate layer containing different concentrations of trace elements. In the present study, we have employed this system to study the effect of copper, zinc, strontium, fluoride and carbonate ions on proliferation and differentiation of MC3T3-E1 osteoblasts as well as on the attachment and resorptive activity of primary osteoclasts. AlarmaBlue and Alkaline Phosphatase activity were used as assays for MC3T3 proliferation and differentiation, respectively. Number of resorbing and non-resorbing osteoclasts and number of resorption pits were measured in order to assess the attachment and resorptive activity of osteoclasts. All investigated trace elements, showed an inhibitory effect on resorptive activity by primary osteoclasts. The effect on proliferation and differentiation of MC3T3 osteoblasts depended on the type of trace element and concentration tested. In general, copper and zinc ions showed an inhibitory effect on osteoblast proliferation, the effect of strontium was concentration dependent, whereas coatings containing fluoride and carbonate, respectively showed stronger osteoblast proliferation as compared to the control. The effect of copper and zinc on osteoblast differentiation was non-existing or mild-inhibitory, while strontium, fluoride and carbonate ions demonstrated a clear decrease in differentiation in comparison to the control coating without trace elements. The observed effects were either direct, by the presence of released elements from the coating in the cell culture medium, or indirect, through the effect of trace elements on coating morphology and dissolution behavior. This study shows that the proposed system can successfully be employed for studying the effect of trace elements on osteoblasts and osteoclasts in vitro in a standardized way. The advantage of this system above a simple addition of dissolved ions into the cell culture medium is that it mimics the environment of bone mineral and calcium-phosphate based bone graft substitutes.

INTRODUCTION

Trace elements play essential roles in various functions of human body. A great number of trace elements are found in bones and teeth and although they are minor components of these tissues, they are of great importance in their development, turnover and degradation. For example, in the metabolism of the skeleton, copper (Cu) performs a key catalytic function in the first step of the maturation of collagen to form stable fibrils [1, 2]. Several reports suggested that mild Cu deficiency may contribute to bone defects such as osteoporotic-like lesions and bone fragility in humans and animals [3, 4], as well as in a variety of bone developmental defects in preterm infants [5, 6]. Oral supplementation with Cu, however, resulted in complete healing of fractures and improvement in other bone defects [5, 6]. Cu was shown to affect both the proliferation and differentiation behavior of Mesenchymal Stem Cells (MSCs) in vitro. It decreased the proliferation rate of MSCs and induced an increase in their differentiation towards the osteogenic and adipogenic lineage [7]. Cu was also reported to affect the timing of expression of Alkaline Phosphatase (ALP) activity, which reached its maximum earlier than in the control samples. Wilson suggested that higher concentrations of Cu (10^{-5}M copper sulfate in culture medium) reduced bone resorption and inhibited hydroxyproline, protein, and DNA synthesis in vitro [8]. Cu was shown to enhance proliferation of endothelial cells and angiogenesis in vivo, a process which is of great importance in healing of large bone defects [9-11].

Zinc (Zn) has multiple important functions in biological systems. It is a trace metal required for the activity of over 300 metalloenzymes, including those involved in nucleic acid and protein synthesis, cellular replication, immune function, and antioxidant systems [12]. It is a constituent of various enzymes and proteins such as ALP, lactate dehydrogenase and carbonic anhydrase, steroid hormone receptors, and transcription factors [13, 14]. There exist about 1,400 zinc-finger proteins that participate in the genetic expression of many proteins [15]. Zn has also been shown to have a stimulatory effect on bone formation and mineralization in vivo and in vitro via bone protein synthesis [16-18]. Stimulatory effects of Zn on ALP [19], protein tyrosine phosphatase activity [20], protein [21], and deoxyribonucleic acid (DNA) syntheses [22] of osteoblast-like MC3T3-E1 cells have also been reported. Furthermore, there exist reports on inhibitory effects of Zn on bone resorption [23, 24] and osteoclast-like cell formation in mouse bone marrow cultures [25], where the metal acts on the later stage of differentiation from bone marrow cells to osteoclasts [26].

Strontium (Sr), together with calcium and magnesium, belongs to the group 2 of the periodic system and, from a chemical point of view, they behave similarly. They all form divalent cations in biological fluids, and have varying degrees of protein binding in biological fluids like serum or plasma, where the protein bindings of Sr and Ca are of the same order of magnitude [27]. In addition, Sr is a bone-seeking element, of which 98% in human body can be found in the skeleton [28]. It is therefore not surprising that among the trace metals present in human bone, Sr was the only one that was correlated with bone compressive strength [29]. Sr was shown to have dose-dependent effects on bone formation: while low doses (0.19% - 0.34% in drinking water) were reported to improve the vertebral bone density and stimulate bone formation in rats [30-32]; high doses (> 0.4% in drinking water) of Sr were shown

to have deleterious effects on bone minerlization in rat [30, 31]. Sr levels of 20-100 ug/ml in culture medium were shown to have an inhibitory effect on osteoblast mineralization (reduced hydroxyapatite formation) in vitro [33]. Sr was also shown to reduce excessive bone resorption in rats with osteopenia and the decrease was associated with the decrease in the number of osteoclasts [34]. Baron [35] further showed that Sr compound dissolved into the culture medium inhibited osteolcast differentiation and osteoclast activity and the inhibition increased with the increase of the dose, while there was no effect on the attachment of the osteoclast. Furthermore, it was also shown that that Sr incorporated into hydroxyapatite could inhibit the bone-resorbing activity in vitro [36].

Fluoride (F) plays a key role in the prevention and control of dental caries. Studies in both humans and animals showed that fluoride affected predominantly the maturation stage of enamel formation [37-41]. F was also found to be the single most effective agent for increasing bone volume in the osteoporotic skeleton [42] and an effective anabolic agent to increase spinal bone density by increasing bone formation and mineralization [43, 44]. Like Sr, the effects of F on bone formation are also dose related: low doses of F increased the trabecular bone density of osteoporotic patient at around 50 mg sodium fluoride daily intake [45-47] whereas a dose of 75 mg/day had no beneficial effects on bone mineral density in postmenopausal women [48]. 0.8 mg/kg fluoride intake also stimulated bone formation in rats [32]; however high doses ($>5*10^{-4}$M) of fluoride in culture medium showed inhibitory effect on osteoblast proliferation and differentiation in vitro [49-51].

As for effects on osteoclasts, reports showed that NaF in concentrations of 0.5-1.0 mM in medium decreased the number of resorption lacunae made by individual osteoclasts as well as the resorbed area per osteoclast [52] and that the suppression of the resorption was enhanced by increasing the NaF concentration of the cell culture medium [53].

Carbonate (CO_3) ions play a very important role in skeleton development. Bone mineral, a calcium phosphate apatite, contains multiple ionic substitution, among which carbonate ions at 2-8 wt% are the most abundant [54]. Studies showed that implants made of synthetic sintered apatites containing carbonate perform well in terms of biocompatibility and bioactivity in repair of bone defects [55-57].

The biomimetic coating method, which is based on immersion of a biomaterial into a solution that mimics the inorganic composition of human blood plasma (the so-called Simulated Body Fluid (SBF)) at physiological conditions, was originally developed by Kokubo in 1990 [58], and has since been improved by several groups of investigators. In the previous chapter, we have presented a calcium phosphate coating based system of tissue culture plates to incorporate trace elements for further medium-throughput study on effect of trace elements on cells relevant to bone formation and resorption.

In the present study, we have employed this medium-throughput system to investigate the effect of a number of trace elements (Cu, Zn, Sr, F and CO_3) at varying concentrations on proliferation and differentiation of osteoblast-like MC3T3 cells and attachment and resorptive activity of primary osteoclasts. Eventually, systemic information on the effect of trace elements on behavior of cells relevant to bone formation and resorption could lead to the improvement of the performance of existing bone graft substitutes in repair of large, clinically relevant bone defect.

MATERIALS AND METHODS

Preparation of the biomimetic calcium phosphate coatings

The various coatings were directly prepared into the 48-tissue culture treated well plates (NUNC) following a two-step procedure, discussed in detail in the previous chapter. First, a thin amorphous calcium phosphate layer was deposited at room temperature from a highly supersaturated Simulated Body Fluid (SBFx2.5, buffered with TRIS/HCl buffer at pH=7.4, Table 1) that was daily prepared at 4°C and refreshed for 3 subsequent days (500μl/well). Second, the final biomimetic calcium phosphate coating was obtained by pouring a Calcium Phosphate Solution (CPS, as previously described, Table 1) supplemented with the chosen trace element at a chosen concentration. CPSs were daily refreshed for 3 subsequent days (500μl/well).

Finally, the coated plates were washed with demineralized water and dried at 50°C for approximately 4h.

Table 1: Inorganic composition (mM) of the coating solutions						
	Na^+	Mg^{2+}	Ca^{2+}	Cl^-	HPO_4^{2-}	HCO_3^{2-}
SBFx2.5	366.5	3.75	6.25	370.0	2.5	10.5
CPS	140.4	0.0	4.0	142.9	2.0	0.0

Functionalization of the biomimetic coatings with trace elements

In order to prepare stock solutions, mineral salts (CuAc, ZnAc, SrAc, NaF, $NaHCO_3$; reagent grade, Sigma Aldrich) were dissolved in TRIS solution and buffered with HCl 1M at pH=7.4 to reach the molar concentration of 0.1 M (for Sr^{2+}, F^-, and CO_3^{2-} ions) or 0.01 M (for Cu^{2+} and Zn^{2+}). They were individually added in the CPS solution in order to obtain various concentrations from 0.1 μM to 10000 μM in CPS solution, as shown in table 2. The solutions will be further labelled respectively F-CPS, Sr-CPS, Cu-CPS, Zn-CPS, CO_3-CPS; and the resulting coatings will be further labelled Cu0.1, Cu1, Cu10; Zn0.1, Zn1, Zn10; Sr1, Sr10, Sr100, Sr1000; F1, F10, F100, F1000; $CO_3$1, $CO_3$10, $CO_3$100, $CO_3$1000, $CO_3$10000 respectively.

Full physico-chemical and morphological characterization of the obtained coatings was described in the previous chapter.

Table 2: Ion concentration (μM) in CPS solution used to prepare the functionalized coatings						
	0.01	0.1	1	10	100	1000	10000
$[Cu^{2+}]$	-	x	x	x	-	-	-
$[Zn^{2+}]$	-	x	x	x	-	-	-
$[Sr^{2+}]$	-	-	x	x	x	x	-
$[F^-]$	-	-	x	x	x	x	-
$[CO_3^{2-}]$	-	-	x	x	x	x	x

Effect of osteoblast proliferation and differentiation

Murine osteoblastic cell line MC3T3-E1 was used to study the effect of trace elements on osteoblast

proliferation and differentiation.

In order to study cell proliferation, 5000 cells in 500 μl MC3T3 proliferation medium (Alpha MEM + 1% PS + 2mM L-Glutamine + 1mM sodium pyruvate + 10% FBS) were added to each well of the coated 48-well plate. Uncoated well plates served as a control. The cells were cultured for 7 days (37 °C, 5 % CO2) with medium refreshment on days 2 and 4. AlamarBlue® was used as a proliferation assay and was performed on days 2, 4 and 7. AlamarBlue is a redox indicator that yields a colorimetric change and fluorescent signal in response to metabolic activity. Briefly, a solution containing 10% AlamarBlue dye in fresh proliferation medium was prepared and pre-warmed at 37°C. Then, the proliferation medium from the well plates was replaced by 500ul AlamarBlue solution and the plates were placed in an incubator at 37°C for 4 hours. After incubation, 200ul solution from each well was transferred to a 96-well plate and colorimetric change was read using a luminescent spectrometer (LS 50B, Perkin Elmer) at wavelength of 545 nm^{-1}. Cells were then washed with PBS and kept in culture with new growth medium.

In order to study the effect on osteoblast differentiation, 500 μl MC3T3 proliferation medium with cell density of 5000 cells/well was added to each well. Medium was refreshed on day 2. On day 4, proliferation medium was replaced by 500 μl MC3T3 differentiation medium (Alpha MEM + 1% PS + 2mM L-Glutamine + 1mM sodium pyruvate + 10% FBS + 1% L-ascorbic acid-2 phosphate + 1% β-glycerol phosphate) per well. Cell culture continued until day 10, with medium refreshment on day 7. Alkaline Phosphatase (ALP) activity was chosen as a marker for osteogenic differentiation. ALP and DNA assay were performed on day 10 of the culture. Briefly, 150 μl lysis buffer (0.2% Triton x-100 solution in 100mM postassium phosphate buffer pH7.8) was prepared and added to each well after washing with PBS. The plates were then stored at -20°C overnight. After thawing at room temperature, 15μl lysate from each well was transferred into a well of a 96-well plate. Then 40μl CDP-star (Roche) solution was added to each well according to the manufacturer's protocol and incubation was performed for 30 minutes in dark at room temperature. Luminessence was measured using a VICTOR^3 Luminometer. Meanwhile, the DNA amount inside the lysis buffer was measured using CyQuant™ kit, according to manufacturer's instructions. Finally, the ALP signal was normalized for DNA amount (which was proportional to the cell number).

Osteoclast isolation and culture

5-day old New Zealand White rabbits (Haarlan Nederland B.V., Horst, The Netherlands) were killed by injecting sodium pentobarbitone (150 mg/ml) intrapertoneally. Long bones (humerus, ulna, fibula and tibia) were aseptically dissected and cleaned of adhering tissue. The long bones were minced mechanically at room temperature in 20 ml of minimal essential medium (α-MEM) supplemented with 5 % heat inactivated fetal calf serum (FCS) and 100 U/ml penicillin and 10 μg/ml streptomycin (Gibco Lab, Grand Island, NY). The minced bone fragments were transferred to a 50 ml tube and agitated using a wide-ended Pasteur pipette. The fragments were then allowed to settle for 1 minute, after which the cell suspension was transferred to another tube. Another 20 ml of α-MEM with 5% FCS and antibiotics was

the added to the remaining fragments and the previous step repeated. The resulting suspensions were pooled, centrifuged for 5 min at 800 rpm, and the pellet containing the cells resuspended in 4-6 ml of α-MEM with 5% FCS and antibiotics.

Osteoclast activity

In order to analyze the effect of trace elements on osteoclasts resorptive activity, 500 μl of osteoclast suspension was added to each well of 48-well plates. After an incubation period of 3 h at 37 °C in humidified air containing 5 % CO2, the non-attached cells were washed away and the attached cells, enriched in osteoclasts, were kept in culture for 40 h. After the culture period the conditioned medium was harvested, centrifuged and analyzed for Lactate dehydrogenase (LDH) activity. The attached osteo-clasts were washed with PBS, fixed for 10 min with 4% formaldehyde in PBS and stained for TRACP activity using the leukocyte acid phosphatase (TRACP) kit (Sigma Chemical, St. Louis, MO) according to the manufacturer's instructions. Nuclei was stained with diamidino-2phenylindole dihydrochloride (DAPI). Five micrographs from fixed positions per well were taken with a digital camera (Leica, Wet-zlar, Germany) and analyzed for the following parameters: (1) the number of resorption pits, (2) the number of resorbing osteoclasts (osteoclasts located on a resorption pit) and (3) the number of non-resorbing osteoclasts (osteoclasts located on intact mineral and not associated with a pit). The area of resorption pits was measured using Image-Pro plus (Media Cybernetics, Silver Spring, ML) software.

Lactate dehydrogenase (LDH) activity

To measure cytotoxicity, supernatants of cultured osteoclasts for 40 h were collected, centrifuged to remove wear particles and cell debris, and stored at -20 °C until further testing. Release of the cytoplas-mic enzyme LDH, a marker of cell damage, was measured using the Cytotoxicity Detection kit (LDH) (Roche Diagnostics, Mannheim, Germany). Each supernatant was tested in duplicate.

Statistical analysis

Proliferation and differentiation data of osteoblasts were statistically analyzed using the one way analy-sis of variance (ANOVA) followed by Tukey's HSD multiple comparison post-hoc test. For statistical testing of attachment and resorptive activity of osteoclasts, the Kruskal-Wallis nonparametric analysis of variance test followed by Tukey-Kramer's multiple comparison test was used. Effects were consid-ered statistically significant at $p<0.05$ (two-tailed).

RESULT

Effect on proliferation of MC3T3

Fig. 1 shows the AlamarBlue data for MC3T3 cells cultured on coatings with and without trace ele-ments for 2, 4 and 7 days.

Both Cu^{2+} and Zn^{2+} showed inhibitory effect on proliferation of osteoblasts, however, this effect was only visible after a longer culture period of 7 days. On days 2 and 4, there was no significant difference

between coatings with Cu^{2+} and Zn^{2+} and the control coating. On day 7, however Cu^{2+} significantly decreased the proliferation at all concentration compared to the control coating, whereas Zn^{2+} significantly decreased the proliferation at concentrations Zn0.1 and Zn1.
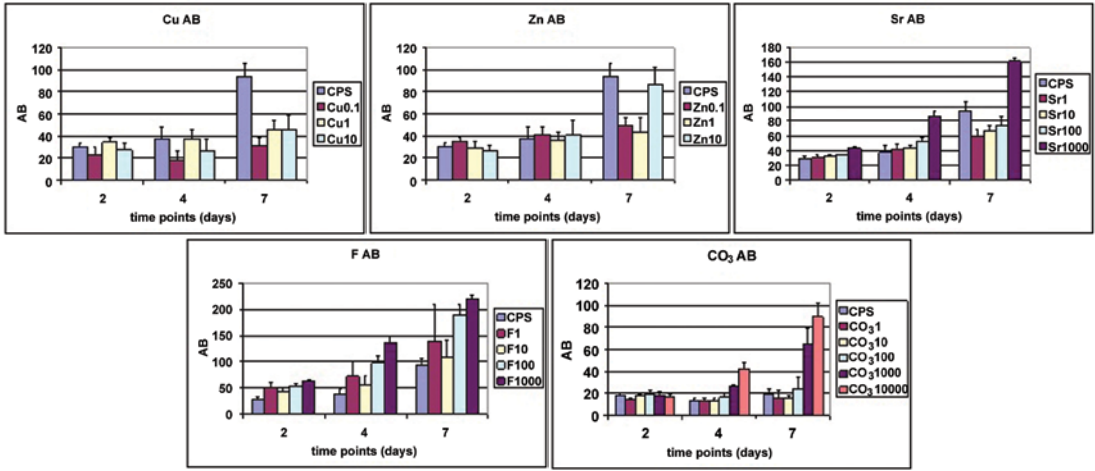

Figure 1: Proliferation of MC3T3 cells
AlamarBlue values showing proliferation of MC3T3 cells on days 2, 4, 7 cultured on control coating and coatings with varying concentrations of a) Cu^{2+}; b) Zn^{2+}; c) Sr^{2+}; d) F^-; and e) CO_3^{2-}.

Regarding the effect of Sr^{2+}, its highest concentration (Sr1000) showed a significantly higher proliferation value than the control coating at all time points tested. On days 2 and 4, coatings with other concentrations of Sr^{2+} did not differ significantly from the control, whereas at day 7, Sr1 and Sr10 coatings showed a lower proliferation than the control. Presence of F^- had a stimulatory effect on osteoblast proliferation at all time points and this effect was dose dependent: the higher the concentration in the coating, the stronger the effect.

Finally, also CO_3^{2-} showed a clear effect on proliferation of osteoblasts. While on day 2, no signifi-
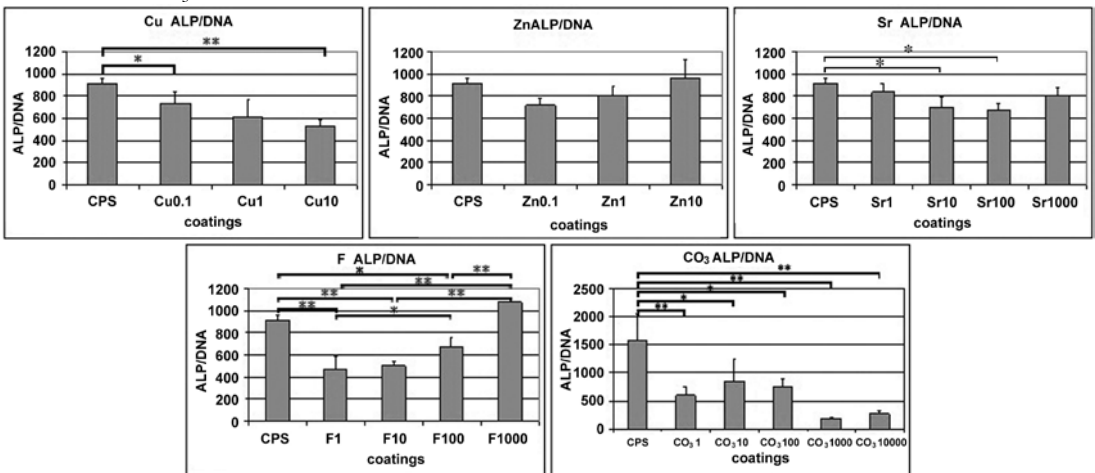

Figure 2: Differentiation of MC3T3 cells
ALP/DNA values representing osteogenic differentiation of MC3T3 cells after subsequent culture for 4 days in proliferation- and 6 days in differentiation medium on control coating and coatings with varying concentrations of a) Cu^{2+}; b) Zn^{2+}; c) Sr^{2+}; d) F^-; and e) CO_3^{2-}. Significant differences: (*) $p<0.05$; (**) $p<0.01$.

cant difference was found between coatings with and without CO_3^{2-}, on days 4 and 7, $CO_3 1000$ and $CO_3 10000$ showed a significantly higher AlamarBlue value than the control coating and coatings with lower CO_3^{2-} concentrations.

Effect on differentiation of MC3T3

After subsequent culture in proliferation medium for 4 days and differentiation medium for another 6 days, the ALP activity of the cells was measured for all conditions. Figure 2 represents the ALP/DNA data.

Similar to the proliferation results, coatings containing Cu^{2+} showed a mild, but significant decrease of ALP/DNA expression as compared to the control coating. In contrast, no effect of Zn^{2+} was observed at any of the tested concentrations.

Sr10 and Sr100 coatings, which showed an inhibitory effect on osteoblast proliferation on day 7 also showed a lower differentiation value than the control coating. No significant difference was observed with coatings containing other Sr^{2+} concentrations tested.

F- showed an inhibitory effect on osteoblast differentiation, but only at lower concentrations and following the trend the lower the concentration, the stronger the inhibitory effect.

Finally, coatings containing CO_3^{2-} showed an inhibitory effect on MC3T3 differentiation and the effect increased with increasing CO_3^{2-} content of the coating.

It should be noted that proliferation of MC3T3 cells in uncoated tissue culture well plates was 2-3 fold faster than that in the coated plates with or without coatings, and that cells were confluent at day 7, which decreased the reliability of the AlamarBlue assay. Also the ALP expression pattern of the cells cultured on uncoated culture plastic was different from that of cells cultured on coated plates (ALP achieved its peak earlier in uncoated than in coated plates). We have therefore decided not to present the data obtained from cultures in uncoated plates in this manuscript.

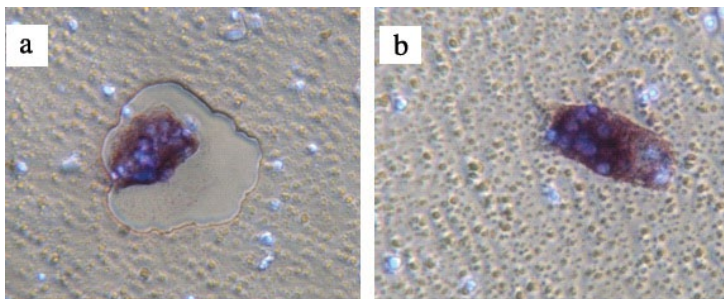## Effect on osteoclast attachment and resorptive activity

Figure 3: After 40 h of culture on CaP coated 48-well plates osteoclasts were stained for TRACP activity. a) resorbing osteoclast and b) non-resorbing osteoclast.. Nucleai were counterstained with DAPI. Phase contrast. Magnification x 400.

Rabbit osteoclasts were plated on culture plates coated with coatings with or without trace elements at different concentrations for 40 h. Figure 3 shows a representative culture after staining for TRACP. Re-

sorbing osteoclasts (osteoclasts located on a resorption pit) and nonresorbing osteoclasts (osteoclasts located on intact mineral and not associated with a pit) can be distinguished (Fig. 3 a and b, respectively). In order to analyze whether the presence of trace elements in the coating influenced osteoclastic resorption, the number of resorption pits were quantified. A significant decrease in the number of resorption pits in osteoclasts cultured on trace element-containing coatings was observed as compared to the control coating. The decrease in the number of resorption pits was observed for all elements tested (Figure 4).
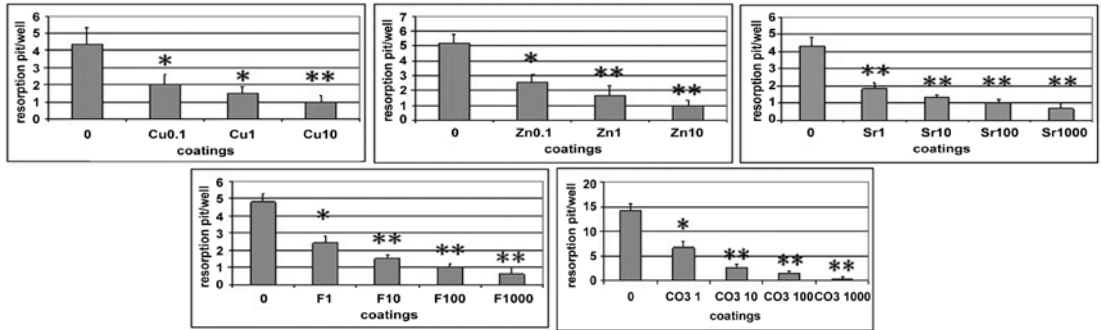
Figure 4: Resorptive activity of osteoclasts
Number of resorption pits/well present after 40 hours of culture of rabbit osteoclasts on control coating and coatings with varying concentrations of a) Cu^{2+}; b) Zn^{2+}; c) Sr^{2+}; d) F^-; and e) CO_3^{2-}. Significant differences: (*) $p<0.05$; (**) $p<0.01$ compared with control coatings.

To test whether trace elements tested affected the viability of osteoclasts, the release of LDH into the medium was determined. Similar levels of released LDH were found in control coatings and coatings containing trace elements at different concentrations (data not shown) indicating that there was no toxic effect of the trace elements at the concentrations tested.

The reduction in the number of resorption pits observed in osteoclasts cultured on coatings containing
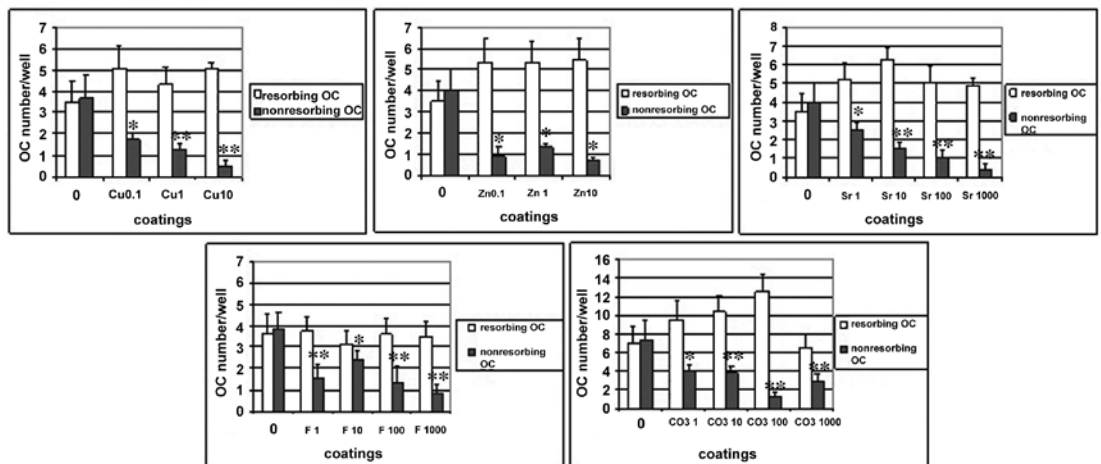

Figure 5: Attachment of osteoclasts
Numbers of resorbing and non-resorbing osteoclasts initially attached onto control coating and coatings with varying concentrations of a) Cu^{2+}; b) Zn^{2+}; c) Sr^{2+}; d) F^-; and e) CO_3^{2-}. Significant differences: (*) $p<0.05$; (**) $p<0.01$ compared with nonresorbing OC of control.

trace elements could be the result of a lower number of osteoclasts initially attached to the coating. Therefore, the number of both resorbing and non-resorbing osteoclasts attached to the coatings were analyzed. As is shown in figure 5, no difference was found in numbers of osteoclasts without or with trace elements tested at different concentrations.

Discussion

Increasing numbers of researches nowadays focus on the effect of trace elements on bone formation and turnover despite the ultra low amounts of these trace elements inside the human body [6, 29, 30, 35, 59-61]. In a previous study, we have successfully setup a medium-throughput in vitro system to study the effect of trace elements on cells related to bone formation and resorption. This system is based on coating multiwell cell culture plates with a thin calcium-phosphate layer containing different concentrations of trace elements. In the present study, we have employed this system to study the effect of Cu^{2+}, Zn^{2+}, Sr^{2+}, F^- and CO_3^{2-} on proliferation and differentiation of osteoblasts as well as on the attachment and resorptive activity of osteoclasts. The choice of trace elements was made based on the literature showing their effect on one or more stages of bone development and turnover in vitro and in vivo.

In an attempt to determine the in vitro biological properties of the biomimetic calcium phosphate coatings containing trace elements on the behavior of osteoblasts, we have chosen MC3T3-E1 cell line as a model. Among the cellular models of osteoblastic differentiation, MC3T3-E1 cell line, a non-transformed model derived from mouse calvaria, was shown to be the best model for examining osteoblast differentiation on the cytochemical, as well as on the transcriptional level, with most marker genes unregulated under osteogenic conditions [20, 62]. Alkaline phosphate activity, an indicator of osteoblast differentiation from non-calcium-mineral-depositing to calcium-mineral-depositing cells, was regarded as an early differentiation marker. It is reported that an enhanced expression of ALP is needed before the onset of matrix mineralization, providing localized enrichment of inorganic phosphate, one of the components of apatite, the mineral phase of the bone [63]. Based on the preliminary experiments, we have chosen to measure the ALP activity at 10 days of culture, because both cell growth and ALP expression occur slower on the calcium-phosphate coated than on the uncoated tissue culture plastic.

Previous studies have shown that there exist a large number of factors that can influence osteoblast attachment, proliferation and differentiation on calcium phosphate surfaces: calcium-phosphate phase, crystallinity, degradability, micro- and macrostructure [36, 55, 64, 65]. In our study, we have added an additional factor which is the effect of trace elements that are released from the coating during cell culture and which have previously been shown to have an effect on the cell behavior when added to the cell culture medium [3, 19, 48, 66].

Regarding the effect of copper, our results showed that although there was little difference in attachment of MC3T3 cells after 2 days, the number of osteoblasts at 7 days was significantly lower on the coatings containing Cu, as compared to the control. These findings are in accordance with those by Fromigue and coworkers with human bone marrow stromal cells [7]. However, in contrast to the study by Fromigue and colleagues, we have observed an inhibitory effect of Cu on MC3T3 differentiation,

which could possibly be explained by the fact that the peak of ALP expression of MC3T3 cells occurred earlier than in the control samples. As the findings of our previous study showed no effect on the presence of Cu on the coating morphology and crystallinity, it can be assumed that the observed effect on the cell behavior was direct, i.e. effect of Cu ions released from the coating into the cell culture medium. Zinc ions present in the coating did not affect the attachment of osteoblasts at 2 days, however, cell proliferation at later time points was significantly increased by higher concentrations tested, which is in accordance with studies by others [16-18]. Cell differentiation on the other hand was not affected by the presence of Zn ions. This finding conflicts with those by others [19-21], which could either be explained by the fact that the concentrations on Zn ions in our study were lower than those in the previous studies or by the fact that the peak of ALP expression occurred earlier in presence than in absence of Zn, as suggested by Storrie and Stupp [67]. Also Zn did not considerably change the morphology or the crystallinity of the coating, suggesting that the observed effect of cell proliferation was directly through the presence of Zn ions.

For both Sr and F, dose dependent effects on proliferation and differentiation were observed: lower concentrations of Sr and F decreased or showed no effect onproliferation and differentiation while higher concentration of both elements increased both MC3T3 proliferation and differentiation. For Sr, the substitution of Ca with Sr in the crystal lattice is expected to increase the dissolution of the coating, increasing therewith the amounts of Ca and Sr in the medium, both of which could have a stimulatory effect on proliferation. High F content produces a low surface potential which favors cell attachment and could therefore have a positive effect on osteoblast proliferation. An increase in differentiation at higher concentrations of Sr and F are consistent with earlier studies showing that both elements can stimulate osteogenic differentiation and bone formation at certain levels within physiological range [30-32, 45]. The incorporation of carbonate into the coating favored the formation of carbonate apatite, with smaller crystals and larger surface area. Carbonated apatite is known to be more soluble than apatites without carbonate, which could have been a reason for the more pronounced osteoblast proliferation in coatings with higher CO_3 content [55]. However, the differentiation was significant decreased in presence of carbonate, which conflicts the data from earlier studies which showed higher cell proliferation on more soluble calcium phosphate phases. A possible reason for our observation of decreased cell differentiation could be local pH changes caused by the release of carbonate from the coating during cell culture. The effect on resorptive activity of osteoclasts was consistent for all trace elements investigated; an inhibitory effect was observed for all elements at all concentrations. For each element, drop in the number of resorption pits increased with the increase of trace element concentration. The observed decrease of resorptive activity was neither related to the number of osteoclasts attached to the coating nor to the toxic effect of trace elements to the cells. For copper, zinc, strontium and fluoride, these results are consistent with earlier reports showing that the presence of these trace elements could inhibit osteoclastic resorption in vitro and in vivo [8, 23, 24, 35, 36, 53]. A recent study using a similar model showed that in contrast to the elements investigated here, cobalt ions increased resorptive activity of osteoclasts [68],. The effect of carbonate on the decreased resorption could either be contributed to the change of

coating morphology or to the local changes of the pH of the medium due to release of carbonate ions, which could affect the activity of osteoclasts [59].

CONCLUSION

In conclusion, this study confirms that the previously developed medium-throughput system based on biomimetic coating method can be used to study the effect of trace elements on the behavior of osteoblasts and osteoclasts. All investigated trace elements, copper, zinc, strontium, fluoride and carbonate showed an inhibitory effect on resorptive activity by primary osteoclasts. The effect on proliferation and differentiation of MC3T3 osteoblasts depended on the type of trace element and concentration tested. In general, copper and zinc ions showed an inhibitory effect on osteoblast proliferation, the effect of strontium was concentration dependent, whereas coatings containing fluoride and carbonate, respectively showed stronger osteoblast proliferation as compared to the control. The effect of copper and zinc on osteoblast differentiation was non-existing or mild-inhibitory, while strontium, fluoride and carbonate ions demonstrated a clear decrease in differentiation in comparison to the control coating without trace elements. The results from this study may give a suggestion as to how calcium-phosphate bone graft substitutes can be modified by addition of trace elements in order to control their activity with regard to bone formation and resorption. This system can also be used for testing the effect of other additives, such as growth factors and anti-biotics on the cell behavior in an environment that mimics bone mineral and calcium-phosphate based bone graft substitutes.

ACKNOWLEDGEMENTS

REFERENCES

1.   O'Dell, B.L., Roles for iron and copper in connective tissue biosynthesis. Philos Trans R Soc Lond B Biol Sci, 1981. 294(1071): p. 91-104.

2.   Tinker, D., N. Romero, and R. Rucker, The role of copper and crosslinking in elastin accumulation., in Trace element in man and animals L. Hurley, et al., Editors. 1988, Plenum Press: New York. p. 277-278.

3.   Howell, J.M. and A.N. Davison, The copper content and cytochrome oxidase activity of tissues from normal and swayback lambs. Biochem J, 1959. 72(2): p. 365-8.

4.   Strain, J.J., A reassessment of diet and osteoporosis--possible role for copper. Med Hypotheses, 1988. 27(4): p. 333-8.

5.   Paterson, C.R., Osteogenesis imperfecta and other bone disorders in the differential diagnosis of unexplained fractures. J R Soc Med, 1990. 83(2): p. 72-4.

6.   Allen, T.M., A. Manoli, 2nd, and R.L. LaMont, Skeletal changes associated with copper deficiency. Clin Orthop Relat Res, 1982(168): p. 206-10.

7.   Fromigue, O., P.J. Marie, and A. Lomri, Bone morphogenetic protein-2 and transforming

growth factor-beta2 interact to modulate human bone marrow stromal cell proliferation and differentiation. J Cell Biochem, 1998. 68(4): p. 411-26.

8. Wilson, T., J.M. Katz, and D.H. Gray, Inhibition of active bone resorption by copper. Calcif Tissue Int, 1981. 33(1): p. 35-9.

9. Parke, A., et al., Characterization and quantification of copper sulfate-induced vascularization of the rabbit cornea. Am J Pathol, 1988. 130(1): p. 173-8.

10. Sen, C.K., et al., Copper-induced vascular endothelial growth factor expression and wound healing. Am J Physiol Heart Circ Physiol, 2002. 282(5): p. H1821-7.

11. Aubin, J.E., et al., Osteoblast and chodroblast differentiation. Bone, 1995. 17(Supplement 2): p. S77-S83.

12. Oteiza, P.I. and G.G. Mackenzie, Zinc, oxidant-triggered cell signaling, and human health. Mol Aspects Med, 2005. 26(4-5): p. 245-55.

13. Vallee, B.L. and D.S. Auld, Zinc coordination, function, and structure of zinc enzymes and other proteins. Biochemistry, 1990. 29(24): p. 5647-59.

14. Vallee, B.L. and K.H. Falchuk, The biochemical basis of zinc physiology. Physiol Rev, 1993. 73(1): p. 79-118.

15. Prasad, A.S., et al., Antioxidant effect of zinc in humans. Free Radic Biol Med, 2004. 37(8): p. 1182-90.

16. Yamaguchi, M., H. Oishi, and Y. Suketa, Stimulatory effect of zinc on bone formation in tissue culture. Biochem Pharmacol, 1987. 36(22): p. 4007-12.

17. Yamaguchi, M., H. Oishi, and Y. Suketa, Zinc stimulation of bone protein synthesis in tissue culture. Activation of aminoacyl-tRNA synthetase. Biochem Pharmacol, 1988. 37(21): p. 4075-80.

18. Yamaguchi, M. and R. Yamaguchi, Action of zinc on bone metabolism in rats. Increases in alkaline phosphatase activity and DNA content. Biochem Pharmacol, 1986. 35(5): p. 773-7.

19. Yamaguchi, M. and J. Ohtaki, Effect of beta-alanyl-L-histidinato zinc on osteoblastic MC3T3-E1 cells: increases in alkaline phosphatase and proliferation. Pharmacology, 1991. 43(4): p. 225-32.

20. Yamaguchi, M. and M. Fukagawa, Role of zinc in regulation of protein tyrosine phosphatase activity in osteoblastic MC3T3-E1 cells: zinc modulation of insulin-like growth factor-I's effect. Calcif Tissue Int, 2005. 76(1): p. 32-8.

21. Yamaguchi, M., S. Kishi, and M. Hashizume, Effect of zinc-chelating dipeptides on osteoblastic MC3T3-E1 cells: activation of aminoacyl-tRNA synthetase. Peptides, 1994. 15(8): p. 1367-71.

22. Yamaguchi, M. and T. Matsui, Stimulatory effect of zinc-chelating dipeptide on deoxyribonucleic acid synthesis in osteoblastic MC3T3-E1 cells. Peptides, 1996. 17(7): p. 1207-11.

23. Moonga, B.S. and D.W. Dempster, Zinc is a potent inhibitor of osteoclastic bone resorption in vitro. J Bone Miner Res, 1995. 10(3): p. 453-7.

24. Togari, A., et al., Alteration of in vitro bone metabolism and tooth formation by zinc. Gen Pharmacol, 1993. 24(5): p. 1133-40.

25. Kishi, S. and M. Yamaguchi, Inhibitory effect of zinc compounds on osteoclast-like cell for-

mation in mouse marrow cultures. Biochem Pharmacol, 1994. 48(6): p. 1225-30.

26.   Yamaguchi, M. and S. Kishi, Zinc compounds inhibit osteoclast-like cell formation at the earlier stage of rat marrow culture but not osteoclast function. Mol Cell Biochem, 1996. 158(2): p. 171-7.

27.   Walser, M., Renal excretion of alkaline earths, in An advanced treatise, C. Comar and F. Bronner, Editors. 1969, Academic Press: New York. p. 235-320.

28.   Skoryna, S., Metabolic aspects of the pharmacologic uses of the trace elements in human subjects with specific reference to stable strontium. Trace Subst Environ Health, 1984(18): p. 3-23.

29.   Jensen, J.-E., H. Stang, and B. Kringsholm, Relationship between trace element content and mechanical bone strength. Bone, 1997(20).

30.   Grynpas, M.D. and P.J. Marie, Effects of low doses of strontium on bone quality and quantity in rats. Bone, 1990. 11(5): p. 313-9.

31.   Marie, P.J., et al., Effect of low doses of stable strontium on bone metabolism in rats. Miner Electrolyte Metab, 1985. 11(1): p. 5-13.

32.   Marie, P.J. and M. Hott, Short-term effects of fluoride and strontium on bone formation and resorption in the mouse. Metabolism, 1986. 35(6): p. 547-51.

33.   Verberckmoes, S.C., M.E. De Broe, and P.C. D'Haese, Dose-dependent effects of strontium on osteoblast function and mineralization. Kidney Int, 2003. 64(2): p. 534-43.

34.   Marie, P.J., et al., S12911, a new agent containing strontium, inhibits bone loss due to immobilization in rats. J bone Miner Res, 1995. 10(Suppl. 1).

35.   Baron, R. and Y. Tsouderos, In vitro effects of S12911-2 on osteoclast function and bone marrow macrophage differentiation. Eur J Pharmacol, 2002. 450(1): p. 11-7.

36.   Capuccini, C., et al., Interaction of Sr-doped hydroxyapatite nanocrystals with osteoclast and osteoblast-like cells. J Biomed Mater Res A, 2008.

37.   Richards, A., Nature and mechanisms of dental fluorosis in animals. J Dent Res, 1990. 69 Spec No: p. 701-5; discussion 721.

38.   Richards, A., et al., Dental fluorosis developed in post-secretory enamel. J Dent Res, 1986. 65(12): p. 1406-9.

39.   Kierdorf, U., et al., Structural changes in fluorosed dental enamel of red deer (Cervus elaphus L.) from a region with severe environmental pollution by fluorides. J Anat, 1996. 188 (Pt 1): p. 183-95.

40.   Larsen, M.J., et al., Enamel fluoride, dental fluorosis and dental caries among immigrants to and permanent residents of five Danish fluoride areas. Caries Res, 1986. 20(4): p. 349-55.

41.   Suckling, G., D.C. Thurley, and D.G. Nelson, The macroscopic and scanning electron-microscopic appearance and microhardness of the enamel, and the related histological changes in the enamel organ of erupting sheep incisors resulting from a prolonged low daily dose of fluoride. Arch Oral Biol, 1988. 33(5): p. 361-73.

42.   Farley, S.M., et al., Fluoride therapy for osteoporosis: characterization of the skeletal response by serial measurements of serum alkaline phosphatase activity. Metabolism, 1987. 36(3): p. 211-8.

43.   Gabuda, S., et al., Structural forms of fl uorides in bone tissue of animals under chronic fluo-

ride intoxication. J Struct Chem (Engl Transl), 2006(47): p. 258-266.

44.   Mackie, E.J., Osteoblasts: novel roles in orchestration of skeletal architecture. Int J Biochem Cell Biol, 2003. 35(9): p. 1301-5.

45.   Briancon, D. and P.J. Meunier, Treatment of osteoporosis with fluoride, calcium, and vitamin D. Orthop Clin North Am, 1981. 12(3): p. 629-48.

46.   Mamelle, N., et al., Risk-benefit ratio of sodium fluoride treatment in primary vertebral osteoporosis. Lancet, 1988. 2(8607): p. 361-5.

47.   Riggs, B.L., et al., Effect of the fluoride/calcium regimen on vertebral fracture occurrence in postmenopausal osteoporosis. Comparison with conventional therapy. N Engl J Med, 1982. 306(8): p. 446-50.

48.   Riggs, B.L., et al., Effect of fluoride treatment on the fracture rate in postmenopausal women with osteoporosis. N Engl J Med, 1990. 322(12): p. 802-9.

49.   Qu, W.J., et al., Sodium fluoride modulates caprine osteoblast proliferation and differentiation. J Bone Miner Metab, 2008. 26(4): p. 328-34.

50.   Burgener, D., J.P. Bonjour, and J. Caverzasio, Fluoride increases tyrosine kinase activity in osteoblast-like cells: regulatory role for the stimulation of cell proliferation and Pi transport across the plasma membrane. J Bone Miner Res, 1995. 10(1): p. 164-71.

51.   Bely, M., G. Ferencz, and K. Itai, Experimental osteofluorosis and arthrofluorosis in rats. Fluoride, 1997(30): p. 113-114.

52.   Okuda, A., J. Kanehisa, and J.N. Heersche, The effects of sodium fluoride on the resorptive activity of isolated osteoclasts. J Bone Miner Res, 1990. 5 Suppl 1: p. S115-20.

53.   Taylor, M.L., et al., The effect of fluoride on the resorption of dentine by osteoclasts in vitro. J Bone Miner Res, 1990. 5 Suppl 1: p. S121-30.

54.   Bigi, A., et al., Chemical and structural characterization of the mineral phase from cortical and trabecular bone. J Inorg Biochem, 1997. 68(1): p. 45-51.

55.   Ellies, L.G., et al., Quantitative analysis of early in vivo tissue response to synthetic apatite implants. J Biomed Mater Res, 1988. 22(2): p. 137-48.

56.   Habibovic, P., et al., Comparative in vivo study of six hydroxyapatite-based bone graft substitutes. J Orthop Res, 2008. 26(10): p. 1363-70.

57.   Landi, E., et al., Carbonated hydroxyapatite as bone substitute. J Eur Ceram Soc, 2003(23): p. 2931-2937.

58.   Kokubo, T., et al., Solutions able to reproduce in vivo surface-structure changes in bioactive glass-ceramic A-W. J Biomed Mater Res, 1990. 24(6): p. 721-34.

59.   Arnett, T.R., et al., Effects of medium acidification by alteration of carbon dioxide or bicarbonate concentrations on the resorptive activity of rat osteoclasts. J Bone Miner Res, 1994. 9(3): p. 375-9.

60.   Burch, R.E., H.K. Hahn, and J.F. Sullivan, Newer aspects of the roles of zinc, manganese, and copper in human nutrition. Clin Chem, 1975. 21(4): p. 501-20.

61.   Dahl, S.G., et al., Incorporation and distribution of strontium in bone. Bone, 2001. 28(4): p.

446-53.

62.   Fatokun, A.A., T.W. Stone, and R.A. Smith, Responses of differentiated MC3T3-E1 osteob-last-like cells to reactive oxygen species. Eur J Pharmacol, 2008. 587(1-3): p. 35-41.

63.   Boyan, B.D., Z. Schwartz, and L.D. Swain, Cell maturation-specific autocrine/paracrine regulation of matrix vesicles. Bone Miner, 1992. 17(2): p. 263-8.

64.   Habibovic, P. and K. de Groot, Osteoinductive biomaterials--properties and relevance in bone repair. J Tissue Eng Regen Med, 2007. 1(1): p. 25-32.

65.   Hott, M., et al., Proliferation and differentiation of human trabecular osteoblastic cells on hydroxyapatite. J Biomed Mater Res, 1997. 37(4): p. 508-16.

66.   Takahashi, N., et al., S 12911-2 inhibits osteoclastic bone resorption in vitro. J Bone Miner Res, 2003. 18(6): p. 1082-7.

67.   Storrie, H. and S.I. Stupp, Cellular response to zinc-containing organoapatite: an in vitro study of proliferation, alkaline phosphatase activity and biomineralization. Biomaterials, 2005. 26(27): p. 5492-9.

68.   Patntirapong, S., P. Habibovic, and P.V. Hauschka, Effects of soluble cobalt and cobalt incorporated into calcium phosphate layers on osteoclast differentiation and activation. Biomaterials, 2008.

Chapter 6

Plasmid DNA containing calcium phosphate coatings on titanium alloy surfaces

Calcium phosphates have been known for several decades as inexpensive and safe non-viral transfection agents in gene therapy. In the present study, we have attempted to develop a gene delivery system by co-precipitating plasmid DNA into calcium phosphate coating on titanium alloy surfaces using a biomimetic coating method. The DNA plasmids used had a gene either coding for Bone Morphogenic Protein Reporter-Luciferase (BRE-Lu), Green Fluorescent Protein (GFP) or Bone Morphogenic Protein 2 (BMP2). They were added in varying concentrations to the calcium phosphate coating solution and deposited on the metal surface. The effect of DNA presence on the coating formation and the efficiency of incorporation were studied. All three types of plasmid DNA were successfully incvorporated into and homogenously distributed throughout the coating. The efficiency of incorporation could be controlled by controlling the coating volume and its DNA concentration. The presence of DNA influenced the coating morphology, which was obvious from the decreased calcium phosphate crystal size. This system should further be tested in vitro and in vivo with regard to the transfection efficiency.

INTRODUCTION

Gene therapy is the insertion of genes into an individual's cells and tissues to treat e.g. a hereditary disease in which a defective mutant allele is replaced with a functional one. Although the technology is still in its infancy, there have been some clinical successes [1, 2].

Since Urist isolated Bone Morphogenetic Protein (BMP) from bone as a glycoprotein extract which can induce the differentiation of cartilage and bone [3], large number of studies focused on the effects of biologically active molecules for bone regeneration [4, 5]. However, to be clinically successful, relatively large, supra-physiological quantities of BMP-2 and Osteogenic Protein-1 (OP-1/BMP-7) are needed, making the treatment with these growth factors highly expensive. One of the ways to decrease the cost of clinical therapy based on BMPs and other growth factors is by optimizing their carrier, which can lead to a more controlled release and better efficiency of the treatment. Another approach could be gene therapy, in which genes of osteogenic proteins, such as BMP- 2, are introduced into local cells which can in turn produce these osteogenic proteins, inducing thereby new bone formation.

Many different gene therapy methods have been developed so far. The osteogenic gene transfer can either be performed ex vivo [6, 7] or in vivo [8, 9]. Using ex vivo approach, patient's cells are cultured and transfected in vitro before being placed back into the patient. Although this is a relatively efficient method, it requires labour intensive cell cultivation and selection. Much effort is therefore put in developing in vivo gene transfer therapies, which can be divided into viral and non-viral therapies. Adenovirus, lentivirus and retrovirus are the most frequently used transfection viral vectors due to their high transfer efficiency [10-12]. However, gene transfer using viral vectors is associated with some safety concerns, such as immune reactions to adenovirus vectors and insertional mutagenesis of retrovirus [13].

More than 30 years ago, calcium phosphates (CaPs) have been reported as possible vectors for gene delivery [14]. Since then, a lot of other non-viral vectors were discovered such as poly(ethylenimine) (PEI) [15], liposomes [16], gene gun administration [17], electroporation [18], peptides [19], plasmid [20] and inorganic vectors [21]. Among all inorganic vectors which are in use nowadays, CaP is the most widely used and studied due to its ability to transfect a large amount of mammalian cells in vitro without immune responses and high toxicity [22]. Recently, there is an emerging trend to use expression plasmid vectors for in vivo gene transfer due to their simplicity and safety. For example, reports showed that for bone tissue engineering, expression plasmid vector encoding osteogenic factors such as BMP, combined with collagen could regenerate bone after transplanted in the bone defective area [20]. The biggest challenge that faces gene therapy is the transfection efficiency. Transfection efficiency can be improved by improving one of the aspects of transfection: the physical and chemical stability of DNA delivered, the uptake process of the cells, DNA's escape from the endosomal network, cytosolic transport and nuclear localization of the DNA delivered [23, 24]. Many studies now focus on combining different vectors to address the problem of low transfection efficiency, such as plasmids with collagen [20], with CaPs [25], with PEI [15] and with DEAE dextran [26].

In our lab, we have been using biomimetic coating process, which is relatively simple, takes place

at low temperature and physiological pH, to provide implant surfaces with a CaP layer alone or in combination with biologically active molecules, such as growth factors [4] and antibiotics [27]. The present study is an attempt to setup an in vivo gene delivery system by co-precipitating plasmid DNA into biomimetic CaP coating on surface of titanium, a metal that is often used in orthopaedic and dental implants.

MATERIALS & METHODS
Preparation of plasmid DNA
First, LB medium ampicilin plate was prepared. Then, the transformation by heat shock was performed using the competent cell and DNA. Finally, different types of plasmid DNA were prepared using Hi-Speed Plasmid kit (Qiagen) according to the manufacturer's protocol. The quality and quantity of DNA were analyzed by gel electrophoresis and spectrophotometer, respectively. The DNA plasmids had a gene either coding for Bone Morphogenic Protein Reporter-Luciferase (BRE-Lu), Green Fluorescent Protein (GFP) or Bone Morphogenic Protein 2 (BMP2).

Coating preparation
The coating process consisted of two steps:

<u>Step 1: pre-calcification</u>

First, 10x10x1 mm3 titanium alloy (Ti6Al4V) plates were cleaned successively in acetone, ethanol (70%), and demineralized water in ultrasonic water bath. A solution that was 5 times more concentrated than Kokubo's Simulated Body Fluid [28] was prepared by dissolving carbon dioxide gas (CO_2), into a solution made of reagent grade NaCl (40g), $CaCl_2 \cdot 2H_2O$ (1.84g), $MgCl_2 \cdot 6H_2O$ (1.52g), $NaHCO_3$ (1.76g) and $Na_2HPO_4 \cdot 2H_2O$ (0.89g) salts in 1l of demineralised water at 37°C [29]. The cleaned Ti alloy plates were immersed into the solution for pre-calcification at 37°C for 24 hours under continuous stirring.

<u>Step 2: crystal growth</u>

In the second step, pre-calcified Ti alloy plates were treated with a calcium phosphate solution (CPS) at physiological pH of 7.40 to deposit a crystallized layer onto the amorphous calcium phosphate layer formed in Step 1.

CPS were prepared by dissolving 0.14M NaCl, 4mM $CaCl_2 \cdot 2H_2O$, 2.25mM $Na_2HPO_4 \cdot H_2O$ and 50 mM Tris in MilliQ water, adjusting the pH of the solution to 7.4 using 1M HCl. Per Ti alloy plate, different volume of CPS (5 ml, 10 ml, 15 ml) were prepared followed by addition of pDNA in varying quantities to obtain CPS solution with following plasmid DNA concentrations: 10 μg/ml, 20 μg/ml, 30 μg/ml. For each volume of CPS solution, CPS solution without pDNA was taken as control. After stirring for 15 minutes, Ti alloy plates were placed in the closed vials with coating solution for 24 hours in a shaking waterbath at room temperature.

Efficiency of plasmid DNA co-precipitation

The concentration of calcium and inorganic phosphate of the plasmid DNA CPS solution was analyzed using VITROS DT60 II system (JOHNSON & JOHNSON GATEWAY®) after removal of Ti alloy plates from the solution.

The pDNA content of CPS solution was measured before and after the coating process using Gene Quant II (Pharmacia Biotech).

The total amount of pDNA in the coating was esyimated using the formula:

$$M_{pDNA} = ([pDNA]_{t-0} - [pDNA]_{t-24h}) * V_{cps}$$

where $[pDNA]_{t=0}$ is plasmid DNA concentration of the solution at the start of coating process, $[pDNA]_{t-24h}$ concentration of coating solution at the end of coating process and V_{cps} volume of the solution.

Coating analysis

The morphology and the presence of plasmid DNA were investigated on gold-sputtered coated Ti alloy plates using Environmental Scanning Electron Microscopy (ESEM, XL-30 ESEM-FEG, Philips) in the secondary electron mode. After the coating process, coating was scratched off the Ti alloy plates and characterized by Fourier Transform Infra-Red spectroscopy spectroscopy (FTIR, 8 scans, Perkin-Elmer, Spectrum 1000).

To determine the presence of plasmid DNA, coated Ti alloy plates with and without DNA were stained with ethidium bromide and micrographs were taken by digital camera under UV light.

RESULTS

ESEM and FTIR analysis

Figures 1a and 1b show the ESEM micrographs of control coating and coating formed in 15 ml CPS solution containing 30 μg/ml p-DNA encoding for GFP. The morphology of this coating is representative for all coatings containing plasmid DNA. Ti alloy plates coated in solution without plasmid DNA were covered with needle-like crystal with the size of around 20 μm that were perpendicularly oriented on the substrate surface and are typical of octacalcium phosphate. In presence of plasmid DNA, and independent on plasmid DNA concentration and coating solution volume, the morphology of the coating considerably changed. Coatings containing plasmid DNA consisted of small crystals with the size of about 2 μm. When plasmid DNA was co-precipitated into coating, the coating structure changed, the crystal size reduced from 20 μm to around 2 μm. Ethidium-bromide stained plates containing plasmid DNA showed a homogenous distribution of DNA in the coating as is demonstrated in figure 1c for BRE-Lu, which is representative for all other coatings with plasmid DNA. The control coating without plasmid DNA and uncoated Ti alloy plates showed no red staining (pictures not shown). Figure 2 shows the FTIR spectra of control coating and coating co-precipitated with plasmid DNA encoding for BMP2 and representative for other plasmid DNA coatings. The spectrum of the control coating was typical of octacalcium phosphate, with sharp P-O bands at about 1100, 1170 and 1023 cm^{-1} (P-O stretching in PO_4^{3-} and HPO_4^{2-}) and a HPO_4^{2-} band at 906 cm^{-1} (P-O stretching in HPO_4^{2-}). The two sharp P-O bands

at 560 and 600 cm^{-1} (P-O deformation in PO_4^{3-}) exhibited shoulders 624 cm^{-1} (H_2O libation) and 526 cm^{-1} (P-O twisting in HPO_4^{2-}) [30].

In the spectrum of the DNA-containing coating, additional peaks were observed at around 1505, 1465 and 1292 cm^{-1}, suggesting formation of carbonated apatitic phase among the OCP. In addition, small bands appeared at about 2959 and 2871 cm^{-1}, corresponding to C-H aliphatic vibrations, suggesting presence of an organic phase in the lattice.
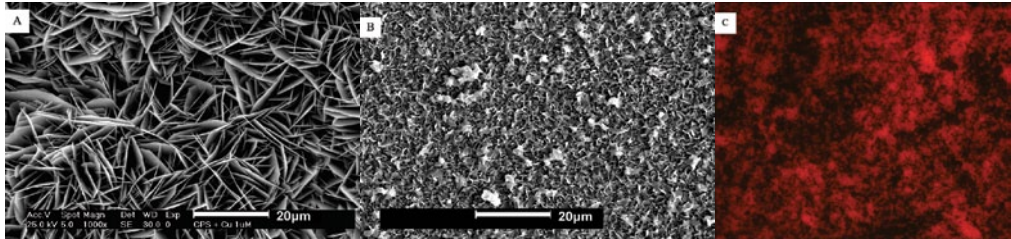
Figure 1: a) ESEM micrograph of control coating without plasmid DNA; b) ESEM micrograph of coating with GFP-DNA (representative of all coatings containing plasmid DNA); c) Ti alloy plate coated with coating containing BRE-Lu-DNA stained with EtBr under UV light (representative of all coatings containing plasmid DNA).
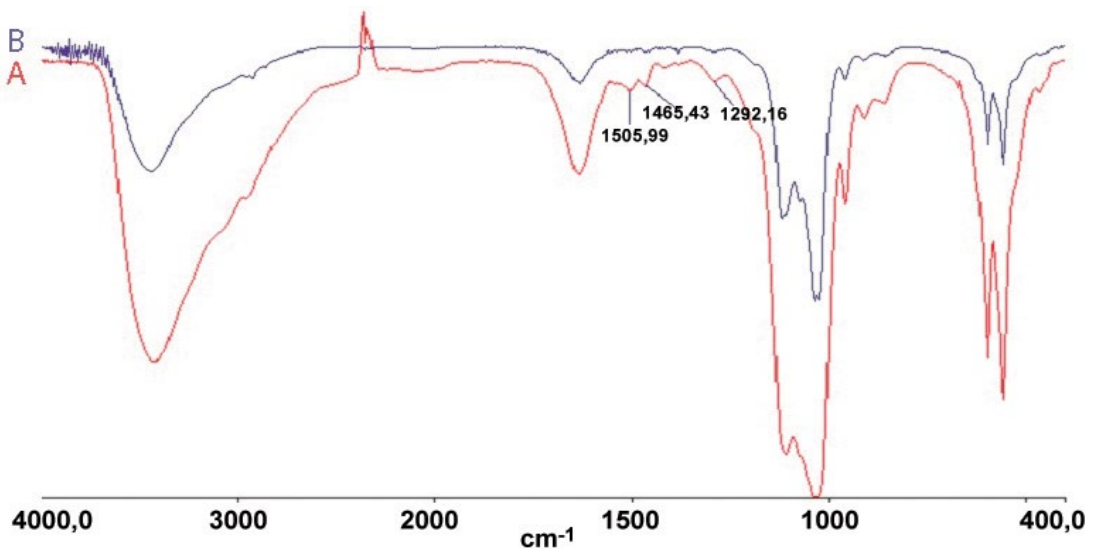

Figure 2: FTIR spectra of: a) coating with BMP2-DNA (representative of all coatings containing plasmid DNA) (red).; b) control coating without plasmid DNA (blue)

Efficiency of plasmid DNA co-precipitation

Figure 3 shows the total amount of plasmid DNA which was incorporated into coatings prepared under different conditions. Independent on the type of DNA, general trend was that the total amount of incorporated DNA increased with the increasing concentration of DNA in the coating solution. An increase in the solution volume from 5 ml to 10 ml also resulted in more DNA in the coating for all three types of DNA tested. However, further increase to 15 ml positively influenced the efficiency of incorporation for BMP2-DNA, whereas for GFP and BRE-Lu, no further increase of incorporated DNA amount

was observed. Maximum amount of incorporated plasmid DNA for GFP-DNA and BRE-Lu-DNA was about 50 μg, whereas the maximum amount of incorporated BMP2-DNA was as high as 90 μg, without reaching the limit. During biomimetic coating process, decrease of Ca and inorganic P from the coating solution was higher in solutions containing plasmid DNA than in the solution without DNA (data not shown).
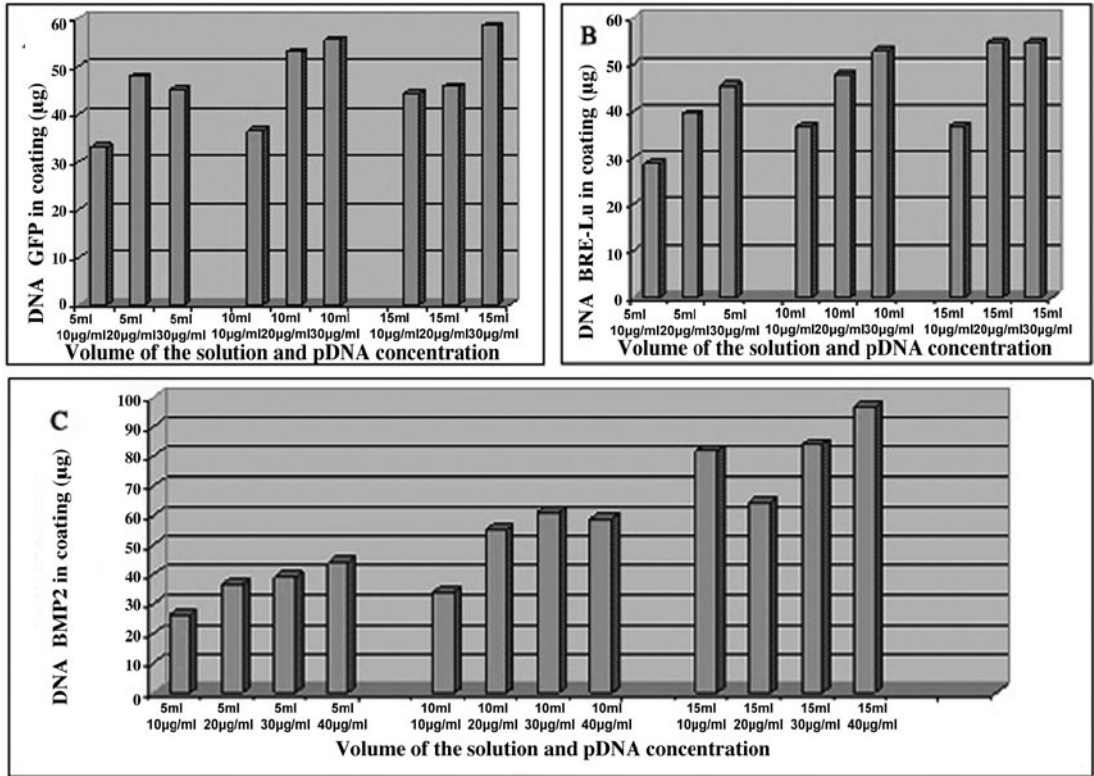

Figure 3: total amount of plasmid DNA incorporated into the coating as a function of coating solution volume and DNA concentration of the coating solution: a) GFP-DNA; b) BRE-Lu-DNA; C) BMP-DNA.

Discussion

More than 40 years ago, the use of uptake-enhancing chemicals for gene delivery was introduced, which is probably the easiest and the most effective gene delivery method [31]. Among non-viral transfection vectors, plasmid vector is of great potential due to its simplicity and safety [8, 20]. However both plasmid DNA and the outer cellular surface are negatively charged, making it difficult for plasmid DNA to enter the cell through the outer cellular surface. The general principle of applying uptake-enhancing chemical for gene delivery is based on complex formation between positively charged chemicals and negatively charged DNA molecules. Among these chemicals, CaPs, which interact with DNA to form CaP-DNA complexes, are the most extensively used for in vitro gene delivery and currently being applied in in vivo experiments [19, 23, 25]. However, due to high variability in transfection efficiency, which can be contributed to variations in particle sizes and morphology [32], the applicability of CaPs

as gene delivery agent has been limited to only a few cell lines. In addition, earlier studies showed that the CaP-DNA complexes can generate direct cell toxicity in vitro [32].

Nowadays, materials based on CaPs are widely used in as bone graft substitutes and as scaffolds in bone tissue engineering constructs. Among them, CaP coatings, either plasma-sprayed or produced using alternative techniques such as biomimetic method are extensively on orthopaedic and dental implants to improve their osteoconductivity and bone bonding ability [33, 34].

In the present study, we have attempted to develop a gene delivery system by coprecipitating plasmid DNA into CaP coating using a biomimetic coating method. This simple approach consisted of deposition of a thin amorphous calcium phosphate layer onto Ti alloy plates and deposition of a thin homogenous crystalline calcium phosphate layer containing plasmid DNA onto this amorphous layer. Various types of plasmid DNA were successfully incorporated into the CaP coating and the amount of DNA incorporated into the coating could be controlled by adjusting the DNA content of the coating solution. The negatively charged plasmid DNA can be incorporated into the CaP crystal lattice by substitution of phosphate group, by either the phosphate or the carbonate group of the DNA. FTIR spectra of the coatings with DNA showed the presence of carbonate as opposed to the control coating as well as other bands associated with an organic phase, suggesting incorporation of DNA into the coating. The ESEM micrographs indicated that crystals of the coating containing DNA were considerably smaller than those of the control coating. This could be related to the inhibiting effect on crystal growth of the relatively large DNA molecules. The EtBr staining results also showed that plasmid DNA was homogenously incorporated into the coating structure.

Studies on gene delivery systems using CaP particles showed that DNA concentration and initial concentration of calcium and phosphate could influence the transfection efficiency [32]. In the present study, we choose three different types of plasmid DNA: GFP, BRE-Lu and BMP2. Different volumes of solution and different DNA concentrations were used. Results showed that the amount of DNA incorporated into the coating increased with the increase of the solution volume and DNA concentration, suggesting the effect of these factors on the binding capacity of DNA to calcium phosphate coating. For GFP and BRE-Lu, the maximum amount of DNA incorporated was $60\,\mu$g, whereas, for BMP2, the total amount was as high as $100\,\mu$g without reaching the limit. The observed difference could be explained by the difference in size of the molecule as well as to the binding affinity of CaP.

In conclusion, in the present study, we developed a simple and efficient way to coat implant surfaces with a CaP layer containing plasmid DNA. This system should further be tested in vitro and in vivo to study the efficiency of transfection. In addition to Ti alloy surfaces, this coating method can also be applied on other materials, such as polymers and ceramics, independent on their overall geometry and internal structure.

ACKNOWLEDGMENTS

REFERENCES

1.   Matsumoto, K., et al., A Pilot Study of Human Interferon {beta} Gene Therapy for Patients with Advanced Melanoma by in vivo Transduction Using Cationic Liposomes. Jpn J Clin Oncol, 2008.

2.   Gottwald, M.D. and M.J. Aminoff, New frontiers in the pharmacological management of Parkinson's disease. Drugs Today (Barc), 2008. 44(7): p. 531-45.

3.   Urist, M.R., et al., Purification of bovine bone morphogenetic protein by hydroxyapatite chromatography. Proc Natl Acad Sci U S A, 1984. 81(2): p. 371-5.

4.   Liu, Y., K. de Groot, and E.B. Hunziker, BMP-2 liberated from biomimetic implant coatings induces and sustains direct ossification in an ectopic rat model. Bone, 2005. 36(5): p. 745-57.

5.   Dragoo, J.L., et al., Bone induction by BMP-2 transduced stem cells derived from human fat. J Orthop Res, 2003. 21(4): p. 622-9.

6.   Franceschi, R.T., et al., Gene therapy for bone formation: in vitro and in vivo osteogenic activity of an adenovirus expressing BMP7. J Cell Biochem, 2000. 78(3): p. 476-86.

7.   Abe, N., et al., Enhancement of bone repair with a helper-dependent adenoviral transfer of bone morphogenetic protein-2. Biochem Biophys Res Commun, 2002. 297(3): p. 523-7.

8.   Bonadio, J., et al., Localized, direct plasmid gene delivery in vivo: prolonged therapy results in reproducible tissue regeneration. Nat Med, 1999. 5(7): p. 753-9.

9.   Sano, A., et al., Atelocollagen for protein and gene delivery. Adv Drug Deliv Rev, 2003. 55(12): p. 1651-77.

10.   Cockrell, A.S. and T. Kafri, Gene delivery by lentivirus vectors. Mol Biotechnol, 2007. 36(3): p. 184-204.

11.   Lim, K.I. and D.V. Schaffer, Library selection approaches to engineering enhanced retroviral and lentiviral vectors. Comb Chem High Throughput Screen, 2008. 11(2): p. 111-7.

12.   Tosch, C., et al., Adenovirus-mediated gene transfer of pathogen-associated molecular patterns for cancer immunotherapy. Cancer Gene Ther, 2008.

13.   Rundle, C.H., et al., In vivo bone formation in fracture repair induced by direct retroviral-based gene therapy with bone morphogenetic protein-4. Bone, 2003. 32(6): p. 591-601.

14.   Graham, F.L. and A.J. van der Eb, Transformation of rat cells by DNA of human adenovirus 5. Virology, 1973. 54(2): p. 536-9.

15.   Godbey, W.T., K.K. Wu, and A.G. Mikos, Poly(ethylenimine) and its role in gene delivery. J Control Release, 1999. 60(2-3): p. 149-60.

16.   Lasic, D. and N. Templeton, Liposomes in gene therapy. Adv Drug Deliv Rev, 1996(20): p. 221-66.

17.   Cheng, L., P.R. Ziegelhoffer, and N.S. Yang, In vivo promoter activity and transgene expression in mammalian somatic tissues evaluated by using particle bombardment. Proc Natl Acad Sci U S A, 1993. 90(10): p. 4455-9.

18.   Somiari, S., et al., Theory and in vivo application of electroporative gene delivery. Mol Ther, 2000. 2(3): p. 178-87.

19.   Trentin, D., J. Hubbell, and H. Hall, Non-viral gene delivery for local and controlled DNA release. J Control Release, 2005. 102(1): p. 263-75.

20.   Fang, J., et al., Stimulation of new bone formation by direct transfer of osteogenic plasmid genes. Proc Natl Acad Sci U S A, 1996. 93(12): p. 5753-8.

21.   Chowdhury, E.H. and T. Akaike, Bio-functional inorganic materials: an attractive branch of gene-based nano-medicine delivery for 21st century. Curr Gene Ther, 2005. 5(6): p. 669-76.

22.   Crystal, R.G., Transfer of genes to humans: early lessons and obstacles to success. Science, 1995. 270(5235): p. 404-10.

23.   Luo, D. and W.M. Saltzman, Synthetic DNA delivery systems. Nat Biotechnol, 2000. 18(1): p. 33-7.

24.   Wiethoff, C.M. and C.R. Middaugh, Barriers to nonviral gene delivery. J Pharm Sci, 2003. 92(2): p. 203-17.

25.   Batard, P., M. Jordan, and F. Wurm, Transfer of high copy number plasmid into mammalian cells by calcium phosphate transfection. Gene, 2001. 270(1-2): p. 61-8.

26.   Liptay, S., et al., Colon epithelium can be transiently transfected with liposomes, calcium phosphate precipitation and DEAE dextran in vivo. Digestion, 1998. 59(2): p. 142-7.

27.   Stigter, M., et al., Incorporation of different antibiotics into carbonated hydroxyapatite coatings on titanium implants, release and antibiotic efficacy. J Control Release, 2004. 99(1): p. 127-37.

28.   Kokubo, T., et al., Solutions able to reproduce in vivo surface-structure changes in bioactive glass-ceramic A-W. J Biomed Mater Res, 1990. 24(6): p. 721-34.

29.   Barrere, F., et al., Biomimetic calcium phosphate coatings on Ti6AI4V: a crystal growth study of octacalcium phosphate and inhibition by Mg2+ and HCO3. Bone, 1999. 25(2 Suppl): p. 107S-111S.

30.   Fowler, B., M. Markovic, and W. Brown, Octacalcium phosphate 3. Infrared and raman vibrational spectra. Chem Mater, 1993. 15: p. 1417-1423.

31.   Vaheri, A. and J.S. Pagano, Infectious poliovirus RNA: a sensitive method of assay. Virology, 1965. 27(3): p. 434-6.

32.   Jordan, M., A. Schallhorn, and F.M. Wurm, Transfecting mammalian cells: optimization of critical parameters affecting calcium-phosphate precipitate formation. Nucleic Acids Res, 1996. 24(4): p. 596-601.

33.   Habibovic, P., et al., Biological performance of uncoated and octacalcium phosphate-coated Ti6Al4V. Biomaterials, 2005. 26(1): p. 23-36.

34.   Havelin, L.I., et al., The Norwegian Arthroplasty Register: 11 years and 73,000 arthroplasties. Acta Orthop Scand, 2000. 71(4): p. 337-53.

Chapter 7

Biomimetic calcium-phosphate coatings on artificial spider silk fibres

Calcium-phosphate ceramic coatings can be applied on surfaces of metallic and polymeric biomaterials to improve their performance in bone repair and regeneration.

Spider silk is biocompatible, strong and elastic, and has been proposed as an attractive biomaterial for applications in connective tissue repair. Recently, artificial spider silk, with mechanical and structural characteristics similar to those of regenerated and native spider silk, has been produced from recombinant minispidroins.

In the present study, modified Simulated Body Fluid (SBF) was used to deposit biomimetic calcium-phosphate coatings on artificial spider silk in an attempt to produce a combined biomaterial that meets both mechanical and bioactivity requirements for a successful synthetic bone graft substitute or scaffold for bone tissue engineering. In addition, the results of this study contribute to understanding the mechanism of in vivo mineralization of artificial spider silk.

The mineralization process was followed in time using scanning electron microscopy equipped with an energy-dispersive x-ray (EDX) detector and Raman spectroscopy. Focused Ion Beam technology was used to produce a cross section of the fibre with calcium-phosphate coating, which was further analyzed by EDX.

The results of this study showed that recombinant spider silk fibres could successfully be coated with a homogenous and thick crystalline calcium-phosphate layer. In the course of mineralization process from modified SBF, sodium chloride crystals were first deposited on the silk surface, followed by the deposition of a calcium-phosphate layer. Deposition of a homogenous calcium-phosphate layer on the surface of silk fibres occurred faster than on other, previously investigated substrates, such as titanium. The coated silk fibres supported the attachment and growth of human bone marrow stromal cells.

INTRODUCTION

Demand for successful repair and regeneration of bone tissue is expanding with the growing life expectancy as a consequence of the improved quality of life. Despite decades of research and hundreds of potential bone graft substitutes developed, transplantation of patient's own bone remains the only reliably successful method in critical orthopaedic and cranio-facial surgeries such as spinal fusions and repair of large defects caused by tumor and trauma. However, the secondary surgery required for the harvest of autograft may be associated with serious problems such as donor site morbidity and permanent gait disturbance. More importantly, the availability of autograft is limited and will soon be insufficient to meet the needs of our aging population. The development of synthetic bone graft substitutes, which are readily available in unlimited quantities and applicable in different situations, remains therefore an important challenge. In order to be as successful as autograft in bone repair and regeneration, synthetic bone graft substitutes need to meet some important requirements associated with their physico-chemical, structural and mechanical properties. Being biocompatible is not sufficient anymore; synthetic bone graft substitutes are expected to be osteoconductive and preferably even osteoinductive. Depending on the intended application, they should be either dense or porous, allowing insidious infiltration of cells and tissue followed by replacement by new bone. Finally, they should be able to sustain forces present during and after implantation, providing the initial stability, but their fatigue strength and elasticity modulus should not differ much from the surrounding tissue in order to avoid detrimental stress shielding. None of the so far developed bone graft substitutes meet all these different requirements. While calcium-phosphate (CaP) based biomaterials, in the form of sintered ceramics or cements have excellent osteoconductive properties [1-6] and are in some formulations even osteoinductive [7], their poor mechanical properties both in dense and porous forms limit their use to non-load bearing or supported load-bearing applications [4-6, 8]. Metals have excellent mechanical properties and by introducing porosity into their structure they can better adopt to the surrounding tissue both from mechanical and biological point of view [9-10]. However, metals are bioinert and non-degradable and therefore difficult to completely incorporate into the surrounding bone. Also polymers are interesting candidates for bone graft substitution as they may be biodegradable [11], their overall geometry and intrinsic structural properties can easily be manipulated [11-12] and they are suitable for applications of various types of loads under low stresses [6, 11, 13]. But similarly to metals, bioactivity of polymers is often inferior to that of CaP based materials. An approach to design more successful synthetic bone graft substitutes is by combining different biomaterials in order to combine positive aspects of each component [14].

Many natural polymers, such as collagen and silk are biocompatible and biodegradable. Silks are protein polymers that are spun into fibers by certain insect larvae, such as worms, and spiders. Characterized by a highly repetitive primary sequence and structural organization, silks possess impressive mechanical properties [15]. Spider silks, although one of nature's best performing polymers, have not been commercialized for biomedical applications, which is primarily due to the predatory nature of spiders and the relatively low levels of production of these silks when compared to silkworm cocoon silk. Much effort has been put into the production of artificial spider silks employing natural or syn-

thetic gene fragments that encode for parts of silk proteins [16-17]. Recently, a method of production of meter-long fibre bundles of recombinant spider silk, 4RepCT, that are similar to those of dragline silks from the structural point of view was developed [18]. The mechanical strength of the recombinant fibres compares favorably to other artificial silks [19-21]. Their tensile strength (0.2 GPa) is well above that of mammalian bone and tendons [22-23]. Moreover, the 4RepCT fibres have an elastic modulus (7 GPa) comparable to that of native dragline silks [17], that can be further improved by genetic engineering [24].

A biomimetic coating method, which is based on immersion of a biomaterial into a solution that mimics the inorganic composition of human blood plasma at physiological conditions (the so-called Simulated Body Fluid (SBF)), was originally developed by Kokubo in 1990 [25], and has since been improved by several groups of investigators. In our group for example, supersaturating SBF resulted in successful formation of bone-like apatite coatings on metallic surfaces in a considerably shorter period of time than when classical SBF was used [26-27]. Moreover, we have shown that thus formed CaP layer significantly improved osteoconductive properties of metals [28-29]. A biomimetic coating process has many advantages over traditional coating processes. The process is relatively simple, takes place at low temperature and physiological pH allowing incorporation of biological agents, e.g. growth factors, into the coating [30-32] and is applicable to a large range of materials with varying chemical composition and geometrically complex and porous shapes [33-34].

In the present study we have used the biomimetic coating setup to deposit a CaP layer on recombinant silk fibres in an attempt to produce a combined biomaterial that meets both mechanical and bioactivity requirements for a successful synthetic bone graft substitute. The study was performed in a way that may also helps understanding the in vivo mineralization process of silk fibres.

MATERIALS AND METHODS

Production of recombinant spider silk fibres

A miniature construct of the major ampullate spidroin (Masp) 1 of Euprosthenops australis was expressed as a His6Trx-fusion protein in E. coli cells and purified under native conditions as previously described [18, 35]. The fusion tag was released by proteolytic cleavage, which induced fibre formation. The formed fibre bundles were washed in water and autoclaved (20 min 121°C, 2.8 bar).

Biomimetic coating

In order to determine optimal conditions for coating spider silk fibres with CaP, the following coating methods were applied:

1.Pre-calcification

A 5 times concentrated Simulated Body Fluid solution (SBFx5A) was prepared by dissolving carbon dioxide gas (CO_2), into a solution made of reagent grade NaCl (40g), $CaCl_2 \cdot 2H_2O$ (1.84g), $MgCl_2 \cdot 6H_2O$ (1.52g), $NaHCO_3$ (1.76g) and $Na_2HPO_4 \cdot 2H_2O$ (0.89g) salts (all salts were purchased from Merck) in 1l of demineralised water at 37°C [26].

Silk fibre bundles were soaked in SBFx5A for periods of time varying from 10 minutes to 1 day. This process was previously shown to result in a formation of thin, amorphous CaP layer on titanium substrates [26].

2.Pre-calcification + crystal growth

Another SBFx5 solution with decreased Mg^{2+} and CO_3^{2-} concentration (SBFx5B) was prepared by dissolving carbon dioxide gas (CO_2), into a solution made of reagent grade NaCl (40g), $CaCl_2 \cdot 2H_2O$ (1.84g), $MgCl_2 \cdot 6H_2O$ (0.30g), $NaHCO_3$ (0.88g) and $Na_2HPO_4 \cdot 2H_2O$ (0.89g) salts in 1l of demineralised water at 50°C. Upon soaking in SBFx5A solution for 1 day, pre-calcified fibres were immersed in the SBFx5B solution for periods of time varying from 10 minutes to 1 day.

Coating characterization

The surface of silk fibres was studied at different time points during coating process by Environmental Scanning Electron Microscopy (ESEM, XL-30 ESEM-FEG, Philips) in the secondary electron mode, coupled with Energy Dispersive X-Ray Analyzer (EDX) and a custom made confocal Raman microscope using a diode laser (λ = 685 nm) with 15-20 mW effective power at the sample surface and a spatial resolution of 700nm, in order to determine the dynamics of coating formation.

Analysis of the fibre cross section

The coated fibre was attached to a carbon tape which was placed onto a piece of silicon and tilted to 52° in a FEI Strata DB235 focused ion beam/scanning electron microscope (FIB/SEM). A 30 keV gallium ion beam was used at a current of 5-7 nA in order to make a rough cross section of the fiber. The cross section was then fine polished by gentle cleaning with a series of currents decreasing from several nA down to a current of 30 pA. The increased smoothness of the fibre cross section after the fine polishing step revealed clear and detailed structure of the fibre.

The FIB polished cross section was placed in a LEO 440 SEM and tilted to 52° for EDX analysis. An EDX spectrum of the entire fibre including the coating was acquired at 15 keV using a probe current of about 15 nA. Live mapping was also performed with the same probe current and with a dwell time of 500 μs, an amplification time of 10 μs and the image size of 256x200 pixels. The mapping was performed for Ca, P, Na and Cl.

Cell culture

Recombinant silk fibre bundles (diameter about 500 μm, length approximately 3 cm), pre-calcified in SBFx5A solution for 24 hours and subsequently coated in SBFx5B solution for another 24 hours, were used for cell culture experiments to study the attachment and growth of bone marrow derived human mesenchymal stem cells (hMSCs). The fibre bundles were individually placed into wells of non-cell culture treated 25-well plates. hMSCs at density of 3x105 cells/sample were added to each well in 1 ml cell culture medium (Alpha MEM + 1% PS + 2mM L-Glutamine + 1mM sodium pyruvate + 10% FBS). The cells were cultured for up to 14 days, with the refreshment of medium every 2 days. Small pieces of

fibres were removed from the medium at different time points, gently rinsed twice with PBS, followed by fixation in 4% formalin for 1 hour. The samples were then passed through an ethanol series (70%, 80%, 90%, 96%, 100%; 1h per step), critical point-dried and studied by ESEM. Another set of samples was removed from the cell culture medium, rinsed with PBS, fixed in 70% ethanol for 20 minutes, followed by washing with PBS. These samples were then stained with phalloidin for 20 minutes in dark at RT, washed with PBS and finally stained with DAPI for 10 minutes in dark, followed by washing in PBS. After fixation on glass slides, the samples were studied using fluorescence microscopy (435 system, BD Pathway™).

RESULTS

Mineralization of recombinant spider silk in SBFx5A solution
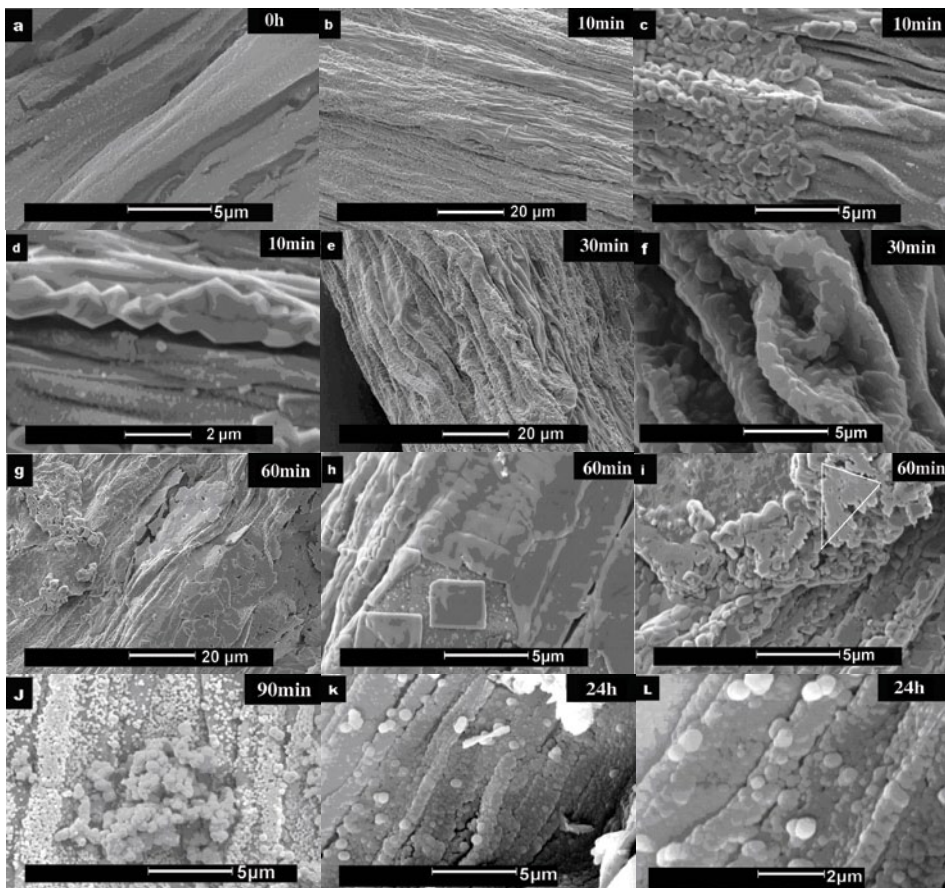
Figure 1: ESEM micrographs of uncoated spider silk fibres (a) and fibres after immersion in SBFx5A solution for 10 minutes magnification 1000x (b), magnification 5000x (c), magnification 10000x (d); for 30 minutes magnification 1000x (e), magnification 5000x (f); for 60 minutes magnification 1000x (g), magnification 5000x (h and i); for 90 minutes magnification 5000x (j); for 24 hours magnification 5000x (k), magnification 10000x (l); At 10 minutes, first polygonal crystals with the size of 0.5 µm to 1 µm appeared on the surface and continued covering the surface for another 50 minutes. After 1 hour of soaking, first globular deposits appeared on the top of polygonal crystals, slowly forming a layer on the surface within 90 minutes.
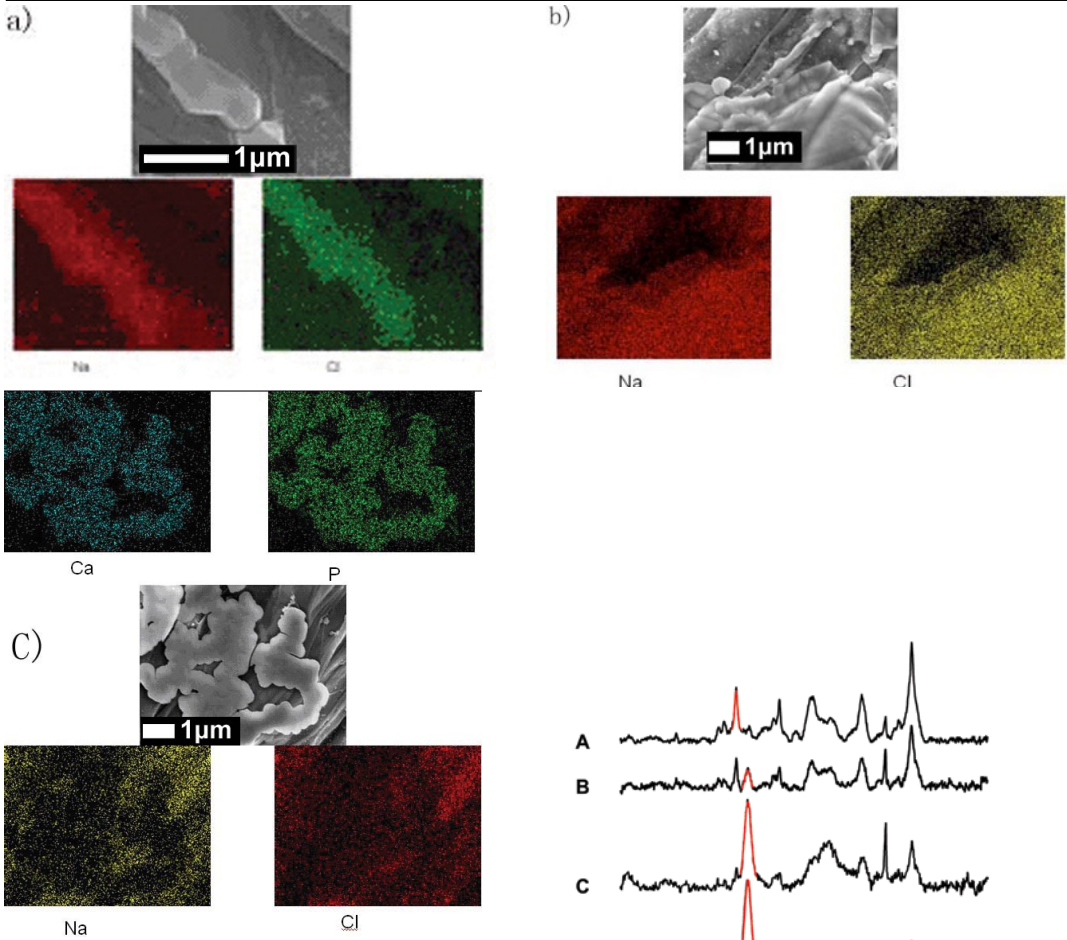
Figure 2: EDX elemental mapping of spider silk fibres after immersion in SBFx5A solution for 10 minutes (a) and 60 minutes (b and c).

The polygon-shaped crystals that first deposit on the silk surface were NaCl crystals (a).

With time, they continued growing and covered the surface after 60 minutes of immersion (b). Following, calcium-phosphate globules started forming on top of the NaCl layer (c).
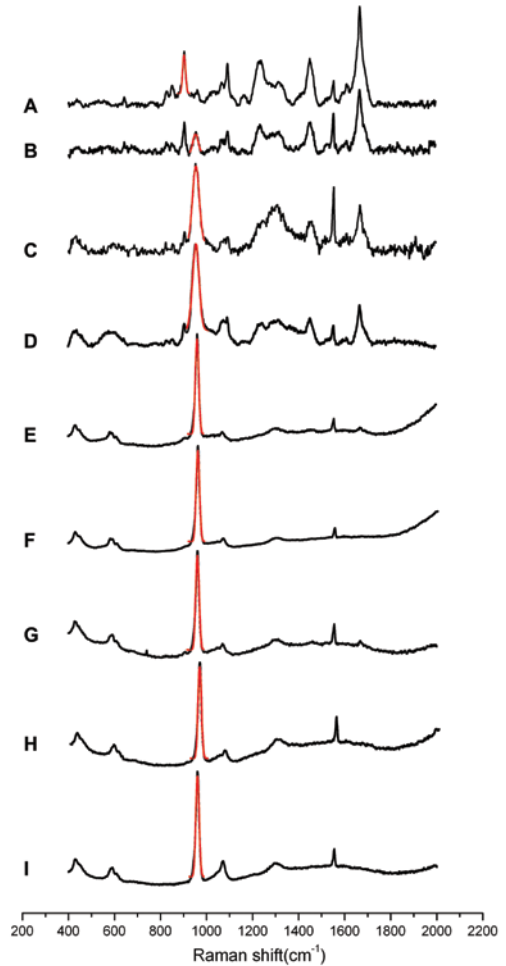

Figure 3: Raman spectra of silk before coating process (a), after soaking in SBFx5A solution for 2 (b), 6 (c), and 24 hours (d); after soaking in SBFx5A for 24 hours followed by soaking in SBFx5B for 1 (e), 2 (f), 3 (g), 5 (h) and 24 hours (i).

The mineralization process in SBFx5A solution was followed in time using ESEM. The ESEM micrograph of the uncoated silk fibres is shown in Figure 1a. After only 10 minutes of immersion in SBFx5A solution, polygon-like particles with a size of 0.5 to 1 μm started depositing on the surface of fibres (Figures 1b-d). Elemental mapping using EDX showed that these particles were sodium chloride crystals (Figure 2a). After 30 minutes in SBFx5A solution, the polygonal-like crystals continued depositing on the surface, slowly covering it (Figure 1e-f). Elemental mapping confirmed that only sodium chloride was present on the surface (not shown). After 1 hour of immersion, the surface of the silk fibre was almost completely covered by the crystalline layer (Figure 1g-i) consisting of sodium chloride (Figure 2b). After 1 hour of immersion, formation of new globules with a size of 0.2 to 0.5 μm was also observed in some areas of the fibres (Figure 1i). Elemental mapping showed that these globular deposits consisted of calcium-phosphate (Figure 2c) with approximate calcium to phosphorus ratio of 1.5. Continued immersion in SBFx5A solution for another half an hour led to growth of globular calcium-phosphate deposits on top of the thin sodium chloride layer (Figure 1j). After 24 hours, silk fibres were completely covered with a calcium-phosphate layer consisting of globules, 0.2 to 0.5 μm in size (Figure 1k-l). EDX analysis (not shown) indicated only presence of calcium and phosphorus, suggesting that the coating was relatively thick.

Raman spectroscopy analysis of uncoated silk fibres showed a spectrum with typical silk protein bands at around 904 cm^{-1} and 1665 cm^{-1} (Figure 3a). After immersion for 2 hours in SBFx5A solution, a peak appeared at around 955 cm^{-1} which is a typical phosphate band (Figure 3b). The Full Width at Half Height (FWHH) of this band was around 29 cm^{-1}, suggesting low crystallinity, which was consistent with the ESEM findings of amorphous calcium phosphate deposition (Figure 1). With time, the height of the phosphate peak increased, suggesting more calcium-phosphate deposition, however, its FWHH value remained the same, confirming that the calcium-phosphate layer remained amorphous until the end of the coating process in SBFx5A (Figure 3c-d).

Crystal growth on pre-calcified recombinant silk fibres

Recombinant spider silk fibres pre-calcified by soaking for 24 hours in the SBFx5A solution were then immersed in SBFx5B solution, with lower concentration of magnesium and carbonate ions, in order to promote crystal growth on the first layer that acted as a collection of nucleation sites. Immersion of pre-calcified fibres in SBFx5B solution did not result in deposition of sodium chloride crystals as was the case when uncoated silk fibres were immersed in SBFx5A solution. After 10 minutes of immersion, no obvious changes were observed on the pre-calcified fibres (Figure 4a-b). However, after 20 minutes, small crystals, with the size of about 0.5 μm started forming on top of the amorphous calcium phosphate layer (Figure 4c-d). This crystalline calcium-phosphate layer continued to grow up to 24 hours of immersion. Also crystal size increased with time and the final coating was composed of sharp crystals with the size of about 5 μm (Figure 4e).

Raman spectra of the coating formed by immersion in SBFx5B solution (after 24-hour pre-calcification in SBFx5A solution) showed a shift in the position of phosphate peak from 955 cm^{-1} (Figure 3b-d) to
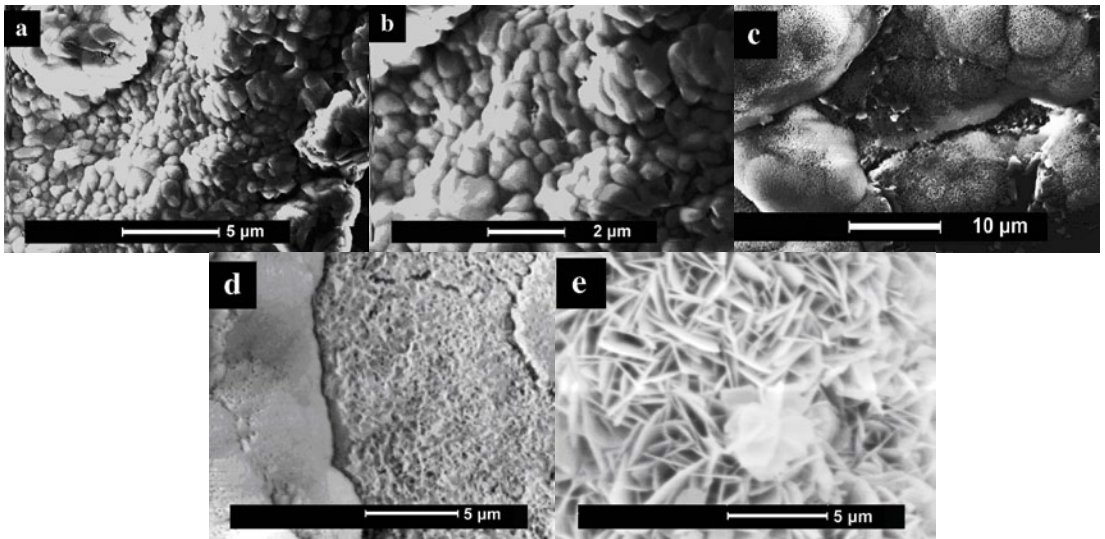
Figure 4: ESEM micrographs of spider silk fibres after immersion in SBFx5A solution for 24 hours followed by immersion in SBFx5B solution for 10 minutes, magnification 1000x (a) and magnification 5000x (b); for 20 minutes, magnification 1000x (c) and magnification 2000x (d); and for 24 hours, magnification 5000 (e).
Immersion in SBFx5B solution after pre-calcification resulted in the formation of crystals with the size of 0.5 µm as early as after 20 minutes (c,d), which then continued growing and eventually forming a thick, homogenous and highly crystalline coating with the crystal size of about 5 µm at 24 hours (e).

961 cm^{-1} (Figures 3e-i) as early as after 1 hour (Figure 3e). With time, the position of the peak remained at about 961 cm^{-1}, and its FWHH value decreased by half as compared to the coating formed during the pre-calcification step. Both shift in the peak position and decrease of the FWHH value suggested the formation of a more crystallized coating, confirming the findings of the ESEM analysis.

Analysis of the fibre cross section

The cross section of the coated fibre after the ion beam polishing at a 52° tilt, is shown in Figure 5a. The diameter of the fibre was about 15 μm and the thickness of the final coating was about 17 μm, slightly varying along the fibre. The thickness of the coating increased with time, indicating that it can be controlled by controlling the process duration. The EDX spectrum of the FIB polished cross section is shown in Figure 5c. The elements found in the analysis were C, O, Na, Ga, Si, P, Cl and Ca. The Ga signal in the spectrum came from the ions that remained inside and around the fibre after the ion beam polishing, whereas the Si signal originated from the substrate to which the coated fibre was attached. Figure 5b shows the mapping of the elements Ca, P, Na and Cl. Both the Ca and P were homogenously distributed within the fibre and the coating. The Na appeared slightly more concentrated in the areas of coating in the vicinity of the silk fibre. The Cl seemed more evenly distributed and the amounts of both Na and Cl were very low in both the fibre and the coating.

Cell culture

Bone marrow derived hMSCs were cultured for up to 14 days on silk fibres coated with thick, crystalline calcium-phosphate layer formed through the two-step method.
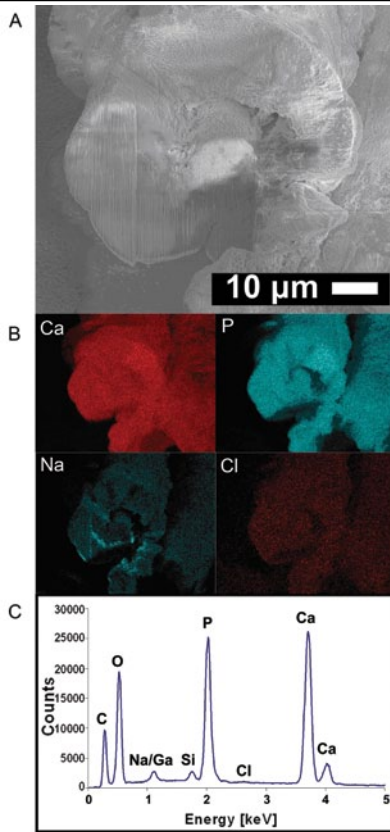
114

Figure 5: SEM micrograph of a cross section of a coated fibre prepared by using the gallium ion beam inside the FIB/SEM (a). The fibre had a diameter of about 15 µm and the coating thickness was approximately 17 µm.
EDX maps of the fibre cross section of the elements Ca, P, Na and Cl, respectively (b). EDX spectrum of the fibre shown in (a) in the energy range of 0 to 5keV.
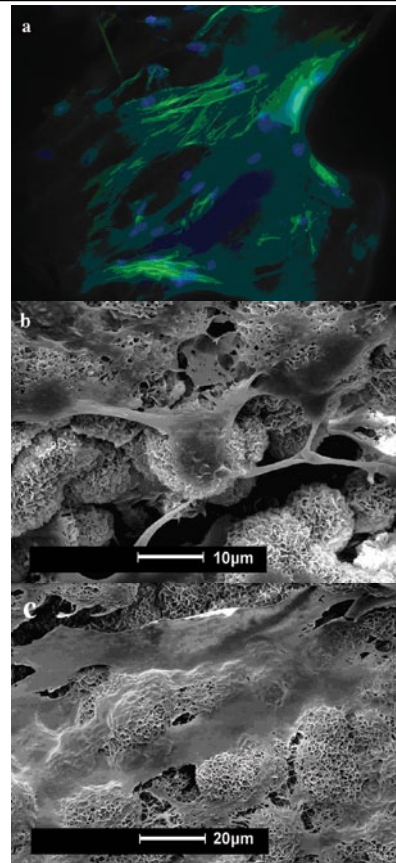

Figure 6: Fluorescence (a) and ESEM (b,c) micrographs of hMSCs cultured for 6 days (a,b) and 14 days (c) on silk fibres coated with crystalline calcium-phosphate layer. (green is phalloidin-stained cytoskeleton and blue is DAPI-stained cell nuclei).

After 6 days of culture, spreading cells were observed on the coated fibres (Figure 6a,b). Cells continued spreading, and completely covered the whole surface of the fibres after 14 days (Figure 6c).

Discussion

Although silk has a long history of use as suture material, it was not until recently that it became heavily investigated with regard to its potential role as scaffold for bone tissue engineering [36-37]. Important advantages of silk as compared to other scaffold materials are its impressive mechanical properties, biodegradability, and biocompatibility [15, 38]. Both natural- and recombinant silk have previously been tested as materials in bone repair and regeneration [39-40]. Two different approaches were used to improve the bioactivity of the silk material, one aiming at combining consensus sequences from silk with

another special gene sequence which resulted in improved calcium-binding ability [39], and another at combining natural silk with a protein containing hydroxyapatite-binding sites [40].

In the present study, we applied a biomimetic coating method to provide recombinant spider silk fibres with a CaP layer so as to improve bioactivity of silk while retaining its mechanical properties. The results of the study showed that it is indeed possible to deposit a thick and homogenous crystalline coating on the silk fibres by using a two-step biomimetic approach which consisted of immersion of silk fibres into supersaturated SBF to obtain an amorphous pre-coating, followed by immersion in supersaturated SBF with decreased amounts of crystal growth inhibitors. Supersaturation of the solution was achieved by bubbling CO_2 gas, which decreased its pH and allowed supersturation of the solution. The coating process was initiated by removing the CO_2 source and allowing the gas to slowly escape, which led to pH increase and CaP precipitation.

Similar approach was previously used to coat titanium substrates, and these experiments showed that the coating formed was crystalline carbonated apatite type AB [26-27, 41-42]. In 2003, Takeuchi etc. also showed that bone-like apatite was deposited onto the silk fibres after immersing into SBF1.5x solution [43]. As the silk fibres used in the present study were small, not enough coating could be obtained to perform Fourier Transform Infra Red (FTIR) Spectroscopy or X-ray diffraction. Nevertheless, as exactly the same coating process was used as for earlier investigated titanium, and based on the estimated calcium to phosphorus ratio, it can be assumed that the CaP coating on silk fibres was also of carbonated apatite type. Interestingly, while the coating process of titanium plates started with deposition of amorphous CaP globules [43-44], in this study we observed sodium-chloride crystals on the surface of silk fibres, prior to the CaP deposition. One possible reason for the deposition of the sodium-chloride layer on the silk surface could be that the silk contained specific binding sites for sodium-chloride, and although the bonding strength may be weak, the strong supersaturation of the solution may allow sodium-chloride crystal deposition. As previously reported [27], lower ionic strength of the solution causes a more rapid increase of the pH and therewith a more rapid precipitation of CaP. The fast deposition of sodium-chloride crystals we observed here may have led to a local depletion of sodium and chloride ions (lower ionic strength) in the microenvironment in the vicinity of the silk fibre, causing local increase of the pH and thus faster deposition of CaP. This local low ionic strength level could possibly explain the early formation of CaP layer, which took place as early as one hour after immersion in SBF-5A and eventually covered the whole surface of fibres in no more than 1.5 hours. This was in contrast with the coating process of titanium alloy substrates, where more than 4 hours of immersion in the same solution were needed to completely cover the surface with CaP layer [44].

ESEM observations of the final coating after immersion in SBFx5A showed that the fibres were covered with a uniform and dense amorphous Ca-P film composed of globules of 0.2 μm to 1 μm in size. When titanium was immersed in the same solution, larger globules were formed (1-5 μm), indicating that the type of substrate is of great importance for coating properties.

After pre-calcification in SBFx5A solution for one day, the silk fibres were immersed in SBFx5B solution, with decreased Mg^{2+} and CO_3^{2-} concentrations. In earlier studies [26, 41], Mg^{2+} and CO_3^{2-} were

shown to act as inhibitors of crystallization of several CaP phases. In line with this finding, the SBFx5B solution with less Mg^{2+} and CO_3^{2-} led to the formation of a thick crystalline coating. Immersion of pre-calcified fibres in SBFx5B solution resulted in a direct deposition of crystalline CaP layer, i.e. without intermittent deposition of sodium-chloride crystals. This again suggests that deposition of sodium-chloride before CaP is related to the nature of silk fibres. Raman spectra showed that the phosphate peak at around 955 cm^{-1} found on silk mineralized in SBFx5A solution, shifted to 961 cm^{-1} upon immersion in SBFx5B, and that the FWHH of this peak gradually decreased by half indicating formation of a more crystalline coating structure. With immersion time, this phosphate peak intensified and the crystal size increased. The amorphous pre-calcification Ca-P layer acted as a seeding surface for the formation of crystalline coating. The gradual decrease of FWHH of the phosphate peak at 961cm^{-1}, suggested that this was a dynamic process involving partial dissolution of the amorphous layer followed by (re)pre-cipitation of the crystalline phase from SBFx5B.

In order to further analyze the coating on the silk fibres, focused ion beam (FIB) was used to produce a cross section of the coated fibre, which was then investigated for chemical composition by EDX. The analysis of the cross section revealed a possible presence of a thin sodium-chloride layer between the silk and the CaP coating that had a thickness of about 17 μm. In addition, the analysis of the cross section showed that the CaP coating was not only present on the outside of the silk fibre bundle, but also between individual fibres within the bundle.

The biomimetic approach described here can be used to provide artificial silk fibres with a homogenous and thick crystalline carbonated apatite layer, which is able to support attachment, growth and extra-cellular matrix formation of hMSCs. A similar coating has previously been shown to have excellent osteoconductivity. The requirement of improved bioactivity of the combined material as compared to individual components is therefore met. This is also consistent with an earlier study on premineral-ized silk scaffolds which showed that the layer of premineralization results in enhanced expression of osteogenic markers [40]. However, whether excellent mechanical properties of silk are retained after the coating process needs to be further investigated. It is expected that the ceramic coating, which is intrinsically brittle, will have negatively affect elastic properties of the silk. However, by varying coat-ing properties, such as crystallinity and thickness, which can be done by controlling the parameters of the coating process, negative effects can be minimized. It is also possible to use the composite material as developed here to initiate bone formation in the beginning of bone healing process by the bioactive coating that is highly resorbable and biodegradable, leaving behind strong silk fibres that are able to mechanically support further bone formation.

CONCLUSIONS

The results of this study showed that recombinant spider silk fibres could successfully be coated with a homogenous and thick crystalline calcium-phosphate layer using a 2-step biomimetic procedure. The coated silk fibres supported the attachment and growth of bone marrow-derived human mesenchymal stem cells. This approach offers possibilities in developing bone graft substitutes that combine me-

chanical properties of silk with bioactivity of calcium phosphates.

Another interesting finding from this study was that the coating process from the supersaturated simulated body fluid started with deposition of sodium-chloride crystals, which was in contrast with coating process on other substrates. The reason behind this observation, which may also be important for understanding the in vivo mineralization of silk fibres, should be revealed in future studies.

ACKNOWLEDGEMENTS

REFERENCES

1.   Zaffe, D., Some considerations on biomaterials and bone. Micron, 2005. 36(7-8): p. 583-92.

2.   Yuan, H., et al., Tissue responses of calcium phosphate cement: a study in dogs. Biomaterials, 2000. 21(12): p. 1283-90.

3.   Gosain, A.K., et al., A 1-year study of osteoinduction in hydroxyapatite-derived biomaterials in an adult sheep model: part I. Plast Reconstr Surg, 2002. 109(2): p. 619-30.

4.   El-Ghannam, A., Bone reconstruction: from bioceramics to tissue engineering. Expert Rev Med Devices, 2005. 2(1): p. 87-101.

5.   Damien, C.J. and J.R. Parsons, Bone graft and bone graft substitutes: a review of current technology and applications. J Appl Biomater, 1991. 2(3): p. 187-208.

6.   Laurencin, C., Y. Khan, and S.F. El-Amin, Bone graft substitutes. Expert Rev Med Devices, 2006. 3(1): p. 49-57.

7.   Habibovic, P. and K. de Groot, Osteoinductive biomaterials - properties and relevance in bone repair. J Tissue Eng Regen Med, 2007. 1: p. 25-32.

8.   Vallet-Regi, M., Revisiting ceramics for medical applications. Dalton Trans, 2006(44): p. 5211-20.

9.   Kokubo, T., H.M. Kim, and M. Kawashita, Novel bioactive materials with different mechanical properties. Biomaterials, 2003. 24(13): p. 2161-75.

10.   Kokubo, T., et al., Bioactive metals: preparation and properties. J Mater Sci Mater Med, 2004. 15(2): p. 99-107.

11.   Rezwan, K., et al., Biodegradable and bioactive porous polymer/inorganic composite scaffolds for bone tissue engineering. Biomaterials, 2006. 27(18): p. 3413-31.

12.   Bauer, T.W., An overview of the histology of skeletal substitute materials. Arch Pathol Lab Med, 2007. 131(2): p. 217-24.

13.   Li, X., et al., Collagen-based implants reinforced by chitin fibres in a goat shank bone defect model. Biomaterials, 2006. 27(9): p. 1917-23.

14.   Li, X., et al., In vitro evaluation of porous poly(L-lactic acid) scaffold reinforced by chitin fibers. J Biomed Mater Res B Appl Biomater, 2009. 90(2): p. 503-9.

15.   Altman, G.H., et al., Silk-based biomaterials. Biomaterials, 2003. 24(3): p. 401-16.

16.   Huemmerich, D., et al., Novel assembly properties of recombinant spider dragline silk proteins. Curr Biol, 2004. 14(22): p. 2070-4.

17.   Lazaris, A., et al., Spider silk fibers spun from soluble recombinant silk produced in mammalian cells. Science, 2002. 295(5554): p. 472-6.

18.   Stark, M., et al., Macroscopic fibers self-assembled from recombinant miniature spider silk proteins. Biomacromolecules, 2007. 8(5): p. 1695-701.

19.   Bogush, V.G., et al., A Novel Model System for Design of Biomaterials Based on Recombinant Analogs of Spider Silk Proteins. J Neuroimmune Pharmacol, 2008.

20.   Brooks, A.E., et al., Properties of synthetic spider silk fibers based on Argiope aurantia MaSp2. Biomacromolecules, 2008. 9(6): p. 1506-10.

21.   Teulé, F., et al., Modifications of spider silk sequences in an attempt to control the mechanical properties of the synthetic fibers. Journal of Materials Science, 2007. 42(21): p. 8974-8985.

22.   Gosline, J., et al., Elastic proteins: biological roles and mechanical properties. Philos Trans R Soc Lond B Biol Sci, 2002. 357(1418): p. 121-32.

23.   Collins, M.J., et al., A Basic Mathematical Simulation of the Chemical Degradation of Ancient Collagen. Journal of Archaeological Science, 1995. 22: p. 175-183.

24.   Grip, S., J. Johansson, and M. Hedhammar, Engineered disulfides improve mechanical properties of recombinant spider silk. Protein Sci, 2009. 18(5): p. 1012-1022.

25.   Kokubo, T., et al., Solutions able to reproduce in vivo surface-structure changes in bioactive glass-ceramic A-W. J Biomed Mater Res, 1990. 24(6): p. 721-34.

26.   Barrere, F., et al., Nucleation of biomimetic Ca-P coatings on ti6A14V from a SBF x 5 solution: influence of magnesium. Biomaterials, 2002. 23(10): p. 2211-20.

27.   Barrere, F., et al., Influence of ionic strength and carbonate on the Ca-P coating formation from SBFx5 solution. Biomaterials, 2002. 23(9): p. 1921-30.

28.   Barrere, F., et al., Osteogenecity of octacalcium phosphate coatings applied on porous metal implants. J Biomed Mater Res A, 2003. 66(4): p. 779-88.

29.   Habibovic, P., et al., Influence of octacalcium phosphate coating on osteoinductive properties of biomaterials. J Mater Sci Mater Med, 2004. 15(4): p. 373-80.

30.   Liu, Y., K. de Groot, and E.B. Hunziker, Osteoinductive implants: the mise-en-scene for drug-bearing biomimetic coatings. Ann Biomed Eng, 2004. 32(3): p. 398-406.

31.   Liu, Y., et al., Biomimetic coprecipitation of calcium phosphate and bovine serum albumin on titanium alloy. J Biomed Mater Res, 2001. 57(3): p. 327-35.

32.   Stigter, M., et al., Incorporation of different antibiotics into carbonated hydroxyapatite coatings on titanium implants, release and antibiotic efficacy. J Control Release, 2004. 99(1): p. 127-37.

33.   Du, C., et al., Biomimetic calcium phosphate coatings on Polyactive 1000/70/30. J Biomed Mater Res, 2002. 59(3): p. 535-46.

34.   Varma, H.K., et al., Porous calcium phosphate coating over phosphorylated chitosan film by a biomimetic method. Biomaterials, 1999. 20(9): p. 879-84.

35. Hedhammar, M., et al., Structural properties of recombinant nonrepetitive and repetitive parts of major ampullate spidroin 1 from Euprosthenops australis: implications for fiber formation. Biochemistry, 2008. 47(11): p. 3407-17.

36. Furuzono, T., et al., Preparation and characterization of apatite deposited on silk fabric using an alternate soaking process. J Biomed Mater Res, 2000. 50(3): p. 344-52.

37. Sofia, S., et al., Functionalized silk-based biomaterials for bone formation. J Biomed Mater Res, 2001. 54(1): p. 139-48.

38. Panilaitis, B., et al., Macrophage responses to silk. Biomaterials, 2003. 24(18): p. 3079-85.

39. Huang, J., et al., The effect of genetically engineered spider silk-dentin matrix protein 1 chimeric protein on hydroxyapatite nucleation. Biomaterials, 2007. 28(14): p. 2358-67.

40. Kim, H.J., et al., Bone tissue engineering with premineralized silk scaffolds. Bone, 2008. 42(6): p. 1226-34.

41. Barrere, F., et al., Biomimetic calcium phosphate coatings on Ti6AI4V: a crystal growth study of octacalcium phosphate and inhibition by Mg2+ and HCO3. Bone, 1999. 25(2 Suppl): p. 107S-111S.

42. Barrere, F., et al., In vitro and in vivo degradation of biomimetic octacalcium phosphate and carbonate apatite coatings on titanium implants. J Biomed Mater Res A, 2003. 64(2): p. 378-87.

43. Takeuchi, A., et al., Deposition of bone-like apatite on silk fiber in a solution that mimics extracellular fluid. J Biomed Mater Res A, 2003. 65(2): p. 283-9.

44. Barrere, F., et al., Nano-scale study of the nucleation and growth of calcium phosphate coating on titanium implants. Biomaterials, 2004. 25(14): p. 2901-10.

Chapter 8

Calcium-phosphate coated electrospun polymers: Towards improved scaffolds for bone tissue engineering

Electrospun scaffolds are widely used for various tissue engineering applications. In this study, we applied a biomimetic coating method to provide electrospun scaffolds from two polymers, poly(□-caprolactone) (PCL) and block-copolymer poly(ethylene oxide terephthalate) – poly(buthylene tereph-thalate) (PEOT/PBT), with a calcium-phosphate layer to improve their bioactivity, The in vitro studies with human mesenchymal stem cells did not show significant effect of coating in terms of enhanced cell proliferation or alkaline phosphatase expression. Implantation of scaffold-goat mesenchymal stem cells constructs subcutaneously in nude mice resulted in bone formation in the coated samples, in contrast to the uncoated ones, where no new bone formation was observed. The results of this study show that the biomimetic method can successfully be used to coat electrospun scaffolds of different polymers with a calcium-phosphate layer, which improves the in vivo bioactivity of the polymer.

Keywords: Bone tissue engineering, electrospun polymer scaffolds, calcium phosphate coating, in vitro, in vivo.

INTRODUCTION

Recent advances in scaffolding technologies allow for development of well-defined complex structures consisting of one or more materials with the goal of optimizing tissue engineering constructs. Bone tissue engineering is an application where a combination of polymers, with their structural diversity and excellent mechanical properties and highly bioactive calcium-phosphates, clearly results in scaffolds with improved characteristics [1]. Electrospinning has been widely used to prepare fibrous meshes of a variety of polymers for tissue engineering applications [2, 3]. It is a simple and powerful technique that involves the application of a high voltage to a polymer solution or melt to obtain fibres in the nanometre to micrometre range [4, 5]. The polymer-solvent combination, flow rate, applied voltage and the collector distance influence the outcome leading to fibres of different diameters and surface morphologies. Electrospun fibrous meshes can be used as a delivery vehicle for drugs, proteins and other growth factors or as a carrier of cells for regenerating tissue function. Polymers can be combined with calcium phosphates in a number of ways, e.g. by forming bulk composite scaffolds or by coating the polymer surface with a calcium phosphate layer using various techniques. Plasma spraying is the classical coating method for providing metallic implants with hydroxyapatite for total hip arthroplasty (HA) [6]. Although this technique has led to excellent clinical results [7], its use is associated with important drawbacks. This line-of-sight process that takes place at very high temperatures does not allow coating of geometrically complex and porous shapes, and its use is limited to thermally stable calcium-phosphate phases, such as hydroxyapatite [8]. Biomimetic coating methods based on the immersion of implants in solutions resembling body fluids have been developed to coat polymeric and metallic substrates with biologically relevant carbonated apatite and octacalcium phosphate coatings [9-11]. Combining bioactive but brittle ceramics with a mechanically strong and processible polymer seems to be a logical approach for the design of bone tissue engineering scaffolds. In this study, we electrospun and biomimetically coated Polycaprolactone (PCL) and PEOT/PBT, two widely used polymers in bone tissue engineering [9], [12]. In vitro and in vivo experiments for evaluating osteogenic potential and bone formation were performed.

Materials and Methods
Materials

PCL (Mn = 42,500) was purchased from Aldrich. PEOT/PBT block co-polymer was prepared in-house. Following an aPEOTbPBTc nomenclature, the composition used in this study was 300PEOT55PBT45 where, (a) is the molecular weight in g/mol of the starting poly(ethylene glycol) (PEG) blocks used in the copolymerization, while (b) and (c) are the weight ratios of the PEOT and PBT blocks, respectively. All the salts and reagents used for the preparation of the coating were purchased at either Merck or Sigma-Aldrich.

Electrospinning

Known amounts of PCL and PEOT/PBT were dissolved in chloroform and a mixture of chloroform

– hexafluoroisopropanol (HFIP) (78%-22%v/v) respectively. A 20% and 22.5% weight/volume (w/v) concentration of PCL in chloroform and a 28% (w/v) PEOT/PBT solution in chloroform – HFIP were prepared and stirred overnight at room temperature.

Electrospun scaffolds of PCL and PEOT/PBT were fabricated by using the following procedure. First, the solution of choice was loaded into a syringe and a desired flow rate was set using a syringe pump (KDS 100, KD Scientific). The other end of the syringe was connected to a needle which acted as the positive pole when a high voltage generator (NCE 30000, Heinzinger Electronic GmbH, Germany) was turned on. A metallic sheet of stainless steel was the collector (ground). An electrostatic field was formed between the needle and the collector when the generator was turned on. The polymer solution was pushed through the syringe to the tip of the needle. When the electrostatic field strength overcame the surface tension of the liquid drop at the tip of the needle, the drop was stretched and deposited onto the collector. The voltage was fixed at 12 kV for all conditions. The distance between the needle and collector was set at 15 cm (PEOT/PBT) or 20 cm (PCL). Flow rate and the distance between the collector and the needle were adjusted depending on the type of polymer solution used.

Preparation of biomimetic coatings on electrospun scaffolds

Electrospun scaffolds were biomimetically coated using a two step coating process.

<u>Step 1: Pre-calcification</u>

A supersaturated simulated body fluid solution (SBFx5) was prepared by dissolving reagent grade NaCl (40 g), $CaCl_2.2H_2O$ (1.84 g), $MgCl_2.6H_2O$ (1.52 g), $NaHCO_3$ (1.76 g) and $Na_2HPO_4.2H_2O$ (0.89 g) salts in 1l of demineralised water at 37° C under CO_2 gas bubbling. The CO_2 source was then removed from the solution and electrospun discs (diameter 15 mm) were immersed in the solution in a partly open vial and left to coat for 24 hours under continuous gentle stirring at 37 °C. This process was previously shown to result in a formation of thin, amorphous CaP layer.

<u>Step 2: Crystal growth</u>

Electrospun discs from step 1 were immersed in a calcium phosphate solution (CPS) at physiological pH of 7.4 for 24 hours to deposit a crystallized layer onto previously formed amorphous CaP layer. CPS was prepared by dissolving NaCl (8 g), $CaCl_2.2H_2O$ (0.59 g), $Na_2HPO_4.H_2O$ (0.36 g) and Tris (6.05 g) in MilliQ water and the pH of the solution was adjusted to 7.4 with 1M HCl. The coated electrospun discs were dried overnight at 50°C.

Characterization of scaffolds

The amount of coating in the scaffolds was calculated by weighing the scaffolds (n=60) before and after the coating process. The architecture and composition of coated and uncoated scaffolds were characterized using Environmental Scanning Electron Microscopy in secondary electron mode (ESEM) coupled to Energy Dispersive X-Ray (EDX) analyzer (XL 30 ESEM – FEG, Philips), Fourier transform infra red spectroscopy (FTIR) (Perkin Elmer Spectrum 1000) and Raman spectroscopy(home built setup). Thin films of the polymer solutions were cast and the contact angle was measured using a Dataphysics

OCA 20 contact angle system. Porosity was calculated using density measurements from a pycnometer (AccuPyc 1330, Micromeritics). Fibre diameters of electrospun scaffolds were measured from SEM images using an image analysis software. A total of 45 fibres were measured for each condition.

In vitro study

hMSC aspiration and expansion

Bone marrow aspirates were obtained from donors after written informed consent, and hMSCs were isolated and proliferated as described previously [13]. Briefly, aspirates were resuspended by using 20-gauge needles, plated at a density of 5 10^5 cells per square centimetre and cultured in hMSC proliferation medium containing α-MEM (Life Technologies), 10% FBS (Cambrex), 0.2 mM ascorbic acid (Asap; Life Technologies), 2 mM l-glutamine (Life Technologies), 100 units/ml penicillin (Life Technologies), 10 μg/ml streptomycin (Life Technologies), and 1 ng/ml basic FGF (Instruchemie). Cells were grown at 37°C in a humid atmosphere with 5% CO_2. Medium was refreshed twice a week, and cells were used for further sub-culturing or cryopreservation. The hMSC basic medium was composed of hMSC proliferation medium without basic FGF and hMSC osteogenic medium was composed of hMSC basic medium supplemented with 10^{-8} M dex (Sigma). Cells were trypsinised prior to seeding on scaffolds.

Cell seeding on scaffolds

The in vitro experiments were performed with cells from one donor and repeated three times.

Uncoated and coated electrospun discs with a diameter of 15 mm were soaked in 70% ethanol for 30 minutes and left overnight in a laminar flow cabinet to dry. The scaffolds were washed twice with sterile PBS, transferred to a 24 well non-treated plate (NUNC) and incubated at 37°C in a humid atmosphere with 5% CO_2 for four hours in basic cell culture medium. After removing the medium, each scaffold was seeded with 15,000 cells (7,500 cells/cm^2) in 50 μl basic medium. The cell-scaffold constructs were incubated for three hours to allow the cells to attach and topped up to 1 ml with the appropriate medium (basic or osteogenic). Medium was refreshed every three days.

The scaffolds were washed with PBS and 200 μl of cell lysis buffer containing 0.2% Triton X-100 buffered with 0.1 M potassium-phosphate at pH 7.8 was added to the scaffolds to lyse the cells. After 30 minutes, the cell lysates were transferred to eppendorf tubes and stored at -80°C.

DNA assay

DNA assay was performed on days 1, 7 and 14. Cell numbers were determined using the Cyquant DNA quantification kit (Invitrogen) with 50 µl of cell lysate according to the manufacturer's protocol. Fluorescence at an excitation wavelength of 480 nm and an emission wavelength of 520 nm was measured using a Perkin Elmer LS50B plate reader.

ALP assay

ALP activity was assessed biochemically on days 7 and 14. 40 μl of CDP-star reagent (Roche) was added to a 10 μl aliquot of cell lysate and incubated for 30 minutes in the dark at 25°C. Chemo luminescence was measured in a Victor plate reader (Perkin Elmer, Wellesley, MA, USA).

In vivo study

Goat Mesenchymal stem cell (gMSC) aspirates were isolated from the iliac crest and cultured as previously described [14]. Culture medium consisted of α-MEM supplemented with 15% FBS, antibiotics, 0.1 mM l-ascorbic acid-2-phosphate, 2 mM l-glutamine and 1 ng/ml basic fibroblast growth factor (Instruchemie, The Netherlands) [15]. Cells were cultured at 37 °C in a humid atmosphere with 5% CO_2. Cells were either cryopreserved or subcultured further. 200,000 gMSCs were seeded on 7 mm x 5 mm scaffolds (thickness 50 -180 μm) in basic cell culture medium containing 15% FBS (Cambrex). Cells were allowed to attach overnight at 37°C in a humid atmosphere with 5% CO_2 before implantation.

Subcutaneous implantation

The four types of scaffolds – electrospun PEOT/PBT (ePEOT/PBT), PCL (ePCL), electrospun and biomimetically coated PEOT/PBT (ecPEOT/PBT), PCL (ecPCL) seeded with goat MSCs were implanted in immuno-deficient mice obtained from Charles River laboratories, The Netherlands (Crl:NMRI-Foxn1<nu>) to assess ectopic bone formation.

Animals were housed at the Central Laboratory Animal Institute (Utrecht University, The Netherlands). All animal experiments were approved by the local Animal Care and Use committee (DEC) and performed in adherence to the local and national ethics guidelines. Prior to implantation, the tissue-engineered constructs were washed with PBS. Six mice were anesthetized using isoflurane. The surgical sites were cleaned with ethanol, four subcutaneous pockets were created using blunt incision and one scaffold from each type was implanted. The sites were closed using resorbable vicryl 4-0 sutures. After 6 weeks, the animals were euthanized and the implants were retrieved and fixed in 4% formalin. The fixed samples were washed with PBS and dehydrated in ethanol series (70%, 80%, 90%, 96%, and 100% x 2, one day in each concentration) and embedded in methyl methacrylate. Sections with a thickness of approximately 10-15 μm were obtained using a histological diamond saw (Leica SP1600, Wetzlar, Germany) and stained with 1% methylene blue (Sigma) and 0.3% basic fuchsin solution (Sigma) after etching with HCl/ethanol mixture. The sections were observed using a Nikon Eclipse E600 microscope.

Statistical Analysis

Statistical analysis on the in vitro data were performed in SPSS 15.0 software using a one way ANOVA test with a LSD Post Hoc comparison. The level of significance was set at 0.05.

RESULTS

Material preparation and characterization

Electrospun scaffolds of PCL and PEOT/PBT were successfully fabricated. Figure 1 shows the SEM mi-
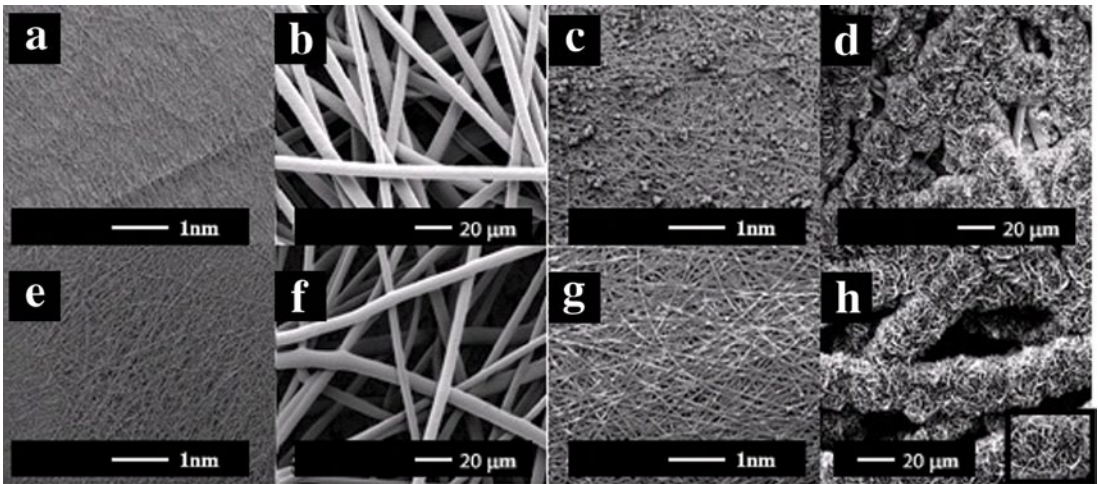
Figure 1: SEM micrographs of ePCL (A and B), ecPCL (C and D), ePEOT/PBT (E and F) and ecPEOT/PBT (G and H) at various magnifications. The insert in H shows the calcium phosphate crystals in high magnification (2500x)

crographs of electrospun fibre mats at low (1A, 1E) and high magnification (1B, 1F) of both polymers. Uniform, non-woven fibres of identical fibre diameters were prepared by adjusting the flow rate, distance from the collector and the concentration of the polymer as indicated in Table 1. The diameter, porosity and the contact angle were measured and are shown in Table 1. The biomimetic coating process resulted in an uniform coating on both polymers (Figs 1C, D, 1G, H). The coating thickness of ecPCL was slightly lower than that of ecPEOT/PBT (12.03 ± 1.71 μm, 13.16 ± 1.89 μm respectively). Weight measurements indicated that PEOT/PBT scaffolds contained 10% more coating compared to the PCL scaffolds (Table 1). EDX mapping of Ca, P and O (Fig 2) confirmed that the coating was uniformly present over the entire surface. The FTIR spectra in Figure 3A indicate the presence of P-O bands at 560 cm^{-1} and 600 cm^{-1} in both polymers. Characteristic HPO_4^{2-} bands of Octacalcium Phosphate (OCP) were observed at 906 cm^{-1} and 852 cm^{-1}. The carbonate bands at 1410 cm^{-1} and 1450 cm^{-1} were also seen in both PCL and PEOT/PBT. The FTIR spectra suggest that the coating was a mixture of OCP and carbonated apatite (CA) phases. Figures 3B and C show the Raman spectra of the two polymers before and after coating. The presence of sharp peak at 960 cm^{-1} confirms the presence of phosphate group.

S.Nr	Type	Concentration of solution (w/v)%	Distance from collector (cm)	Flow rate(ml/hr)	Fiber diameter (μm)	Porosity (%)	Contact angle (°)	Amount of coating (%)
1	PEOT/PBT	28% in 78/22 CHCl3-HFIP	15	15,20,25	6.47 ± 1.46	68.5 ± 2.2	66.8 ± 3.65	24.47 ± 6.13
2	PCL	20 or 22.5% in CHCl3	20	1	6.52 ± 1.51	79.3 ± 11.3	75.6 ± 2.29	14.01 ± 5.4

Table 1: Spinning conditions and scaffold characterization in terms of fibre diameter, porosity, contact angle and the amount of coating present. A voltage of 12kV was applied in all cases
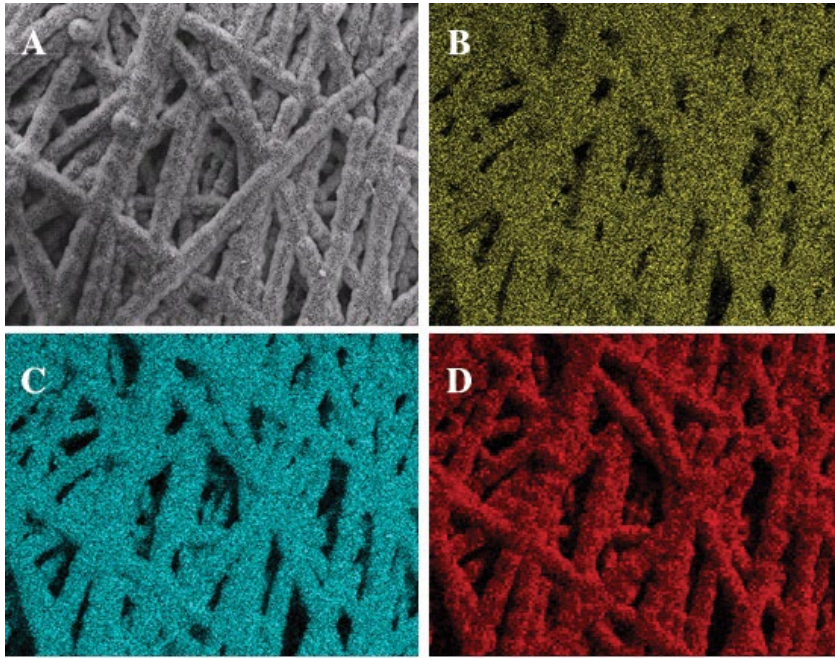
Figure 2: SEM Micrograph (A) of ecPEOT/PBT and the corresponding elemental mapping of Calcium (B), Phosphorus (C) and Oxygen (D) acquired by EDX. These findings are also representative for ecPCL scaffolds.
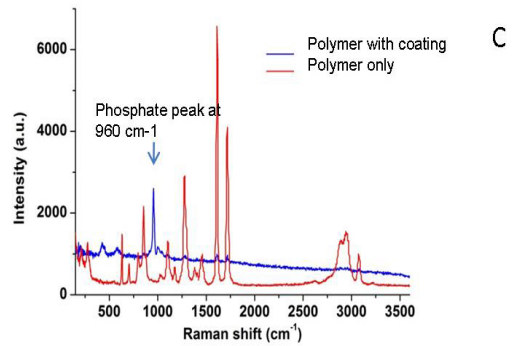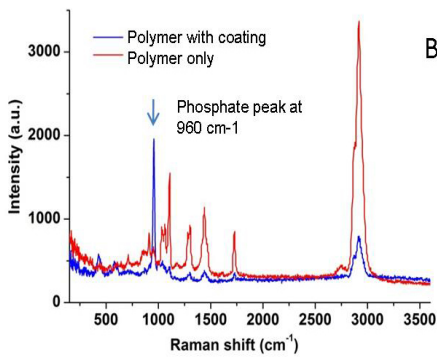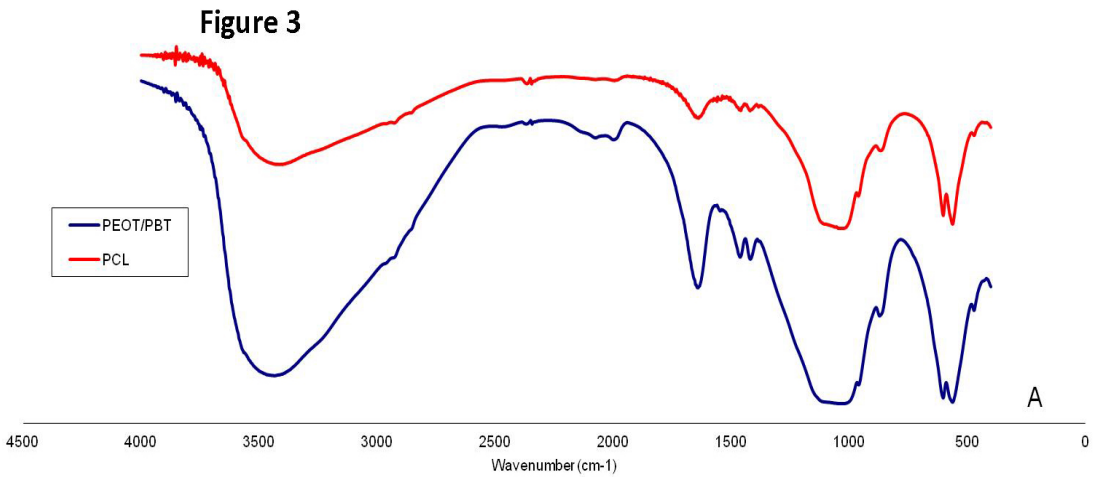

Figure 3: Spectroscopic characterisation. (A) FTIR spectra of biomimetically coated PCL and PEOT/PBT. Raman spectra of coated and uncoated (B) PCL and (C) PEOT/PBT

In vitro study

Cell proliferation

Results of DNA assay on days 1, 7 and 14 are shown in Figure 4A. On day 1, there were no significant differences in cell numbers between constructs cultured in basic and osteogenic medium. Similarly, no effect was observed of the presence of coating or polymer type. Also on day 7, no significant differences in cell numbers were found when the effect of culture medium, coatings and polymers was tested. The type of medium used did not have a significant effect on cell numbers on day 14, except in the case of PCL coated scaffolds. The presence of coatings decreased cell numbers on both PCL and PEOT/PBT. In addition, significant difference in cell number at day 14 was found between uncoated PCL and PEOT/PBT constructs.
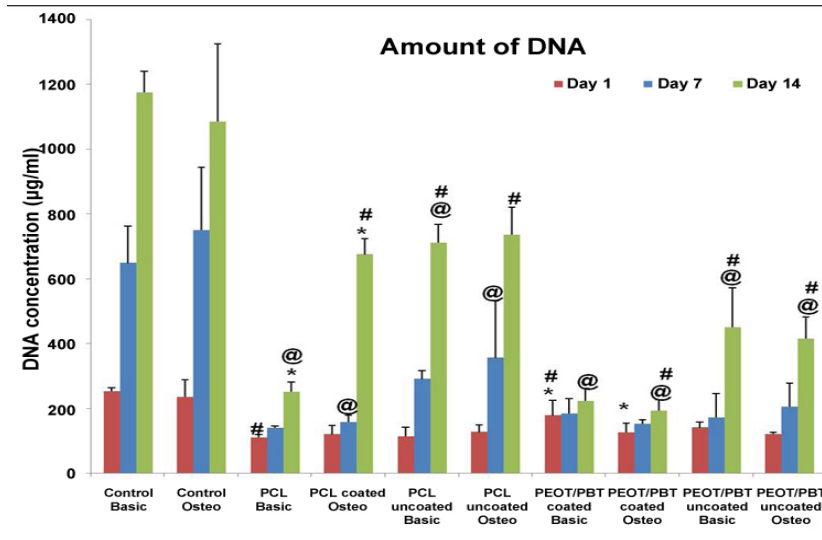

*Figure 4a: Amount of DNA in the various conditions on days 1,7 and 14. A LSD Post Hoc calculation was performed. * represents significant differences between scaffolds in basic and osteogenic medium (compared within the same polymer and coating type) @ represents significant differences between coated and uncoated scaffolds (compared within the same medium and polymer) and # represents significant differences between PCL and PEOT/PBT (compared within the same medium and coating type). p = 0.05.*
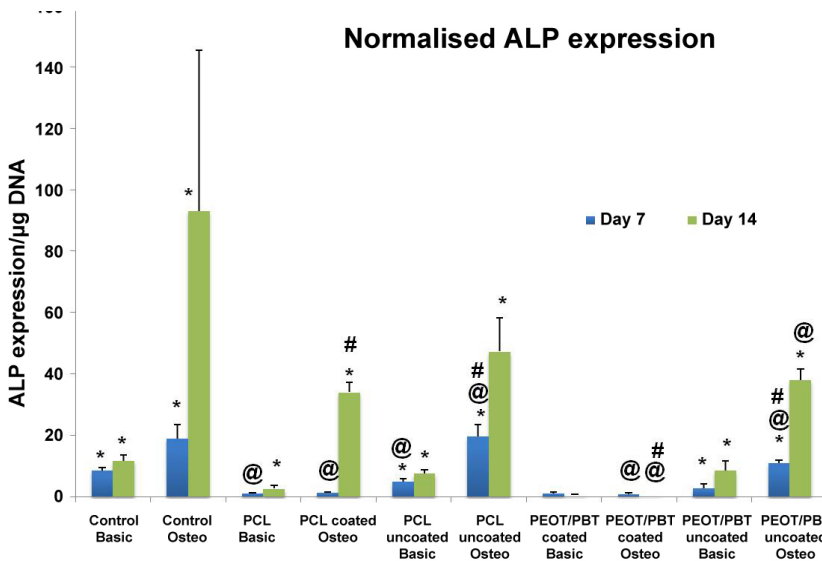

*Figure 4b: Normalised ALP in the various conditions on days 7 and 14. A LSD Post Hoc calculation was performed. * represents significant differences between scaffolds in basic and osteogenic medium (compared within the same polymer and coating type) @ represents significant differences between coated and uncoated scaffolds (compared within the same medium and polymer) and # represents significant differences between PCL and PEOT/PBT (compared within the same medium and coating type). p = 0.05.*

Osteogenic differentiation

The ALP expression on days 7 and 14 is shown in Figure 4B. On day 7, osteogenic medium significantly increased the normalized ALP expression in control TC plates and on uncoated electrospun fibres. In contrast, no significant difference in ALP expression between basic and osteogenic medium was found for ecPCL and ecPEOT/PBT. In most cases, the scaffolds with coatings had a significantly lower expression of ALP compared to the uncoated ones. There were no significant differences in the ALP expression when the two polymers were compared. On day 14, constructs in the osteogenic medium showed a significantly higher ALP expression compared to the cultures in basic medium for all
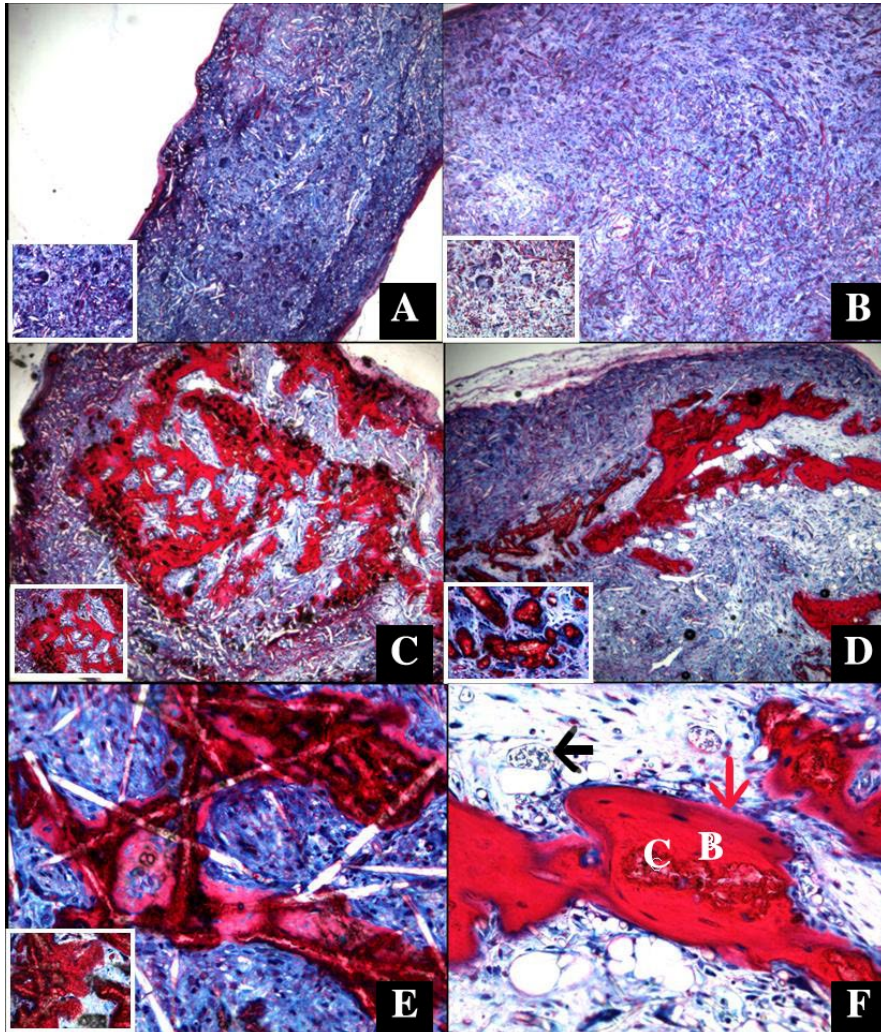

Figure 5: Histological sections from the in vivo study after Methylene blue and Basic fuchsin staining . (A) ePCL (B) ePEOT/PBT. Both scaffolds show presence of macrophages (insert) and fibrous tissue but no bone formation. (C) ecPCL showing bone formation. The insert shows the presence of bone surrounding the biomimetic coating. (D) ecPEOT/PBT showing bone formation. The insert shows the presence of macrophages around remnant of the coating. (E) ecPEOT/PBT shows bone in very early stage of formation (pink). The insert shows early mineralisation under high magnification. (F) ecPEOT/PBT with the biomimetic coating C and bone B. The black arrow indicates erythrocyte like cells present in the vicnity of the bone. The red arrow indicates bone lining cells

conditions. No significant differences were found between coated and uncoated constructs. In general, polymer type did not significantly affect the ALP expression on day 14.

In vivo study

During explantation, one sample of both coated and uncoated PCL were lost. No bone formation was observed in any of the uncoated PCL and PEOT/PBT samples (Fig 5A, 5B). Multi-nucleated giant cells were present in both types of scaffolds suggesting an inflammatory response (inserts in 5A, 5B). Bone formation was observed in one out of five ecPCL (Figure 5C) and in four out of six ecPEOT/PBT (Figure 5D) constructs. In some samples, new mineral formation was observed, without osteoblasts and bone lining cells and the bone formed had immature woven appearance (Fig 5E). Some remnants of coating were found in areas with new bone formation, incorporated into new bone, whereas in general, the coating had degraded. Figure 5F shows the presence of newly formed bone with osteoblasts, bone lining cells and erythrocytes.

Discussion

Electrospinning is a simple and versatile technique to produce polymeric meshes consisting of fibres in the nanometre to micrometre range and is therefore widely used for fabricating scaffolds for tissue engineering. In the present study, electrospun scaffolds were successfully made from PCL and PEOT/PBT, both of which have found several applications in regenerative medicine. It was ensured that the fibre diameter of the electrospun constructs from the two polymers was the same to avoid another variable in the study. In an earlier study, Moroni et al [17] showed that fibre diameter and morphology of electrospun PEOT/PBT fibres have an effect on hMSC proliferation. Since a lower flow rate was used to obtain PCL fibres of diameter identical to that of PEOT/PBT, the number of fibres in the PCL mesh was lower compared to PEOT/PBT, also explaining a higher porosity for the PCL scaffolds. Contact angles indicated that PEOT/PBT was slightly more hydrophilic, probably due the presence of a hydrophilic segment in the PEOT/PBT copolymer.

Biomimetic coatings have been widely used to coat various substrates like titanium and polymers [9-11]. As the biomimetic coating process takes place at physiological pH and low temperatures, it allows addition of bioactive agents such as proteins and growth factors to the coating, which would not be possible if plasma spraying was used. Furthermore, the biomimetic coating process that employs inorganic solutions resembling human blood plasma can be used for coating porous structures. In this study, the biomimetic coatings were uniform on both polymer types, but more coating was found on PEOT/PBT scaffolds, which may be contributed to its stronger hydrophilicity as compared to PCL. Characterisation of the coatings by EDX, FTIR and Raman spectroscopy indicated the presence of a mixture of OCP and carbonated apatite phases.

In vitro cell culture with hMSCs was performed over 14 days. The effect of the medium, coatings and the two polymers used were studied. Overall, the type of medium used did not have a great effect on cell numbers. After one day of culture, no significant differences were found in the amount of DNA be-

tween coated and uncoated fibres. At 7 days, it was observed that coatings negatively influenced DNA amounts, although differences between coated and uncoated scaffolds were not significant. Nevertheless, for the in vivo study, we have chosen to use peroperative seeding as described by Siddappa et al [16] in order to keep cell number on all scaffold types as equal as possible. As was shown by Siddappa et al [16] and from our prior experience, hMSCs seeded peroperatively do not lead to in vivo bone formation in subcutaneous nude mouse model in contrast to gMSCs, which were therefore chosen for the in vivo part of this study. The coated scaffolds had lesser DNA content compared to their uncoated counterparts on day 14, suggesting that coatings slow down cell growth.

The presence of dexamethasone, a known stimulus for osteogenic induction, in the osteogenic medium contributed to a significantly higher normalized ALP expression on day 7 in uncoated scaffolds only. On day 14, PCL coated scaffolds in osteogenic medium also showed a significantly higher ALP expression. These results suggest that the effect of dexamethasone is only sensed at a later time point by cells present on the coated scaffolds. The ALP activity of the cells cultured on coated scaffolds was lower than on the uncoated ones on day 7 though this effect was not visible on day 14. This can be explained by the late peaking between day 7 and day 14 of ALP expression of cells cultured on coated scaffolds. When viewed in conjunction with the DNA assay data, these data suggest that though there were significantly fewer cells in the coated scaffolds, no significant difference was observed in the ALP expression. The type of polymer did not have an obvious effect on the ALP expression.

The in vivo experiments showed that the uncoated scaffolds of either polymers combined with gMSCs did not lead to bone formation. Before implantation, gMSCs were expanded and allowed to attach to scaffolds in basic cell culture medium meaning that the cell culture medium could not have provided the osteogenic stimuli to the cells to trigger bone formation upon ectopic implantation. Porous PEOT/PBT scaffolds previously showed bone ingrowth and in vivo calcification when implanted in the femur of goats [17]. Biomimetic calcium phosphate coatings, similar to the one described in this study have led to bone formation inside porous metallic implants in rats [18] and goats [10]. Upon implantation, calcium phosphate coatings start dissolving [19], releasing thereby calcium and phosphorus ions, which is considered to be the first step towards de novo bone formation. Following the dissolution, a new carbonated apatite layer is precipitated on the substrate surface that contains endogenous factors. This process may act as a stimulus for osteoprogenitor cells to colonize the biomaterial eventually leading to new bone formation [10]. In the case of ectopic implantation, this stimulus is given to the implanted cells on the scaffold. The PEOT/PBT scaffolds contained a higher percentage of coating and the thickness of the biomimetic coating was also greater compared to PCL scaffolds. Studies by Chim [12] and co-workers showed that precalcification of 3-D PCL scaffolds in SBF did not result in increased osteoconductivity which might explain the low incidence of bone formation in PCL scaffolds. Relatively more coating on PEOT/PBT scaffolds possibly due to stronger adhesion of the coating may have been the reason for the higher bone incidence in PEOT/PBT constructs in comparison to the PCL ones. Although electrospinning is an attractive technique to provide an environment for cell attachment similar to that of extracellular matrix, electrospun structures cannot be used as sole scaffold for load bearing

applications in bone tissue engineering due to their poor mechanical properties. The combination of electrospinning with other scaffold fabrication technologies could lead to the development of a more complete scaffold for tissue engineering applications. Moroni et al [20] showed that combining an electrospun PEOT/PBT polymer mesh with a 3-D printed scaffold leads to enhanced cartilage tissue formation. More recently, Kuraishi et al [21] used Polyurethane fibres to cover a stent in the treatment of cerebral aneurysms. Since this study has shown that ecPEOT/PBT can initiate new bone formation, the next step was to combine it with a 3-D fibre deposited scaffold (Figure 6). The bioactive coated electrospun fibres in combination with the 3-D scaffold whose mechanical properties can be tailored [22] based on the requirementscould therefore be a promising scaffold for bone tissue engineering.
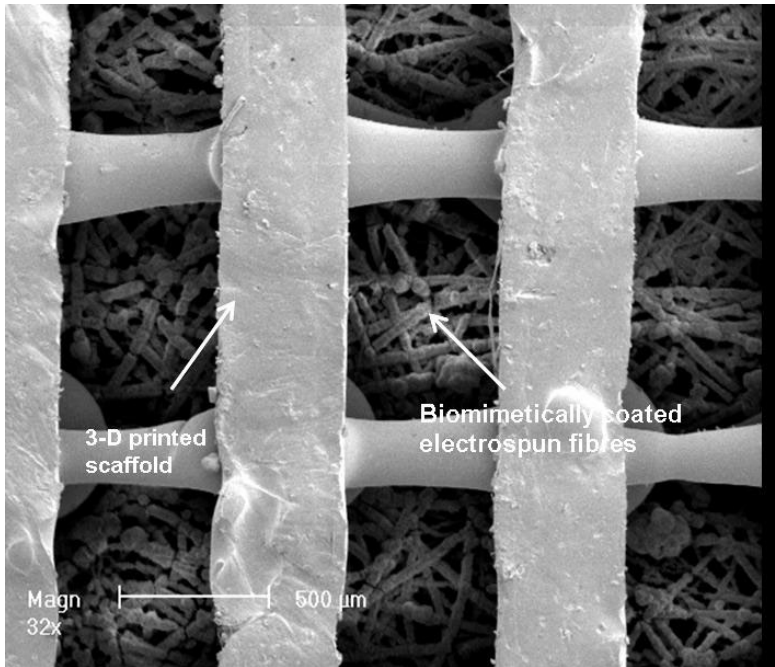

Figure 6: Combination of a 3-D fibre deposited scaffold and biomimetically coated electrospun fibres

CONCLUSIONS

Electrospun scaffolds were prepared from two widely used polymers and they were coated with a calcium phosphate layer using biomimetic coating process. Though in vitro results did not indicate a significantly high ALP expression of the coated scaffolds, in vivo experiments in a nude mouse model have demonstrated the osteogenic ability of the coated fibres. These bioactive coated electrospun scaffolds, in combination with a mechanically more suitable 3D scaffold could be used for bone tissue engineering applications.

ACKNOWLEDGEMENTS

work EC project STEPS (FP6-500465).

REFERENCES

1.   Bhattacharyya S, Kumbar SG, Khan YM, Nair LS, Singh A, Krogman NR, et al. Biodegradable Polyphosphazene-Nanohydroxyapatite Composite Nanofibers: Scaffolds for Bone Tissue Engineering. Journal of Biomedical Nanotechnology 2009 Feb;5(1):69-75.

2.   Li CM, Vepari C, Jin HJ, Kim HJ, Kaplan DL. Electrospun silk-BMP-2 scaffolds for bone tissue engineering. Biomaterials 2006 Jun;27(16):3115-3124.

3.   Yang F, Murugan R, Wang S, Ramakrishna S. Electrospinning of nano/micro scale poly(L-lactic acid) aligned fibers and their potential in neural tissue engineering. Biomaterials 2005 May;26(15):2603-2610.

4.   Doshi J, Reneker DH. Electrospinning Process and Applications of Electrospun Fibers. Journal of Electrostatics 1995 Aug;35(2-3):151-160.

5.   Dalton PD, Grafahrend D, Klinkhammer K, Klee D, Moller M. Electrospinning of polymer melts: Phenomenological observations. Polymer 2007 Nov 2;48(23):6823-6833.

6.   He DY, Sun XF, Zhao LD. Hydroxylapatite coatings by microplasma spraying. Journal of Inorganic Materials 2007 Jul;22(4):754-758.

7.   Geesink RGT, Hoefnagels NHM. 6-Year Results of Hydroxyapatite-Coated Total Hip-Replacement. Journal of Bone and Joint Surgery-British Volume 1995 Jul;77B(4):534-547.

8.   Ellies LG, Nelson DGA, Featherstone JDB. Crystallographic Changes in Calcium Phosphates during Plasma-Spraying. Biomaterials 1992;13(5):313-316.

9.   Du C, Meijer GJ, van de Valk C, Haan RE, Bezemer JM, Hesseling SC, et al. Bone growth in biomimetic apatite coated porous Polyactive((R)) 1000PEGT70PBT30 implants. Biomaterials 2002 Dec;23(23):4649-4656.

10.   Habibovic P, Li JP, van der Valk CM, Meijer G, Layrolle P, van Blitterswijk CA, et al. Biological performance of uncoated and octacalcium phosphate-coated Ti6A14V. Biomaterials 2005 Jan;26(1):23-36.

11.   Barrere F, Layrolle P, van Blitterswijk CA, de Groot K. Biomimetic coatings on titanium: a crystal growth study of octacalcium phosphate. Journal of Materials Science-Materials in Medicine 2001;12(6):529-534.

12.   Chim H, Hutmacher DW, Chou AM, Oliveira AL, Reis RL, Lim TC, et al. A comparative analysis of scaffold material modifications for load-bearing applications in bone tissue engineering. International Journal of Oral and Maxillofacial Surgery 2006 Oct;35(10):928-934.

13.   Both SK, Van der Muijsenberg AJC, Van Blitterswijk CA, De Boer J, De Bruijn JD. A rapid and efficient method for expansion of human mesenchymal stem cells. Tissue Engineering 2007 Jan;13(1):3-9.

14.   J.D. de Bruijn IvdB, Y.P. Bovell and C.A. van Blitterswijk. Tissue engineering of goat bone: osteogenic potential of goat bone marrow cells. Bioceramics 1998(11):497-500.

15.   Janssen FW, Oostra J, van Oorschot A, van Blitterswijk CA. A perfusion bioreactor system capable of producing clinically relevant volumes of tissue-engineered bone: In vivo bone formation showing proof of concept. Biomaterials 2006 Jan;27(3):315-323.

16.   Siddappa R, Martens A, Doorn J, Leusink A, Olivo C, Licht R, et al. cAMP/PKA pathway activation in human mesenchymal stem cells in vitro results in robust bone formation in vivo. Proceedings of the National Academy of Sciences of the United States of America 2008 May 20;105(20):7281-7286.

17.   Radder AM, Leenders H, vanBlitterswijk CA. Application of porous PEO/PBT copolymers for bone replacement. Journal of Biomedical Materials Research 1996 Mar;30(3):341-351.

18.   Dekker RJ, de Bruijn JD, Stigter M, Barrere F, Layrolle P, van Blitterswijk CA. Bone tissue engineering on amorphous carbonated apatite and crystalline octacalcium phosphate-coated titanium discs. Biomaterials 2005 Sep;26(25):5231-5239.

19.   Barrere F, van der Valk CM, Dalmeijer RAJ, van Blitterswijk CA, de Groot K, Layrolle P. In vitro and in vivo degradation of biomimetic octacalcium phosphate and carbonate apatite coatings on titanium implants. Journal of Biomedical Materials Research Part A 2003 Feb 1;64A(2):378-387.

20.   Moroni L, Schotel R, Hamann D, de Wijn JR, van Blitterswijk CA. 3D fiber-deposited electrospun integrated scaffolds enhance cartilage tissue formation. Advanced Functional Materials 2008 Jan 11;18(1):53-60.

21.   Kuraishi K, Iwata H, Nakano S, Kubota S, Tonami H, Toda M, et al. Development of Nanofiber-Covered Stents Using Electrospinning: In Vitro and Acute Phase In Vivo Experiments. Journal of Biomedical Materials Research Part B-Applied Biomaterials 2009 Jan;88B(1):230-239.

22.   Moroni L, de Wijn JR, van Blitterswijk CA. 3D fiber-deposited scaffolds for tissue engineering: Influence of pores geometry and architecture on dynamic mechanical properties. Biomaterials 2006 Oct;27(7):974-985.

General discussion and conclusion

I – Trace elements containing calcium phosphate coatings (Chapters 3-5)

In the first part of the thesis, a selected number of trace elements known to play a role in various biological processes related to bone repair and regeneration were incorporated into CaP coatings. In Chapter 3, lithium ions containing CaP coatings were prepared using two coating methods, electrolytic deposition and biomimimetic method. Lithium has previously been shown to play a role in Wnt signaling, a cell signaling pathway associated with mesenchymal stem cell proliferation. Both ELD and biomimetic coating method allowed for incorporation of lithium ions into the CaP coatings deposited on titanium alloy surfaces, the metal that is frequently used for implants in load-bearing orthopaedic and dental applications. The efficiency of lithium incorporation could successfully be controlled by changing the lithium concentration of the coating solutions. The presence of lithium interfered with CaP crystal formation, decreasing the crystallinity and crystal size of the coating. The in vitro lithium release from both ELD and biomimetic coatings showed a burst profile, probably because the majority of lithium ions were not incorporated into the CaP crystal lattice.

In Chapter 4, a medium-throughput screening method based on biomimetic CaP coatings was developed for investigating the effect of trace elements on the osteoblast- and osteoclast behavior. Tissue culture well plates were coated with thin CaP layer containing different concentrations of copper-, zinc-, strontium-, fluoride- or carbonate ions, allowing for subsequent cell culture in a standardized way. The selected trace elements have all been shown to play a role in some of the processes related to bone formation and turnover, namely angiogenesis, osteoblast proliferation, osteogenic differentiation and osteoclastogenesis, as was also discussed in the review of Chapter 2. Positively charged ions, such as Sr^{2+}, Cu^{2+} and Zn^{2+}, occupied the Ca^{2+} sites in the CaP crystalline lattice and large amounts of these elements clearly affected structural properties of the coating. For example, higher concentrations of Sr^{2+} in the coating solution reduced the crystallinity of the coating, probably due to the replacement of Ca^{2+} with Sr^{2+} which has a larger ionic radius than Ca^{2+}. Negatively charged ions, F^- and CO_3^{2-}, can occupy the sites of the phosphate group or the hydroxyl group in the crystalline lattice. For example, earlier reports showed that the replacement of OH^- with F^- can decrease solubility of calcium phosphate crystal,

and bring about a reduction in the volume of the unit cell [4-7]. Experimental results of Chapter 3 also showed that the presence of F^- increased the crystallinity which was in accordance with earlier studies [8, 9]. In the case of CO_3^{2-}, two types of lattice substitution could occur: phosphate substitution (A type) and/or hydroxyl substitution (B type) [8, 10]. Results of Chapter 4, showing a decrease of coating crystallinity in presence of CO_3^{2-}, suggested the prevalence of the type A substitution, which is consistent with other reports [11, 12].

In Chapter 5, trace elements containing CaP coatings described in Chapter 4 were investigated with regard to their effects on the behavior of osteoblasts and osteoclasts. The presence of Cu^{2+} showed an inhibitory effect on ALP expression by MC3T3-E1 osteoblasts. Zn^{2+} increased the proliferation of MC3T3 in a dose-dependent manner, which was in accordance with earlier reports [13-15].

For both Sr^{2+} and F^-, dose dependent effects on osteoblast proliferation and differentiation were observed: lower concentrations of both elements decreased or showed no effect on proliferation and differentiation while higher concentration increased both proliferation and differentiation. These results are consistent with earlier studies showing that both elements can stimulate osteogenic differentiation and bone formation at certain levels within physiological range [16, 17].

The incorporation of CO_3^{2-} increased the proliferation of MC3T3 cells, probably due to the surface structure change. In contrast, decreasing differentiation was observed in the presence of CO_3^{2-} which could result from the local pH changes caused by the release of carbonate from the coating during cell culture.

The effects on resorptive activity of rabbit osteoclasts were consistent for all trace elements investigated; an inhibitory effect was observed for all elements at all concentrations. These results were in accordance with earlier reports showing inhibitory effects of these trace elements on osteoclastic resorption in vitro and in vivo [18-20].

II – Plasmid-DNA containing calcium phosphate coatings (Chapter 6)

In this part of the thesis, the possibility to co-precipitate plasmid DNA with calcium phosphate on titanium substrate was investigated in order to develop a gene delivery system that is able to combine the advantages of the calcium phosphate and gene therapy for bone tissue engineering.

Three types of pDNA were used, which had the gene encoding for either Bone Morphogenetic Protein Reporter-Luciferase (BRE-Lu), Green Fluorescent Protein (GFP) or Bone Morphogenetic Protein 2 (BMP2). All three types of plasmid DNA were successfully and homogenously incorporated into the CaP coatings using the biomimetic coating method, as suggested by the FTIR, ESEM and staining results, and the amount of pDNA incorporated into the coating could be controlled by adjusting the pDNA content of the coating solution. Coatings made in presence of pDNA exhibited changes in the morphology due to the inhibitory effect on crystal growth of the relatively large DNA molecules.

III – Combinations of calcium phosphate coatings with polymers (Chapter 7 & 8)

In order to be as successful as autograft in bone repair and regeneration, synthetic bone graft substitutes

need to meet some important requirements associated with their physico-chemical, structural and mechanical properties including biocompatibility, osteoconductivity, osteoinductivity, initial stability and fatigue strength and elasticity modulus similar to the surrounding tissue. None of the so far developed bone graft substitutes meet all these different requirements and new research lines focus on combining different biomaterials in order to optimize the properties of the final product. In this part of the thesis, the osteoconductive calcium phosphates were successfully combined with the polymers of impressive mechanical properties to produce a combined biomaterial that meets both mechanical and bioactivity requirements for a successful synthetic bone graft substitute.

In Chapter 7, recombinant spider silk fibres were coated with a layer of CaP by applying the biomimetic coating method. The preliminary cell culture experiments showed that the homogenous and thick crystalline carbonated apatite layer provided an environment to support attachment, growth and extracellular matrix formation of hMSCs which is consistent with an earlier study on premineralized silk scaffolds which showed that the layer of premineralization results in enhanced expression of osteogenic markers [21]

In Chapter 8, electrospun fibres of two polymers were successfully coated with CaP, but the in vitro experiments showed no significant effect of the coating on proliferation and differentiation of hMSCs. However, coated polymer fibres loaded with gMSCs induced bone formation upon subcutaneous implantation in nude mice, in contrast to the uncoated ones. In vivo, calcium phosphate coatings are expected to start dissolving [23], releasing thereby calcium and phosphorus ions, which are considered to be the first step towards de novo bone formation. Following the dissolution, a new carbonated apatite layer is precipitated on the substrate surface that contains endogenous factors. This process may act as a stimulus for implanted osteoprogenitor cells to induce new bone formation [24].

IV – Conclusion and future perspectives

The results of the present thesis showed that the biomimetic coating process that uses supersaturated body fluids and takes place at physiological pH and low temperatures is an attractive method to deposit a variety of calcium phosphate coatings on different substrates. The most valuable property of this process is that a variety of molecules, ranging from the earlier investigated antibiotics and growth factors, to plasmid DNA and trace elements described here, can successfully be co-deposited with calcium phosphate coatings. The efficiency of incorporation can easily be controlled by controlling the composition of the coating solution. The effect of the incorporated compound on the coating characteristics and the release profile are dependent on the physico-chemical nature of the compound, which determines whether or not it is incorporated into the calcium phosphate crystal lattice. The biological effect of the incorporated compounds can easily be investigated using standardized in vitro assays, as the CaP coatings can also be deposited on the tissue culture well plates.

The studies described here also showed that certain trace elements incorporated into CaP have an effect on proliferation and differentiation of osteoblasts as well as on resorbing capacity of osteoclasts making them a potentially valuable alternative to biologically complex and relatively expensive growth

factors. Another attractive alternative to growth factors based tissue engineering is gene delivery and this thesis showed that such a delivery system can be developed by co-depositing plasmid DNA with CaP onto a substrate. Further studies are needed to better control the temporal release of the compounds incorporated into CaP coatings, considering that some compounds showed a burst release profile. Understanding cellular and molecular pathways by which the incorporated compounds exert an effect on osteoblasts and osteoclasts is another topic of further investigation. Finally, in vivo studies should be performed to determine the effect of CaP coatings containing various compounds on bone formation and the resorption of the CaP coatings.

In addition to the fact that a variety of compounds can be co-precipitated into the coatings, the biomimetic methods, that take place in a solution at the near-physiological conditions allow for coating geometrically complex and porous shapes of a range of substrates, including thermally sensitive ones. This property makes it an attractive method to combine CaP with other biomaterials. In the thesis it has been shown that CaP coatings can be deposited on nano- and micro-sized fibres of natural and synthetic polymers with excellent strength and elasticity. Further studies should aim at developing 3D polymeric scaffolds with a compressive strength suitable for load-bearing applications, which are then combined with nano- and microfibers coated with CaP. Eventually, such constructs should be investigated in vivo in clinically relevant orthotopic defects to test the hypothesis that combination of polymers that possess excellent mechanical properties with bioactive CaP leads to improved synthetic bone graft substitutes.

REFERENCES

1.   Legeros, R.Z., et al. effect of the strontium on some properties of apatites. in the 5th Interantional Symposium. 1989.

2.   Wang, X. and J. Ye, Variation of crystal structure of hydroxyapatite in calcium phosphate cement by the substitution of strontium ions. J Mater Sci Mater Med, 2008. 19(3): p. 1183-6.

3.   Verberckmoes, S.C., et al., Effects of strontium on the physicochemical characteristics of hydroxyapatite. Calcif Tissue Int, 2004. 75(5): p. 405-15.

4.   Elliott, J., Structure and Chemistry of the Apatites and Other Calcium Orthophosphates. ed. . Vol. . 1994, Amsterdam-London-New York-Tokyo: Elsevier. 389.

5.   Young, R. large effects from the small structural differences in apatites. in Pro Int Cong Phosphorous Compounds. 1980.

6.   legeros, R.Z. and J.P. Legeros, in An introduction to bioceramics, L.W. Hench, J, Editor. 1993, World Scientific: Singpore.

7.   Aoba, T., The effects of the fluoride on apatite structure and growth. Crit Rev Oral Dent Med, 1997(8): p. 136-153.

8.   Elliott, J.C., D.W. Holcomb, and R.A. Young, Infrared determination of the degree of substitution of hydroxyl by carbonate ions in human dental enamel. Calcif Tissue Int, 1985. 37(4): p. 372-5.

9.   Shimoda, S., et al., Effect of solution composition on morphological and structural features of carbonated calcium apatites. J Dent Res, 1990. 69(11): p. 1731-40.

10.   Aoba, T. and E.C. Moreno, Changes in the nature and composition of enamel mineral during porcine amelogenesis. Calcif Tissue Int, 1990. 47(6): p. 356-64.

11.   Vignoles, M., et al., Influence of preparation conditions on the composition of type B carbonated hydroxyapatite and on the localization of the carbonate ions. Calcif Tissue Int, 1988. 43(1): p. 33-40.

12.   Gibson, I.R. and W. Bonfield, Novel synthesis and characterization of an AB-type carbonate-substituted hydroxyapatite. J Biomed Mater Res, 2002. 59(4): p. 697-708.

13.   Yamaguchi, M., H. Oishi, and Y. Suketa, Stimulatory effect of zinc on bone formation in tissue culture. Biochem Pharmacol, 1987. 36(22): p. 4007-12.

14.   Yamaguchi, M., H. Oishi, and Y. Suketa, Zinc stimulation of bone protein synthesis in tissue culture. Activation of aminoacyl-tRNA synthetase. Biochem Pharmacol, 1988. 37(21): p. 4075-80.

15.   Yamaguchi, M. and R. Yamaguchi, Action of zinc on bone metabolism in rats. Increases in alkaline phosphatase activity and DNA content. Biochem Pharmacol, 1986. 35(5): p. 773-7.

16.   Grynpas, M.D. and P.J. Marie, Effects of low doses of strontium on bone quality and quantity in rats. Bone, 1990. 11(5): p. 313-9.

17.   Briancon, D. and P.J. Meunier, Treatment of osteoporosis with fluoride, calcium, and vitamin D. Orthop Clin North Am, 1981. 12(3): p. 629-48.

18.   Vallet-Regi, M., Revisiting ceramics for medical applications. Dalton Trans, 2006(44): p. 5211-20.

19.   Moonga, B.S. and D.W. Dempster, Zinc is a potent inhibitor of osteoclastic bone resorption in vitro. J Bone Miner Res, 1995. 10(3): p. 453-7.

20.   Baron, R. and Y. Tsouderos, In vitro effects of S12911-2 on osteoclast function and bone marrow macrophage differentiation. Eur J Pharmacol, 2002. 450(1): p. 11-7.

21.   Kim, H.J., et al., Bone tissue engineering with premineralized silk scaffolds. Bone, 2008. 42(6): p. 1226-34.

22.   Barrere, F., et al., Osteogenecity of octacalcium phosphate coatings applied on porous metal implants. J Biomed Mater Res A, 2003. 66(4): p. 779-88.

23.   Barrere, F., et al., In vitro and in vivo degradation of biomimetic octacalcium phosphate and carbonate apatite coatings on titanium implants. J Biomed Mater Res A, 2003. 64(2): p. 378-87.

24.   Habibovic, P., et al., Biological performance of uncoated and octacalcium phosphate-coated Ti6Al4V. Biomaterials, 2005. 26(1): p. 23-36.

Summary

As a novel approach to repair and regenerate damaged and degraded bone tissue, tissue engineering has recorded tremendous growth for the last thirty years. This is an emerging interdisciplinary field applying the principles of biology and engineering to the development of viable substitutes that restore and maintain the functions of human bone tissues. Tissue engineering constructs usually are natural or synthetic scaffolds in combination with cells and/or growth factors. Ideally, the engineered bone, called bone graft substitute, becomes integrated within the patient, affording a potentially permanent and specific cure of the tissue. These engineered constructs are commercially attractive for their off-the-shelf availability in large quantities and relatively low production and storage costs. Bone-graft substitute should ideally be: biocompatible, to be accepted by the body without adverse tissue responses; osteoconductive, able to facilitate and guide new bone formation from the host bone; osteoinductive, able to induce new bone formation; bio-resorbable, and structurally similar to bone.

This thesis contains two parts. The first part is to study the effects of the selected additives: trace elements (Chapter 2-5) and pDNA (Chapter 6) on the calcium phosphate materials, and the effects on in vitro cell behavior. The second part is to combine calcium phosphate with other synthetic material or scaffolds to produce a better biomaterial that meets both mechanical and bioactivity requirements for a successful bone graft substitute.

Chapter 2 gives a review on improving the biological performance of calcium phosphate ceramics as bone graft substitutes by adding inorganic compounds as additives. Five inorganic additives have been selected: zinc, copper, strontium, fluoride and carbonate. Zinc has shown positive effects on proliferation and osteogenic differentiation of bone forming cells and decreased osteoclastic resorption in vitro; copper was shown to have similar effect on crystal properties as zinc; strontium has also shown positive effects on proliferation and osteogenic differentiation of osteoblastic cells whereas negative effects on osteoclast growth; in a dose dependent manner, fluoridated apatites can stimulate osteoblast proliferation and osteogenic differentiation; carbonated ceramics have shown poorer attachment of osteoblastic cells, whereas higher osteoclast proliferation and resorption potential.

In chapter 3, lithium ions were successfully introduced into CaP coatings via electrolytic deposition and biomimetic method. The efficiency of lithium incorporation is controllable while the vitro release showed a burst profile.

Chapter 4 and 5 introduced a novel medium-throughput screening method based on biomimetic coating method to investigate the effect of trace elements on the osteoblast and osteoclast behavior. The same ions were chosen as in the chapter 2. Structural effects were discussed such as effects on crystallinity, solubility and etc. The effects of those elements on the behavior of osteoblasts and osteoclasts were further investigated in chapter 5. Copper showed an inhibitory effect on osteoblastic ALP expression, while zinc amd carbonate showed a positive effect on osteoblastic proliferation. The effects of strontium and fluoride on osteoblasts are dose dependent. All those elements showed an inhibitory effect on resorptive activity of rabbit osteoclasts.

Chapter 6 successfully combined pDNA with calcium phosphate coating on titanium substrate and the efficiency was controllable via adjusting the pDNA content of the coating solution. Three types of pDNA were used, which had the gene encoding of GFP, BRE-Lu, or BMP2. Because of the inhibitory effects on crystal growth of the relatively large DNA molecules, the presence of pDNA exhibited changes on the morphology of coating.

To be a successful bone graft substitute, biomaterial should meet some important requirements, which were addressed in the second part of this thesis by combining osteoconductive calcium phosphates with polymers of impressive mechanical properties via biomimetic coating process. Preliminary cell culture experiments in chapter 7 showed that the combination of calcium phosphate and recombinant spider silk fibres did help to support hMSCs' attachment, growth and extracellular matrix formation. In vivo experiments in chapter 8 showed that loaded with gMSCs and implanted in nude mice, the combination of calcium phosphate and electrospun polymer fibres induced bone formation, in contrast to the pure polymer fibres.

The final chapter summarized and discussed all results of this thesis, and raised ideas for the future work. Future work should focus on develop 3D polymeric scaffolds combined with nano- spider fibers coated with CaP, which should bear a compressive strength suitable for load-bearing applications and an improved bioactivity.

Acknowledgements

I will never forget that ignorant young boy with poor English standing in the arrival hall of the schipol airport alone, and probably because of the nervousness, failing to even notice that there were several Chinese stood at the entrance, holding a board with his name on it (deeply sorry for wasting your precious time, HuiPing and JiaPing). When I look back, I feel that I am extremely lucky because I have met so many smart and kind people. Without you guys, I will never manage to come this far. It is so hard to acknowledge all you guys, and if I fail to list your name here, I want you to know that my gratitude is not less than for these listed below.

First and foremost I would like to express my deep and sincere gratitude to my supervisors: Prof. Dr. C.A. van Blitterswijk, Dr. F. de Groot-Barrere, and Dr. P. Habibovic. Clemens, your profound insight will always inspire me not only on scientific research but on many other things in my life as well. Florence, thank you for giving me the opportunity to work in tissue engineering field, in spite of my poor English and ignorance in this particular field. Pamela, thank you for your contribution of time, ideas, and all the other things, which have made my PhD life productive and stimulating. Your enthusiasm, attitude, and good organization always set examples for me. Your encouragement and understanding made my PhD life much easier and happier.

The work described in Chapter 4 and 5 were done together with Florence and Soledad, without your contribution, this chapter would not have been possible. And Anand, thank you for all the work you have done to make chapter 8 so interesting and all suggestions you gave to me. My special thanks to Aart. You have spent lots of precious time with me on ESEM and Raman, which made the work very fun and I really enjoyed it.

I would like to thank all the group members who during my stay at Bilthoven and Twente, have provided such a pleasant and friendly environment where we had so much fun. Aart, Anouk, Aliz, Ana, Anand, Andre, Audrey, Gustavo, Hemant, Hugo, Ineke, Jacqueline, Joyce, Liliana, Nicolas, thank you all guys for your help and suggestions.

My special thanks to my Chinese friends Liujun, Lingnan, Jiaping, Sunkang, Huipin, Ruiqing, Yanling, Yuelian, Mabin, Wulin, ChenWei, Yizi, Xiaojun, Maxiao, Leimong, Xuexin, Shuhan, Songyue, Qiubing, Yanhong, Minliang, Shuilingling, Baiwei, Pushi, Zhixun, Chunlin, Yizhi, Sangxiang, Xiaoli, Yiyu, Yangjing, Yixuan, Bianxia, Hongliang, Zhangxiao, Yingzhun, Zhangyang, Zhangpeng, Jiwu, Yangqi, Dingqi, Haiyan, Guoai, Yunkai, Gaonan, Xuda, Lice, Dunting, Shanlin, King, Xiaotong, Sundan, Jianan, Nan, Jiajing, Enxin, Tingting, Zhangrong, Wenwen, and etc. Thanks you guys for all the supports in my research and my life in Holland. Last, but not least, I thank my family: my parents, for giving birth, for educating me and for unconditional affection; my girlfriend Yunjie, for your encouragements, supports, endless love and happiness you brought to me. xoxoxoxox

Liang Yang
Enschede, the Netherlands
May 2010

Curriculum Vitae

Liang Yang was born on June 12th 1982 in LinChuan, JiangXi Province, China. He obtained his B.Sc and Master degrees at Tsinghua University, Peking, China in 2002 and 2005. After that, he went to University of Twente, Enschede, the Netherlands, as a PhD student under the supervision of Prof. Dr. C.A. van Blitterswijk and Dr. P. Habibovic. The subject of his research was to explore the possibilities to improve the biological performance of the existing biomaterials in bone repair and regeneration, without the use of cells and growth factors and the results are described in this thesis.

List of Publications

Yang L, Harink H and Habibovic P, Calcium-phosphate ceramics with inorganic additives, in: Comprehensive Biomaterials, Paul Ducheyne et.al., editors, submitted for publication 2010.

Yang L, Perez-Amodio S, Barrere-de Groot FYF, Everts V, van Blitterswijk CA and Habibovic P, The effect of inorganic additives to calcium phosphate on in vitro behavior of osteoblasts and osteoclasts, Biomaterials 3: 2976-2989 (2010).

Nandakumar A, Yang L, Habibovic P, van Blitterswijk C, Calcium phosphate coated electrospun fiber matrices as scaffolds for bone tissue engineering, Langmuir, 2010, in press.

Yang L, Hedhammar M, Blom T, Leifer K, Johansson J, Habibovic P and van Blitterswijk CA, Biomimetic calcium phosphate coatings on artificial spider silk fibres, submitted for publication to Biomedical Materials, 2010.

Yang L, van Blitterswijk CA and Florence Barrere, pDNA and calcium phosphate co-preicipitation on titanium alloy plate, Key Engineering Materials 330-332: 621-624 (2007).

Other publications:
Yang L, Zhang Y and Cui FZ, Two types of mineral-related matrix vesicles in the bone mineralization of zebrafish, Biomedical Materials 2: 21-25 (2007)